INVESTIGATION OF THE ACQUISITION PROBLEM IN SATELLITE ATTITUDE CONTROL

A. SABROFF
R. FARRENHOPF
A. FREW
M. GRAN

TRW/SPACE TECHNOLOGY LABORATORIES
REDONDO BEACH, CALIFORNIA

FOREWORD

This report was prepared by TRW/Space Technology Laboratories, Redondo Beach, California, in a study entitled "Investigation of the Acquisition Problem in Satellite Attitude Control," Contract AF33(615)-1535, Project No. 8219, Task No. 821904. The work was administered under the direction of the Air Force Flight Dynamics Laboratory, Research and Technology Division, Air Force System Command, Wright-Patterson Air Force Base, Ohio. Mr. A. Connors was the RTD project engineer and Dr. A. Sabroff was the project manager for TRW/Space Technology Laboratories.

The permanent members of the Program Review Board consisted of Mr. N.W. Trembath, Chairman, Mr. E. I. Reeves, and Dr. E.I. Ergin. In addition, acknowledged credit is given to those technical staff members who contributed to the study effort. In particular, the authors thank Dr. G. Bekey, STL Consultant, for his help in initiating the optimization studies, to Mr. J. C. Fox for his efforts in the quantitative comparison of various systems and to Messrs. E. Hartsfield, M. Reagan and A. Wong for invaluable assistance in programming the digital computer algorithms for the optimization and stability studies.

This is the final report for the subject contract. The contractors report number is 4154-6008-RU001.

The manuscript was released by the authors 31 March 1965 for publication as an RTD Technical Report.

This report has been reviewed and is approved.

C. B. Westbrook

C. B. WESTBROOK
Chief, Control Criteria Branch
Flight Control Division
AF Flight Dynamics Laboratory

ABSTRACT

The acquisition function of a spacecraft attitude control system consists of properly orienting the vehicle with respect to specified reference directions starting from large initial attitude and rate errors. The resulting control system design problem was examined by establishing suitable mathematical representations, comparing competing control concepts, developing a practical optimization approach, and evaluating a new technique for applying Lyapunov stability theory to the acquisition problem.

All potentially practical kinematic representation for specifying rigid body attitude are presented and compared. The bases for comparison are with respect to their applicability for analytic studies and simulation studies. In each case the ease of visualization and interpretation, simplicity of system representation, order of the representation, as well as the basic characteristics of the representations themselves are considered.

An analytic study which proves complete stability of a particular acquisition system is presented. The effects of modifications in this ideal analytic model are quantitatively evaluated. Included are control torque saturation, attitude error sensor saturation and simplified schemes for providing satellite body rate information. All effects are evaluated for both direction cosine attitude sensors and Euler angle attitude sensors.

Algorithms for parametric optimization of acquisition systems are developed and compared. A practical approach to optimal design of the high order nonlinear acquisition systems with many degrees of parametric freedom is presented. A particular acquisition system is optimized with varying degrees of parametric freedom and various performance criteria. Minimum acquisition time with fuel constraint, minimum fuel with an acquisition time constraint, and minimum allowable control torque level within a specified acquisition time are considered.

A new and potentially useful approach of stability of acquisition systems based on Lyapunov stability theory is developed. A digital computer algorithm for proving the sign definiteness of a function over a bounded region of state space is described. A unified approach to stability studies is given and the developed technique is demonstrated.

TABLE OF CONTENTS

TABLE OF CONTENTS

TABLE OF CONTENTS

TABLE OF CONTENTS

TABLE OF CONTENTS

TABLE OF CONTENTS

LIST OF ILLUSTRATIONS

LIST OF ILLUSTRATIONS

LIST OF ILLUSTRATIONS

LIST OF ILLUSTRATIONS

LIST OF ILLUSTRATIONS

LIST OF TABLES

LIST OF TABLES

SECTION I

INTRODUCTION

The primary objective of this study was the investigation of analytical and computational design procedures for automatic control systems used for properly orienting satellites (spacecraft) with respect to specified reference directions starting from unknown initial conditions on vehicle attitude and tumbling rates. This flight control problem is commonly called the "acquisition" problem. Although the applications of the analytic and simulation techniques developed during the course of this study are directed to the acquisition problem, they are generally applicable to any nonlinear control system problem. Major emphasis of the study was the development of "practical" or "potentially practical" techniques for the analysis and design of these and other high order nonlinear control systems.

1.1 Statement of the Problem

The "acquisition"function of a spacecraft attitude control system consists of properly orienting the spacecraft with respect to specified (stationary or time-varying) reference directions starting from unknown initial conditions on the spacecraft attitude and bounded, but otherwise arbitrary, tumbling rates. The acquisition problem is the task of formulating performance and stability criteria, establishing concepts of operation, synthesizing control laws and instrumentation (compatible with the normal mode attitude stabilization) for an automatic control system to perform the acquisition functions.

In several respects, the conceptual and analytical aspects of the acquisition design problem are among the most difficult and least understood in the attitude control field. In general, small angle approximations are not valid and dynamical cross-coupling terms are

not negligible. Generally, therefore, control action cannot be applied about one control axis independently of the vehicle motion about the others. Also, performance and stability criteria for acquisition have not been adequately defined. Perhaps the most critical problem is that design concepts as well as detailed procedures for many acquisition situations have not been adequately formulated. One of the critical features of acquisition is to evaluate the effects of saturating behavior of actuators, sensors, etc.

Analytic techniques for investigation of the acquisition problem must provide capability of including the effects of these control system imperfections. "Idealized" analytic models provide only qualitative information in relation to the highly complex nature of readily implemented physical systems. Numerous important performance constraints must be considered. Among these are the time to achieve a suitable equilibrium, the amount of energy expended in the acquisition process, the attitude error sensor characteristics including saturations and regions of no signal output, mission constraints such as eclipse, control torque source limitations with respect to amplitude and operating characteristics, the degree of control system complexity in relation to weight, power, and reliability of the acquisition system, the interrelation of the acquisition system to the "normal mode" (near equilibrium) control system and others.

Because of the complex nonlinear character of the acquisition problem, relatively sophisticated mathematical and computational tools are required to arrive at reasonable solutions for the design problems. Even the mathematical formulation of the dynamical aspects of the spacecraft motion is complex. Results of numerical investigation of specific acquisition design problems cannot be generalized to a reasonably large class of similar problems. Instead, it seems

likely that numerical investigations of reasonable duration will be valuable only after an analytical framework for the acquisition problem has been constructed.

The two basic considerations attending the acquisition requirements are Stability and Optimality. The latter assures the first only for the general "closed loop" optimal control, a result not attainable in a general form within the scope of the present study. Therefore, it is important to seek practical solutions to the stability problem which include all basic system nonlinearities. Concurrently, a suitable quasi-optimum form of control, which satisfies the basic performance constraints but is at the same time practically implemented, was a reasonable goal.

1.2 Discussion of the Problem

The first operation of the satellite attitude control system after it is activated will be to orient and stabilize the vehicle with respect to specified reference directions starting from particular sets of initial conditions. At other times during the satellite lifetime, a repetition of the act of acquiring a proper attitude starting from unfavorable initial conditions may be necessary. For example, loss of reference can occur due to occulting of the vehicle sensors by nearby bodies or from temporary power outage. In these cases, however, the bounded rates are usually less than during "initial acquisition". Stabilization modes initiating from these arbitrary attitudes but small initial rates are often referred to as "reacquisition". In this study all such requirements are considered as subproblems of the general acquisition problem.

Analytic complexities arise because sensors and actuators suitable for normal operation in attitude control are subject to saturating behavior during acquisition. It is usually desirable to utilize the

same equipment for both operational modes because of weight, cost, and reliability considerations. These additional constraints - more philosophical than analytical - further complicate the acquisition problem.

Certain approaches such as Lyapunov stability criteria and Dynamic Programming have been used to obtain preliminary results on this problem [1].* It appears that these techniques cannot be easily extended to more realistic acquisition problems. This is because of the apparently perplexing computational problems involved in the Dynamic Programming approach for continuous time dynamic systems, and the extreme cost of implementing this approach. Additionally, no unified approach to application of Lyapunov techniques to general nonlinear control problems yet exists.

1.2.1 Acquisition Requirements and Design Problems

It has previously been indicated that the control concept for an acquisition system is strongly dependent not only on the acquisition phase requirements, but also on the overall mission requirements, since such requirements to a great extent dictate the possible sensing and control torque generation mechanisms to be used. In discussing various acquisition situations, it is desirable to relate them to missions with their associated requirements and constraints. The several acquisition situations can be classified by either the dynamical and physical character of the reference frame with which the vehicle coordinate axes must be aligned at the completion of acquisition, and/or by the particular control mechanisms which are available to force the vehicle into its final desired orientation in space.

Dynamic Character of the Reference Frame: The reference frame defines the ideal orientation of the vehicle as a function of time. If the reference frame is inertially fixed, it is independent of time and

* Numbers in brackets refer to references of Section X.

the acquisition problem may be somewhat simplified. For orbiting vehicles, however, the reference frame will in general be time dependent; the nature of this dependence being determined by the orbit characteristics and the vehicle orientation requirements. Even in orbital situations, it may be possible to neglect the rotation of the reference frame if the acquisition can be accomplished in a relatively short period of time compared to the motion of the reference frame.

Physical Character of the Reference Frame: The physical character of the reference frame will, in general, determine the nature of sensing devices (and to an extent the control torque mechanisms). For inertial references, sensing devices such as star sensors, gyros, and sun sensors may be utilized. For orbiting vehicles where one of the vehicle axes may always be required to point along the local vertical, devices such as horizon trackers may be more suitable. The choice of the sensing device will strongly influence the performance and design of the acquisition system.

Character of Control Torque Sources: Since the design of an attitude control system for space vehicles is primarily based on the overall mission requirements and constraints, the selection of the control torque sources is normally accomplished prior to detailed acquisition considerations. The acquisition system is, then, usually constrained to use the same torque sources (as well as sensors) in order to avoid penalties in the weight and the reliability of the control system. Torque sources may be either internal (ones which do not change the total vehicle angular momentum, e.g., reaction wheels) or external (those that do change the total angular momentum). In addition, the external torque sources may either be natural (such as gravity gradient, or Earth's magnetic field) or vehicle-generated (such as those obtained by mass expulsion systems). The major

difference in design in the latter situation arises from the fact that the control system designer has much greater latitude in the selection and the specification of vehicle-generated torque sources. The design of the systems utilizing natural ambient fields for torque generation is complicated by two factors:

(1) Limited design flexibility because of the uncertainties and anamolies in the ambient fields, and/or because of the influence of vehicle parameters (such as moments of inertia, or the residual magnetism of the vehicle) on the system design.

(2) Difficult design problems because of the natural dependence of the ambient control torques on the vehicle orientation itself, i.e., additional dynamical coupling.

It is important to investigate the acquisition design problems associated with control systems utilizing ambient fields since they offer, in many cases, advantages of simplicity and light weight over other control configurations. It is, of course, undesirable to utilize different torque sources for acquisition, when they are not absolutely required, so that unnecessary weight and reliability penalties may be avoided.

In Section II several acquisition situations, which utilize various combinations of the above-mentioned torque sources and reference frames, are discussed and some of the significant problems are pointed out. These acquisition situations cover a variety of design problems that can be encountered in the design of present and future satellites. The examples given are selected as representative of the problems that are being discussed and have been encountered in the field of attitude control.

1.2.2 General Considerations

The acquisition system designer must formulate performance and stability criteria, establish concepts of operation, and synthesize control laws and instrumentation. Before the specific acquisition situations can be discussed, it is necessary to consider briefly the selection of criteria and the influence of initial conditions on the system design.

Criteria and Constraints: The design criteria for space vehicle attitude control systems are normally selected as system weight, power requirements, and reliability. The objective of the design is to minimize the first two and to maximize the last. The same basic measures may be used for the acquisition systems for most mission requirements. Even though a general mathematical formulation of the above-mentioned criteria does not appear feasible at present, certain design approaches may achieve a near optimum acquisition system with respect to these criteria.

The total control system weight is normally determined on the basis of studies of the normal system operation. Hence, weight minimization in the acquisition case may be interpreted as minimization of the amount of special acquisition equipment (such as logic) and minimization of the amount of propellant required for control torque generation during acquisition.

The minimum control system power is similarly defined, in the acquisition case, as a minimum expenditure of stored energy during the acquisition process, and is strongly related to the first consideration (particularly since the propellant can also be considered as stored energy).

The maximum reliability in the acquisition case may be obtained by adding a minimum of complex equipment to the normal control system in order to achieve proper acquisition. This approach may not be satisfactory if the acquisition system performance places excessive demands on the normal control system operating characteristics. It would be ineffective to maximize the reliability of the acquisition system if in so doing the reliability of the normal mode control system was decreased.

A fourth criterion, minimum acquisition time, may be an important consideration for certain missions. At least for scientific missions, acquisition time can be considered as a constraint rather than a performance criterion. That is, the acquisition process must be completed within a specified time. For some tactical orbital operations this may no longer be a valid approach and the important design criterion may become minimum time.

Major acquisition constraints are derived from the nonlinearities in sensing and torque generating devices, particularly saturation characteristics of these control system elements. An additional important constraint (usually known) in the design process is the maximum initial tumbling rates from which the vehicle is to recover, reorient, and stabilize.

Influence of Initial Conditions: Since the dynamical character of the satellite during acquisition is highly nonlinear, the system response and hence the selection of system parameters for performance optimization are strong functions of initial conditions. As a result, the problem of determining the optimum acquisition approach is a formidable one. Indeed, even being able to ascertain the proven stability of the system over reasonable limits on initial conditions has not been resolved except for particular cases.

1.3 Study Approach

The objectives of the present program of investigation are threefold:

(1) Evolution and quantitative evaluation of competing means of providing satellite acquisition control.

(2) Development and/or refinement of analysis techniques applicable to the acquisition problem.

(3) Evaluation of the practical feasibility and benefits of specific optimal acquisition schemes.

Useful fulfillment of these objectives requires establishment of specific areas of investigation and a suitable set of ground rules. Each of these is necessary to assure that one aspect of the problem is not overly penetrated at the exclusion of other, perhaps equally important, areas of investigation. For example, a priori decisions relating the importance of reorientation (single axis) maneuvers to the true acquisition problem must be made. Again, the acquisition categories to be investigated as well as the extent of investigation need be considered at the outset. Basically the decision becomes one of establishing the relative importance of investigation and development of analytic and simulation techniques applicable to specific acquisition requirements as compared to detailed evaluation of particular acquisition systems. The basic approach of this study has been the development of analytic and simulation techniques.

1.3.1 Areas of Investigation

Four major areas of investigation were selected:

(1) Investigation of dynamics and kinematics with major emphasis on the means of representation of rigid body attitude.

(2) Quantitative comparison of various practical acquisition systems with an aim toward establishing relative importance of implementation constraints.

(3) Development and evaluation of parameter optimization schemes suitable for practical application to realistic acquisition systems and demonstration of their utility.

(4) Development and evaluation of computer aided analyses for proving the stability of complex nonlinear systems over a bounded region of possible initial conditions.

These areas of investigation cover the basic problems associated with practical analysis of acquisition systems.

A fundamental limitation of acquisition system analysis and simulation is the lack of a completely satisfactory means of formulating the system kinematics. The general requirement for all-attitude information coupled with the need and desire for simplicity of representation and ease of interpretation presents a formidable obstacle. Therefore, as a starting point for further investigations it was important to review all available representations in a quantitative manner and thereby establish the basic characteristics of each. The desire of low order representations in analytic hand analyses may grossly complicate the formulation for simulation studies. Therefore, it may prove beneficial to utilize different representations for different phases of investigation of the acquisition problem.

Since no unified approach to conceptual development of acquisition systems exists, it appeared beneficial to quantitatively compare various acquisition systems. In this case the goal was to establish the implications of various implementation constraints. For example,

general conclusions relating the importance of saturation in attitude sensors are not presently available. Also of importance are the relative tradeoffs between linear type torque sources such as may be available from a proportional gas jet system and the more practical bang-bang type operation. Finally, the effects on system performance of various schemes of sensing and computing satellite body rates about control axes were to be considered. This type investigation will provide not only quantitative evaluations of these various considerations but will help to establish significant further areas of investigation where important comparison studies can be performed.

No rational approach to optimization of satellite acquisition systems has yet been undertaken. To date most satellite control system designs have been accomplished based on the more analytically tractable small angle performance. Unfortunately this approach often gives rise to undesirable complexities of logic and/or mode switching to insure a "satisfactory" acquisition capability. Design based primarily on small angle behavior may not provide acquisition behavior which could be accomplished via a unified approach to the design of both. Therefore, optimization of the acquisition system while employing constraints which guarantee acceptable small angle behavior represents a potentially useful approach. This is particularly true when the basic torque sources used for acquisition and normal mode control are different so that less influence of optimal design of one is felt by the other. For example, a gas jet - reaction wheel system may primarily utilize the gas system for acquisition and the reaction wheel system for normal control, the only constraint being the ability of the wheels to assume control of the system and the gas system being able to provide momentum removal for the normal phase of operation. In other missions the acquisition mode may predominate the system objective such that its optimization becomes a prime design requirement. Along these lines, an immediately applicable approach to

optimization of acquisition systems can be of considerable practical value. A major goal of the present study was the development, evaluation and demonstration of utility of a practically implemented optimization scheme.

The development of a practical approach to system optimization does not necessarily guarantee system stability. That this is so will be more readily appreciated later. Therefore, in order to stand on firm ground an independent evaluation of system stability would be required. Unfortunately, for high order nonlinear systems no entirely suitable approach exists. Therefore, it is desirable to investigate potentially useful means for such analysis. In particular, since the acquisition problem (1) is characterized by bounded initial conditions, (2) can be analytically represented in a straightforward way, and (3) represents a physical process so that intuition becomes an important factor, it appeared that techniques not generally applicable to high order nonlinear control systems might be of considerable value here.

Although other areas of investigation pertinent to the acquisition problem are presented in this report, the four delineated and discussed above constituted a majority of the effort.

1.3.2 Study Ground Rules

For purposes of application of the developed analysis techniques the study scope was limited. However, in no case are the basic techniques themselves limited in application to either more complex acquisition systems or for evaluation of most nonlinear systems. The basic ground rules and their resulting limitation in scope can be categorized with respect to:

(1) System mission and requirements

(2) System implementation

The established considerations in each of these areas and their significance on the present study are of interest.

System Mission and Requirements: For purposes of presenting examples of application of the developed optimization technique as well as for the quantitative comparison of acquisition systems with respect to implementation constraints the following ground rules were established.

First, rotation about a single axis initiating from an essentially zero momentum state was not considered to be representative of the acquisition problem and therefore was not studied. Reorientations of a satellite fall into this category. The exclusion of this problem from the present study should not be construed as an attempt to minimize its practical significance. Indeed, the reorientation of a satellite can represent a major mode of operation. In addition, techniques not readily applicable to the acquisition problem can be of great advantage here. In particular, the Pontryagin Maximum Principle has been successfully employed for such single axis - nominally second order - systems[2].

Second, acquisition systems for spin stabilized vehicles need not be considered. Since a spin stabilized vehicle with a passive wobble damper has a stable inertial orientation, all subsequent maneuvers can be classified as reorientations of the spin axis to some new inertial position.

Third, acquisition systems for gravity gradient stabilized satellites need not be considered. In this case the acquisition characteristics of the system are more a function of basic physical phenomena than of the acquisition system design. Although some tradeoffs exist, the time to acquire from an initial tumbling condition is strongly dependent on the initial satellite momentum. Once the satellite has entered a libration phase of operation, i.e.,

the earth pointing axis no longer crosses the local horizontal plane, some tradeoffs exist. In this case the tradeoffs are more from the system approach viewpoint than from the parametric sensitivity of a particular design.

Fourth, no serious attempt was made to invent new acquisition approaches. Hence, acquisition systems utilizing magnetic torquing, with or without reaction wheels, were not considered. Considerable interest would attend such an acquisition system and some advanced work is being performed in this area[3]. Although the development of new approaches was not considered a primary effort in this study, some interesting results pertaining to as yet untried systems are presented.

Fifth, two fundamental acquisition requirements can be established: (a) one axis*, and (b) three axis. In the first case the acquisition maneuver is to establish a desired attitude of one satellite axis, reduce the final body rate about this axis to a predetermined value, or zero as desired, and to reduce the remaining body rates to zero or their limit cycle values. In the second case all three satellite axes are established with a desired attitude relative to the reference coordinate system and all body rates are reduced to their minimum value. In general, the latter problem is more difficult from both the analytic and simulation points of view. The three axis problem can be reduced to the one axis problem by considering a reorientation maneuver about the attitude controlled axis after acquisition. Because of this consideration the acquisition systems considered for this study were of the one axis type.

---

*There is a profound difference between the "one axis" system considered here and the "single axis" system discarded previously. The change from "single axis" to "one axis" increases the study complexity greatly whereas the change from "one axis" to "three axis" is more a straightforward extension.

System Implementation: Several ground rules were established relative to the form of implementation of the acquisition systems considered.

First, the primary momentum removal means utilized for quantitative evaluation was mass expulsion, e.g. gas jets. For "high performance" systems the required large torque levels can be easily attained only with mass expulsion torquing. Additionally, use of reaction wheels as the basic control torque requires an external torque source which becomes overly dependent on mission constraints and vehicle configuration. The advantage of the gas jet assumption is the ready applicability to a wide range of missions and satellite configurations.

Second, the attitude error sensing was assumed proportional to appropriate direction cosines from the body to the reference attitude direction. This constraint is satisfied by a majority of available and proposed Earth and Sun sensors. The notable exception to this assumption is the case of utilizing gimbal angle pickoffs for attitude error measurement relative to an inertial-or-rotating-platform reference. A special study of the effects of particular forms of acquisition systems utilizing the gimbal angle pickoff approach was undertaken.

Third, satellite inertias were not considered as free parameters. No defense of this constraint is possible except that it was necessary, within the present scope of study, to limit the degrees of parametric freedom to reasonable bounds.

Although, in some cases, the established ground rules may appear arbitrary, the essential study objective of evaluating approaches rather than systems would justify even more restriction. As will be seen, the analytic approaches studied are not restricted by any of these ground rules.

1.4 Contents of the Report

Section II considers in more detail the implications of various acquisition missions with respect to desired final attitudes, momentum removal sources and sensing requirements and capabilities. Many of the above listed ground rules are readily justified when this broad look at the acquisition problem is critically reviewed.

Section III presents an organized review and evaluation of the dynamic and kinematic representation aspects of the acquisition problem. The fundamental limitations of the available kinematic representations are qualitatively and quantitatively evaluated. The relative advantages and disadvantages of these approaches for analysis, simulation, interpretation and implementation are discussed.

Section IV presents the results of analytic investigations of a particular idealized acquisition system. The system is analyzed utilizing Lyapunov's Second Method and proven completely stable. The system described in this section forms a base point for the studies to follow.

Section V evaluates the effects on system performance of less ideal sensing and control from that available in the analytic study of Section IV. The implications on system performance of control torque saturation, bang-bang control, sensor saturation, and less ideal body rate information are evaluated in a quantitative manner. Additionally, the effects of utilizing gimbal angles as the basic attitude error sensor are evaluated for a variety of practically implementable situations.

Section VI presents a practical unified approach to acquisition system optimization. Several parametric optimization schemes are evaluated with respect to application efficiency. Using the results of Section V a reasonable practical acquisition system is optimized

using the developed techniques. Optimization criteria of minimum time (with fuel constraint), minimum fuel (with time constraint) and minimum control capability within minimum time are evaluated.

Section VII describes a potentially useful approach for analysis of stability of high order nonlinear systems. A digital computer algorithm is developed for augmenting stability studies via the Second Method of Lyapunov.

Section VIII discusses the major conclusions for the analytic studies presented in this report.

Several appendices are included to supplement the material of the main text. Appendix A presents an analytic study due to R. Mortenson of a particular three axis acquisition system. The summary of this work is included since it is apparently unavailable in the published literature and demonstrates several interesting applications to acquisition system design. Appendices B, C and D describe the simulation studies supporting the results of Sections V, VI, and VII, respectively.

SECTION II

MISSIONS AND SYSTEMS

Before embarking on the detailed analytic developments of the study, it is useful to establish logical categories for Earth satellite missions and associated acquisition systems. The mission may provide important limitations concerning the type of stabilization system to be employed. In some cases the choice may be easily established. However, even if this occurs for the normal mode requirements it is possible that the acquisition system to be employed will remain relatively undefined. More generally a variety of possible approaches to stabilization, both with respect to the normal operational mode and acquisition, must be weighed, one against the other, to establish the "best" combined approach.

2.1 Mission Categories

Although numerous specific missions can be readily delineated, for purposes of the present study, a more useful categorization is with respect to the final desired acquisition reference system. Two generalized categories exist:

(1) Systems with an inertial acquisition reference

(2) Systems with a moving acquisition reference.

Within these categories the general missions of interest can be classified. Figure 2.1 delineates the potential missions wherein the final desired attitude is with respect to an inertial reference. Shown are some of the spacecraft existing, or under consideration as potential missions, in each of these categories. Notice the preponderance of spin stabilized applications for inertially referenced satellites.

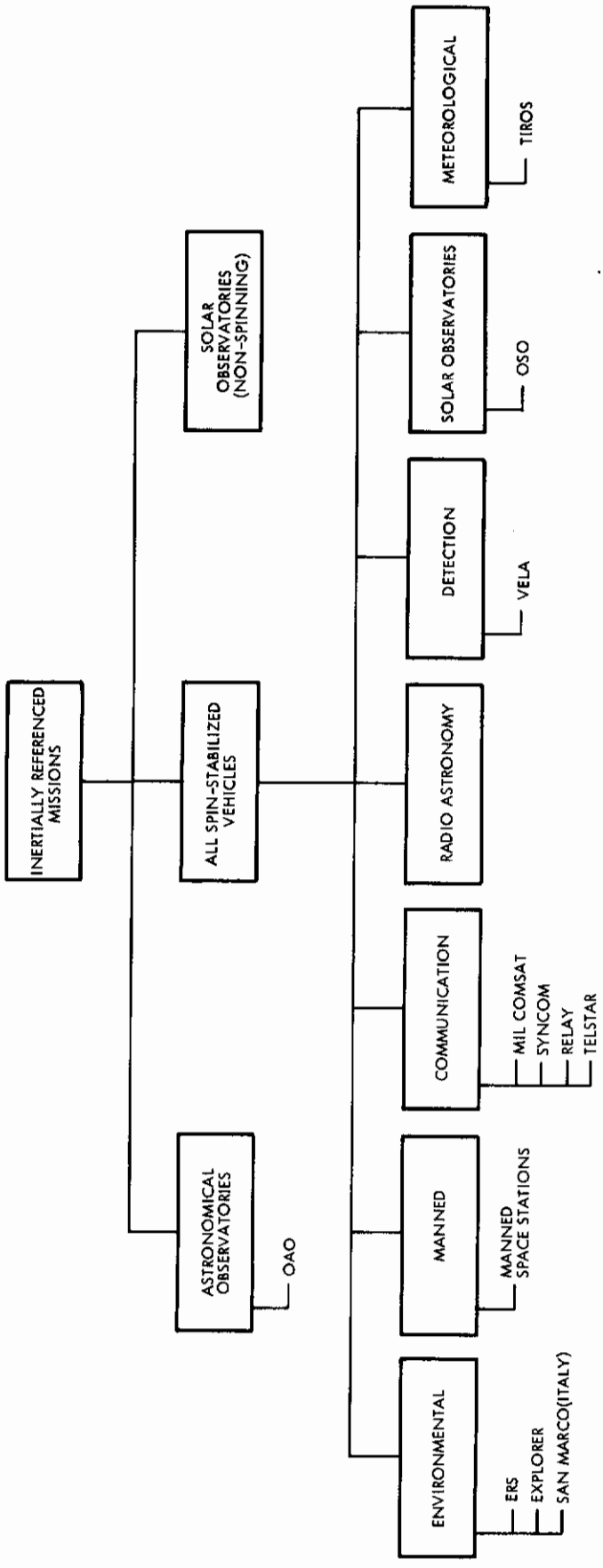

Figure 2.1 Inertially Referenced Missions

Figure 2.2 presents a similar consideration for moving reference system missions. Here the moving references have been subdivided into "earth oriented," "magnetic field oriented" and "other". Again, particular missions within these categories have been shown. A system which employs a moving reference for its nominal operational use may utilize an inertial reference for the basic acquisition maneuver. For example, the Orbiting Geophysical Observatory (OGO), performs a sun acquisition whereas normal mode pointing is directed toward the Earth. Additionally, systems which may be classified as Earth oriented may employ added degrees of freedom between portions of the satellite to control part of the satellite to an inertial reference. For example, both OGO and Nimbus utilize movable solar arrays to maintain the Sun vector normal to the plane of the solar array. In these cases both inertial and moving references are employed.

2.2 Acquisition Systems

Within the connotation developed here it is possible to further summarize the characteristics of the various acquisition systems to be employed. Of interest are both the conceptual design and implementation of the acquisition system. Figure 2.3 depicts the basic considerations in the development of an acquisition system with respect to an inertial reference. Of importance are:

(1) The method of momentum removal, i.e., magnetic or mass expulsion.

(2) The form of control for magnetic torquing, i.e., on board or command, and with or without reaction wheels.

(3) The form of mass expulsion, i.e., torque magnitude available and form of torque.

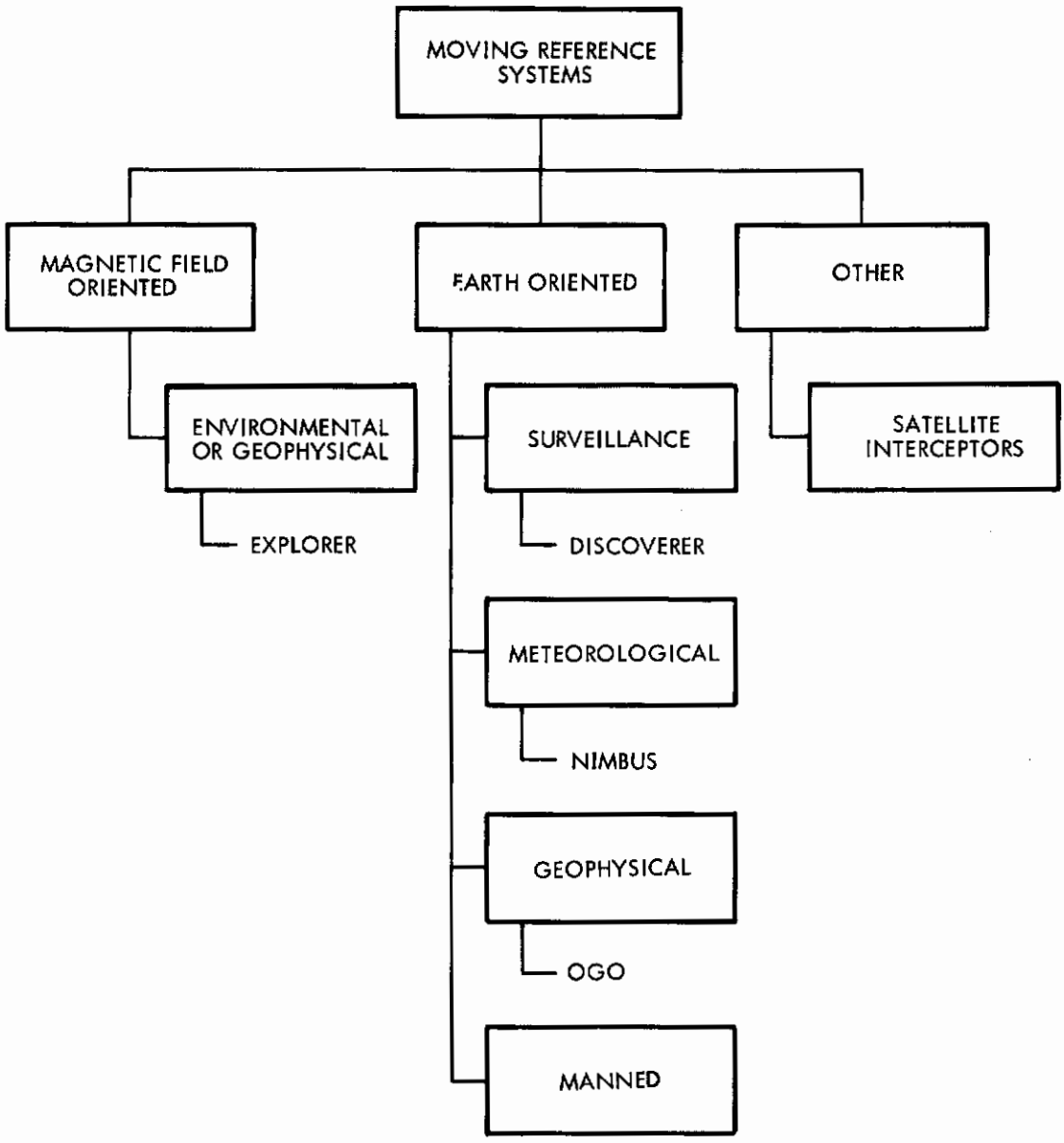

Figure 2.2 Moving Reference Missions

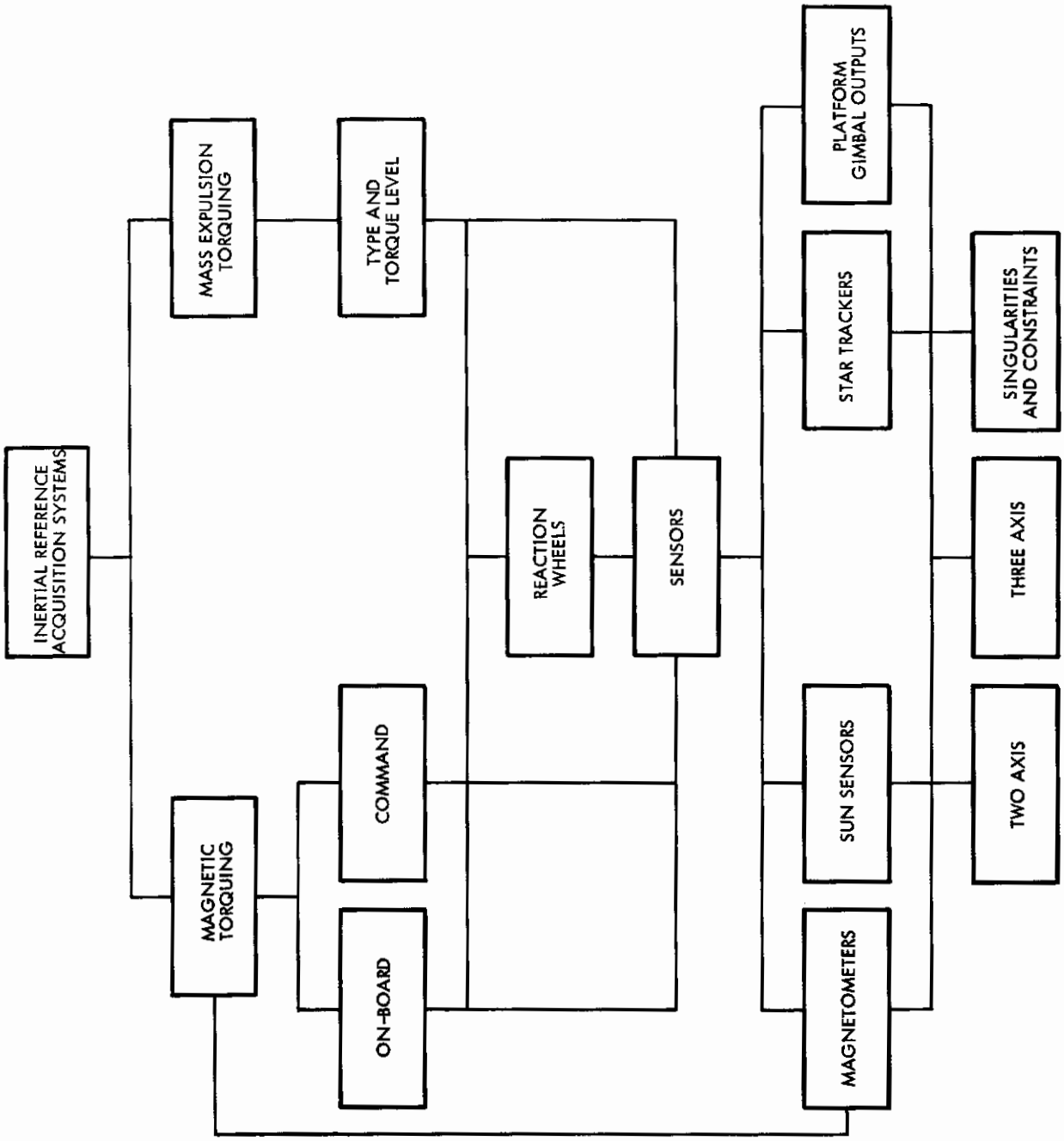

Figure 2.3 Inertial Reference Acquisition Systems

(4) The attitude and rate sensing employed.

(5) The limitations imposed by the sensing technique.

Figure 2.4 presents the same information relative to moving reference systems. For the case of an Earth oriented system an additional control torque is available, viz., gravity gradient.

Some general considerations for each of the acquisition systems implied by Figures 2.3 and 2.4 as well as their relation to the present study are given in the following paragraphs.

2.2.1 Acquisition of Inertial Reference Using Mass Expulsion

A relatively simple type of acquisition situation arises in a mission in which the desired reference directions can be assumed inertially fixed. Both one axis and three axis situations arise. The acquisition of a particular satellite axis toward the Sun represents an important one axis case. A three axis inertial reference can be established by sensing the positions of the Sun and a near-polar star.

It may be important to perform acquisition of a desired attitude relative to the Sun rapidly. The vehicle attitude relative to the Sun is important both with respect to solar energy conversion and with respect to temperature control. Fortunately, Sun sensors with a full spherical field of view can be reliably constructed with a relatively low weight penalty.

If the mass expulsion torquing system is to be used for normal control, the accelerations available may be relatively small in order to reduce the impulse which is expended in limit cycling. Alternatively, if pulsed gas jets [4] are employed to obtain low limit cycle rates during normal control, a large torque may be available for acquisition.

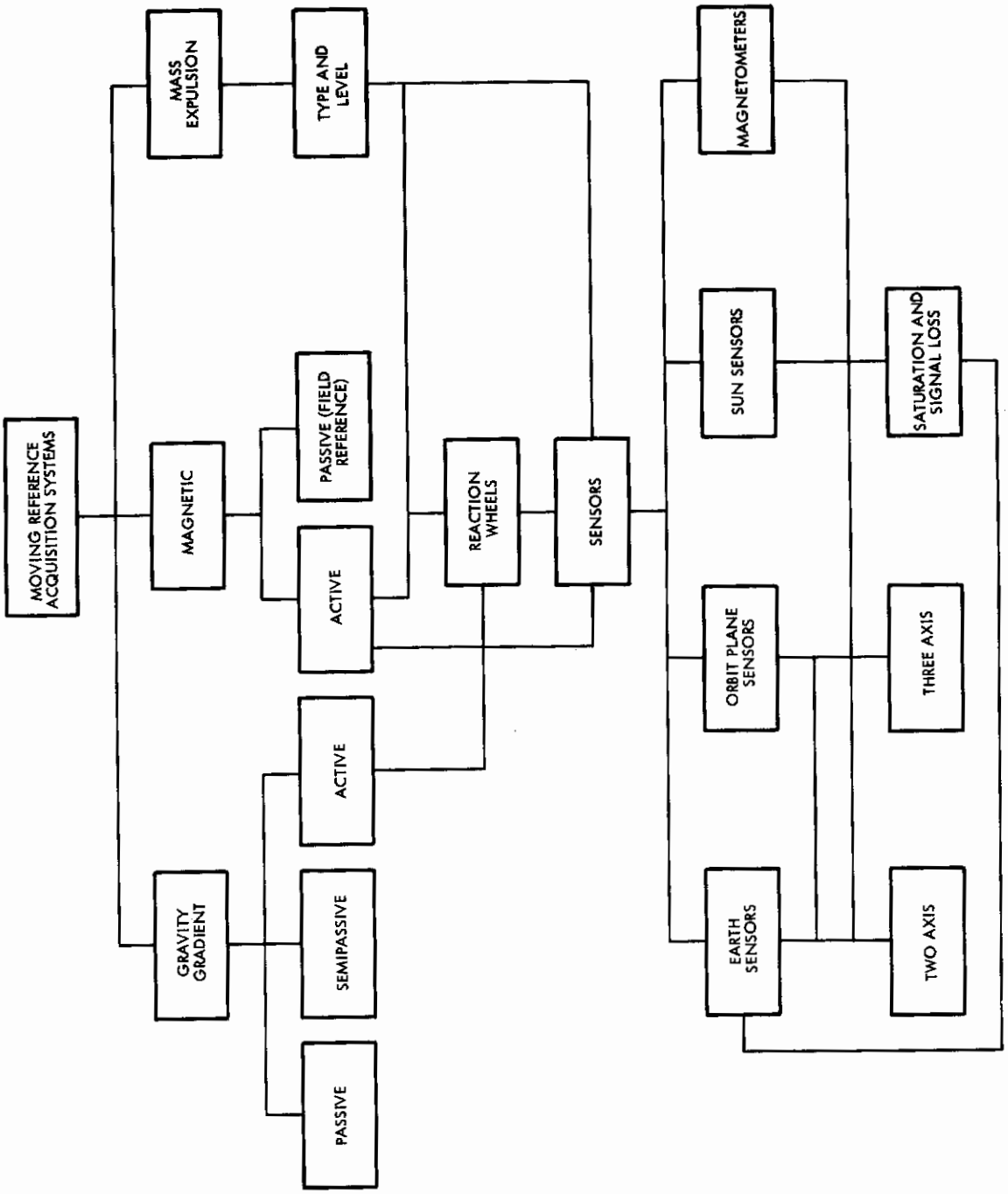

Figure 2.4 Moving Reference Acquisition Systems

In either case, the total pneumatic impulse requirement for acquisition will be of prime importance since the propellant supply must be carried as a direct weight penalty. On the other hand, if the mass expulsion system is to be used only for acquisition, then the total time required to orient the vehicle may assume design importance.

To minimize fuel consumption during acquisition it will be shown (Sections V and VI) that flexibility in the design of the mass expulsion system is desirable. However, as described in these sections, pulsed operation (approximation to proportional torquing system) of the mass expulsion system may not provide significant improvements in acquisition performance. Thus although the pulsed control may be of considerable practical importance for the normal mode of operation no performance advantage may exist during acquisition. On the other hand, if the use of pulsed control allows larger torque levels to be utilized then, as will be shown, significant performance advantages may accrue. The disadvantage of the pulsed torquing system may be the reduced reliability attending multiple on-off operations during acquisition.

The mass expulsion system may be augmented by a momentum storage system (reaction wheels) to be used during the normal mode of the vehicle operation. If reaction wheels are present, they may either aid or degrade the acquisition performance. There are two major characteristics of reaction wheels which will be significant in acquisition: torque saturation and momentum saturation. The wheels can only exert a fixed maximum value of torque regardless of their input. Likewise, they can only store a fixed maximum amount of momentum. Furthermore, the reaction wheel control design is usually such that momentum saturation occurs for small attitude error angles. The reaction wheel torque saturation characteristic may greatly affect their performance in acquisition. The time required for a reaction wheel to accelerate from zero to full speed (i.e., full momentum storage) is inversely proportional to the torque exerted by the wheel.

Thus even if the wheels can store enough angular momentum to have a significant effect on acquisition, they will not do so in a reasonable length of time if their torque level is too low. The reaction wheel rise time must be small enough to allow the wheels to respond to the control signals they receive in the dynamic acquisition process. An additional feature of the use of reaction wheels in the three dimensional acquisition problem is the additional cross coupling between control axes that can be introduced. If the reaction wheel momentum storage is large, reaction wheel cross coupling terms can be larger than the direct rigid body difference of inertia torques.

Two basic sensing techniques have immediate application to the acquisition of an inertial reference. First, Sun sensor-star tracker combinations for Sun acquisition or pure star tracking for other inertial orientations and second, the gimbal angle outputs of an inertially oriented platform. In the later case the inertial reference orientation can be arbitrarily established before launch with resulting increased flexibility.

Sun sensing, or other star sensing, establishes only a single line reference in space and therefore is inadequate for three axis acquisition. Sun and star sensing in combination allow complete control providing the two reference lines are not colinear. An all-attitude gimballed platform can easily provide complete three axis sensing in a straightforward manner. However, even in this case it may be preferable to first acquire a line in space - the one axis acquisition problem - and then to perform a controlled rotation (reorientation) to establish the final attitude. Gimbal angle pickoffs provide some interesting variations in control as compared to other sensing techniques. For example, it appears, in many cases, as easy to provide the resolved gimbal angles, sine and cosine of the angle, as the angle themselves. An evaluation of this consideration

is given in Section V. Further, if an all-attitude platform is to be utilized the gimbal rotation sequence, as well as the servo control approach of the redundant gimbal, may influence the performance and mechanization of the acquisition system utilizing this information as a basic attitude error sensing mechanism.

Obviously there exist numerous tradeoffs in the design of an inertially referenced system. The type and characteristics of the mass expulsion system, the use or non-use of reaction wheels, the sensing technique and their limitations and influence on design are all of importance.

Since the mass expulsion acquisition of an inertial reference covers a broad range of application and includes all major implementation constraints as well as a variety of sensing techniques, major emphasis was placed on this approach in this study.

2.2.2 Spinning Vehicle Acquisition Using Mass Expulsion

Another acquisition situation of considerable practical importance is concerned with a spinning vehicle. Such a vehicle can be used for a variety of orbital missions in which an inertial (or nearly inertial) orientation of the spin axis is desirable. A simple and reliable active control system can be incorporated for acquisition that will use very little power and be of light weight.

A rigid body will perform stable rotation about a principle axis of inertia for which the moment of inertia has the largest or the smallest value. If a passive damping device is used to eliminate precession, the equatorial moments of inertia must be less than the moment of inertia about the spin axis. In this case the minimum energy condition is pure rotation about the maximum moment of inertia axis.

Spin stabilized satellite acquisition systems have been developed both for sun acquisition and for acquisition of the spin vector perpendicular to the vehicle-sun line. The latter would permit inertial stabilization of a vehicle in near equatorial orbits while still permitting an efficient utilization of the surface of the vehicle for solar energy conversion. For orbital operations stabilization of the spin vector normal to the orbit plane provides a useful system for numerous applications.

In principle, the acquisition of the spin axis to any of these inertial - or nearly inertial - references represents acquisition of the simplest type. For this reason spin stabilized systems were given no further consideration in the present study.

2.2.3 Acquisition of Inertial Reference Using Magnetic Torquing

A significantly more complex acquisition problem exists in utilizing magnetic torquing for control. In this approach, control torques are generated by energizing vehicle-fixed coils to establish magnetic moments which interact with the Earth magnetic field. The torque applied to the spacecraft is given by the equation

$$\bar{T} = \bar{M} \times \bar{B}$$

where $\bar{T}$ is the torque

$\bar{M}$ is the generated magnetic moment

$\bar{B}$ is the Earth field density

Clearly, torque can be generated only perpendicular to the plane formed by the $\bar{M}$ and $\bar{B}$ vectors. Therefore, no torque component about the axis defined by the vector $\bar{B}$ is possible. However, because of orbital motion of the satellite, except for stationary synchronous orbits, the components of the vector $\bar{B}$ along the satellite body axes

are time varying. Hence torques can be generated about all body axes of the vehicle at a particular time during each orbit. By definition, large attitude excursions occur during the acquisition maneuver so that variation of the vector $\bar{B}$ components in body coordinates is more dependent on the satellite attitude excursions than the orbital motion itself. Generally the magnetic torquing approach to acquisition will be useful only for low altitude Earth orbits. Since the magnetic field strength decreases as the cube of the geocentric orbital radius, excessively large satellite generated magnetic moments would be required at higher orbital altitudes. This, of course, implies increases in weight and power of the magnetic torquing system.

A further disadvantage of this approach is the need for additional sensing in the form of a magnetometer field measurement system. In order to establish a reasonable closed loop control for on-board operation, the instantaneous values of the Earth field components in spacecraft coordinates must be known so that an appropriate vector $\bar{M}$ can be established in the satellite. If, on the other hand, ground computation and command can be utilized this additional complexity might be circumvented. For example, the satellite attitude can be obtained from the inertial reference sensing system and telemetered to the ground. Here the components of magnetic field in satellite coordinates can be computed using a priori knowledge of the field model and satellite ephemeris data. Additionally, the required spacecraft magnetic moments are ground computed and a command system utilized to establish the proper control. In this case the entire control law mechanism is ground based with only the current carrying coils being on board the spacecraft.

Acquisition systems utilizing magnetic torquing have not been employed, at least in this complete form. The development of a suitable stable control concept is not a trivial task. Some work, as yet unpublished, is underway along these lines [3].

The basic magnetic torquing system may be augmented with a reaction wheel system. Again the implementation of the control concept is not simple. It appears reasonable that the reaction wheel system may efficiently supplement the capabilities during periods of unsatisfactory alignment of the vector $\bar{B}$ relative to the spacecraft axes for purposes of magnetic torquing. However, since the control torque capability available from magnetic torquing is usually small, the additional coupling effects introduced by the wheel momentum storage may significantly affect the control complexity.

2.2.4 Moving Reference Acquisition Using Mass Expulsion

For an orbital mission with a vehicle using mass expulsion control, the basic features of the acquisition process are essentially the same as those discussed in Section 2.2.1. However, the time varying reference directions may impose additional control complexities. Total impulse requirement and total acquisition time must again be major considerations for the design of the acquisition system.

The fact that the acquisition reference is time-varying makes the acquisition problem more difficult to handle analytically (or to simulate) than the corresponding problem for a mission with an inertially fixed reference frame. Whether this time-varying characteristic is important depends upon available control torques and the speed of response of the acquisition system itself as well as upon orbital characteristics. It is possible to neglect the time-varying aspects of the acquisition reference whenever a step-wise acquisition sequence is used and when each acquisition step can be completed before significant motion of the reference frame occurs.

When one of the reference directions in an orbital mission is the local vertical, a moving-reference acquisition problem occurs. However, the reference motion can be conveniently used to facilitate an acquisition sequence for a Sun-Earth referenced vehicle by first

acquiring the Sun and subsequently using the orbital motion to aid in a search for the Earth (using directional sensors). Precisely such an approach is implemented for the OGO acquisition system.

A basic acquisition difference between a moving reference and an inertial reference attends the attitude sensing techniques. In acquiring the Earth, the moving reference is the rotating geocentric set. The simplest sensing device from the point of view of control law design becomes an Earth sensor for establishing the orientation of the desired satellite Earth pointing axis. Practical Earth sensing devices to date do not possess a complete spherical field of view. Although such is possible, e.g., by using additional sensors, it may not be either practical or desirable. In Sections V and VI it is demonstrated that optimal acquisition with respect to particular performance criteria demands saturation of the attitude sensors. Additionally, the loss of signal (blanking) of the sensors may also be desirable for some forms of control. Thus, even if full field of view is available, optimal control may require that certain portions of these attitude measurements not be utilized.

If complete three-axis attitude reference of an Earth oriented vehicle is required, an additional sensor is required. For example, if while directing one axis of the satellite toward the Earth it is also required to maintain a second axis in the orbit plane, a means for detecting rotations about the Earth pointing axis is required. For normal mode control a gyro compassing system is adequate. For acquisition the gyro compass measurement would be seriously affected by the satellite body rates. Proposed ion detectors can establish the orientation of the satellite velocity vector over reasonably large angular excursions. For acquisition as well as normal mode control this may prove to be a superior approach.

For thermal control, or for orientation of a movable (or fixed) solar array, it may be necessary to provide control about the Earth pointing axis to give a preferred Sun orientation. For example, it may be desirable to orient about the Earth pointing axis so as to place an orthogonal satellite axis in the plane containing the geocentric local vertical and the satellite-Sun line. This can be accomplished by means of an appropriately placed Sun sensor. This technique is utilized on OGO to keep the solar array plane perpendicular to the satellite-Sun line for maximum energy conversion efficiency.

Other situations utilizing mass expulsion for acquisition of a moving reference can be visualized. The acquisition of one satellite to another with subsequent tracking and perhaps homing and/or rendezvous is of current interest. Although the orbital dynamics grossly affect any guidance maneuvers, the attitude acquisition problem is unchanged. In this case the rate of motion of the reference system may be of considerable significance. Additionally, the sensing techniques will be different in form.

2.2.5 Moving Reference Acquisition Using Magnetic Torquing

The significance of the motion of the acquisition reference system is more pronounced when employing magnetic torquing than when utilizing most types of mass expulsion. This arises because of the usually low level of control torque available via magnetics. Hence it can be expected that significant motion of the reference will occur before the acquisition can be completed. Although this may not make the accomplishment of acquisition any more difficult, it will complicate the formulation of the problem.

In other respects the acquisition of a moving reference with magnetic torques is not significantly different than acquiring an inertial reference. As described previously the sensing implementa-

tion will differ between the two problems, but the basic control requirements are essentially the same.

If the moving reference is the rotating geocentric local vertical system and if magnetic torquing is to be utilized both for acquisition and normal mode control, it is likely that a reaction wheel system will be available. In this case the reaction wheel system can be of considerable value during the normal mode control and may greatly simplify the control logic otherwise required. The probable existence of the reaction wheel system makes the consideration of its practical value during acquisition a more immediate problem. However, the concern for acquisition with a combined magnetic torquing - reaction wheel control approach is basically the same as with the inertial reference case. A significant difference may attend the intercoupling of the stored wheel momenta with the rotation rates implied by the motion of the reference frame itself.

A particularly simple form of magnetic torquing acquisition to a moving reference has been employed on several past satellite missions. In this case the moving reference becomes the Earth magnetic field vector itself. In application, permeable rods (termed hysteresis rods) are mounted in the spacecraft body. As the satellite tumbles relative to the magnetic field these rods remove energy by magnetic hysteresis losses in the permeable material. In this way the energy stored in the satellite at acquisition initiation can be dissipated. Note that no attitude control is provided for the system in this form. However, if in addition to the rods a permanent magnet is included, the magnet will tend to align with the Earth's field so that a pseudo-attitude control of this axis is provided. No attitude control about the magnet axis is provided, but neither can substantial rate exist because of the damping action of the permeable rods.

This passive acquisition system with attending attitude control has been utilized as the only control on some Explorer satellites. Several satellites in the NRL launch series have used this scheme for initial energy removal before deploying a gravity gradient stabilization system. In the latter case the permanent magnet may be replaced with an electromagnet so that upon deployment of the gravity gradient system the magnet-induced disturbance torques can be eliminated.

2.2.6 Earth Acquisition Using Gravity Gradient Torquing

Reaction Wheel Damping: An acquisition situation which has become increasingly important attends orbital missions employing gravity gradient torques plus momentum storage devices for control. Gravity gradient control systems afford a significant improvement in control system reliability. In order to stabilize a satellite by use of gravity gradient torque, an auxiliary damping system is required. Such damping can be provided by reaction wheels driven from sensors within the satellite.

There are several aspects of the acquisition problem for this type of system (gravity gradient plus reaction wheels) which are appreciably different from the systems discussed previously. The largest control torques available will generally be those supplied by the reaction wheels. If the reaction wheels have sufficient momentum storage capacity to absorb all of the initial angular momentum in the system a very efficient acquisition can be obtained. The stored angular momentum may then be removed over a long period of time using the gravity gradient torque. The length of time required for momentum removal will depend upon the initial momentum in the system, the allowable attitude offset error, and the vehicle moments of inertia.

If the reaction wheels reach momentum saturation before the initial rates are reduced to zero*, the acquisition problem becomes more formidable. Even if the wheels are driven to saturate, the vehicle will continue to tumble in a situation where the external gravity gradient torque can be utilized to provide acquisition. The reaction wheel torques must be sufficiently large and appropriate control of the reaction wheel system is required. In this case, the reaction wheels must be able to accelerate from full momentum storage in one direction to full momentum storage in the other direction rapidly enough to allow the gravity gradient torque to achieve some net momentum removal each revolution. This process will eventually reduce the momentum in the vehicle until the wheels can store it. Whether or not this type of process will achieve acquisition in a reasonable time will depend upon the size of the reaction wheel motor and the magnitude of the gravity gradient torques. The latter in turn depend on the vehicle mass properties and upon the orbital altitude. Note that this acquisition process will in general require a considerable length of time and the motion in orbit must be considered.

Gyro Dampers: The use of gyros appears to be an attractive method of achieving both damping and acquisition capability for gravity gradient stabilized satellites [5]. Its chief advantage rests in the fact that no external sensors are required to provide attitude or body rate information. The damping gyros are their own sensors.

Each gyro is torqued externally by a spring or small torque generator in such a way that any satellite motion other than the orbital rate causes the gyro to precess. The use of a viscous restraint on the gyro output axis then provides the necessary energy

---

* For geocentric local vertical acquisition the final body rates are not all zero. Rather the rate about an axis normal to the orbital plane must be equal to orbital rate.

sink for satellite motion damping. The minimum energy state (kinetic and potential) of the system corresponds to an attitude in which the axis of the minimum satellite moment of inertia remains aligned with the local vertical and the axis of maximum moment of inertia is normal to the orbit plane.

Even though the gyro damper is not a true active control system, proper design assures acquisition from reasonable initial vehicular attitudes and attitude rates. Clearly the gyro and satellite kinetic and positional (or potential) energies plus the energy dissipated viscously remain constant with time. The minimum mechanical energy state (corresponding to the desired attitude) is possible only if the gyros continue to precess to increase the viscous energy. Should the attitudes and body rates be such that every gyro remains against its limit stop, acquisition cannot occur. Even if this is not the case, there exist non-unique attitude conditions corresponding to the minimum energy state. Attainment of the proper one, however, does not appear to be a formidable task. It is possible to design a gyro system which is known to continuously dissipate energy for reasonable initial satellite momenta.

Previous studies have indicated that use of two gyros provides very adequate normal mode performance. In addition, simulation studies have demonstrated a practical acquisition capability. The use of gyros, however, suffers from several practical considerations. A high degree of precision is required in their construction. Small changes in the momenta of the gyro wheels, or in their torque generator outputs result in adverse effects on the satellite attitude. The effect generally becomes more severe the higher the orbital altitude. The gyro precision required, however, is well within existing "state-of-the-art."

Passive Damping: For acquisition of, and long-term stabilization with respect to, an Earth reference system, interest in passively damped gravity gradient systems has been increasing [6-9]. Since no sensing is required, no power is consumed, and the devices are very simple, this control scheme appears ideal for many Earth pointing missions.

Depending on system design, acquisition may be feasible utilizing only the passive damping mechanism. In this case only the time to acquire is of major concern. The time to acquire the Earth pointing orientation is strongly dependent upon the initial momentum of the satellite. Variation of parameters in the stabilization system design will generally only have a small effect on the acquisition time. This latter observation is valid only if simultaneous to establishing satisfactory acquisition characteristics the normal mode stabilization capability is evaluated.

For passive damping techniques, or for constraining mission requirements, auxiliary acquisition systems may be either required or desired. The rapid increase of time to acquire with initial satellite momentum, the possible unstable - no damping - operation of certain systems with sufficient initial momentum, the constraints of suitable normal mode stabilization accuracy, as well as other considerations, may all demand auxiliary acquisition capability. In this respect, the passive magnetic acquisition approach has been successfully employed [9].

SECTION III

DYNAMICS AND KINEMATICS

In order to conduct a satisfactory general investigation of analytical and computational design procedures for application to satellite acquisition systems, it is first necessary to establish suitable mathematical representations of acquisition system dynamics and kinematics. The dynamic and kinematic representation of the system must be characterized in such a form as to be suitable for use with advanced mathematical control system techniques. Further, it is important that these characterizations lend themselves easily to the various machine-aided studies considered in Sections VI and VII as well as being attractive for the use of hand analysis. The purpose of this section is to investigate various methods for dynamic characterization of rigid body attitude in order to establish a set of suitable dynamic and kinematic equations which will facilitate the application of generalized design techniques.

There are a number of particular considerations that are involved in settling upon a particular characterization: 1) The ability, with a reasonable amount of effort, to apply various hand analysis techniques to the resultant systems of equations and obtain a simplicity of physical interpretation of the analytic results, 2) The ease of implementing and interpreting machine-aided studies while minimizing hardware requirements, programming needs, costs, and solution times, and 3) The physical realizability which constrains the manner in which various control sources and attendent control laws must be represented. As will be shown, the above criteria do not appear to be so easily satisfied for any particular choice of representation. The relative merits of a number of systems, however, will be delineated in order to establish a basis for choice of representation according to the general form and demands of the system.

3.1 State Variable Formulation

The applicability of modern control theory presupposes a particular form of the system mathematical model. In particular, this formulation has become known as the general state variable approach. In order to establish a firm basis for further technical discussion, it is important at this point to consider formulation of the acquisition problem using state variable notation. Into this mold, then, will be fitted the dynamic and kinematic equations of motion. By definition, the state variables are considered to be a set of the least number of quantities necessary to describe the state of the dynamical system (i.e., to characterize each degree of freedom). For continuous time dynamical systems, the motion of the system is defined by the vector differential equation

$$\dot{\bar{x}} = \bar{f}\,[\bar{x}(t),\ \bar{u}(t),\ t],\ -\infty < t < \infty \qquad (3.1)$$

which is equivalent to the set of n scalar differential equations

$$\dot{x}_i = f_i\,(x_1, \ldots, x_n, u_1, \ldots, u_r, t)\ ,\ i = 1, \ldots n \qquad (3.2)$$

The vector $\bar{x}(t)$ is defined as the state of the system and the components $x_i(t)$ are known as the state variables. The vector $\bar{u}(t)$ is the control function of the system; its components, $u_j(t)$, are the control variables. Note that the relations,

$$\bar{u} = \bar{u}(\bar{x}) \qquad (3.3)$$

by which the control variables are related to the state variables, are commonly called the "control laws" of the system, and that the form of the equation implies that feedback control is to be employed. Other classes of equations arise to describe some particular systems.

For discrete-time dynamical systems, the state of the system is characterized by the vector difference equation

$$\bar{x}(t_{k+1}) = \bar{f}\,[\bar{x}(t_k),\ \bar{u}(t_k),\ t_k] \qquad (3.4)$$

Here the system is not a function of a continuous variable and the state is determined with respect to an index, k. Definitions of the quantities in Equation (3.4) follow analogously from those defined in Equation (3.1). If a digital device is employed, this sort of equation arises naturally; e.g., sampled data theory may be developed using this form. Similarly, integral equations, difference-differential equations, and stochastic differential equations may be fitted into a general state-variable formulation. Characterization of the acquisition problem in the form of first order equations allows general mathematical techniques developed for the general state variable approach to be employed for analysis and synthesis. Conversely, however, if these powerful techniques are to be employed, representation of the controlled system dynamics in this form must, in general, be valid. This implies that a set of well behaved variables must be found which determine completely the state of the satellite system during acquisition. Three of these will be directly related to the angular rates (i.e., body rates) of the spacecraft. The others will constitute a suitable kinematic representation for determining the attitude of the satellite.

3.1.1 Dynamics

The dynamical characteristics of the system to be controlled in satellite acquisition are those of rigid-body rotational motion*. This dynamical system is acted upon by external perturbing torques

---

*Acquisition of non-rigid satellites is, of course, a practical problem. Inclusion of structural flexibility or fluid motions internal to the satellite will increase the order of the dynamic representation. Since no extension of concept is involved, the simpler rigid-body case is used for discussion purposes.

resulting from interactions with various natural field and fluid phenomena and possible mass expulsion from the vehicle. In treating the acquisition problem, the angular orientation (attitude) of the vehicle with respect to a prescribed reference frame must be controlled.

For purposes of attitude control, a space vehicle can be considered as a lumped-parameter mechanical network whose elements are rotating rigid bodies. The interconnections between the various rotating parts may be 1) rigid, as when torque is transmitted by supporting bearings in a direction normal to the axis of rotation, or 2) elastic, as when torque motors or servo motors are deliberately used to control the rotation of one of the parts. The design of an attitude control acquisition system for a space vehicle requires the creation of a suitable scheme for transferring angular momentum among elements within the vehicle to the external universe. In general, the motions of the bodies are merely constrained by bounds on their allowable angular velocities or displacements.

Denote by $(\omega_1, \omega_2, \omega_3)$ the angular velocity of the satellite about its principal axes of inertia $(\bar{x}_1, \bar{x}_2, \bar{x}_3)$, respectively. These quantities are commonly referred to as the "body rates" of the satellite. Define the corresponding principal moments of inertia as I_1, I_2, I_3, respectively.

The total angular momentum of the body, $\bar{H}$, may be resolved into components, H_i, along these same body-fixed axes and defined as

$$H_i = \mathcal{H}_i + h_i \; ; \quad i = 1, 2, 3 \tag{3.5}$$

where $H_i = I_i \omega_i$ = total angular momentum of the spacecraft about its i^{th} principal axis less angular momentum attributable to internal rotating parts (e.g., reaction wheels)

h_i = total angular momentum stored in internal rotating parts resolved onto the i^{th} body-fixed axis.

Similarly, one may define components of the total external torque, $\bar{M}$, along body axes as (M_1, M_2, M_3), respectively. The fundamental equations of rigid body motion in inertial coordinates may be simply written in vector notation as

$$\frac{d}{dt} \bar{H}^I = \bar{M}^I \tag{3.6}$$

Equivalently, with respect to body fixed coordinates, the equations of motion are defined as the Euler equations

$$\frac{d}{dt} \bar{H} + \dot{\bar{\omega}} \times \bar{H} = \bar{M} \tag{3.7}$$

where $\bar{\omega} \times \bar{H}$ denotes the vector cross product. These equations relate the body rates and angular momentum to the external torques acting on the vehicle resolved into components in the body-fixed system. Equation (3.7) is equivalent to:

$$\frac{d}{dt} \bar{H} + [P(\omega)] \bar{H} = \bar{M} \tag{3.8}$$

where

$$\left[P(\omega)\right] \triangleq \begin{bmatrix} 0 & -\omega_3 & \omega_2 \\ \omega_3 & 0 & -\omega_1 \\ -\omega_2 & \omega_1 & 0 \end{bmatrix} \tag{3.9}$$

Note that Det $P(\omega) = 0$. Thus, $P(\omega)$ is a <u>singular</u> matrix and as such possesses no inverse. Also, note that

$$\left[P(\omega)\right]^T = -\left[P(\omega)\right] \tag{3.10}$$

Expanding Equation (3.7) into the three equivalent scalar equations gives

$$\begin{aligned}
\dot{\omega}_1 + \frac{I_3-I_2}{I_1}\omega_2\omega_3 + \frac{1}{I_1}(\omega_2 h_3 - \omega_3 h_2) &= \frac{M_1}{I_1} + \frac{\dot{h}_1}{I_1} \\
\dot{\omega}_2 + \frac{I_1-I_3}{I_2}\omega_1\omega_3 + \frac{1}{I_2}(\omega_3 h_1 - \omega_1 h_3) &= \frac{M_2}{I_2} + \frac{\dot{h}_2}{I_2} \\
\dot{\omega}_3 + \frac{I_2-I_1}{I_3}\omega_1\omega_2 + \frac{1}{I_3}(\omega_1 h_2 - \omega_2 h_1) &= \frac{M_3}{I_3} + \frac{\dot{h}_3}{I_3}
\end{aligned} \tag{3.11}$$

In the equations, $\dot{h}_i$ is the direct reaction wheel torque on the i^{th} body-fixed axis. M_i is the external torque acting about the i^{th} axis and, in general, consists of a component which is introduced for control purposes plus a component due to disturbances, (i.e., $M_i = u_i + d_i$).

These equations are highly nonlinear with cross-coupling terms occurring both from interaction of the body rates and interaction of (reaction wheel) momentum stored in one body axis with non-zero angular rates about the others.

Inertial cross-coupling terms become most pronounced when relatively large differences exist between the vehicle moments of inertia about the three control axes and when the body rates about these axes are appreciable. Hence, the cross-coupling terms need to be carefully evaluated in determining convergence and stability from large initial attitude errors and error rates, and when attitude accuracy requirements are stringent.

3.1.2 Kinematics

The dynamics of a rigid body is essentially a separate field from the dynamics of a particle or systems of particles without constraints. Thus, the kinematics of a rigid body possess certain peculiarities which arise basically from the geometric properties of spatial rotations.

The Euler equations described in the preceding section constitute but part of the description of the rotating satellite since the body rates, ω_i, must be related to the attitude or body orientation to obtain the complete description of the motion. It is the essence of this and the following sections, then, to present a discussion of rigid body kinematics and establish a formulation of the acquisition problem especially suitable for the application of advanced control theory and simulation techniques.

In defining and controlling the attitude of a spacecraft it is necessary to use certain reference coordinate systems. The number of reference coordinate systems as well as suitable definition for each

depends upon the particular mission for which a satellite is to be designed. It is difficult to generalize, but some definitive remarks about satellite coordinate systems may be made.

Basically, in treating the rotational motion of a rigid body, two sets of three orthogonal reference vectors are required, the origin of each usually being chosen coincident with the rigid body center of mass. As is well known, by so choosing the origins the translational and rotational motions may be divorced. The rotation of the body will then be equivalent to the rotation about its center of mass as a point, fixed in space. The directions of one set are considered fixed in inertial space. Hence, with respect to this set, the basic rotational equations of motion for the rigid body (Euler Equations) may be written, i.e., the time derivatives of the angular momentum components resolved along the inertial reference vectors are equal to the respective components of externally applied torque (similarly resolved along inertial directions).

A second set of reference vectors is defined to be body-fixed. The directions of the reference vectors are usually chosen to coincide with the principal axes of inertia of the body (the latter always form an orthogonal set). Chosen in this fashion, cross-products of inertia vanish with respect to those reference vectors and considerable simplification in the equations of motion transformed from inertial to body-fixed coordinates is realized.

In the particular case of Earth satellites, of course, the rigid body (or system of such bodies) translates, as well as rotates, with respect to inertial space. Thus, in order to study long term effects, it is often desirable to define a third coordinate system as an orbital reference system. For many purposes, the origin of this third reference system may be chosen to coincide with the center of the

Earth without introducing significant errors. The directions of the unit reference vectors of this coordinate system (as in the case of the first system mentioned) are orthogonal and inertially fixed. The motion of the satellite in orbit may be conveniently described with respect to this third coordinate system.

In case the desired satellite attitude rotates with respect to inertial space, occurring, for example, when a principal axis of inertia is to "track" the Earth's local vertical, it is convenient to define another coordinate system with origin at the satellite center of mass. The directions of the unit reference vectors are defined as those required for perfect attitude control, i.e., this defines the ideal satellite attitude as a function of time. Generally, this latter system is a rotating coordinate system and its definition must be chosen carefully with due regard for the sensors to be used and for the objectives to be achieved by attitude control.

A comprehensive discussion of possible choices of coordinate systems for Earth pointing satellites is contained in [10]. Here, with regard to "small" differences between coordinate system choices, it is pointed out that a poor choice may cause the attitude control system to "constantly strive to correct a small difference it should not have to correct," with the result that "net power consumption may be prohibitive." In defining the attitude of the satellite, the relation between the body fixed axes and the "ideal attitude" axes are of primary interest. These two coordinate systems are related by a transformation involving a minimum of three independent time varying parameters. In normal mode operation of the attitude control system, of course, the coordinate systems are to be aligned within small angular deviation. (Thus, "small angle" approximations ordinarily can be applied to the description of this transformation.) This, of

course, is not true for characterizing the acquisition problem where a well behaved characterization of the large angle motion is required.

It is useful, as an introduction to the kinematic properties of a satellite as they arise in attitude control considerations, to examine the characteristics of the fundamental matrix transformation involved in relating a body-centered inertial reference coordinate system to a corresponding body-fixed system. Only the rotational motion of a rigid spacecraft is considered here and, as a result, only two coordinate systems are used. This does not restrict the generality of the equations to be derived.

Let a set of unit vectors, $(\bar{x}_1^I, \bar{x}_2^I, \bar{x}_3^I)$ which form an orthogonal, right-hand set be fixed in inertial space with the origin coincident with the satellite center of mass. Choose a second orthogonal set of unit vectors, $(\bar{x}_1, \bar{x}_2, \bar{x}_3)$, as a right-handed set also with origin coincident with the spacecraft center of mass. Let the members of the latter set be body fixed and coincide, respectively with the principal moments of inertia of the satellite.

At any time, each of the body-fixed unit vectors may be resolved into components along the inertial directions. This fundamental concepts allows one to express mathematically each body-fixed reference vector as a linear combination of the inertially-fixed unit vectors as follows:

$$\bar{x}_i = \sum_{j=1}^{3} a_{ij} \bar{x}_j^I, \quad i = 1, 2, 3 \tag{3.12}$$

where it is clear that the coefficients a_{ij} are time-varying if the spacecraft rotates with respect to inertial space. These equations written in vector-matrix notation give

$$\bar{x} = [A] \bar{x}^I \tag{3.13}$$

where

$$[A] = \begin{bmatrix} a_{11} & a_{12} & a_{13} \\ a_{21} & a_{22} & a_{23} \\ a_{31} & a_{32} & a_{33} \end{bmatrix} \tag{3.14}$$

As the matrix A, defined in Equation (3.14), plays such a central role in kinematic characterization, it is important to briefly establish some of its properties. The elements, a_{ij}, of the transformation matrix A, are direction cosines. In other words,

$$a_{ij} = \cos \theta_{ij} \tag{3.15}$$

where θ_{ij} is defined as the plane angle between the vectors $\bar{x}_i$ and $\bar{x}^I_j$. Further, since the vectors are orthogonal,

$$\bar{x}_i \cdot \bar{x}_j = \delta_{ij} \tag{3.16}$$

where δ_{ij} is the Kronecker delta.

$$\delta_{ij} = \begin{cases} 1 & i = j \\ 0 & i \neq j \end{cases} \tag{3.17}$$

Equations (3.13), (3.14) and (3.16) yield

$$\sum_{j=1}^{3} a_{ij}\, a_{kj} = \delta_{ik} \quad (i, k = 1, 2, 3) \tag{3.18}$$

Further, since A is a unitary orthogonal matrix the value of the determinant of A is unity

$$\det A = |A| = 1 \tag{3.19}$$

Relations between A, its inverse, A^{-1}, and its transpose, A^{T}, are given as

$$\left.\begin{aligned} AA^{-1} &= A^{-1}A = I \\ A^{T} &= A^{-1} \\ A^{T}A &= AA^{T} = I \end{aligned}\right\} \tag{3.20}$$

where I is the identity matrix. As a consequence of Equations (3.20)

$$a_{ij} = \text{co-factor}\,(a_{ij}) \equiv A_{ij} \tag{3.21}$$

and

$$\sum_{i=1}^{3} a_{ij}\, a_{ik} = \delta_{jk} \quad (k, j = 1, 2, 3) \tag{3.22}$$

In the next section, differential equations of motion involving the a_{ij}'s and their time derivatives will be considered. It is clear that a number of the expressions in the a_{ij}'s obtained above may be differentiated with respect to time in order to yield (equivalent) identities in which the $\dot{a}_{ij}$'s are involved. For some purposes, it may be more convenient to use the following expressions.

Differentiation of Equation (3.18) yields

$$\sum_{j=1}^{3} (a_{ij}\,\dot{a}_{kj} + \dot{a}_{ij}\,a_{kj}) = 0 \quad (i, k = 1, 2, 3) \tag{3.23}$$

and, similarly, differentiating Equation (3.22) gives

$$\sum_{i=1}^{3} (a_{ij}\,\dot{a}_{ik} + \dot{a}_{ij}\,a_{ik}) = 0 \quad (k, j = 1, 2, 3) \tag{3.24}$$

An interesting consequence is obtained from differentiating Equation (3.19) to yield

$$\frac{d}{dt}\left|A\right| = \left|\frac{d}{dt}\,A\right| = \left|\dot{A}\right| = 0 \tag{3.25}$$

Thus, the matrix $\dot{A}$ is singular and therefore possesses no inverse. By differentiating the third relation of Equation (3.20) the following is obtained

$$\left[A\right]\,\frac{d}{dt}\left[A^{T}\right] + \left(\frac{d}{dt}\left[A\right]\right)\cdot\left[A^{T}\right] = 0 \tag{3.26}$$

which is equivalent to Equation (3.23). Finally, differentiation of Equation (3.21) gives nine relations of the form

$$\dot{a}_{ij} = \frac{d}{dt} [\text{co-factor } a_{ij}] \quad (i, j = 1, 2, 3) \tag{3.27}$$

Except for the case when A is the identity matrix or the rotation is through an angle which is an exact multiple of π, the matrix A has three distinct eigenvalues, λ_i, which satisfy the equation

$$\det (A - \lambda_i I) = 0 \tag{3.28}$$

By direct expansion and use of Equation (3.21) the characteristic equation is found to be

$$\lambda^3 - (a_{11} + a_{22} + a_{33}) \lambda^2 + (a_{11} + a_{22} + a_{33}) \lambda - 1 = 0 \tag{3.29}$$

By inspection, it is obvious that one of the eigenvalues is always +1. Associated with each eigenvalue is an eigenvector, $\bar{e}$, defined by

$$(A - \lambda_i I) \bar{e}_i = 0 \tag{3.30}$$

Denote by $\hat{e}$ the eigenvector of A associated with the eigenvalue +1. From Equation (3.30) this eigenvector satisfies the equation

$$\hat{e} = A \hat{e} \tag{3.31}$$

Thus, the eigenvector components of $\hat{e}$ remain invariant under the transformation. Recall the Euler kinematic theorem; "any finite rotation of a rigid body may be expressed as a rotation through some angle about some fixed axis." Evidently, the eigenvector $\hat{e}$ corresponds to the direction in space about which a single rotation would yield the same relative orientation of the $\bar{x}$ and $\bar{x}^I$ axes as the transformation A, thus yielding a proof of the theorem. Denote the "equivalent angle of rotation" as Φ. This angle of rotation may be easily obtained in terms of the a_{ij}. As shown in Goldstein [11], by means of some similarity transformation it is always possible to transform the

matrix A to a system of coordinates where the $\bar{x}_3$ axis coincides with $\hat{e}$. In such coordinates the matrix A_1, which represents the rotation about $\hat{e}$ through the angle Φ, has the form

$$A_1 = \begin{bmatrix} \cos\Phi & \sin\Phi & 0 \\ -\sin\Phi & \cos\Phi & 0 \\ 0 & 0 & 1 \end{bmatrix} \tag{3.32}$$

Since A and A_1 are similar matrices, they possess the same trace. The trace is then obtained as

$$\text{tr } A = a_{11} + a_{22} + a_{33} = 1 + 2\cos\Phi \tag{3.33}$$

From Equations (3.29) and (3.33), it is established that the eigenvalues, λ_i, of A are defined as:

$$\lambda_i = +1,\ \epsilon^{j\Phi},\ \epsilon^{-j\Phi} \quad (i = 1, 2, 3) \tag{3.34}$$

When the rotation is zero or an even integral multiple of π, there are three real eigenvalues at +1. When the rotation is an odd integral multiple of π, there is one eigenvalue at +1 and two at -1.

Denote the components of the eigenvector $\hat{e}$ by e_1, e_2, and e_3. Carrying out the matrix manipulations involved in solving Equation (3.31) and using the relation given in Equation (3.33), these components of $\hat{e}$ are given as

$$e_1 = \frac{a_{23}-a_{32}}{2\sin\Phi};\quad e_2 = \frac{a_{31}-a_{13}}{2\sin\Phi};\quad e_3 = \frac{a_{12}-a_{21}}{2\sin\Phi} \tag{3.35}$$

where Φ is simply determined from Equation (3.33).

By restricting Φ to the range $0 \leq \Phi \leq \pi$, and allowing e_1, e_2, and e_3 to take on any values between +1 and -1 consistent with the condition

$$e_1^2 + e_2^2 + e_3^2 = 1 \tag{3.36}$$

one may generate any possible distinguishable rotation.

The vector $\hat{e}$ will always be considered to have unit magnitude. The set of all distinguishable spatial rotations, and hence their corresponding matrices A, form a group as shown by Smirnov [12]. Furthermore, as Smirnov points out by considering the vector $\hat{e}$ defined above, the rotation group is isomorphic to the points in a solid sphere of radius π. Thus, the basic kinematic properties of the transformation matrix, A, have been obtained.

The kinematic state equations are obtained from a set of variables and their derivatives which may be used to equivalently represent the transformation defined by the matrix A. Since only three degrees of freedom are involved, it would be expected that three kinematic state variables would be sufficient for solution of the problem. As will be described in the following section, however, the problem of finding a wholly satisfactory set of three kinematic state variables has never been completely resolved.

3.2 Kinematic Representations

It is clear that for a given relative orientation of two sets of axes, the elements a_{ij} of the transformation matrix A may be determined through using any one of a number of schemes for parametric representation. This section serves to review and extend what is known in this area through discussion of a number of attractive sets of kinematic variables for describing the attitude of a satellite during acquisition.

3.2.1 Direction cosines

The elements of the matrix, A, are themselves a suitable characterization of attitude. The coordinate transformation matrix, of course, is given by Equation (3.14) as

$$A = \begin{bmatrix} a_{11} & a_{12} & a_{13} \\ a_{21} & a_{22} & a_{23} \\ a_{31} & a_{32} & a_{33} \end{bmatrix} \tag{3.37}$$

The kinematic state equations using this representation are found in the following fashion. Using the identity

$$\frac{d}{dt}\,\bar{H}^I = \frac{d}{dt}\left\{\left[A\right]^T \bar{H}\right\} \tag{3.38}$$

the following equation is obtained.

$$\frac{d}{dt}\,\bar{H} + \left[A\right]\frac{d}{dt}\left[A^T\right]\bar{H} = \bar{M} \tag{3.39}$$

Comparison of this equation to Euler's equations given in Equation (3.8) yields the identity:

$$A\,\frac{d}{dt}\,A^T = P(\omega) \tag{3.40}$$

Equation (3.40) is then rearranged by taking the matrix transpose of each side and applying several identities to yield:

$$\frac{d}{dt}\left[A\right] + \left[P(\omega)\right]\left[A\right] = 0 \tag{3.41}$$

where $[P(\omega)]$ is defined in Equation (3.9).

Writing out the nine scalar equations obtained from equating coefficients in Equation (3.41) gives:

$$
\begin{aligned}
\dot{a}_{11} &= \omega_3 a_{21} - \omega_2 a_{31} \\
\dot{a}_{12} &= \omega_3 a_{22} - \omega_2 a_{32} \\
\dot{a}_{13} &= \omega_3 a_{23} - \omega_2 a_{33} \\
\dot{a}_{21} &= \omega_1 a_{31} - \omega_3 a_{11} \\
\dot{a}_{22} &= \omega_1 a_{32} - \omega_3 a_{12} \\
\dot{a}_{23} &= \omega_1 a_{33} - \omega_3 a_{13} \\
\dot{a}_{31} &= \omega_2 a_{11} - \omega_1 a_{21} \\
\dot{a}_{32} &= \omega_2 a_{12} - \omega_1 a_{22} \\
\dot{a}_{33} &= \omega_2 a_{13} - \omega_1 a_{23}
\end{aligned}
\qquad (3.42)
$$

where ω_i is the angular velocity of the body about the i^{th} body fixed axis.

These expressions are differential equations of the first order for all of the a_{ij}'s. Equations (3.42) plus the Euler equations of motion, Equation (3.7) or (3.8), form a set of twelve first order differential equations describing the motion of the spacecraft. As can readily be seen, twelve variables appear where intrinsically only six are required. There must be six equations which relate the redundant direction cosines. These equations may be derived from the matrix A by applying the orthogonality conditions as defined in Equation (3.18).

A decrease in dimensionality of this method to six state variables can be accomplished, but at the expense of destroying symmetry in the equations. Any attempt at further reduction (i.e., use of less than six direction cosines as state variables) results in a problem of determining the proper sign of square root functions, since the basic algebraic identities are of second order. This will be dealt with in more detail in a following section in discussing the suitability of this set of variables for analog and digital computation.

A greater usefulness for the scheme of using direction cosines as state variables in solving the acquisition problem results when it is necessary to control only the final orientation of a single axis. Under these conditions it is possible to describe the dynamical problem using only three direction cosines as kinematic state variables. The previously described one axis acquisition problem is of this type. As can readily be seen from Equations (3.42), any three equations relating a single inertial axis to the three body axes form a self-contained set of variables. For example, in a "sun acquisition problem" is is desired to align a body fixed axis along an inertial axis directed toward the sun. Defining the sun line to be the $\bar{x}_3^I$ inertial axis, the state variable formulation could be given as:

$$\begin{aligned} \dot{a}_{13} &= \omega_3 a_{23} - \omega_2 a_{33} \\ \dot{a}_{23} &= \omega_1 a_{33} - \omega_3 a_{13} \\ \dot{a}_{33} &= \omega_2 a_{13} - \omega_1 a_{23} \end{aligned} \tag{3.43}$$

A slightly different formulation of this problem for which Asymptotic Stability in the Large has been proved using the Second Method of Lyapunov is discussed in Section IV.

3.2.2 Euler Angles

One of the best known and most frequency used schemes for representing the displacement of a rigid body about a fixed point is the method of Euler angles. The rigid body orientation is specified by means of three ordered rotations about a set of orthogonal axes. There are two basic types of Euler transformations, each distinguished by the particular manner of rotation. In one case, the rotations take place successively about each of the three body axes. This will be referred to as a Type I Euler transformation. Furthermore, the axes about which the rotations take place may be permuted, so that six distinct transformations matrices result. The following transformation matrix, A, corresponds to a first rotation, θ_1, about $\bar{x}_1$; a second rotation, θ_2, about the resulting $\bar{x}_2$ axis; and the third rotation, θ_3, about the resultant $\bar{x}_3$ axis.

$$\begin{bmatrix} x_1 \\ x_2 \\ x_3 \end{bmatrix} = [A] \begin{bmatrix} x_1^I \\ x_2^I \\ x_3^I \end{bmatrix} \tag{3.44}$$

where:

$$A = \begin{bmatrix} \cos\theta_2\cos\theta_3 & \cos\theta_3\sin\theta_2\sin\theta_1 + \sin\theta_3\cos\theta_1 & -\cos\theta_3\sin\theta_2\cos\theta_1 + \sin\theta_3\sin\theta_1 \\ -\sin\theta_3\cos\theta_2 & -\sin\theta_3\sin\theta_2\sin\theta_1 + \cos\theta_1\cos\theta_3 & \sin\theta_3\sin\theta_2\cos\theta_1 + \cos\theta_3\sin\theta_1 \\ \sin\theta_2 & -\cos\theta_2\sin\theta_1 & \cos\theta_2\cos\theta_1 \end{bmatrix}$$

The expressions for the rates of change of the Euler angles for the particular ordered rotations as defined in the matrix A above are found as:

$$\dot{\theta}_1 = \frac{1}{\cos\theta_2}\,(\omega_1 \cos\theta_3 - \omega_2 \sin\theta_3)$$

$$\dot{\theta}_2 = \omega_1 \sin\theta_3 + \omega_2 \cos\theta_3 \qquad (3.45)$$

$$\dot{\theta}_3 = \omega_3 - (\omega_1 \cos\theta_3 - \omega_2 \sin\theta_3) \tan\theta_2$$

A second general type of transformation using Euler angles can be obtained. This is defined by taking the first rotation about a body axis, the second rotation about a second body axis, and the third rotation about the same axis (now displaced) about which the first rotation took place. This will be defined as a Type II Euler rotation. The axes about which the rotations take place may again be permuted, so that six distinct transformation matrices are obtained. The following transformation matrix A corresponds to a rotation, θ_1, about the $\bar{x}_1$ axis; θ_2 about the resulting $\bar{x}_2$ axis; and θ_3 about the $\bar{x}_1$ axis resulting from the first two rotations.

$$\begin{bmatrix} x_1 \\ x_2 \\ x_3 \end{bmatrix} = [A] \begin{bmatrix} x_1^I \\ x_2^I \\ x_3^I \end{bmatrix} \qquad (3.46)$$

where

$$A = \begin{bmatrix} \cos\theta_2 & \sin\theta_1\sin\theta_2 & -\sin\theta_2\cos\theta_1 \\ \sin\theta_2\sin\theta_3 & \cos\theta_3\cos\theta_1 - \sin\theta_1\sin\theta_3\cos\theta_1 & \cos\theta_3\sin\theta_1 + \sin\theta_3\cos\theta_1\cos\theta_2 \\ \sin\theta_2\cos\theta_3 & -\sin\theta_3\cos\theta_1 - \sin\theta_1\cos\theta_2\cos\theta_3 & -\sin\theta_3\sin\theta_1 + \cos\theta_1\cos\theta_2\cos\theta_3 \end{bmatrix}$$

The rates of change of the Euler angles defined in Equations (3.46) are given as:

$$\dot{\theta}_1 = \frac{1}{\sin\theta_2} (\omega_2 \sin\theta_3 + \omega_3 \cos\theta_3)$$

$$\dot{\theta}_2 = \omega_2 \cos\theta_3 - \omega_3 \sin\theta_3 \qquad (3.47)$$

$$\dot{\theta}_3 = \omega_1 - \cot\theta_2 (\omega_2 \sin\theta_3 + \omega_3 \cos\theta_3)$$

Any of the other Type I or Type II Euler matrices can be obtained from the matrices A defined in Equations (3.44) and (3.46). This is possible by observing the following rules on some arbitrary initial reference frame (y_1, y_2, y_3) about which ordered rotations ϕ, θ, ψ take place.

1) Order the corresponding columns as

$$\begin{bmatrix} x_i \\ x_j \\ x_k \end{bmatrix} \quad \text{and} \quad \begin{bmatrix} y_i \\ y_j \\ y_k \end{bmatrix} \qquad (i, j, k = 1, 2, 3)$$

where the first rotation is taken about the y_i axis, the second about the y_j axis, the third about the y_k axis, thus satisfying the equation:

$$\begin{bmatrix} x_i \\ x_j \\ x_k \end{bmatrix} = [A] \begin{bmatrix} y_i \\ y_j \\ y_k \end{bmatrix} \qquad (3.48)$$

2) If the order of i, j, k is left-handed (e.g., 2, 1, 3), replace all the θ_i in the matrix A by $(-\theta_i)$ for all i.

3) Form a new matrix, B, from the elements of A as modified in 2) above by defining the i^{th} column of B as the 1st column of A, the j^{th} column of B as the 2nd column of A, and the k^{th} column of B as the 3rd column of A.

4) Form another matrix, C, from the components of B by defining the i^{th} row of C as the 1st row of B, the j^{th} row of C as the 2nd row of B, and the k^{th} row of C as the 3rd row of B.

5) In the matrix $C = f(\theta_i)$, replace θ_1 by the angle of rotation taken about y_i, θ_2 by that about y_j, and θ_3 by that taken about y_k, thus yielding a matrix $C = f(\phi, \theta, \psi)$.

The matrix $C = f(\phi, \theta, \psi)$ will now yield the required Euler matrix, i.e.,

$$\begin{bmatrix} x_1 \\ x_2 \\ x_3 \end{bmatrix} = [C] \begin{bmatrix} y_1 \\ y_2 \\ y_3 \end{bmatrix} \tag{3.49}$$

To obtain the expressions for the rates of change of the Euler angles which correspond to the permuted rotations defined by C in Equation (3.49), the following rules should be followed.

1) If the order of the i, j, k in the Equations (3.48) is left-handed (e.g., 2, 1, 3), replace all the θ_i in the expressions of Equation (3.45) or (3.47) by $(-\theta_i)$. The signs of the corresponding $\dot{\theta}_i$ are <u>not</u> to be changed.

2) Replace θ_1 and $\dot{\theta}_1$, respectively, with the angle and rate of change of the angle taken about the y_i axis defined in Equation (3.48). Similarly, replace θ_2 and $\dot{\theta}_2$ with the angle about the y_j axis, and θ_3 and $\dot{\theta}_3$ with the angle taken about the y_k axis. The body rate, ω_1, is then measured about the $\bar{x}_i$ axis, ω_2 about the $\bar{x}_j$ axis, and ω_3 about the $\bar{x}_i$ axis.

Thus, each type of Euler rotation may yield six distinct transformations, for a total of twelve matrices. The choice of which transformation to use is prompted by the particular problem being solved. For example, if the elements a_{i1} (i = 1, 2, 3) are to be used in the equations of motion (e.g. in the control law), the use of the particular matrices in either Equation (3.44) or (3.46) would be attractive, as the elements are algebraically simple. On the other hand, these matrices would not be attractive if the elements a_{3i} (i = 1, 2, 3) were of importance. Except for the disadvantage of unsymmetrical participation of the three variables θ_1, θ_2, and θ_3, it would appear that Euler angle transformations are quite useful for the analytic treatment of rigid body dynamics since only three variables are involved and no constraint equations are required. However, a closer look at the expressions for the rates of change of the angles, Equations (3.45) and (3.47), reveals that mathematical difficulties are encountered. This results because the time derivatives of a set of Euler angles do not, in general, form an orthogonal set.

Note that there exists a particular attitude of the body for which transformation is not unique. This case is commonly referred to as "gimbal lock." For the Type I Euler transformation, this singularity occurs for $\theta_2 = \pi/2$, whereas for the Type II Euler rotation the singularity occurs for $\theta_2 = 0$. It becomes obvious that the Type I Euler rotation must be used for study of system motion near the origin. The Type II rotations, however, are easier to

visualize and may be more convenient for some applications in mechanics. This basic failure in the formulation eliminates consideration of the three Euler angles as state variables for study of the acquisition problem. A solution to this dilemma, however, may be the inclusion of a fourth Euler angle (i.e., a redundant variable) to uniquely specify the attitude. This is done by defining four ordered rotations, θ_1, θ_2, θ_3, and θ_4 from the $\bar{x}^I$ coordinates to the $\bar{x}$ coordinates, where three of these are independent, say θ_1, θ_2, θ_3. The "gimbal lock" situation again will occur if the second angle of rotation, θ_2, passes through the singular point. However, to prevent the angle from approaching the singular point, certain conditions are placed upon the fourth angle θ_4.

3.2.3 Euler Symmetrical Parameters

The formulation of this four parameter system has been credited to Euler who introduced this kinematic representation in 1776. The oldest treatment generally available today is that of Whittaker[13], who arrives at them from direct geometrical considerations. These parameters may also be defined by considering the components of the eigenvector $\hat{e}$, defined in Equation (3.31). Three of the parameters define the "equivalent axis of rotation," and the fourth parameter determines the magnitude of the "equivalent angle of rotation, Φ." Define:

$$\begin{aligned} \xi &= e_1 \sin\left(\frac{\Phi}{2}\right) \\ \eta &= e_2 \sin\left(\frac{\Phi}{2}\right) \\ \zeta &= e_3 \sin\left(\frac{\Phi}{2}\right) \\ \chi &= \cos\left(\frac{\Phi}{2}\right) \end{aligned} \tag{3.50}$$

As there are four parameters and only three degrees of freedom, a constraint equation is necessary. This is given by the identity

$$\xi^2 + \eta^2 + \zeta^2 + \chi^2 = 1 \tag{3.51}$$

The parameter χ is seen to be positive for any value of the angle of total rotation Φ between $-\pi$ and $+\pi$, and $\chi = +1$ if and only if $\Phi = 0$ or an integral multiple of 4π. The relation of the parameters defined in Equation (3.50) to the elements of the transformation matrix may be obtained by considering A as a dyadic (see Gibbs [14]). In terms of the unit vector $\hat{e}$ and the angle Φ, the rotational dyadic $\bar{\bar{A}}$ is given by

$$\bar{\bar{A}} = \cos\Phi\, \bar{\bar{I}} + (1 - \cos\Phi)\, \hat{e}\hat{e} + \sin\Phi\, (\bar{\bar{I}} \times \hat{e}) \tag{3.52}$$

If the components of $\hat{e}$ are represented parametrically in terms of the symmetrical parameters as defined in Equation (3.50), use of the identity in Equation (3.51) gives the corresponding direction cosine matrix, A, as:

$$A = \begin{bmatrix} \xi^2 - \eta^2 - \zeta^2 + \chi^2 & 2(\xi\eta + \zeta\chi) & 2(\xi\zeta - \eta\chi) \\ 2(\xi\eta - \zeta\chi) & -\xi^2 + \eta^2 - \zeta^2 + \chi^2 & 2(\eta\zeta + \xi\chi) \\ 2(\xi\zeta + \eta\chi) & 2(\eta\zeta - \xi\chi) & -\xi^2 - \eta^2 + \zeta^2 + \chi^2 \end{bmatrix} \tag{3.53}$$

For small angles, χ is close to +1 and 2ξ, 2η, and 2ζ correspond to the angles θ_1, θ_2, θ_3, respectively, for a Type I Euler rotation.

Substitution of Equation (3.53) into Equation (3.41) will yield an equation involving the Euler parameters, their time derivatives, and the body rates. Only three of the resultant equations are independent, so a fourth equation is obtained by taking the time derivative of the identity in Equation (3.51) to obtain

$$2(\xi\dot{\xi} + \eta\dot{\eta} + \zeta\dot{\zeta} + \chi\dot{\chi}) = 0 \tag{3.54}$$

Placing these equations in vector-matrix notation yields

$$\bar{\omega} = 2\, B\, \dot{\bar{\rho}} \tag{3.55}$$

where

$$\bar{\omega} = \begin{bmatrix} \omega_1 \\ \omega_2 \\ \omega_3 \\ 0 \end{bmatrix} \quad ; \; \bar{\rho} = \begin{bmatrix} \xi \\ \eta \\ \zeta \\ \chi \end{bmatrix} ; \; B = \begin{bmatrix} \chi & \zeta & -\eta & -\xi \\ -\zeta & \chi & \xi & -\eta \\ \eta & -\xi & \chi & -\zeta \\ \xi & \eta & \zeta & \chi \end{bmatrix} \tag{3.56}$$

One can easily show that the matrix B is orthogonal (i.e., $B^{-1} = B^T$) and obtain the inverse relationship of that given in Equation (3.55), namely:

$$\dot{\bar{\rho}} = \frac{1}{2} B^{-1} \bar{\omega} = \frac{1}{2} B^T \bar{\omega} \tag{3.57}$$

Since the terms are linear in both ω_1, ω_2, ω_3 and ξ, η, ζ, χ, the above expression may be rearranged and written in a slightly different way as:

$$\dot{\bar{\rho}} = \frac{1}{2}\, \Omega\, \bar{\rho} \tag{3.58}$$

where:

$$\Omega = \begin{bmatrix} 0 & \omega_3 & -\omega_2 & \omega_1 \\ -\omega_3 & 0 & \omega_1 & \omega_2 \\ \omega_2 & -\omega_1 & 0 & \omega_3 \\ -\omega_1 & -\omega_2 & -\omega_3 & 0 \end{bmatrix} \tag{3.59}$$

For solution of problems in rigid body dynamics, the body rates may be obtained from the dynamic equations of motion and the matrix Ω constructed accordingly. Solving Equations (3.58) for ρ by state variable techniques then becomes straightforward if the ω_i are known as functions of time. The elegance and simplicity of this approach is evident.

While dealing with Euler's Symmetrical Parameters, consider some interesting identities and relationships. Extend the three by three direction cosine matrix, A, to a four by four matrix by adding 1 to the main diagonal, thus

$$\mathbf{A} = \begin{bmatrix} a_{11} & a_{12} & a_{13} & 0 \\ a_{21} & a_{22} & a_{23} & 0 \\ a_{31} & a_{32} & a_{33} & 0 \\ 0 & 0 & 0 & 1 \end{bmatrix} \tag{3.60}$$

Define a matrix, C, as follows:

$$C = \begin{bmatrix} 1 & 0 & 0 & 0 \\ 0 & 1 & 0 & 0 \\ 0 & 0 & 1 & 0 \\ 0 & 0 & 0 & -1 \end{bmatrix} \tag{3.61}$$

With these definitions and the matrix B in Equation (3.56), the entire set of relations given by Equation (3.53) may be found from the matrix identity

$$A = B\,C\,B\,C \tag{3.62}$$

Note that the matrix C is symmetric and that the effect of the similarity transformation CBC on the matrix B is to reverse the signs of the off-diagonal elements in the last row and column. By direct expansion, the characteristic equation of the matrix B is found to be

$$(\lambda^2 - 2\lambda\chi + 1)^2 = 0 \tag{3.63}$$

The eigenvalues are therefore

$$\lambda = \chi + \sqrt{\chi^2 - 1} = \cos\frac{\Phi}{2} \pm j\sin\frac{\Phi}{2} = \epsilon^{\pm j\frac{\Phi}{2}} \tag{3.64}$$

Another interesting identity is given by

$$B = \epsilon^{\frac{\Phi}{2}E} \tag{3.65}$$

where E is a matrix constructed from the components of $\hat{e}$:

$$E = \begin{bmatrix} 0 & e_3 & -e_2 & -e_1 \\ -e_3 & 0 & e_1 & -e_2 \\ e_2 & -e_1 & 0 & -e_3 \\ e_1 & e_2 & e_3 & 0 \end{bmatrix} \tag{3.66}$$

The matrix exponential given in Equation (3.65) may be expanded in a power series. Note from Equations(3.66) and (3.36) that

$$[E]\ [E] = E^2 = -I \tag{3.67}$$

where I is the identity matrix. Using Equation (3.67), the series may be written as:

$$\epsilon^{\frac{\Phi}{2}E} = I + \frac{\Phi}{2}E + \frac{(\frac{\Phi}{2}E)^2}{2!} + \frac{(\frac{\Phi}{2}E)^3}{3!} + \ldots$$

$$= I\left[1 - \frac{(\frac{\Phi}{2})^2}{2!} + \frac{(\frac{\Phi}{2})^4}{4!} + \ldots\right] \qquad (3.68)$$

$$+ E\left[\frac{\Phi}{2} - \frac{(\frac{\Phi}{2})^3}{3!} + \frac{(\frac{\Phi}{2})^5}{5!} + \ldots\right]$$

Recognizing terms in the series expansions as $\sin\frac{\Phi}{2}$ and $\cos\frac{\Phi}{2}$, Equation (3.68) may be written as:

$$\epsilon^{\frac{\Phi}{2}E} = I\cos\frac{\Phi}{2} + E\sin\frac{\Phi}{2} \qquad (3.69)$$

Direct substitution of the definitions given by Equation (3.50) into the matrix B defined in Equation (3.56) and expansion of Equation (3.69) yields proof of the identity given in Equation (3.65). The analogy of this identity with Euler's identity for the imaginary exponential is evident.

3.2.4 Quaternions

One particularly elegant formulation of a four parameter system was introduced by Hamilton in 1843 [15] for the study of classical mechanics. Euler's Symmetrical Parameters may be regarded as the components of an entity defined as a quaternion

$$q = \chi + i\,\xi + j\,\eta + k\,\zeta \qquad (3.70)$$

where the i, j, k are hypercomplex numbers defined by the following rules:

$$\begin{aligned} i^2 &= -1, \qquad ij = -ji = k \\ j^2 &= -1, \qquad jk = -kj = i \\ k^2 &= -1, \qquad ki = -ik = j \end{aligned} \tag{3.71}$$

Such a designation becomes obvious through consideration of the following. In terms of the components e_1, e_2, e_3 of the eigenvector $\hat{e}$ and the angle of total equivalent rotation, Φ, q may be defined as

$$q = \epsilon^{\frac{\Phi}{2}(ie_1 + je_2 + ke_3)} \tag{3.72}$$

Recalling the definitions of the Euler parameters in terms of $\hat{e}$ and Φ, and substituting into the definition of q in Equation (3.70), the following identity is obtained.

$$\epsilon^{\frac{\Phi}{2}(ie_1 + je_2 + ke_3)} = \cos\frac{\Phi}{2} + (ie_1 + je_2 + ke_3)\sin\frac{\Phi}{2} \tag{3.73}$$

This identity is seen to be an extension of Euler's identity, i.e., $\epsilon^{j\theta} = \cos\theta + j\sin\theta$, and in analogy to the identity in Equation (3.65).

The various functions of quaternions may be defined in analogy with ordinary algebra. Quaternion multiplication, however, even though done in a manner similar to that of complex numbers, requires that the order of operations be taken into account. The conjugate of the quaternion is defined as

$$q^* = \chi - i\xi - j\eta - k\zeta \tag{3.74}$$

The norm (i.e., length) of a quaternion is defined as:

$$q\, q^* = q^*\, q = \chi^2 + \xi^2 + \zeta^2 + \eta^2 \tag{3.75}$$

According to the identity in Equation (3.51) this norm is unity, resulting in defining a special form of the quaternion known as a versor (i.e., quaternion with unit norm).

Consider how the quaternion formulation provides the necessary kinematic characterization. The vector $\bar{x}^I$, having components x_1^I, x_2^I, x_3^I, may be represented in quaternion notation as

$$\bar{x}^I = i\, x_1^I + j\, x_2^I + k\, x_3^I \tag{3.76}$$

An interesting result is obtained from examining the equation

$$\bar{F} = q\, \bar{x}^I\, q^* \tag{3.77}$$

It may be shown that the operation defined in Equation (3.77) transforms the components x_1^I, x_2^I, x_3^I of the vector $\bar{x}^I$ into the components x_1, x_2, x_3 of the vector $\bar{x}$ to give results identical to those obtained from the transformation matrix A, i.e., $\bar{F} = \bar{x}$.

3.2.5 Cayley-Klein Parameters

This four parameter set was introduced in order to implement the solution of gyroscopic problems. The approach is to apply a 2 x 2 complex matrix to represent a transformation, rather than a 3 x 3 real matrix. The approach is described in Goldstein [11], with particular emphasis toward application to quantum mechanics. The following is more adapted to showing correspondence between this and other four parameter sets and is a development similar to that of Robinson [16]. Consider the following 2 x 2 complex matrix:

$$H = \begin{bmatrix} h_{11} & h_{12} \\ h_{21} & h_{22} \end{bmatrix} \tag{3.78}$$

It is required that the matrix be unitary and therefore

$$\det H = |H| = 1 \tag{3.79}$$

and

$$H H^{*} = I \tag{3.80}$$

where H^{*} is the transposed matrix conjugate of H.

The complex quantities h_{11}, h_{12}, h_{21}, h_{22} are referred to as the Cayley-Klein parameters. It is convenient, since the h_{ij} are complex, to introduce four other quantities, g_1, g_2, g_3, g_4, which are defined as follows:

$$\begin{aligned} h_{11} &= g_1 + i\, g_2 \\ h_{12} &= g_3 + i\, g_4 \end{aligned} \tag{3.81}$$

From the conditions in Equations (3.79) and (3.80), it may be shown that

$$\begin{aligned} h_{22} &= h_{11}^{*} \\ h_{21} &= -h_{12}^{*} \end{aligned} \tag{3.82}$$

Using the definitions in Equations (3.81) and (3.82), the matrix H may be written as

$$H = \begin{bmatrix} g_1 + i\, g_2 & g_3 + i\, g_4 \\ -g_3 + i\, g_4 & g_1 - i\, g_2 \end{bmatrix} \tag{3.83}$$

The following interesting result may then be shown:

$$\begin{aligned} g_1 &= \chi \\ g_2 &= \zeta \\ g_3 &= \eta \\ g_4 &= \xi \end{aligned} \tag{3.84}$$

where the quantities on the right are Euler's Symmetrical Parameters. Therefore, the Cayley-Klein Parameters may be defined as:

$$\begin{aligned} h_{11} &= \chi + i\zeta \\ h_{12} &= \eta + i\xi \\ h_{21} &= -\eta + i\xi \\ h_{22} &= \chi - i\zeta \end{aligned} \tag{3.85}$$

All of this serves to demonstrate that each variation of the four parameter system is essentially a slightly different method of representing the same thing.

3.2.6 The Gibbs Vector

Consider a slightly different formulation of the kinematic reference using the four Euler parameters. Dividing the first three quantities in Equation (3.50) by the fourth yields the following relationship.

$$\begin{aligned} \alpha &= \frac{\xi}{\chi} = e_1 \tan\frac{\Phi}{2} \\ \beta &= \frac{\eta}{\chi} = e_2 \tan\frac{\Phi}{2} \\ \gamma &= \frac{\zeta}{\chi} = e_3 \tan\frac{\Phi}{2} \end{aligned} \tag{3.86}$$

These quantities α, β, γ, can be defined as components of a vector referred to as the Gibbs vector [14]. No fourth parameter is necessary since the tangent is periodic in 2π for a half angle argument. Using the definitions in Equation (3.86) and the matrix of Equation (3.53), the elements of the transformation matrix A are given as:

$$\mathbf{A} = \frac{1}{1+\alpha^2+\beta^2+\gamma^2} \begin{bmatrix} 1+\alpha^2-\beta^2-\gamma^2 & 2(\alpha\beta+\gamma) & 2(\alpha\gamma-\beta) \\ 2(\alpha\beta-\gamma) & 1-\alpha^2+\beta^2-\gamma^2 & 2(\beta\gamma+\alpha) \\ 2(\alpha\gamma+\beta) & 2(\beta\gamma-\alpha) & 1-\alpha^2-\beta^2+\gamma^2 \end{bmatrix} \tag{3.87}$$

To determine the expressions relating the body rates ω_1, ω_2, ω_3 to the components of the Gibbs vector, the time derivatives are first obtained for α, β, and γ by direct differentiation of the quantities defined in Equation (3.86).

$$\dot{\alpha} = \frac{x\dot{\xi} - \xi\dot{x}}{x^2}$$

$$\dot{\beta} = \frac{x\dot{\eta} - \eta\dot{x}}{x^2} \qquad (3.88)$$

$$\dot{\gamma} = \frac{x\dot{\zeta} - \zeta\dot{x}}{x^2}$$

Writing Equations (3.88) in matrix form and augmenting them with a form of the relation in Equation (3.54) yields the formulation

$$\begin{bmatrix} \dot{\alpha} \\ \dot{\beta} \\ \dot{\gamma} \\ 0 \end{bmatrix} = \frac{1}{x^2} \begin{bmatrix} x & 0 & 0 & -\xi \\ 0 & x & 0 & -\eta \\ 0 & 0 & x & -\zeta \\ \xi & \eta & \zeta & x \end{bmatrix} \begin{bmatrix} \dot{\xi} \\ \dot{\eta} \\ \dot{\zeta} \\ \dot{x} \end{bmatrix} \qquad (3.89)$$

Substituting in the relation for $\dot{\rho}$ from Equation (3.57) gives the expression:

$$\begin{bmatrix} \dot{\alpha} \\ \dot{\beta} \\ \dot{\gamma} \\ 0 \end{bmatrix} = \frac{1}{2x^2} \begin{bmatrix} x^2+\xi^2 & \xi\eta-x\zeta & \xi\zeta+x\eta & 0 \\ \xi\eta+x\zeta & x^2+\eta^2 & \eta\zeta-x\xi & 0 \\ \xi\zeta-x\eta & \eta\zeta+x\xi & x^2+\zeta^2 & 0 \\ 0 & 0 & 0 & 1 \end{bmatrix} \begin{bmatrix} \omega_1 \\ \omega_2 \\ \omega_3 \\ 0 \end{bmatrix} \qquad (3.90)$$

Notice that, as expected, the four-dimensional vector formulation has been reduced to a three-dimensional formulation since the last row and column of Equation (3.90) is trivial. Using the definitions in Equation (3.86), Equation (3.90) may be written as:

$$\begin{bmatrix} \dot{\alpha} \\ \dot{\beta} \\ \dot{\gamma} \end{bmatrix} = \frac{1}{2} \begin{bmatrix} 1 + \alpha^2 & \alpha\beta - \gamma & \alpha\gamma + \beta \\ \alpha\beta + \gamma & 1 + \beta^2 & \beta\gamma - \alpha \\ \alpha\gamma - \beta & \beta\gamma + \alpha & 1 + \gamma^2 \end{bmatrix} \begin{bmatrix} \omega_1 \\ \omega_2 \\ \omega_3 \end{bmatrix} \tag{3.91}$$

An equivalent form of this equation is given as:

$$\dot{\bar{G}} = \frac{1}{2} \left[\bar{\omega} + \bar{\omega} \times \bar{G} + \bar{G} \left(\bar{G} \cdot \bar{\omega} \right) \right] \tag{3.92}$$

where:

$$\bar{G} = \begin{bmatrix} \alpha \\ \beta \\ \gamma \end{bmatrix} \quad ; \quad \bar{\omega} = \begin{bmatrix} \omega_1 \\ \omega_2 \\ \omega_3 \end{bmatrix} \tag{3.93}$$

Equation (3.91) involves only α, β, and γ and their time derivatives, thereby giving expressions which relate three independent kinematic parameters α, β, γ and the body rates ω_1, ω_2, and ω_3.

There is, however, a significant problem in the application of such a formulation. From the definitions in Equation (3.86), it can be seen that the variables are unbounded, i.e., α, β, $\gamma \rightarrow \infty$ as $\phi \rightarrow \pi$. This disadvantage, however, may be overcome by judicious analytic constraints. As is shown in Appendix A, Mortensen has been able to formulate analytically a general acquisition problem using these variables and prove asymptotic stability in-the-large.

3.2.7 Conclusions

Due to the geometric constraints inherent in rigid body rotation, a basic problem in attitude characterization has been shown to exist. In each case considered, there appears to be some ambiguity of position or discontinuity in rate that cannot be avoided with the

use of three kinematic state variables. This occurs for some singular rotation at which time either the attitude or the rate cannot be described uniquely. This is evident from Equations (3.45) and (3.47) in describing the rate of change of the Euler angles. When the second rotation has a certain singular value, the rates of change of the other two angles become infinite (i.e., undefined). Similarly, for the Gibbs vector as defined in Equation (3.86), when the total angle of rotation, Φ, is $\pm \pi$, the variables themselves as well as their rates of change are infinite (i.e., undefined). As would be expected, these ambiguities will occur for angles where trigonometric functions are zero or have singularities.

Even simple rotations lead to ambiguity, as can be noted by the problem which arises when a body has undergone a complete rotation and assumes its original position. Euler angles may be used to indicate the complete angle of rotation and may get arbitrarily large if a vehicle remains spinning. Direction cosines and the components of the Gibbs vector, however, are periodic and yield position unambiguously only up to a rotation of 2π radians. The Euler parameters, however, can supply complete information for rotations up to 4π radians since the argument is of the half angle of rotation.

With these problems of ambiguity and unboundedness in various characterizations, it becomes important to evaluate the use of a given parametric representation for the solution of particular problems. This topic is further discussed in the following section.

3.3 Evaluation of Kinematic Representations

As noted earlier, in considering the state variable formulation for the acquisition problem, it is important to characterize the problem in such a form to be suitable for use with advanced analytic and machine-aided control system techniques. The three broad areas

of concern are: 1) applicability of hand and machine-aided analysis techniques, 2) applicability of simulation techniques and ease of interpretation, and 3) physical constraints and the analytic representation of various control sources and control laws. It is important to consider these concerns in light of the various dynamical and kinematic representations discussed previously.

The first point is important during the preliminary analytic evaluation of various acquisition systems. For example, the ability to show stability in the large or convergence to a small region near the equilibrium position is a powerful result in acquisition control system design. This approach alleviates the usual brute force attack on such problems which result in extrapolating the results obtained for a certain set of points in state space to the whole space. This important result has been accomplished for particular acquisition situations discussed in Section IV and Appendix A.

Control system design and analysis is complemented by use of digital and analog computation for processing complex algorithms and/or providing simulation of the dynamic characteristics of the system. This will become particularly apparent in later sections of this report where both approaches have been exercised. Machines become invaluable aids in the analysis of acquisition systems and a following section will deal particularly with the constraints on implementing and interpreting such studies. It will be left to Sections V, VI and VII to discuss the actual results from particular machine-aided studies of acquisition systems.

The third consideration is important from a practical point of view. The actual physical situation must be ever present in the design approach. If an acquisition scheme can be designed to be optimum in some way, and yet the corresponding control law is not physically realizable or is overly complex, the system

design has little meaning. Conversely, if a system with given sensor characteristics and control laws is to be studied, but the representation of these quantities is highly complex using a given set of state variables, the analysis task becomes heavily impaired simply in terms of writing the state equations. These problems are by no means remote, and will be discussed in detail.

3.3.1 Analytic Considerations

There are several important considerations when discussing the applicability of a particular parametric representation of satellite attitude for analysis. The most important concern is the complexity which the equations assume under various formulations. Contributing to this complexity are the number of state variables, the symmetry of the resulting equations, and the manner in which various control laws or torques must be written. It is clear that hand analysis and manipulation using a system of equations with the nine direction cosines in conjunction with Euler's equations would be overly tedious, as the state vector would have twelve components. The use of the Gibbs vector, however, might provide a simpler approach. Here only six state equations are necessary, and certain symmetry is still maintained in the formulation. Euler parameters also could be used with some degree of ease, as only seven state variables are involved and symmetry in the formulation is evident.

It is important to realize that the analysis approach to complex control problems does not usually seek the explicit solutions to the state equations. Rather, techniques are used to determine behavior or obtain control laws without explicit solution. Therefore, the problem of visualizing the solution or transient motion of the system appears to be of little importance in choice of a set of variables with which to work the analysis problem. For example, if stability in some sense is to be proved using Lyapunov techniques, it is important only that for some initial point or region in state space, the

solution be shown to be forced to a particular defined region about the equilibrium point. It is only important, then, that the final state of the system have meaning, as the explicit motion is of little importance for such a problem. Therefore, a set of kinematic variables which will result in mathematical simplicity may have some real advantage in application to such problems. Two particular examples which apply powerful analytic control techniques to the acquisition problem are discussed in Section IV and Appendix A. The first deals with a one axis acquisition problem. The kinematic representation employed is a set of three direction cosines which relate the three body axes to an inertially fixed reference axis. Asymptotic stability in the large is shown using the Second Method of Lyapunov. The second example deals with three-axis acquisition and stability starting from any initial state. The components of the Gibbs vector are used to represent the attitude of the system and, although the variables themselves are unbounded, certain conditions are placed upon the initial state such that stability in the large may be shown for such a system.

Computing machines become helpful in solving the analysis problem as tools to carry out an algorithm which would be too complex or tedious to carry out by hand. An example of such usage would be the computation and manipulation required in solving matrix equations, e.g., computing the inverse, determinant, eigenvalues, etc. This is computational labor which may be alleviated using a computer to carry out the manipulations. The digital computer is used in such a fashion for some of the analyses detailed later in this study. One particular example is the use of the digital computer to obtain the region in state space for which a certain given function satisfies the property of being positive definite. When using a machine in this way, it is important to keep the order of the system (i.e., number of state variables) to a minimum. The compelling reason for this is to minimize the machine computation time which is necessary to perform the

required operations. This time increases rapidly with an increase in the order (i.e., dimensionality) of the system. For example, if a sixth-order state space (the minimum order for the acquisition problem) must be searched to obtain a region, this is considerably simpler and less costly than searching, for example, a twelfth-order state space. Again, for this application, the explicit motion of the system is not required, and minimizing the order of the system becomes of concern to minimize the cost of running the program. This particular application of computing machines, then, is essentially carrying out the manipulations which are required from the application of some of the more powerful analysis techniques. Another important, although considerably different, approach to using machines is discussed in the following section.

3.3.2 Simulation Considerations

An important way in which computers (both digital and analog) are used is in simulation of the actual system dynamics, i.e., obtaining the explicit solutions of the equations of motion. There are a number of problem constraints which must then be considered. It is important to minimize solution time and computer cost, to maintain good accuracy in the solution, and to be able to interpret easily the motion of the system. Two references, DeBra [17] and Robinson [16], deal particularly with such problems. DeBra is particularly concerned with the applicability of various parametric schemes for representing attitude to solution by digital quadrature. Further discussion involves determining the error which results from digital solution and what type of integration algorithm is particularly suitable to the dynamical problem of satellite attitude control. Robinson is more concerned with the comparison of various methods, particularly four-parameter methods, for analog simulation. The following discussion is particularly indebted to these references.

In considering each of the more important parametric representations discussed earlier, both the Euler angles and Gibbs vector appear to be unsuited for simulation purposes. Although the integration of Euler angles is straightforward and only three equations are involved, the important singularity results in loss of accuracy and the use of trigonometric functions makes computation slow. The Gibbs vector, although having been of some convenience for analytic work, also possesses a singularity which leads to similar difficulties in unboundedness and loss of accuracy in simulation.

The use of direction cosines or Euler Symmetrical parameters, however, appears attractive. Several procedures can be implemented to obtain the time solution of the attitude using direction cosines. Mathematically, the complete transformation matrix can be obtained using three non-zero elements and the sign of a fourth. However, Robinson was unable to obtain a computationally stable scheme for solution on the analog computer using less than six integrations. It appears, therefore, that six of the direction cosines must be integrated and the other three obtained using algebraic relationships. In writing the equations, conditions must be applied to maintain the unity magnitude and orthogonality of the elements of the matrix. This correction scheme is necessary due to errors which build up during digital numerical integration procedures or to problems of drift which occur during analog computation. Robinson delineates a method of correction which, although applied particularly to analog computation, might equally apply to the analogous problem in digital integration. The equations, including the correction terms, are given below:

$$
\left.
\begin{aligned}
\dot{a}_{11} &= \omega_3 a_{21} - \omega_2 a_{31} + k_1 a_{11}(1 - \bar{i}\cdot\bar{i}) \\
\dot{a}_{21} &= \omega_1 a_{31} - \omega_3 a_{11} + k_1 a_{21}(1 - \bar{i}\cdot\bar{i}) \\
\dot{a}_{31} &= \omega_2 a_{11} - \omega_1 a_{21} + k_1 a_{31}(1 - \bar{i}\cdot\bar{i}) \\
\dot{a}_{12} &= \omega_3 a_{22} - \omega_2 a_{32} + k_1 a_{12}(1 - \bar{j}\cdot\bar{j}) - k_2 a_{11}(\bar{i}\cdot\bar{j}) \\
\dot{a}_{22} &= \omega_1 a_{32} - \omega_3 a_{12} + k_1 a_{22}(1 - \bar{j}\cdot\bar{j}) - k_2 a_{21}(\bar{i}\cdot\bar{j}) \\
\dot{a}_{32} &= \omega_2 a_{12} - \omega_1 a_{22} + k_1 a_{32}(1 - \bar{j}\cdot\bar{j}) - k_2 a_{31}(\bar{i}\cdot\bar{j}) \\
a_{13} &= a_{21} a_{32} - a_{22} a_{31} \\
a_{23} &= a_{12} a_{31} - a_{11} a_{32} \\
a_{33} &= a_{11} a_{22} - a_{12} a_{21} \\
\bar{i}\cdot\bar{i} &= \sum_{i=1}^{3} a_{i1}^2 \\
\bar{j}\cdot\bar{j} &= \sum_{i=1}^{3} a_{i2}^2 \\
\bar{i}\cdot\bar{j} &= \sum_{i=1}^{3} a_{i1} a_{i2}
\end{aligned}
\right\} \quad (3.94)
$$

The k terms on the right-hand side of the first six equations are the required correction terms. The k_i are the error coefficients, and are adjusted to maintain small error and computational stability.

DeBra[17] contends that such a procedure is lengthy and unnecessary, and that when errors are small, first order approximations may be used. He suggests an averaging process that, hopefully, will reduce the integration errors. Averaging procedures are discussed that force the averaged direction cosines to satisfy the normality conditions and therefore come closer to satisfying the orthogonality conditions. Both cases are discussed where either all nine elements

or only six elements are integrated. This approach, of course, is based on the assumption that the errors are small.

The Euler parameters, however, appear to offer the greatest potential for implementation. At most, each of the four parameters would be integrated and the constraint given by Equation (3.51) used to check and correct the magnitudes of the integrated parameters. These parameters share an advantage with direction cosines since there is no singular point with which to cope and simple algebraic equations are involved rather than trigonometric functions.

A further point of comparison becomes of considerable importance if many coordinate transformations must be accomplished. The use of direction cosines, of course, is by far the simplest method to obtain a vector transformation since only the elements themselves are required, as is apparent from Equation (3.13). When using Euler parameters, however, certain functions of the parameters must be precomputed in order to determine the transformation. This is clear from consideration of the matrix in Equation (3.53). This, of course, gives a slight computational advantage to the use of direction cosines if many vector transformations are to be computed. However, the savings in time for performing only four integrations using Euler parameters as opposed to six using direction cosines should considerably offset the time to compute the elements of the transformation matrix. This yields an overall greater efficiency in the use of Euler parameters as the kinematic representation for simulation of the acquisition problem.

A further consideration for purposes of simulation is the ease with which the motion may be visualized. All the systems of representation which have been considered are quite good for visualization of small angle motion. In fact, for small angle rotations both

the Euler parameters and the Gibbs vector as defined become equivalent to one-half the corresponding Type I Euler angles, i.e.,

$$\begin{aligned} \alpha &\cong \xi \cong \frac{\theta_1}{2} \\ \beta &\cong \eta \cong \frac{\theta_2}{2} \\ \gamma &\cong \zeta \cong \frac{\theta_3}{2} \\ \chi &\cong 1 \end{aligned} \tag{3.95}$$

Similarly, the diagonal elements of the direction cosine matrix become unity and the off-diagonal elements satisfy the equation

$$a_{ij} = - a_{ji} \tag{3.96}$$

where the a_{ij} may each be associated directly with a Type I Euler angle as shown below:

$$A \cong \begin{bmatrix} 1 & \theta_3 & -\theta_2 \\ -\theta_3 & 1 & \theta_1 \\ \theta_2 & -\theta_1 & 1 \end{bmatrix} \tag{3.97}$$

For large angle motions the direction cosines and Euler parameters provide the easiest visualization, although each system takes some experience for rapid interpretation. An example may help to illustrate these representations of the motion. Constant rates of one-third, one-half, and one cycle per second have been placed about the body fixed $\bar{x}_1$, $\bar{x}_2$, $\bar{x}_3$ axes, respectively. The resultant motion is depicted using direction cosines in Figures 3.1 through 3.3 and Euler parameters in Figure 3.4.

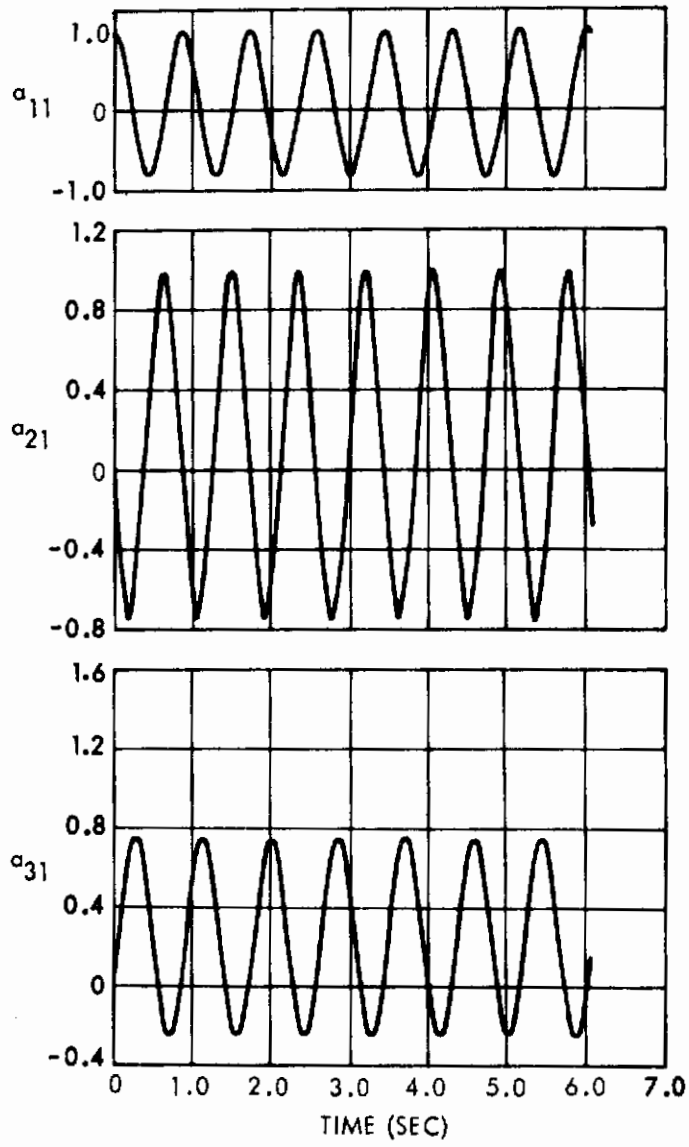

Figure 3.1 Direction Cosine Elements a_{il} (i = 1,2,3) as a Function of Time for Constant Body Rates

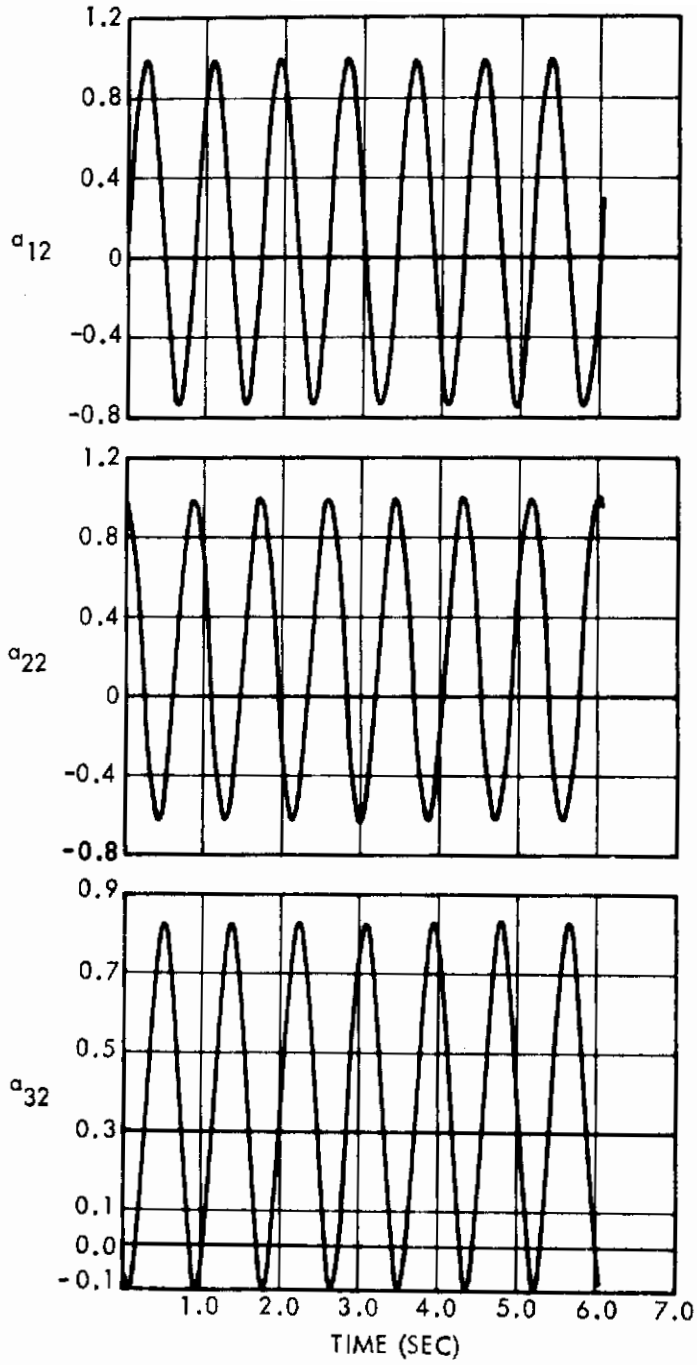

Figure 3.2 Direction Cosine Elements a_{i2} (i = 1,2,3) as a Function of Time for Constant Body Rates

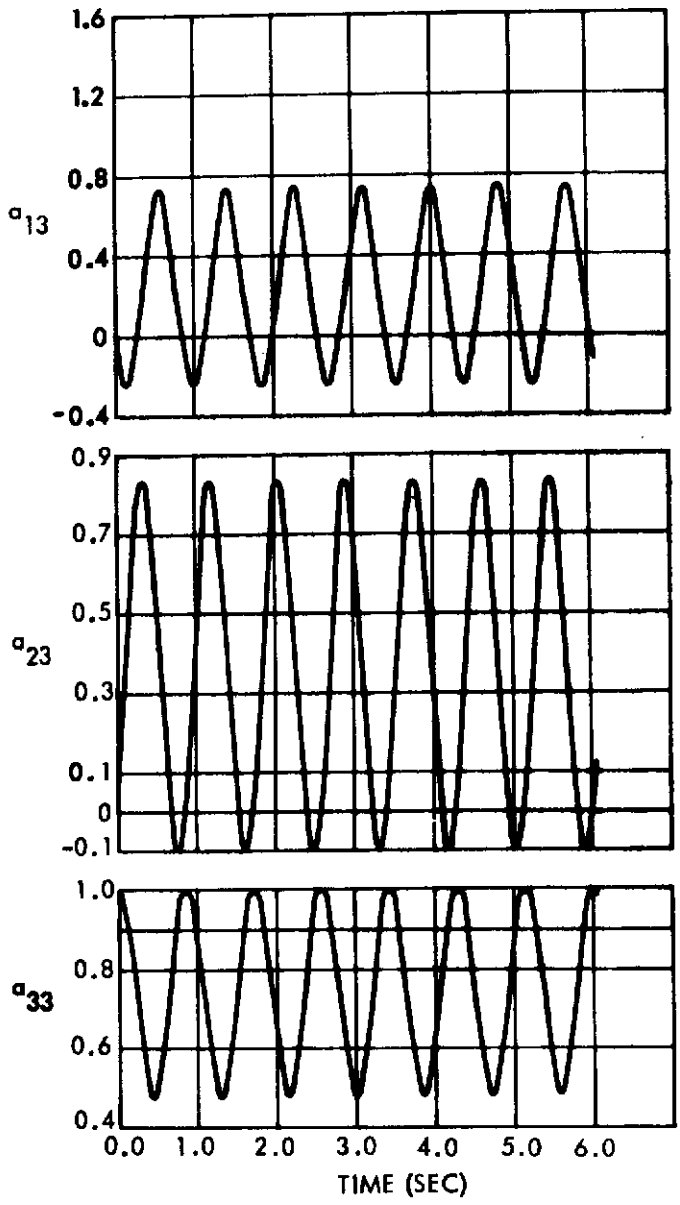

Figure 3.3 Direction Cosine Elements a_{i3} (i = 1,2,3) as a Function of Time for Constant Body Rates

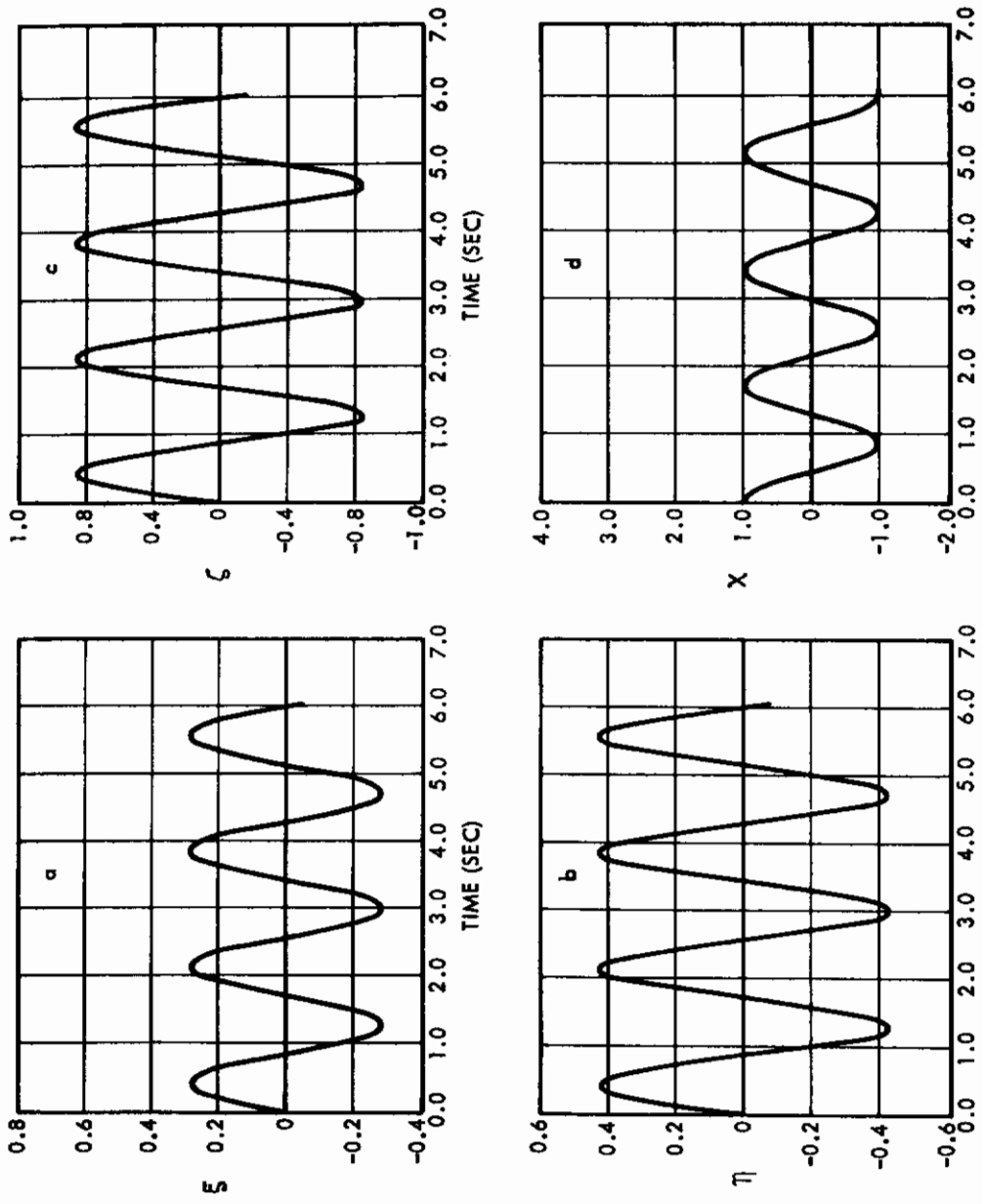

Figure 3.4 Euler Symmetric Parameters as a Function of Time for Constant Body Rates

Recalling the definitions of the Euler parameters from Equation (3.50), it can be seen that ξ, η, and ζ are directly proportional to the components of the eigenvector $\hat{e}$ as resolved along the body axes $\bar{x}_1$, $\bar{x}_2$, and $\bar{x}_3$. The instantaneous position of the axis of equivalent rotation, therefore, can be easily visualized. The fourth parameter χ is, by definition, the cosine of half the equivalent angle of rotation and may again be easily visualized. For the particular motion pictured, note that for all time, $\eta = \frac{\zeta}{2}$. Therefore, the axis of equivalent rotation always lies in a plane containing the $\bar{x}_1$ axis and rotated +64 degrees from the $\bar{x}_2$ axis. The position of the body can then be quickly established for any time and the overall motion visualized. The direction cosines are somewhat more difficult to visualize, as it is necessary to coordinate the variation of more quantities. It can be seen that the a_{ij} $(i \neq j)$ are equal except for the phase angle. Also, a_{33} is always positive and the elements a_{11} and a_{22} have a positive bias. Coordinating these facts may then yield a reasonable visualization of the satellite motion. It becomes apparent, however, that the use of Euler parameters facilitates the visualization of large angle motion.

Other plots also can be very useful. For example, a plot of a_{ik} vs. a_{jk} yields a projection of the motion of the tip of the $\bar{x}_k^I$ unit vector in a plane normal to the $\bar{x}_k$ unit vector. This is particularly enlightening when dealing with problems employing sensors or optical scanners. Similar sort of plots involving the Euler parameters may also prove helpful. Individual experimentation can be used to yield displays of particular usefulness to the analyst.

Table 3.1 provides a brief capsule summary of the preceding discussion relating the suitability of various kinematic representations for machine-aided analysis and simulation.

TABLE 3.1

SUMMARY OF KINEMATIC REPRESENTATIONS AND APPLICABILITY TO DIGITAL AND ANALOG MACHINE-AIDED ANALYSIS

	Kinematic Representations			
	Direction Cosines	Euler Angles	Euler Parameters	Gibbs Vector
I. Machine aids to implementing techniques in control analysis				
Ease in writing equations	Good	May become complex	Poor in some cases	May become complex
Relation to physical situation	Good	Good	Poor	Poor
Order and symmetry of resultant system	9th order w/ symmetry	3rd order and trig. func. req'd, some symmetry	4th order and symmetric	3rd order and symmetric
Overall usefulness for analysis	Fair	Poor	Good	Good
II. Machine simulation				
Number of integrals required	6-9	3	3-4	3
Singularities	None	$\theta_2 = 0, \pm\pi$ or $\pm\pi/2$	None	$\Phi = +\pi$
Calculation necessary	Algebra	trig. func.	Algebra	Algebra
Range of unambiguous orientation	$0-2\pi$	$0-\infty$	$0-4\pi$	$0-2\pi$
Visualization Small Angle	Good	Good	Good	Good
Large Angle	Good w/experience	Poor	Good	Good
Range of Variables	Magnitude ≤ 1	Bounded for finite rates	Magnitude ≤ 1	Unbounded
Range of Rates of change of variables	Bounded for finite rates	Unbounded	Bounded for finite rates	Unbounded
Overall usefulness for simulation	Good	Poor	Good	Poor

3.3.3 System Representation and Realizability

It is important in the analysis and simulation of the acquisition control problem to consider the constraints on the representation and physical realizability of the system. An inherent constraint is present in the design since control laws are required to have some physical meaning which can be incorporated into actual hardware implementation. For example, if a system is to be optimized in some sense, the control law obtained must be physically realizable to have any real application. This section, then, will deal with the representation and realizability of sensor outputs, control laws, and external torque sources in relation to various kinematic representations.

An important consideration in implementing a suitable analytic representation of the acquisition problem is the mathematical complexity necessary to adequately represent the required sensor reference frame for implementing certain control laws. Consider the required reference frame whose physical character will, in general, be determined by the nature of necessary sensing devices. For inertial references, devices such as star trackers, gyros, and sun sensors may be utilized. For orbiting vehicles, where orientation with respect to the local vertical may be required, some form of earth sensor would be more suitable. It is the output quantities of such devices which are required as control signals, and as such must be realizable in some tractable analytic form.

A similar situation arises when attempting to describe various torque sources which act as disturbances or may be utilized for control. Such torques may be internal (those which do not change the total vehicle angular momentum, e.g., reaction wheels) or external (those which do change the total angular momentum). Further, the external torques may arise from natural sources (such as the earth's gravitational and magnetic fields) or be vehicle-generated (such as

obtained by mass expulsion systems). A number of acquisition systems which are acted upon by various combinations of the above-mentioned torque sources and utilize particular sensor or reference frames are discussed in this section. Considered are the representation of sensor and scanner outputs, control laws for various systems, and the representation of ambient fields.

One need not pursue the problem very far before discovering that the use of direction cosines appears as the simplest and most straightforward manner to describe analytically such quantities as sensor outputs and control torques. This is to be somewhat expected, considering the great redundancy inherent in such a choice of variable formulation. Nonetheless, the disadvantages of complexity in the analytical representation (e.g., twelve equations) must be weighed with the rewards in the reduction of dimensionality of the problem.

Consider the natural way in which certain kinematic representations arise. In the use of direction cosines, for example, consider the two elements a_{13} and a_{23}. The first is representative of a measure of the plane angle between the $\bar{x}_3^I$ inertial reference axis and the $\bar{x}_1$ body axis. The second, a_{23}, is reprsentative of the plane angle between the $\bar{x}_3^I$ inertial reference axis and the $\bar{x}_2$ body axis. Using these quantities, therefore, one may relate the positioning of the $\bar{x}_3$ body axis to the $\bar{x}_3^I$ inertial reference axis. If the $\bar{x}_3$ axis were to be controlled to point along $\bar{x}_3^I$, a_{13} and a_{23} may represent directly quantities proportional to the outputs of sensors which measure the error. These quantities, however, will yield no information concerning position measured <u>about</u> the $\bar{x}_3$ axis. Note that the same sort of development could be extended to any of the three body axes.

In a similar way, the Euler angles are very naturally represented as gimbal angles and are commonly used for control and navigation in airplane, missile, and shipboard systems. The singularity inherent in such a system, however, places constraints upon their use. For example, in missile application the middle gimbal angle is restricted below some value and flight maneuvers must take this into account. Systems using four gimbal platforms have been used in aircraft and some boosters to achieve all-attitude capability. The mechanization, however, is essentially done by "slaving" the redundant gimbal to the middle gimbal to avoid the singularity problem. This represents more of a servo design problem than a useful approach to kinematic representation. Because this particular set of variables appears unsuitable for the acquisition problem, their use is precluded for the remainder of this discussion.

The Euler parameters and components of the Gibbs vector appear to have no direct relation to physically sensed quantities. However, functions of these parameters may be related to sensed quantities which are easily recognizable. The components of the matrices in Equations (3.53) and (3.87) may each be associated directly with a direction cosine and thus represent a single sensed quantity. Other equations and functions of the parameters may characterize a combination of sensed quantities involving more than single axis observations. It is clear, however, that the direction cosine elements are of primary importance in obtaining physically realizable sensed quantities.

In order to minimize confusion for purposes of illustrating particular control laws, only the direction cosine elements a_{13} and a_{23}, and their representation in other parametric systems will be dealt with. Of course, these results may be generalized to any

set of elements using analogous relations and identities. The use of Euler parameters results in characterizing these particular elements as

$$\begin{aligned} a_{13} &= 2(\xi\zeta - \eta\chi) \\ a_{23} &= 2(\eta\zeta + \xi\chi) \end{aligned} \tag{3.98}$$

By direct differentiation, the rates of change of the elements are:

$$\begin{aligned} \dot{a}_{13} &= 2\left[\xi\dot{\zeta} + \dot{\xi}\zeta - (\dot{\eta}\chi + \eta\dot{\chi})\right] \\ \dot{a}_{23} &= 2\left[\eta\dot{\zeta} + \dot{\eta}\zeta + (\dot{\xi}\chi + \xi\dot{\chi})\right] \end{aligned} \tag{3.99}$$

The quantities in Equation (3.99) are representative of "derived rate", and are used in a number of control laws to provide the damping term.

Similar results may be obtained using the components of the Gibbs vector. From Equation (3.87):

$$\begin{aligned} a_{13} &= \frac{2(\alpha\gamma - \beta)}{1+\alpha^2+\beta^2+\gamma^2} \\ a_{23} &= \frac{2(\beta\gamma + \alpha)}{1+\alpha^2+\beta^2+\gamma^2} \end{aligned} \tag{3.100}$$

and

$$\begin{aligned} \dot{a}_{13} &= \frac{2\left[(1+\alpha^2+\beta^2+\gamma^2)(\alpha\dot{\gamma}+\dot{\alpha}\gamma-\dot{\beta}) - 2(\alpha\gamma-\beta)(\alpha\dot{\alpha}+\beta\dot{\beta}+\gamma\dot{\gamma})\right]}{(1+\alpha^2+\beta^2+\gamma^2)^2} \\ \dot{a}_{23} &= \frac{2\left[(1+\alpha^2+\beta^2+\gamma^2)(\beta\dot{\gamma}+\dot{\beta}\gamma+\dot{\alpha}) - 2(\beta\gamma+\alpha)(\alpha\dot{\alpha}+\beta\dot{\beta}+\gamma\dot{\gamma})\right]}{(1+\alpha^2+\beta^2+\gamma^2)^2} \end{aligned} \tag{3.101}$$

As an example, a particular type of control law is defined which might be considered typical for an acquisition system. Two forms of the basic law are given, both employing position information using direction cosines, but differing in the use of a rate dependent term. In one case, the measured body rates, ω_i, are used whereas in the second case the "derived rates," $\dot{a}_{13}$ and $\dot{a}_{23}$, supply the necessary signal. These so-called "proportional plus lead" control law formulations are given in Table 3.2 expressed equivalently in various kinematic sets, where u_i is the control law for the i^{th} axis, and the α_{ij} are "gains". It is clear that the complicating factor in expressing such control laws is the "derived rate" term. Control laws employing body rate information are not greatly complicated by expressing direction cosine control laws in terms of other parametric representations. Section V deals in greater detail upon actual control law formulation, whereas what is presented here is merely an example of obtaining equivalence among various kinematic representations.

It is obvious, however, from Table 3.2 that some control laws which are expressed in a simple fashion in terms of direction cosines can become quite complex if expressed in terms of other kinematic representations. It may be of interest, therefore, to consider control laws formulated directly in terms of the various kinematic parameters, i.e., control laws based directly upon Euler parameters or components of the Gibbs vector. Consider the usefulness of the following quantities for control law formulation

$$\frac{\alpha}{1+\alpha^2+\beta^2+\gamma^2} = \xi\chi = \frac{1}{4}(a_{23} - a_{32})$$

$$\frac{\beta}{1+\alpha^2+\beta^2+\gamma^2} = \eta\chi = \frac{1}{4}(a_{31} - a_{13}) \qquad (3.102)$$

$$\frac{\gamma}{1+\alpha^2+\beta^2+\gamma^2} = \zeta\chi = \frac{1}{4}(a_{12} - a_{21})$$

TABLE 3.2

EQUIVALENT CONTROL LAW FORMULATION

$(u_{31} = \alpha_{31}\,\omega_3)$

Kinematic Representation	Proportional Plus Lead Using Derived Rate Information	Proportional Plus Lead Using Body Rate Information
Direction Cosines (a_{13}, a_{23})	$u_1 = \alpha_{11}\,(a_{13} + \alpha_{12}\,\dot{a}_{13})$ $u_2 = \alpha_{21}\,(a_{23} + \alpha_{22}\,\dot{a}_{23})$	$u_1 = \alpha_{11}\,(a_{13} + \alpha_{12}\,\omega_1)$ $u_2 = \alpha_{21}\,(a_{23} + \alpha_{22}\,\omega_2)$
Euler Symmetric Parameters (ξ, η, ζ, χ)	$u_1 = \alpha_{11}\,(\xi\zeta - \eta\chi) + \alpha_{12}(\xi\dot{\zeta} + \dot{\xi}\zeta - (\dot{\eta}\chi + \eta\dot{\chi}))$ $u_2 = \alpha_{21}\,(\eta\zeta + \xi\chi) + \alpha_{22}(\eta\dot{\zeta} + \dot{\eta}\zeta + (\dot{\xi}\chi + \xi\dot{\chi}))$	$u_1 = \alpha_{11}\,(\xi\zeta - \eta\chi) + \alpha_{12}\,\omega_1$ $u_2 = \alpha_{21}\,(\eta\zeta + \xi\chi) + \alpha_{22}\,\omega_2$
Gibbs Vector (α, β, γ)	$u_1 = \frac{2\,\alpha_{11}}{1+\alpha^2+\beta^2+\gamma^2}\left[(\alpha\gamma - \beta) + \alpha_{12}(\alpha\dot{\gamma} + \dot{\alpha}\gamma - \dot{\beta}) - \frac{\alpha_{12}(\alpha\gamma - \beta)(\alpha\dot{\alpha} + \beta\dot{\beta} + \gamma\dot{\gamma})}{1 + \alpha^2 + \beta^2 + \gamma^2}\right]$ $u_2 = \frac{2\,\alpha_{21}}{1+\alpha^2+\beta^2+\gamma^2}\left[(\beta\gamma + \alpha) + \alpha_{22}(\beta\dot{\gamma} + \gamma\dot{\beta} + \dot{\alpha}) - \frac{\alpha_{22}(\beta\gamma + \alpha)(\alpha\dot{\alpha} + \beta\dot{\beta} + \gamma\dot{\gamma})}{1 + \alpha^2 + \beta^2 + \gamma^2}\right]$	$u_1 = \frac{\alpha_{11}}{1+\alpha^2+\beta^2+\gamma^2}\left[(\alpha\gamma - \beta) + \alpha_{12}\,\omega_1\right]$ $u_2 = \frac{\alpha_{21}}{1+\alpha^2+\beta^2+\gamma^2}\left[(\beta\gamma + \alpha) + \alpha_{22}\,\omega_2\right]$

The quantities on the right are, of course, functions of the direction cosine elements and provide the clearest relation to physical implementation. The use of the quantities on the left, although complex to measure, may have much to recommend them because of the relatively simple representation when using either Euler parameters or the Gibbs vector as the kinematic characterization. An example control law may take the form

$$\begin{aligned} u_1 &= \alpha_{11} (\pi x + \alpha_{12} \omega_1) \\ u_2 &= \alpha_{21} (\zeta x + \alpha_{22} \omega_2) \\ u_3 &= \alpha_{31} \omega_3 \end{aligned} \tag{3.103}$$

At this point, however, such control laws have not been investigated since the most important emphasis has been toward achieving a greater simplicity in the physical systems rather than the analytic representation - and correctly so. However, it may be of future interest to pursue such systems, particularly in light of Mortensen's example (see Appendix A) where the following control law was found to yield asymptotic stability in the large.

$$\begin{aligned} u_1 &= \alpha_{11} \omega_1 + \alpha_{12} (1 + \alpha^2 + \beta^2 + \gamma^2) \alpha \\ u_2 &= \alpha_{21} \omega_2 + \alpha_{22} (1 + \alpha^2 + \beta^2 + \gamma^2) \beta \\ u_3 &= \alpha_{31} \omega_3 + \alpha_{32} (1 + \alpha^2 + \beta^2 + \gamma^2) \gamma \end{aligned} \tag{3.104}$$

Experimentation with such systems may lead to increased simplicity and a greater ability to achieve the desired performance for an acquisition system.

As seen from the discussion on formulating control laws for an acquisition system, a problem of undesired complexity may exist in writing the equations of motion in terms of some particular attitude

characterization. This is directly related to the problem of vector transformation discussed in an earlier section, and is increasingly the case when control torque sources are included. The torque sources of particular interest, and those which are included in the discussion below, are gravity gradient, magnetic, solar, and aerodynamic. The first two are of particular concern to the acquisition problem because of presently demonstrated capability of using such sources for acquisition control. The latter two sources have been employed for "normal-mode" stabilization, and may be of interest in the future for acquisition problems. To demonstrate the complexity introduced to incorporate these control torque sources, the general form of the required equations is given in Table 3.3 using the elements of the direction cosine matrix as the kinematic variables. The A_{ij} are (constant and time varying) coefficients which are vehicle and mission dependent and are not given explicitly since only the form of the equations is important for the present purposes. If these equations were to be expressed in another kinematic frame (e.g., Euler parameters or the Gibbs vector), the complexity will increase considerably due to the increased algebra involved. This is evidenced by referring to the matrices in Equations (3.53) and (3.87). For gravity gradient torques, the use of other kinematic representations will not add great complexity, as the equations are quite simple in terms of direction cosines and involve only three elements. Magnetic torques become more complicated since all elements of the direction cosine matrix are involved. This is a direct example of the problem involved to perform vector transformations, since the equations simply reflect a transformation of the magnetic field components from an orbital reference coordinate system to the body fixed reference coordinate system. Similar comments apply to both solar torques and aerodynamic torques, although additional complexity is introduced since the basic equations themselves are more involved. As would be expected, expressing these equations in terms of Euler parameters will require less complex expressions than using

TABLE 3.3

EQUATIONS FOR VARIOUS CONTROL TORQUE SOURCES EXPRESSED IN TERMS OF DIRECTION COSINES AND VEHICLE PARAMETERS A_{ij}

Gravity Gradient Torques

$$T_{g1} = A_{11}\, a_{23}\, a_{33}$$

$$T_{g2} = A_{21}\, a_{13}\, a_{33}$$

$$T_{g3} = A_{31}\, a_{13}\, a_{23}$$

Magnetic Torques

$$T_{m1} = A_{11}\, a_{21} + A_{12}\, a_{22} + A_{13}\, a_{23} + A_{14}\, a_{31} + A_{15}\, a_{32} + A_{16}\, a_{33}$$

$$T_{m2} = A_{21}\, a_{11} + A_{22}\, a_{12} + A_{23}\, a_{13} + A_{24}\, a_{31} + A_{25}\, a_{32} + A_{26}\, a_{33}$$

$$T_{m3} = A_{31}\, a_{11} + A_{32}\, a_{12} + A_{33}\, a_{13} + A_{34}\, a_{21} + A_{35}\, a_{22} + A_{36}\, a_{23}$$

Aerodynamic Torques

$$T_{a1} = A_{11}a_{31}|a_{31}| + A_{12}a_{21}|a_{31}| + A_{13}a_{31}(1-a_{31}^{2})^{1/2} + A_{14}a_{21}(1-a_{31}^{2})^{1/2}$$

$$T_{a2} = A_{21}a_{31}|a_{31}| + A_{22}a_{11}|a_{31}| + A_{23}a_{31}(1-a_{31}^{2})^{1/2} + A_{24}a_{11}(1-a_{31}^{2})^{1/2}$$

$$T_{23} = A_{31}a_{21}|a_{31}| + A_{32}a_{11}|a_{31}| + A_{33}a_{21}(1-a_{31}^{2})^{1/2} + A_{34}a_{11}(1-a_{31}^{2})^{1/2}$$

Solar Torques

$$T_{s1} = A_{11}\,(A_{41}a_{31} + A_{42}a_{32} + A_{43}a_{33})\,|A_{41}a_{31} + A_{42}a_{32} + A_{43}a_{33}|$$
$$+ A_{12}\,(A_{41}a_{21} + A_{42}a_{22} + A_{43}a_{23})\,|A_{41}a_{31} + A_{42}a_{32} + A_{43}a_{33}|$$
$$+ A_{13}\,(A_{41}a_{31} + A_{42}a_{32} + A_{43}a_{33})\left[1-(A_{41}a_{31} + A_{42}a_{32} + A_{43}a_{33})^{2}\right]^{1/2}$$

TABLE 3.3 (Continued)

$$+ A_{14}\,(A_{41}a_{21} + A_{42}a_{22} + A_{43}a_{23})\left[1-(A_{41}a_{31} + A_{42}a_{32} + A_{43}a_{33})^2\right]^{1/2}$$

$$+ A_{15}\,(A_{41}a_{21} + A_{42}a_{22} + A_{43}a_{23})(A_{41}a_{31} + A_{42}a_{32} + A_{43}\,a_{33})$$

$$T_{s2} = A_{21}\,(A_{41}a_{11} + A_{42}a_{12} + A_{43}a_{13})\left|A_{41}a_{31} + A_{42}a_{32} + A_{43}a_{33}\right|$$

$$+ A_{22}\,(A_{41}a_{31} + A_{42}a_{32} + A_{43}a_{33})\left|A_{41}a_{31} + A_{42}a_{32} + A_{43}a_{33}\right|$$

$$+ A_{23}\,(A_{41}a_{31} + A_{42}a_{32} + A_{43}a_{33})\left[1-(A_{41}a_{31} + A_{42}a_{32} + A_{43}a_{33})^2\right]^{1/2}$$

$$+ A_{24}\,(A_{41}a_{11} + A_{42}a_{12} + A_{43}a_{13})\left[1-(A_{41}a_{31} + A_{42}a_{32} + A_{43}a_{33})^2\right]^{1/2}$$

$$+ A_{25}\,(A_{41}a_{11} + A_{42}a_{12} + A_{43}a_{13})(A_{41}a_{31} + A_{42}a_{32} + A_{43}a_{33})$$

$$T_{s3} = A_{31}\,(A_{41}a_{21} + A_{42}a_{22} + A_{43}a_{23})\left|A_{41}a_{31} + A_{42}a_{32} + A_{43}a_{33}\right|$$

$$+ A_{32}\,(A_{41}a_{11} + A_{42}a_{12} + A_{43}a_{13})\left|A_{41}a_{31} + A_{42}a_{32} + A_{43}\,a_{33}\right|$$

$$+ A_{33}\,(A_{41}a_{21} + A_{42}a_{22} + A_{43}a_{23})\left[1-(A_{41}a_{31} + A_{42}a_{32} + A_{43}a_{33})^2\right]^{1/2}$$

$$+ A_{34}\,(A_{41}a_{11} + A_{42}a_{12} + A_{43}a_{13})\left[1-(A_{41}a_{31} + A_{42}a_{32} + A_{43}a_{33})^2\right]^{1/2}$$

the Gibbs vector because of the redundancy in the kinematic formulation. For machine simulation studies, this additional complexity does not become too great a problem since the elements a_{ij} may be formed directly and substituted in appropriately at each instant. For analysis studies, however, the complete equations must appear directly, thus adding a computational burden. This additional complexity of manipulating an algebraically cumbersome set of state equations may then lead to increasing the order of the system (e.g., using direction cosines instead of Euler parameters or the Gibbs vector) in order to proceed.

3.3.4 Conclusions

In dealing with the dynamic and various kinematic state equations, it becomes evident that particular characterizations of the acquisition state equations should be used for particular classes of problems. For example, when considering control of a single axis, three direction cosines combined with Euler's dynamical equations yield the best and most useful formulation. This is true, in this case, for both analysis and simulation of acquisition. For three axis control, several formulations appear suitable. For analysis, the use of the Gibbs vector or Euler's symmetrical parameters yield suitable representations with low dimensionality. If characterizing the system becomes burdensome due to the complexity of the algebra resulting from these particular representations, then the use of direction cosines may allow the problem to be tractable even with the attendant increase in dimensionality. For simulation, Euler parameters and direction cosines are the most suitable representations. The Euler parameters are recommended because the advantages of a lower dimensional state vector will normally be greater than the disadvantages due to increased algebraic complexity in carrying out vector transformations.

The discussion on physical realizability makes clear the important role of the elements of the direction cosine matrix. Representation of these quantities with other parametric variables is straightforward, even though considerably more complex, and for machine studies and much hand analysis should not be overly cumbersome.

SECTION IV

AN ACQUISITION SYSTEM

4.1 Introduction

In this chapter, consideration is focused upon a specific acquisition system for which, under certain conditions, asymptotic stability in the large can be proven. The acquisition under consideration is that described in Sections I and II, namely the removal of the satellite angular momentum while pointing one of the satellite principle axes to an inertial reference. This type of acquisition was studied in detail by T. G. Windeknecht [18], whose results are summarized in this chapter. The control law utilized to perform this mission assumes the use of three ideal linear external torque sources, such as proportional gas jets. Body kinematic information consists of angular velocity measurements along each principal axis, and attitude information is provided in terms of the direction cosines relating the axis to be pointed to an inertially fixed coordinate set.

The body attitude can be conveniently described by relating the right handed, orthogonal body-fixed set which form the principal axes to a similar inertially-fixed set which possesses an axis, x_3^R, pointing in the direction of the desired satellite orientation. Denoting the former coordinate set by (x_1, x_2, x_3) and the latter by (x_1^R, x_2^R, x_3^R), an orthogonal matrix (a_{ij}) can be used to describe the vehicle attitude as in Equation (3.13). For convenience this transformation is repeated here.

$$\begin{bmatrix} x_1 \\ x_2 \\ x_3 \end{bmatrix} = \begin{bmatrix} a_{11} & a_{12} & a_{13} \\ a_{21} & a_{22} & a_{23} \\ a_{31} & a_{32} & a_{33} \end{bmatrix} \begin{bmatrix} x_1^R \\ x_2^R \\ x_3^R \end{bmatrix} \tag{4.1}$$

It is clear that once the body is properly aligned, $a_{13} = a_{23} = 0$, $a_{33} = 1$ while the remaining elements of (a_{ij}) can have any value subject to the constraints imposed by the orthogonal matrix.

Before considering this acquisition system in detail, a somewhat simpler system will be analyzed.

4.2 Momentum Removal

The acquisition requirements in this subsection are such that the final orientation of the satellite is immaterial. The only consideration of importance is the removal of the satellite angular momentum. Since the requirement involving the final orientation of a specific body principal axis is lifted, the analysis of this system is considerably easier.

4.2.1 Dynamic Equations of Motion

If ω_1, ω_2, and ω_3 represent the projections of the body angular rate $\bar{\omega}$ on its principal x_1, x_2, x_3 axes respectively, and if I_1, I_2, and I_3 are the corresponding moments of inertia, the dynamical equations are of the conventional Eulerian form of Equation (3.7). The three scalar components can be written as

$$\begin{aligned} I_1 \dot{\omega}_1 &= (I_2 - I_3)\,\omega_2\omega_3 + M_1 \\ I_2 \dot{\omega}_2 &= (I_3 - I_1)\,\omega_3\omega_1 + M_2 \\ I_3 \dot{\omega}_3 &= (I_1 - I_2)\,\omega_1\omega_2 + M_3 \end{aligned} \qquad (4.2)$$

where a super dot denotes differentiation and M_1, M_2, and M_3 are the control torques along the axis in question.

4.2.2 Asymptotic Stability in the Large

The most convenient way to establish sufficient conditions such that $(\omega_1, \omega_2, \omega_3)$ tend to (0, 0, 0) is to employ the Second Method of Lyapunov. That is, if $\bar{x} = (\omega_1, \omega_2, \omega_3)$, a scalar function $V(\bar{x})$ with continuous first partial derivatives is sought such that

$$\left.\begin{array}{lll} \text{(i)} & V(\bar{x}) > 0 & \text{for } \bar{x} \neq \bar{0} \\ \text{(ii)} & V(\bar{0}) = 0 & \\ \text{(iii)} & \dot{V}(\bar{x}) < 0 & \text{if } \bar{x} \neq \bar{0} \\ \text{(iv)} & V(\bar{x}) \to \infty & \text{as } ||x|| \to \infty \end{array}\right\} \tag{4.3}$$

For the problem at hand, the following function is considered

$$V = I_1^2 \omega_1^2 + I_2^2 \omega_2^2 + I_3^2 \omega_3^2 \tag{4.4}$$

Clearly this function satisfies conditions (i), (ii) and (iv) of Equation (4.3). Condition (iii) can be checked by time differentiating Equation (4.4) and utilizing Equations (4.2). The result is

$$\dot{V} = 2 [I_1 \omega_1 M_1 + I_2 \omega_2 M_2 + I_3 \omega_3 M_3] \tag{4.5}$$

Thus a sufficient condition to satisfy (iii) is that

$$\omega_i M_i < 0 \qquad (i = 1, 2, 3) \tag{4.6}$$

or, in other words, each body axis torque should be opposite in sign to the corresponding body rate.

A specific example of Equation (4.6) is to set

$$M_i = -k_i \omega_i \qquad (i = 1, 2, 3) \tag{4.7}$$

where k_i is a constant for each i. The practical implementation of Equation (4.7) then utilizes a rate gyro and a linear torquer on each body principal axis.

Note that the Lyapunov function defined by Equation (4.4) is merely the inner product of the angular momentum vector with itself. Denoting the magnitude of this vector by H(t), it is possible to bound the decay rate of the angular momentum in this example:

$$\epsilon^{-\tau_\ell (t-t_o)} \leq \frac{H(t)}{H(t_o)} \leq \epsilon^{-\tau_u (t-t_o)} \tag{4.8}$$

where

$$\left.\begin{aligned} \tau_u &= \frac{I_1^2 + I_2^2 + I_3^2}{\gamma_1} \\ \tau_\ell &= \frac{\gamma_2}{k_1 I_1 + k_2 I_2 + k_3 I_3} \end{aligned}\right\} \tag{4.9}$$

and

$$\left.\begin{aligned} \gamma_1 &= \min (k_1 I_1, k_2 I_2, k_3 I_3) \\ \gamma_2 &= \min (I_1, I_2, I_3) \end{aligned}\right\} \tag{4.10}$$

Utilizing Newton's rotational law directly, it is possible also to place a lower bound on the fuel consumed to remove the momentum. This lower bound is clearly proportional to $H(t_o)$ itself. In fact, $H(t_o)$ gives the greatest lower bound since a very large torque co-linear and opposite to the initial angular momentum vector will instantly reduce the momentum to zero before the body has had an opportunity to move. Clearly the integral of this torque is the impulse required and equals $H(t_o)$.

If a body axis requires pointing in addition to removing $H(t_o)$, a greater fuel penalty must be paid. This type of acquisition system will now be considered.

4.3 One Axis Acquisition

The requirement that a specific body axis must eventually point at some fixed reference point involves consideration of the direction cosine matrix given in Equation (4.1) in order to aptly describe the vehicle orientation. Actually, only three elements of the matrix (a_{ij}) must be determined in order that the body x_3 axis be completely described relative to the fixed inertial set. These elements, a_{13}, a_{23}, and a_{33} are easily determined via the kinematic equations of motion.

4.3.1 Kinematic Equations

Equations (3.43) can be written

$$\begin{aligned} \dot{a}_{13} &= -\omega_2 + \omega_2 \beta + \omega_3 a_{23} \\ \dot{a}_{23} &= \omega_1 - \omega_1 \beta - \omega_3 a_{13} \\ \dot{\beta} &= \omega_1 a_{23} - \omega_2 a_{13} \end{aligned} \tag{4.11}$$

where

$$\beta = 1 - a_{33} \tag{4.12}$$

4.3.2 Control Law

It remains to select a control law, namely, to precisely specify M_1, M_2, and M_3 of Equation (4.2). In attempting to establish the proper control philosophy in orienting a single axis, Windeknecht demonstrated the desirability of incorporating in M_1 a term proportional to $-a_{23}$ and including in M_2 a term proportional to a_{13}. The results of Section 4.2.2 indicate that rate dependent terms should also be included in the driving torques, and thus the following control law is suggested.

$$\left.\begin{aligned} M_1 &= -k_1 \omega_1 - c_2 a_{23} \\ M_2 &= -k_2 \omega_2 + c_1 a_{13} \\ M_3 &= -k_3 \omega_3 \end{aligned}\right\} \qquad (4.13)$$

Equations (4.2), (4.11), (4.12), and (4.13) completely describe the problem being analyzed. Interest is now focused upon the stability of this system, namely under what conditions (ω_1, ω_2, ω_3, a_{13}, a_{23}, β) approach zero with increasing time.

4.3.3 Asymptotic Stability

As in Section 4.2.2, the aim is again to establish a Lyapunov function in order to prove asymptotic stability in the large; that is, to find a function $V(\bar{x})$ which satisfies Equation (4.3) where in this case $\bar{x} = (\omega_1, \omega_2, \omega_3, a_{13}, a_{23}, \beta)$. The corresponding linear system suggests, as a possible candidate function

$$V = \frac{1}{2}\left[I_1 \omega_1^2 + I_2 \omega_2^2 + I_3 \omega_3^2 + 2 A_1 I_1 \omega_1 a_{23} - 2 A_2 I_2 \omega_2 a_{13} + 2 B \beta\right] \qquad (4.14)$$

where A_1, A_2, and B are constants which remain to be specified. If the norm $||\ ||$ is chosen to be the Euclidean norm, conditions (ii) and (iv) of Equation (4.3) are immediately satisfied. By the familiar process of "completing the square," Equation (4.14) can be rewritten in the form

$$V = \frac{1}{2}\left[I_1 (\omega_1 + A_1 a_{23})^2 + I_2 (\omega_2 - A_2 a_{13})^2 + I_3 \omega_3^2 + B\beta^2 + (B - I_2 A_2^2)\, a_{13}^2 + (B - I_1 A_1^2)\, a_{23}^2\right] \tag{4.15}$$

from which it follows that V is positive definite (condition 1), if

$$B > I_1 A_1^2 > 0$$
$$B > I_2 A_2^2 > 0 \tag{4.16}$$

It remains to consider condition (iii). Differentiating Equation (4.14), and utilizing Equations (4.2), (4.11), and (4.13); then employing the arbitrary constraint

$$B = A_1 k_1 + c_2 = A_2 k_2 + c_1 \tag{4.17}$$

and finally employing "completing the square" techniques again, the result is

$$-\dot{V} = (k_1 - A_1 I_1 a_{33})\left\{\omega_1 + \frac{a_{13}[A_2 I_3 + (A_1 - A_2) I_1]}{2[k_1 - A_1 I_1 a_{33}]}\omega_3\right\}^2 + (k_2 - A_2 I_2 a_{33})\left\{\omega_2 + \frac{a_{23}[A_1 I_3 + (A_2 - A_1) I_2]}{2[k_2 - A_2 I_2 a_{33}]}\omega_3\right\}^2 +$$

(Equation continued on next page)

$$+\left\{ k_3 - \frac{a_{13}^2 \left[A_2 I_3 + (A_1 - A_2) I_1\right]^2}{4\left[k_1 - A_1 I_1 a_{33}\right]} - \frac{a_{23}^2 \left[A_1 I_3 + (A_2 - A_1) I_2\right]^2}{4\left[k_2 - A_2 I_2 a_{33}\right]} \right\} \omega_3^2$$

$$+ A_1 c_2 a_{23}^2 + A_2 c_1 a_{13}^2 \qquad (4.18)$$

Sufficient conditions to insure the positive semi-definiteness of $\dot{V}$ (this is adequate since $\dot{V} = 0$ occurs only at $\bar{x} = 0$ or at unstable critical points) can now be deduced. These conditions combined with Equations (4.16) reduce to the following requirements for satisfaction of Equation (4.3).

$$\left.\begin{aligned} & A_1 k_1 + c_2 = A_2 k_2 + c_1 = B \\ & k_1 > A_1 I_1 > 0 \\ & k_2 > A_2 I_2 > 0 \\ & c_1 > 0 \\ & c_2 > 0 \\ & k_3 \geq \frac{\left[A_1 I_1 + A_2 (I_3 - I_1)\right]^2}{4 (k_1 - A_1 I_1)} + \frac{\left[A_2 I_2 + A_1 (I_3 - I_2)\right]^2}{4 (k_2 - A_2 I_2)} \end{aligned}\right\} \qquad (4.19)$$

This gives the final result. The single-axis-pointing acquisition system described by Equations (4.2), (4.11) and (4.13) is asymptotically stable in the large to the origin provided Equations (4.19) are satisfied. It should be noted, however, that these conditions are merely sufficient to insure this result, but are not in general necessary.

4.3.4 Parameter Variations

From the standpoint of physical realizability it is desirable that asymptotic stability in the large be attained for small values of the constants k_1, k_2, k_3, c_1, and c_2 otherwise, severe constraints may be placed upon the required saturation levels of the control system physical hardware. Conditions (4.19) can be used to study this situation.

First of all, it is clear that c_1 and c_2 can be selected arbitrarily small, but positive, without affecting the system stability. A practical lower limit for these parameters is thus dictated by the system response time requirements. On the other hand, arbitrarily small values of all five parameters cannot be implied from Equation (4.19) unless c_1 and c_2 are equal. From a practical standpoint, this condition cannot be guaranteed and thus finite values of the rate gain constants are required to satisfy Equation (4.19).

The interpretation of Equation (4.19) is dependent upon A_1 and A_2 which are not system physical parameters. A more practical insight is obtained by considering computer solutions of this acquisition system, deriving therefrom such information as convergence time and fuel consumption. This is one of the tasks considered in Section V.

4.3.5 Conclusions

The one-axis-pointing acquisition system utilizing the control law of Equation (4.13) has been demonstrated to possess asymptotic stability in the large under suitable restrictions of the control parameters. This is a highly significant result in that stability information regarding a given acquisition system is generally very difficult to obtain by analytic means, and the trial and error

approach based upon computer solutions is normally the only general method of obtaining some sort of stability confidence. This latter method is not foolproof. Thus, from a purely operational viewpoint, if the appropriate equipment is judged suitable for the application, there appears to be no strong motivation for adopting other control forms for most acquisition systems requiring the pointing of a single axis. If cost and reliability constraints are very severe, it may be desirable to alter the control law of Equation (4.16) to form a more suitable to the preferred sensing and control equipment. The comparison of systems employing different sensing and torquing methods is the subject of Section V.

SECTION V

ACQUISITION SYSTEMS COMPARISON

5.1 Idealized Proportional System

5.1.1 Description

The acquisition system described in Section IV was selected as a reference system for the comparison studies discussed in this section. For this idealized proportional-torque system complete stability was established for significant ranges of the system parameters. Therefore, parameter variations required to establish optimal control with respect to various criteria can be accomplished without undue concern for instability. Additionally, control gain changes, as effectively introduced by torque or sensor saturation, would not be expected to affect the proven stability seriously. As additional modifications are incorporated into the idealized design the probability of instability is greater. However, in that case the concepts described in Section VII appear practical in continuing to guarantee the stability.

Although the idealized proportional system of Section IV is physically realizable, at least for bounded initial conditions, its implementation for practical application may require more than minimum weight and power and less than attainable system reliability (from utilization of proportional torque sources). Therefore it is desirable to investigate the effects of more practically implemented torquing and sensing systems on performance. In any case the ideal system can be used as a reference for comparison with the common types of acquisition systems where: 1) bang-bang control of the mass expulsion torquing system is utilized, 2) attitude information is obtained from saturating sensors or gimbal angle pickoffs of inertially referenced platforms, and 3) rate is sensed by rate gyros, computed via suitable body rate approximation formulae, or derived via

lead-lag networks on the attitude errors, or obtained from some combination thereof. The purpose of the comparisons described in this section is to determine the relative performance of various systems comprised of these characteristics. In this way the relative worth of the idealized proportional system as opposed to one of the more practically implemented modifications can be established. Additionally, the significance of the modifications within themselves can be evaluated.

In the simulation study comparing various acquisition systems, the idealized proportional system was first simulated in the previously described form where the roll and pitch axis control signals are obtained from rate gyros and ideal linear direction cosine sensors to produce a linear proportional control torque. The study assumes that only the minimum inertia axis (yaw) is to be pointed, hence the yaw control torque is linearly proportional to a yaw rate gyro signal. In all of the systems investigated, the yaw gyro was always included as a fixed system control law.

The dynamical equations of the idealized proportional system, Equations (4.2) can be written normalized to I_2 as

$$\begin{aligned} \alpha \dot{\omega}_1 &= (1-\beta)\ \omega_2 \omega_3 + \gamma_1 \\ \dot{\omega}_2 &= (\beta-\alpha)\ \omega_1 \omega_3 + \gamma_2 \\ \beta \dot{\omega}_3 &= (\alpha-1)\ \omega_1 \omega_2 + \gamma_3 \end{aligned} \qquad (5.1)$$

where the subscripts 1, 2, 3 refer to roll, pitch, and yaw axes, respectively, and

ω_i - body rate about the i-th principal inertia (control) axis

γ_i - proportional control acceleration about the i-th axis, $\frac{M_i}{I_2}$

α - roll to pitch inertia ratio

β - yaw to pitch inertia ratio

Note that the γ_i terms have dimensions of rad/sec^2 since they represent control torque to pitch inertia ratios. The control acceleration terms can then be expressed as

$$\left.\begin{aligned} \gamma_1 &= -k_1 \omega_1 - c_1 a_{23} \\ \gamma_2 &= -k_2 \omega_2 + c_2 a_{13} \\ \gamma_3 &= -k_3 \omega_3 \end{aligned}\right\} \qquad (5.2)$$

where

k_1 - normalized roll rate gain, sec^{-1}

k_2 - normalized pitch rate gain, sec^{-1}

k_3 - normalized yaw rate gain, sec^{-1}

c_1 - normalized roll position gain, sec^{-2}

c_2 - normalized pitch position gain, sec^{-2}

The kinematic equations are given by Equations (3.43) as

$$\left.\begin{aligned} \dot{a}_{13} &= \omega_3 a_{23} - \omega_2 a_{33} \\ \dot{a}_{23} &= \omega_1 a_{33} - \omega_3 a_{13} \\ \dot{a}_{33} &= \omega_2 a_{13} - \omega_1 a_{23} \end{aligned}\right\} \qquad (5.3)$$

The normalized impulse (I_n) and the convergence time (t_c) are nominally assumed to be the acquisition systems' error criteria. Assuming equal gas jet lever arms, the normalized total impulse over the acquisition time interval t_c is defined to be

$$I_n = \int_o^{t_c} \sum_{i=1}^{3} |\gamma_i| \, dt \quad \text{sec}^{-1} \tag{5.4}$$

In the subsequent comparison of the acquisition systems, the system gains were varied for each new case with the object of minimizing a combination of t_c and I_n through the use of analog repetitive operation visual display techniques. To avoid the necessity for obtaining individual optimal solutions for each performance criterion, it has been found to be of value to define a weighting factor called the impulse utilization ratio to aid in the acquisition systems comparisons. Let the normalized initial momentum vector be defined as

$$\bar{H}_{t_n}(o) = \alpha \omega_x(o) \, \bar{e}_x + \omega_y(o) \, \bar{e}_y + \beta \omega_z(o) \, \bar{e}_z$$

with magnitude

$$\left| H_{t_n}(o) \right| = \left\{ [\alpha \omega_x(o)]^2 + [\omega_y(o)]^2 + [\beta \omega_z(o)]^2 \right\}^{1/2}$$

Then, define the impulse utilization ratio (R) to be

$$R \triangleq \frac{I_n}{\left| H_{t_n}(o) \right|}$$

As discussed in Section 4.2.2, $\left| H_{t_n}(o) \right|$ is a lower bound on the normalized fuel needed for acquisition. A single performance criterion (Φ) which combines the effect of both time and impulse penalties is then given by

$$\Phi = (t_c)(R) \quad \text{sec} \tag{5.5}$$

5.1.2 Performance of Idealized Proportional (IP) System

The idealized proportional system performance is optimized for system gains consistent with maximum analog scaling after appropriate rate to position gain ratios are selected. Runs were taken for initial body rates given by

$$\bar{\omega}(o) = 10 \sum_{i=1}^{3} \delta_i \bar{x}_i \left(\frac{\text{deg}}{\text{sec}}\right)$$

where each δ_i (i = 1, 2, 3) equals either +1 or -1. Table 5.1 presents the average values of t_c, I_n and Φ for the eight possible runs implied by the above equation assuming no initial attitude error. Similar results are also presented for a 4 deg/sec body rate in each axis.

TABLE 5.1

IDEALIZED PROPORTIONAL SYSTEM PERFORMANCE SUMMARY

(α = 1.15, β = .486)

Case	Initial Rate	k_1, k_2	k_3	c_1, c_2	$\bar{t}_c$(sec)	$\bar{I}_n(\text{sec}^{-1})$	Φ(sec)
IP-1	10 deg/sec	.25	.125	.05	26	.65	60
IP-2	4 deg/sec	.20	.10	.02	24	.25	53

Example recordings of the above cases in Table 5.1 are given in Figure 5.1 for Case IP-1 and in Figure 5.2 for Case IP-2. In Table 5.1 notice that the best position gains, c_1 and c_2, vary in direct proportion to the initial rates. On the other hand, the best rate gains, k_1, k_2 and k_3, are nearly independent of the initial rate. Of further significance is that the convergence time, t_c, is nearly the same for the two cases whereas the normalized impulse varies in direct proportion to the magnitude of the initial rates. For both initial rate conditions the impulse utilization ratio, R, is about 1.4. The normalized performance criterion Φ is nearly unchanged for the two cases thereby reflecting its intended insensitivity to the initial conditions.

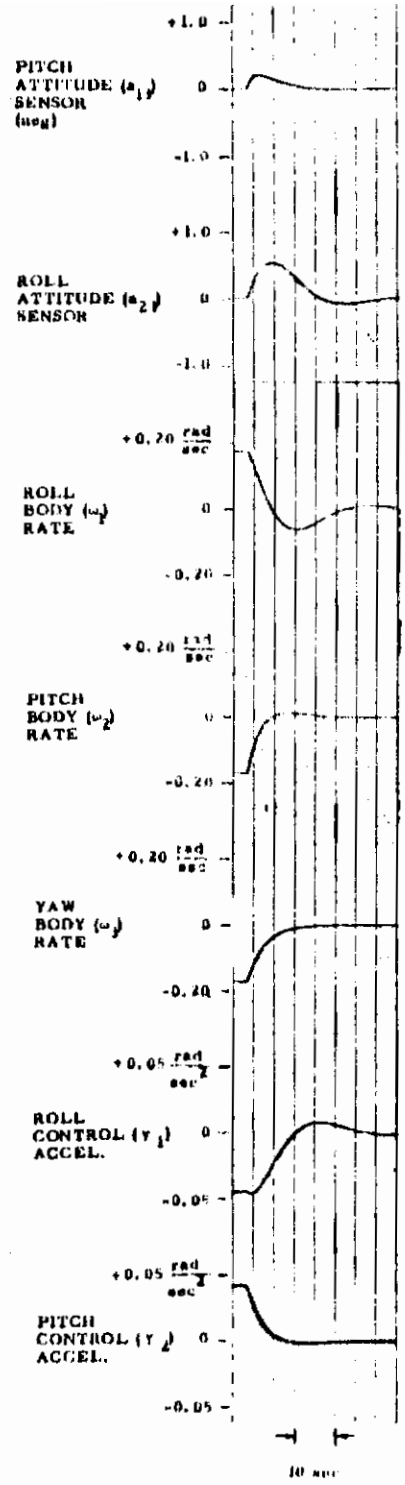

Figure 5.1 Acquisition of Idealized Proportional System (ω_o = 10 deg/sec)

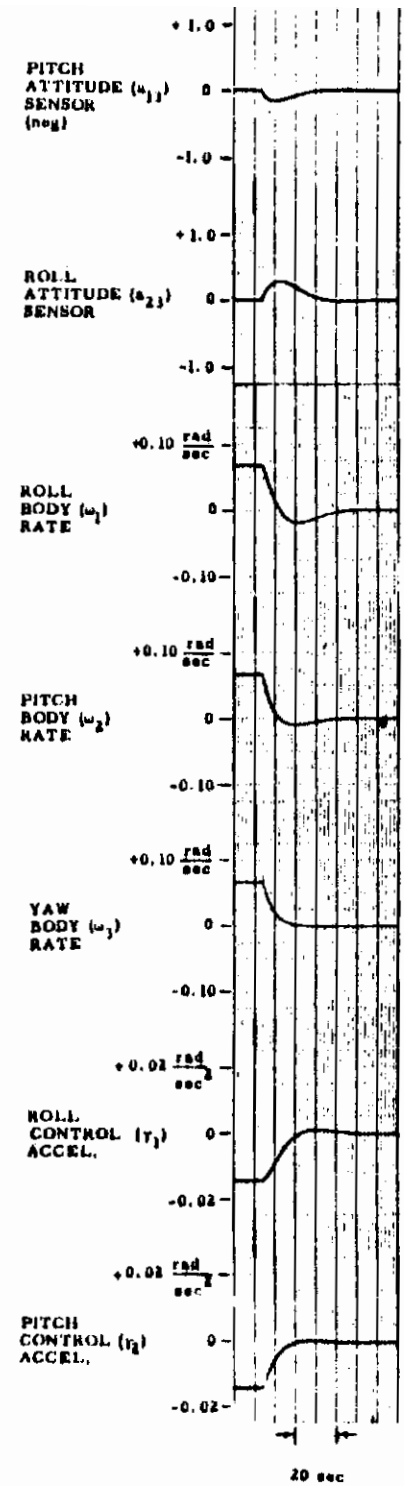

Figure 5.2 Acquisition of Idealized Proportional System (ω_o = 4 deg/sec)

In Figure 5.1, Case IP-1, the initial control accelerations in pitch and roll are nearly 0.05 rad/sec^2 whereas in Figure 5.2, Case IP-2, these initial values are reduced in proportion to the initial rates. Degradation in the noted performance would be expected if the maximum available control accelerations were reduced below these commanded values. In the next section, the performance is considered when these constraints are added to the control sources. Other effects, such as sensor saturation, are also evaluated.

5.2 Direction Cosine Attitude Sensing

5.2.1 Torque Modes

The first comparison of acquisition systems with respect to the IP system was made by considering torque modes other than the proportional mode. Maintaining the control mechanization as direction cosine attitude information and three rate gyros, both saturating proportional (SP) and bang-bang (BB) torque were utilized with three control acceleration saturation levels and the effect on the performance criteria evaluated. The acceleration levels used are noted in Table 5.2. In each case, the value of the acceleration for the first saturation level corresponds to one-half the maximum value required in the idealized proportional case of the previous section. Also shown in Table 5.2 are the ranges of control law gain parameters found effective in establishing the best system performance for the systems to be described.

The results of changing the torque mode are noted in Figure 5.3. These results were obtained in the same way as those reported in Table 5.1 (average over eight initial conditions) for a 4 deg/sec initial velocity on each body axis. In comparison with the IP performance criteria the proportional saturating torque produces a value of Φ about 10% higher. Further altering the system by saturating the direction cosine sensors at 0.7 results in a 15% increase in Φ.

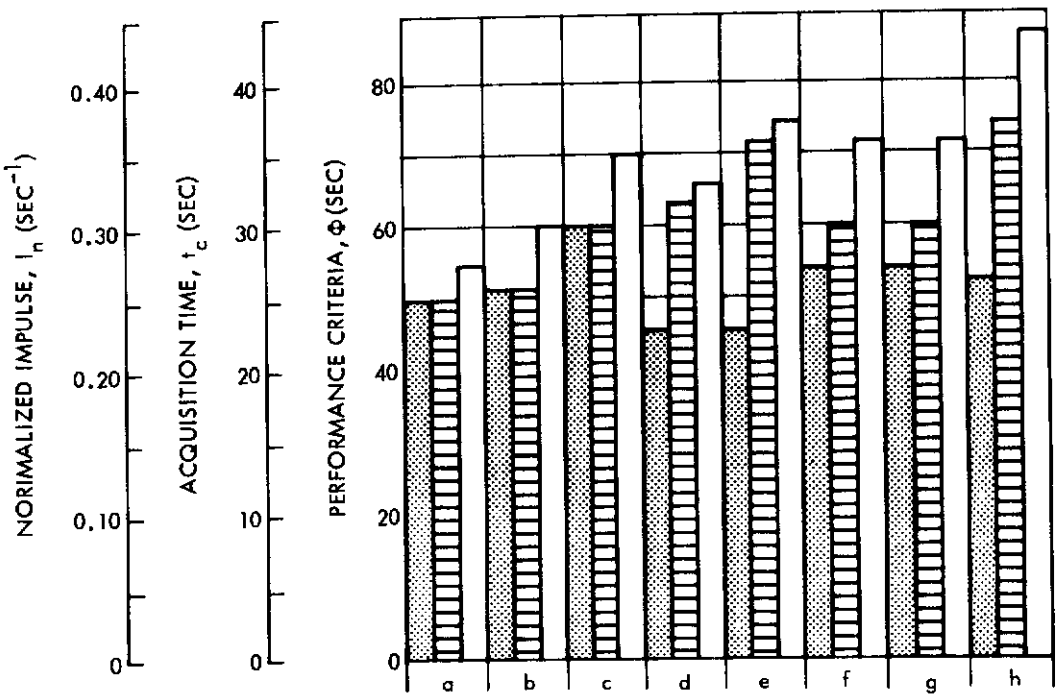

KEY

I_n

t_c

Φ

*IDEAL PROPORTIONAL (IP)
**PROPORTIONAL SATURATING (PS)
***BANG BANG (BB)

CASE	TORQUE MODE	SENSOR SATURATION LEVEL
a	IP*	NONE
b	PS**	NONE
c	PS	0.70
d	PS	0.50
e	PS	0.25
f	BB***	0.70
g	BB	0.50
h	BB	0.25

Figure 5.3 Comparison of Torque Modes for Control Saturation Level One (Direction Cosine and Rate Gyros)

TABLE 5.2

SYSTEM PARAMETERS FOR ACQUISITION

SYSTEMS COMPARISON

System Parameter	Symbol	Range of Values	
Roll control acceleration	γ_1	$\gamma_{1s1} = .0100$ rad/sec^2 $\gamma_{1s2} = .0050$ rad/sec^2 $\gamma_{1s3} = .0025$ rad/sec^2	
Pitch control acceleration	γ_2	$\gamma_{2s1} = .0100$ rad/sec^2 $\gamma_{2s2} = .0050$ rad/sec^2 $\gamma_{2s3} = .0025$ rad/sec^2	
Yaw control acceleration	γ_3	$\gamma_{3s1} = .0050$ rad/sec^2 $\gamma_{3s2} = .0025$ rad/sec^2 $\gamma_{3s3} = .00125$ rad/sec^2	
Roll to pitch inertia ratio	α	1.15	
Yaw to pitch inertia ratio	β	.486	
		Direction Cosine Cases	Euler Angle Cases
Roll rate gain	k_1	$.12 \leq k_1 \leq .20 \text{sec}^{-1}$	$.10 \leq k_1 \leq 1.0 \text{sec}^{-1}$
Pitch rate gain	k_2	$.12 \leq k_2 \leq .20 \text{sec}^{-1}$	$.16 \leq k_2 \leq .20 \text{sec}^{-1}$
Yaw rate gain	k_3	$.005 \leq k_3 \leq .020 \text{sec}^{-1}$	$.005 \leq k_3 \leq .015 \text{sec}^{-1}$
Roll position gain	c_1	$.010 \leq c_1 \leq .020 \text{sec}^{-2}$	$.015 \leq c_1 \leq .080 \text{sec}^{-2}$
Pitch position gain	c_2	$.010 \leq c_2 \leq .020 \text{sec}^{-2}$	$.014 \leq c_2 \leq .040 \text{sec}^{-2}$

Finally, by changing to a bang-bang torque mode (with negligible deadzone) and with the same sensor saturation level, (f), little further increase in Φ results. The total degradation in performance criterion from case (b) to (f) is 20%. Other values of Φ are also given for lower sensor saturation levels while maintaining the same control acceleration level.

From Figure 5.3 notice that both t_c and I_n are slightly degraded in the proportional saturating case, as compared to the idealized proportional system. This was expected, since the saturated acceleration is less than the initial commanded control acceleration of the IP system.

For a particular saturated acceleration level, the normalized impulse decreases as the saturation level of the sensors is reduced. Conversely the time to converge increases. This result was further evidenced in the optimization study to be described in Section VI. There the optimal sensor saturation levels within certain constraints were established.

For a particular sensor saturation value, both the impulse and time increase for lower control acceleration saturation levels. This is evidenced by comparing the general scaling in Figures 5.3 through 5.5 inclusive. Typical recordings of cases (c) and (f) of Figure 5.3 are shown in Figures 5.6 and 5.7, respectively.

5.2.2 Saturated Attitude Sensing

It can be seen that for the relatively large control accelerations, the effect of lowering the sensor saturation level is not large. In Figure 5.4 where the performance criteria are presented for the same conditions as in Figure 5.3, but with half the saturated acceleration level, the proportional saturating torque cases are compared to the bang-bang torque cases for three levels of sensor saturation. There is no significant change in criteria for the various cases, although one notes that the values of Φ for these cases are about twice those for the corresponding cases in Figure 5.3.

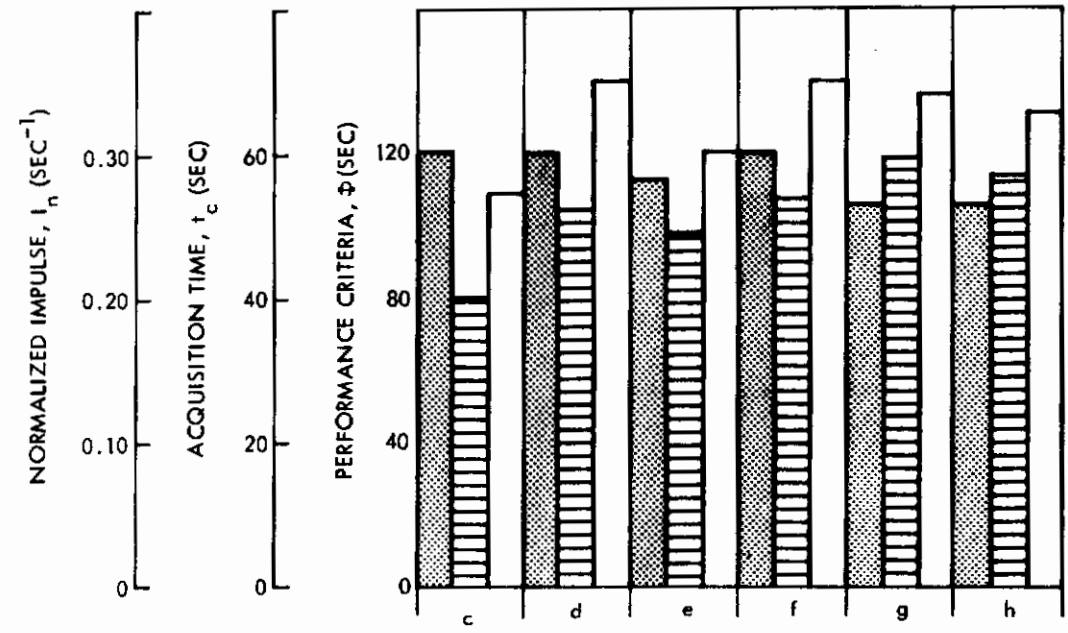

CASE	TORQUE MODE	SENSOR SATURATION LEVEL
c	PS*	0.70
d	PS	0.50
e	PS	0.25
f	BB**	0.70
g	BB	0.50
h	BB	0.25

*PROPORTIONAL SATURATING (PS)
**BANG BANG (BB)

Figure 5.4 Comparison of Torque Modes for Control Acceleration Level Two (Direction Cosine and Rate Gyros)

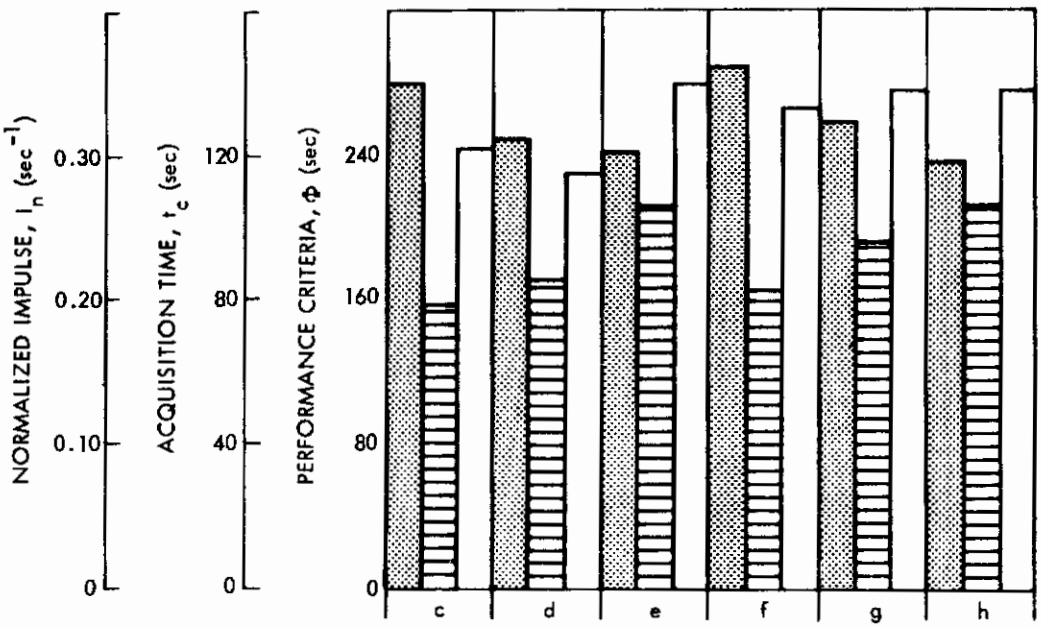

KEY

I_n

t_c

Φ

* PROPORTIONAL SATURATING (PS)
** BANG-BANG (BB)

CASE	TORQUE MODE	SENSOR SATURATION LEVEL
c	PS*	0.70
d	PS	0.50
e	PS	0.25
f	BB**	0.70
g	BB	0.50
h	BB	0.25

Figure 5.5 Comparison of Torque Modes for Control Acceleration Level Three (Direction Cosine and Rate Gyros)

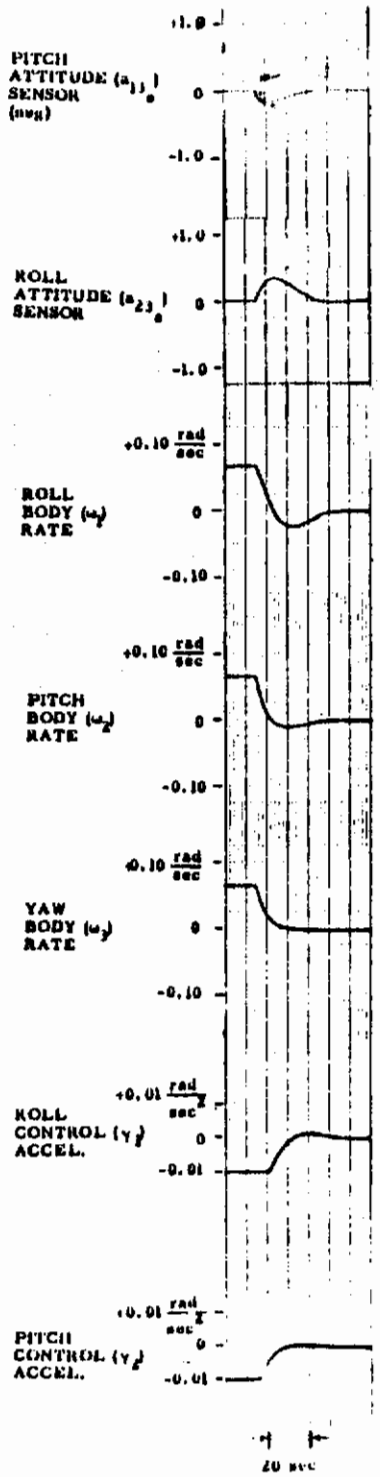

Figure 5.6 Acquisition of Proportional Saturating System (Sensor Saturation Level = 0.7)

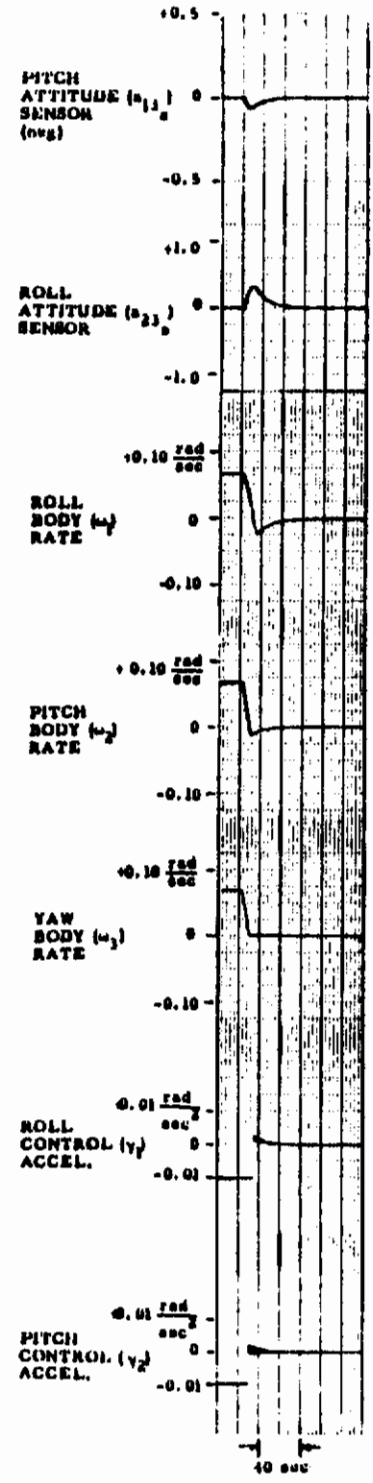

Figure 5.7 Acquisition of Bang-Bang System (Sensor Saturation Level = 0.7)

The same comparison of torque modes for the three sensor saturation levels is repeated in Figure 5.5 for 1/4 the saturation levels considered in Figure 5.3. In this case the decrease in normalized impulse and increase in time with decreases in attitude sensor saturation level is more pronounced. The average value of Φ for all the cases shown is about twice the average value obtained for Figure 5.4. Evidently this performance criterion is nearly linearly related to the control acceleration level for the direction cosine sensors and three rate gyro cases. By maintaining this idealized control law for each axis, the acquisition system performance is clearly dominated by the control acceleration level in a proportional manner, with the sensor saturation level producing a secondary effect over the range of levels considered. A further result of the information contained in Figures 5.3 to 5.5 concerns the bang-bang torque mode performance. Referring to Figure 5.1, note that the bang-bang torque mode at the highest torque saturation level and sensor saturation levels as low as 0.5 (cases (f) and (g)) only results in about a 33% increase in Φ compared to the IP case. The attitude sensor saturation effect is not overly significant at large control acceleration levels and the system is still a good approximation to the IP system.

5.3 Comparison of Rate Sensing Schemes with Saturated Direction Cosine Attitude Sensing and Bang-Bang Torque

Various rate sensing schemes were evaluated for the three levels of sensor saturation and the three levels of control acceleration in the bang-bang torque mode. In all of the rate sensing control laws investigated the yaw gyro is maintained in the system. Therefore, only the method of roll and pitch rate sensing will be discussed. The results of all the different rate sensing modes are presented in tabular form in Table 5.3 where the average values of convergence time ($\bar{t}_c$), normalized impulse ($\bar{I}_n$), and performance criteria (Φ) are presented as obtained from initial rates of 4 deg/sec about all control axes. In each case, the system gains were first selected to "minimize" t_c and I_n by noting the effect of each system gain value independently. The

TABLE 5.3

RATE SENSING MODES VS. CONTROL ACCELERATION LEVEL

RESULTS FOR THREE DIRECTION COSINE SATURATION

AND THREE BANG-BANG TORQUING LEVELS

(Initial rates of 4^{o}/sec each control axis)

Direc. Cosine Sensor Saturation Level	Rate Sensing Roll	Rate Sensing Pitch	Control Acceleration Level** γ_{is1} $\bar{t}_c$	$\bar{I}_n$	Φ	γ_{is2} $\bar{t}_c$	$\bar{I}_n$	Φ	γ_{is3} $\bar{t}_c$	$\bar{I}_n$	Φ
0.70	G	G	30	.27 *	72	52	.30 *	140	82	.36 *	263
	IC	IC	26	.28 *	65	44	.32 *	126	82	.40 *	286
	AC	AC	24	.29 *	62	50	.32 *	143	84	.47 *	352
	SC	SC	32	.29 *	83	52	.31 *	144	120	.54 *	579
	ASC	ASC	27	.30	72	46	.35	144	117	.54	565
	PD	SC	26	.29 *	67	48	.32 *	137	124	.58 *	642
	PD	PD	26	.29 *	67	50	.32 *	143	122	.62 *	675
0.50	G	G	30	.27 *	72	52	.30 *	139	96	.32 *	274
	IC	IC	32	.27 *	77	50	.31 *	138	84	.40 *	300
	AC	AC	32	.28 *	80	56	.30 *	150	88	.47 *	370
	SC	SC	36	.28 *	90	56	.30 *	150	128	.56 *	640
	ASC	ASC				42	.35	132	113	.53 *	535
	PD	SC	28	.28 *	70	50	.31 *	138	124	.57 *	630
	PD	PD				50	.31 *	152	122	.62 *	675
0.25	G	G	36	.23	74	58	.26	135	104	.30	279
	IC	IC	32	.26 *	75	60	.25 *	134	110	.54	530
	AC	AC	30	.28 *	75	60	.26 *	139	110	.43 *	425
	SC	SC	30	.28 *	75	56	.28 *	140	126	.54 *	608
	ASC	ASC	31	.27	75	52	.30	139	119	.50	531
	PD	SC	32	.26 *	74	58	.39 *	202	134	.68 *	814
	PD	PD	28	.31 *	73	72	.39 *	250	167	.79	1180

* not average value of all rate sign combinations.

** the γ_{is} levels are given in Table 5.2

KEY

G - Gyro	ASC - Approximate Simplified Computed
IC - Ideal Computed	PD - Pure Derived
AC - Approximate Computed	
SC - Simplified Computed	

range of system gains required was given in Table 5.2. Symbols appearing in Table 5.3 are defined in the following sections as each rate sensing system is discussed.

5.3.1 Gyro Rate Sensing (G)

The system control laws utilize, as before, saturated direction cosine sensing and three rate gyros. For the largest control acceleration level, γ_{is1}, this case corresponds most closely to the IP system. Referring to Table 5.3, note that for equivalent values of $\bar{I}_n$, the convergence time with the "best" system gains is about 30 sec for γ_{is1} compared to 24 sec for the IP case. As the γ_{is} level is reduced, the degradation is marked as noted previously in Figures 5.3 to 5.5. For γ_{is3} the convergence time is from 82 to 104 sec depending upon the sensor saturation level.

5.3.2 Ideal Computed Body Rate Sensing (IC)

For this control law, the pitch and roll gyros are removed and it is assumed that the derivative of the direction cosine attitude error is available over the nonsaturated region. Practically this may be implemented by differencing the output of a lead-lag following the sensor with the sensor output. To include the effect of sensor saturation, the following variables are defined

$$f_{13} = \begin{cases} a_{13}, & |a_{13}| < a_{13_s} \\ a_{13_s}, & |a_{13}| \geq a_{13_s} \end{cases} \qquad (5.5)$$

where

a_{13_s} = pitch sensor saturation level

$$f_{23} = \left\{ \begin{array}{l} a_{23},\ |a_{23}| < a_{23_s} \\ a_{23_s},\ |a_{23}| \geq a_{23_s} \end{array} \right\} \tag{5.6}$$

where

a_{23_s} = roll sensor saturation level

$$\dot{f}_{13} = \left\{ \begin{array}{l} \dot{a}_{13},\ |a_{13}| < a_{13_s} \\ 0,\ |a_{13}| \geq a_{13_s} \end{array} \right\} \tag{5.7}$$

and

$$\dot{f}_{23} = \left\{ \begin{array}{l} \dot{a}_{23},\ |a_{23}| < a_{23_s} \\ 0,\ |a_{23}| \geq a_{23_s} \end{array} \right\} \tag{5.8}$$

From the kinematic Equation (5.3), the ideal computed body rates are

$$\left. \begin{array}{l} \omega_1 = \dfrac{\dot{a}_{23} + \omega_3 a_{13}}{a_{33}} \\ \omega_2 = \dfrac{-\dot{a}_{13} + \omega_3 a_{23}}{a_{33}} \end{array} \right\} \tag{5.9}$$

Equations (5.9) represent a method of replacing the rate gyros by computational means. With ideal pure derived rate and non-saturating scanners the body rates could be exactly computed by this method. The yaw rate gyro information, ω_3, is still assumed and, although the pitch

and roll gyros have been eliminated, knowledge of a_{33} is assumed. Including the effect of the sensor saturation, the "ideal" computed body rates are defined to be

$$\omega_{1_c} = \frac{\dot{f}_{23} + \omega_3 f_{13}}{a_{33}}$$

$$\omega_{2_c} = \frac{-\dot{f}_{13} + \omega_3 f_{23}}{a_{33}} \qquad (5.10)$$

Equations (5.10) were utilized in the simulation of this control law.

By reference to Table 5.3, note that for sensor saturation levels of 0.7 and 0.5 there is little difference in performance between the (IC) and the gyro (G) control laws. At the low value of sensor saturation (0.25), a degradation of 1% appears for γ_{is2} and a degradation of 90% is obtained for γ_{is3} for the (IC) case.

Typical recordings of the (G) and (IC) cases are shown in Figures 5.8 and 5.9, respectively, for the lowest sensor saturation level and γ_{is3}, the lowest considered acceleration saturation levels.

The required modification to the analog simulation for this control law is given in Appendix B.

5.3.3 Approximate Computed Body Rate Sensing (AC)

A further approximation to the computed body rates may be obtained by neglecting the ω_3 terms in Equations (5.10). This approach possesses merit in attempting to simplify the computational requirements and validity since the neglected terms are of second order near the equilibrium point. The (AC) terms are defined as

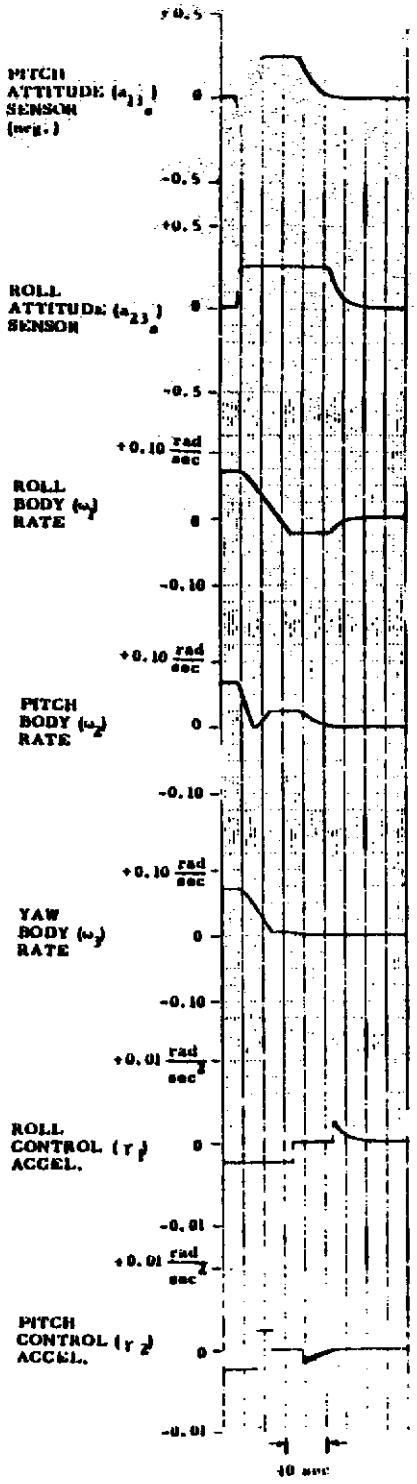

5.8 Acquisition of Bang-Bang System (G, γ_{is3}, Sensor Saturation Level = 0.25)

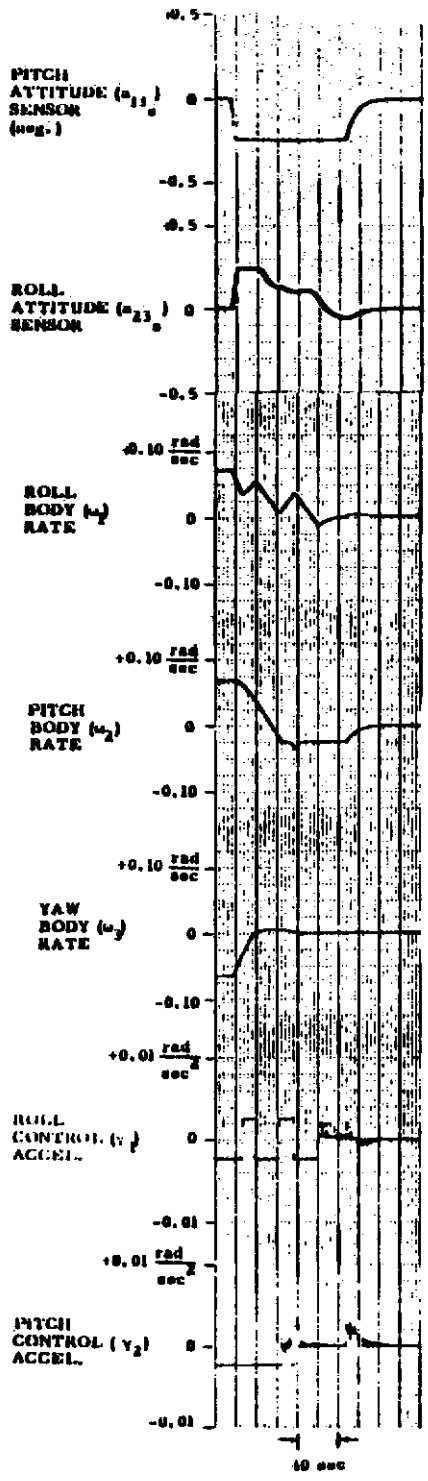

Figure 5.9 Acquisition of Bang-Bang System (IC, γ_{is3}, Sensor Saturation Level = 0.25)

$$\left.\begin{aligned} \omega'_{1c} &= \frac{\dot{f}_{23}}{a_{33}} \\ \omega'_{2c} &= \frac{-\dot{f}_{13}}{a_{33}} \end{aligned}\right\} \qquad (5.11)$$

Replacing the ω_{ic} terms with the ω'_{ic} terms in the simulation, the (AC) results in Table 5.3 are obtained. The values are about the same as for the (IC) case with the exception of lowest sensor saturation and γ_{is3}.

5.3.4 Simplified Computed Body Rate Sensing (SC)

To reduce the amount of required information for this control law, assume that only the sign of a_{33} is available and its magnitude is to be computed from the saturating scanner outputs, i.e.,

$$a_{33_a} = \text{sgn } a_{33} \sqrt{1 - f_{13}^2 - f_{23}^2}$$

and define

$$\left.\begin{aligned} \omega''_{1c} &= \frac{\dot{f}_{23}}{a_{33_a}} \\ \omega''_{2c} &= \frac{-\dot{f}_{13}}{a_{33_a}} \end{aligned}\right\} \qquad (5.12)$$

Replacing the ω'_{ic} terms with the ω''_{ic} terms, the (SC) results in Table 5.3 are obtained. Again for γ_{is1} and γ_{is2} the results are about the same as for all the previous cases. For γ_{is3}, significant performance degradation occurs at all sensor saturation levels with an average increase in performance criteria of 59% with respect to (AC) and 124% relative to (G).

5.3.5 Approximate Simplified Computed Body Rate Sensing (ASC)

For this case the a_{33_a} magnitude information is neglected and only the sign of a_{33} is utilized. In this case the rate information becomes

$$\left.\begin{aligned} \omega'''_{1c} &= \dot{f}_{23} \operatorname{sgn} a_{33} \\ \omega'''_{2c} &= -\dot{f}_{13} \operatorname{sgn} a_{33} \end{aligned}\right\} \qquad (5.13)$$

For practical application this represents the most easily implemented approximation to Equations (5.9) and, therefore, may be of considerable interest.

Referring again to Table 5.3 and taking cognizance of the remarks in Section 5.3.4, it is apparent that the (ASC) results agree with the (SC) results and no further degradation in performance has been obtained by neglecting the a_{33_a} magnitude information. It seems intuitively reasonable to expect this since for γ_{is1} and γ_{is2} the performance is insensitive to sensor saturation level and for γ_{is3} the performance is torque limited such that only the appropriate sign of the rate term is required.

5.3.6 Pure Derived Rate Sensing (PD)

The final approximation to the ideal control law for the direction cosine scanner system consists of the assumption that no a_{33} information is available and the error signals to the bang-bang torquers become

$$\left.\begin{aligned} e_1 &= -k_1 \dot{f}_{23} - c_1 f_{23} \\ e_2 &= k_2 \dot{f}_{13} + c_2 f_{13} \end{aligned}\right\} \qquad (5.14)$$

where Equations (5.14) can be approximated by a lead-lag network operating upon the sensor output.

The (PD) control law is first applied to the roll axis maintaining (SC) in pitch. From Table 5.3, only a small change from the previous case is encountered for γ_{is1}. For γ_{is2} and the lowest sensor saturation level degradation is noted. For γ_{is3} all sensor saturation level results are degraded from 14% to 53% with respect to the previous case.

Using the (PD) control law simultaneously in pitch and roll, the worst case degradation of the direction cosine attitude error sensor system occurs. For the lowest saturation torque level the performance criterion increases approximately 150% for the highest two sensor saturation levels compared to the initial rate gyro control law cases.

Recordings of the (PD) cases for γ_{is3} and the lowest two sensor saturation levels are shown in Figures 5.10 and 5.11, respectively.

5.4 Euler (Gimbal) Angle Attitude Sensing

An alternate method of obtaining attitude information of the body control axes with respect to a set of inertially fixed reference coordinates involves the use of a gimballed inertial platform mounted within the body. Since the gimbal angles correspond to a particular Type I (see Section III) Euler rotation of the body set with respect to the inertia reference set, then for a yaw, pitch, roll rotation sequence the pitch and roll Euler angles can be related to the direction cosines such that

$$\left.\begin{aligned} a_{13} &= -\sin\theta \\ a_{23} &= \sin\phi\cos\theta \\ a_{33} &= \cos\phi\cos\theta \end{aligned}\right\} \qquad (5.15)$$

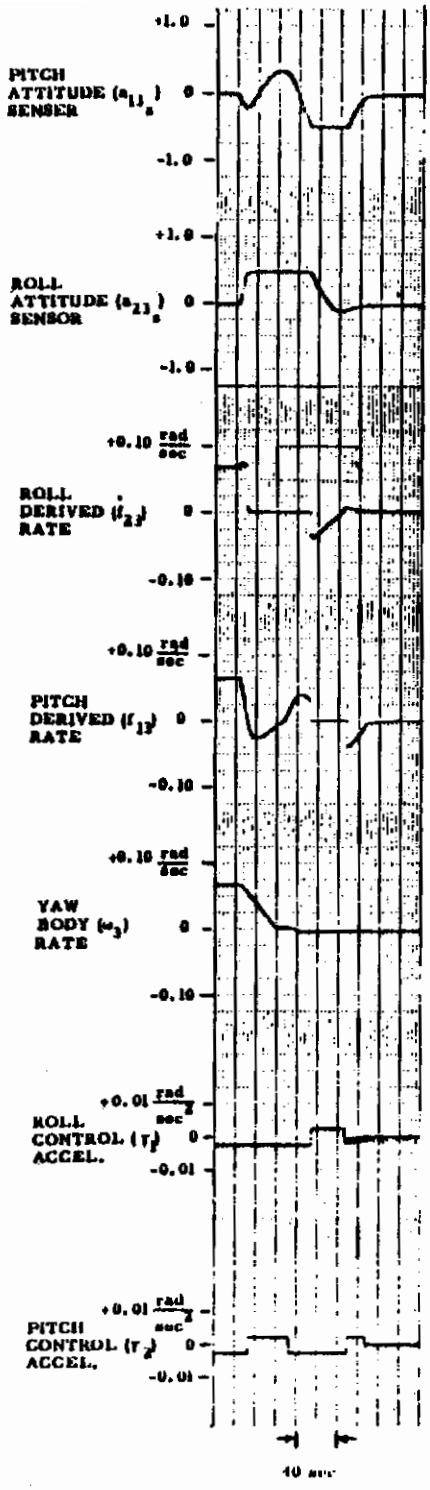

Figure 5.10 Acquisition of Bang-Bang System (PD, γ_{is3}, Sensor Saturation Level = 0.5)

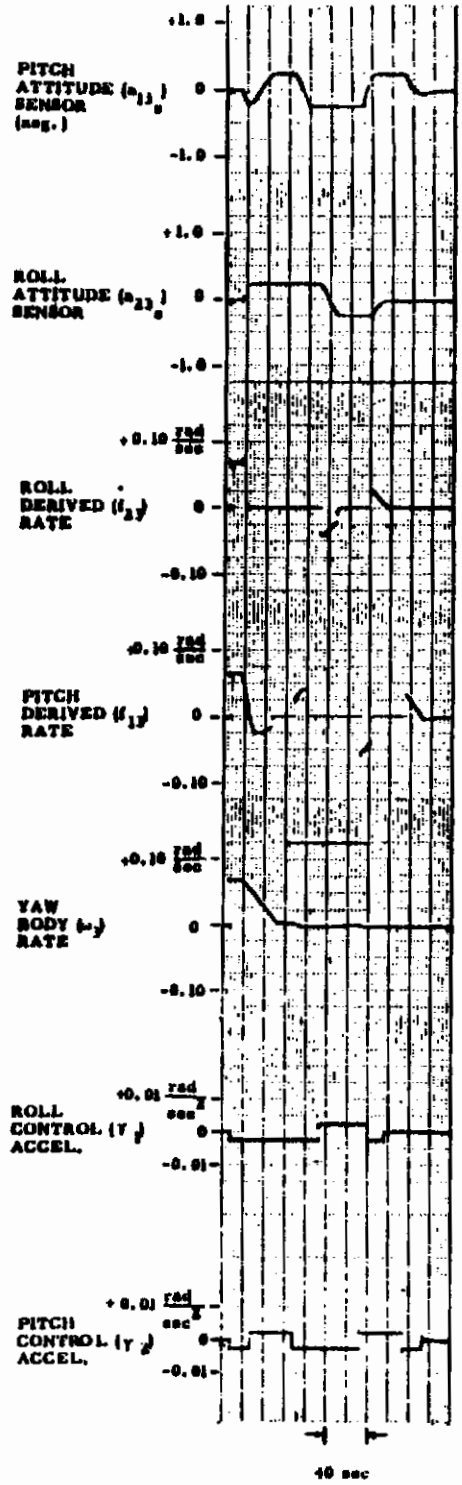

Figure 5.11 Acquisition of Bang-Bang System (PD , γ_{is3}, Sensor Saturation Level = 0.25)

where

θ = pitch Euler angle attitude error

ϕ = roll Euler angle attitude error

Therefore, an alternate form of providing pitch and roll position dependent control torques is to consider signals proportional to θ and ϕ, respectively, as obtained from the gimbal pickoff signals. The system damping may still be obtained from rate gyro information, or alternatively, derived rate in the form of $\dot{\theta}$ and $\dot{\phi}$ may be assumed available.

In application it may be preferable to utilize "resolved" gimbal angle pickoffs so that in place of the θ and ϕ information the quantities sin θ, cos θ, sin ϕ, and cos ϕ are available. This possibility was not considered here since if such is available then the direction cosine can be computed directly from Equations (5.15) and this case reduces to those already considered in detail. Instead, it is desirable to evaluate the effects of using θ and ϕ directly in various forms and thereby establish the relative need or desirability of providing the resolved gimbal angles when large attitude errors between body and platform exist.

For the Euler angle sensor cases it is desired to determine the system performance with similar control laws as for the direction cosine sensors to evaluate the relative merits of the two systems. Since the roll gimbal angle experiences a discontinuity when a_{33} is zero, it is particularly interesting to evaluate the effect of roll sensor "blanking"* for roll errors greater than 90° ($a_{33} < 0$). The system gains were "optimized" for each new case as was done previously.

---

* "Blanking" is a term used here to define the condition where the sensor output is ignored even if one exists.

To avoid the simulation difficulties associated with the formation of the Euler rates and the integration thereof (as discussed in Section III) the Euler angles were solved for explicitly from Equations (5.15) and the Euler rates were formed from differentiation of Equations (5.15) and explicit solution. The kinematic equations for simulation remained in terms of the direction cosines and body rates.

Using Equations (5.15) useful expressions for the Euler angles and rates are easily obtained in accordance with the above as

$$\left.\begin{aligned} \theta &= -\sin^{-1}(a_{13}) \\ \phi &= \begin{cases} \sin^{-1}\left(\dfrac{a_{23}}{\cos\theta}\right) & , a_{33} \geq 0 \\ \left(180^{\circ} - \left|\sin^{-1}\dfrac{a_{23}}{\cos\theta}\right|\right) \operatorname{sgn} a_{23}, & a_{33} < 0 \end{cases} \\ \dot{\theta} &= \frac{-\dot{a}_{13}}{\cos\theta} \\ \dot{\phi} &= \cos^2\phi \left[\frac{a_{33}\,\dot{a}_{23} - a_{23}\,\dot{a}_{33}}{a_{33}^2}\right] \end{aligned}\right\} \qquad (5.16)$$

Notice that several singularities are experienced in attempting to solve Equations (5.16). The roll angle is undefined as $\cos\theta$ approaches zero. The pitch rate becomes unbounded as $\cos\theta$ approaches zero as does the roll rate when a_{33} approaches zero. These, of course, are the same limitations discussed in Section III. However, for simulation purposes no essential difficulty exists. The approach utilized is similar to that employed in driving an "eight ball" for visual pilot display. Here as the angles and rates approach their singular points they are merely bounded at a reasonable level until the computation, in terms

of the accurate direction cosines, is again defined. In this way an instantaneous error can exist in ϕ, $\dot{\theta}$ or $\dot{\phi}$ but no buildup of error is possible. The appropriate analog computer diagrams to obtain these quantities are presented in Appendix B.

5.4.1 Torque Modes

Following the same procedure as in the direction cosine sensor cases, the proportional saturating and bang-bang torque modes were compared with the ideal linear case for initial rates of 4 deg/sec as shown in Figure 5.12. In this case the pitch control law uses derived pitch rate, i.e., $\dot{\theta}$, so that the value of Φ for the nonsaturating proportional torquing case is about 30% higher than the corresponding case for direction cosines and pitch gyro control given in Figure 5.1. In both cases a roll gyro is employed. Note, however, that there is essentially no difference with γ_{is1} and no saturation as shown by cases (a), (b), and (c) in Figure 5.4. Again, the proportional saturating and bang-bang torque modes are compared in Figure 5.13 where γ_{is2} and γ_{is3} are considered with the lowest gimbal angle sensor saturation level*. The relatively large increase in Φ from γ_{is2} to γ_{is3} is due to the blanking condition on the roll attitude error, ϕ, not being imposed for $a_{33} < 0$. Note that for the unblanked cases, increases in Φ of 300% to 400% are obtained for γ_{is3} compared to γ_{is2}. However, from γ_{is1} to γ_{is2} only a 100% increase is experienced.

Typical recordings of the bang-bang torque cases of Figure 5.13 are shown in Figures 5.14 and 5.15 for γ_{is2} and γ_{is3}.

---

*The same numerical saturation levels were utilized in the sensors although in the Euler angle case this corresponds to radians whereas in the direction cosine case it was a per unit value.

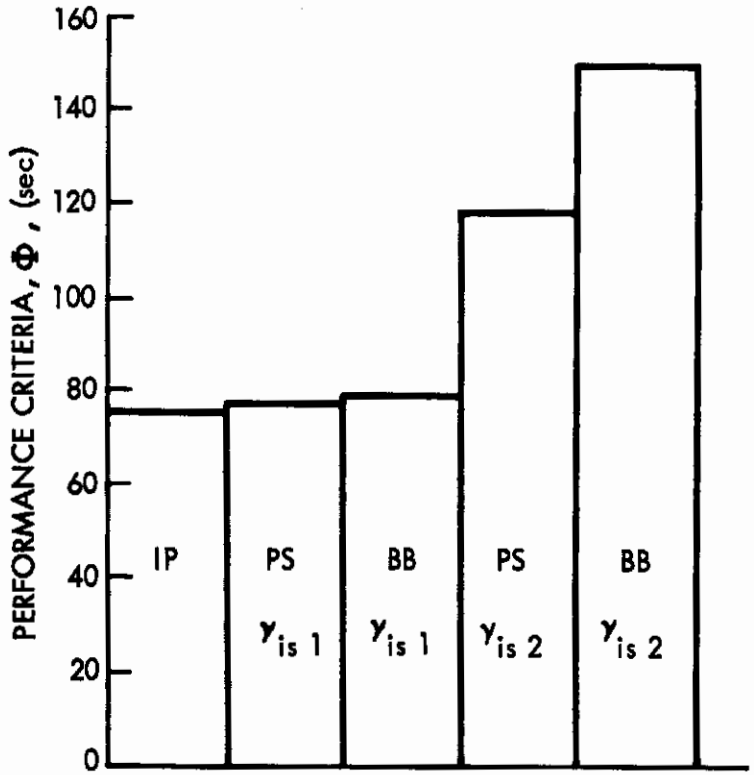

Figure 5.12 Comparison of Torque Modes with No Sensor Saturation (Euler Angles with Roll Gyro and Pitch Derived Rate)

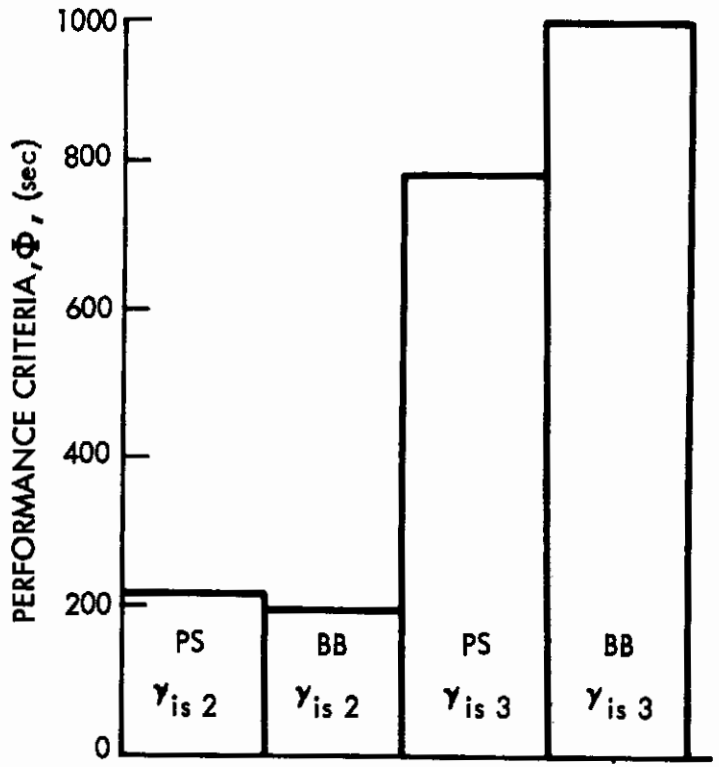

Figure 5.13 Comparison of Torque Modes with Saturation at 0.25 (Euler Angles with Roll Gyro and Pitch Derived Rate)

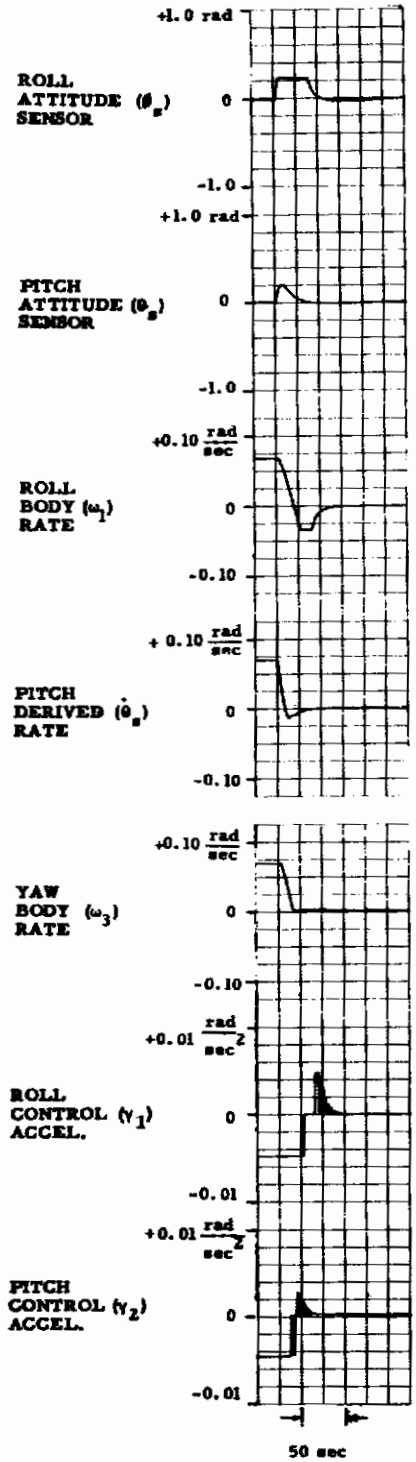

Figure 5.14 Acquisition of Bang-Bang System (Roll-G, Pitch-PD, γ_{is2}, Euler Angle Saturation = 0.25)

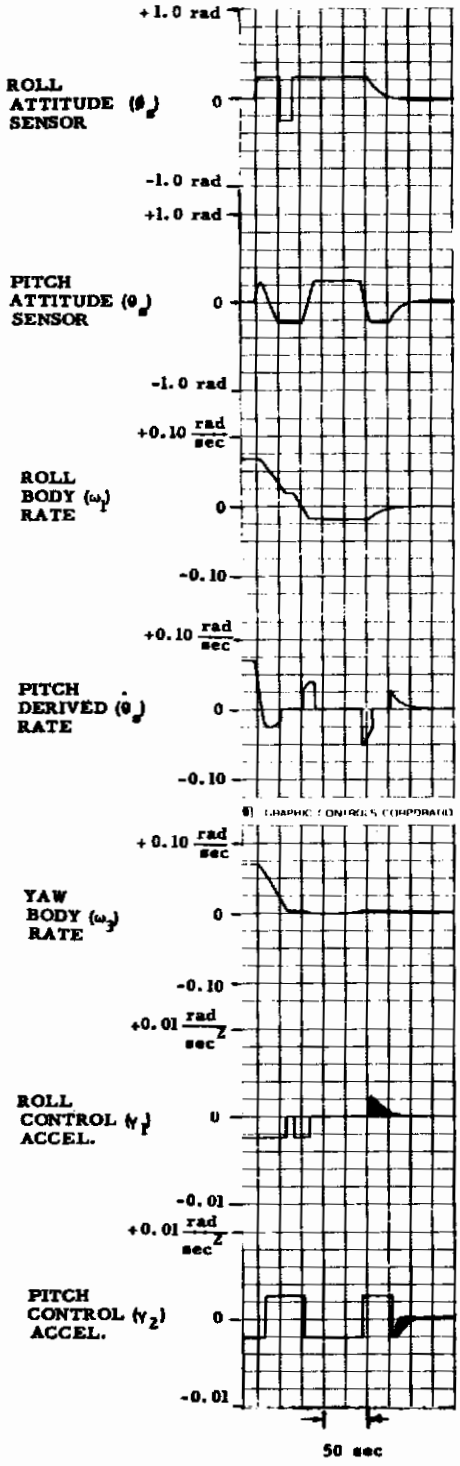

Figure 5.15 Acquisition of Bang-Bang System (Roll-G, Pitch-PD, γ_{is3}, Euler Angle Saturation = 0.25)

5.4.2 Unsaturated and Unblanked Euler Angle Sensors

Using the bang-bang torque mode and the range of system gains specified in Table 5.2 for the Euler angle cases, three different rate control laws were investigated for the full range sensor cases. The results are summarized in Table 5.4 as obtained from initial rates of 4 deg/sec.

Gyro Rate Sensing (G): In this case a rate gyro is used in both pitch and roll control. The error criteria increases proportionately to decreases in γ_{is}.

Pure Derived Rate and Gyro Sensing: Maintaining the gyro in roll and replacing the pitch gyro with pure derived rate ($\dot{\theta}$), given in Equations (5.16), the performance criterion increases 200% for the change from γ_{is2} to γ_{is3}.

Pure Derived Rate: Removing the gyro in roll and replacing with pure derived rate ($\dot{\phi}$), as in Equations (5.16), the performance criteria increases 350% in changing from γ_{is2} to γ_{is3}. This effect results from the undesirability of the control law for large roll errors. First, with γ_{is3}, a significant tumbling of the vehicle occurs from 4^{o}/sec rates. Ideally, one would like to require the roll error to have the form of $\sin\phi$ corresponding to the direction cosine a_{23} which changes sign and decreases in magnitude as ϕ increases from $\pi/2$ to π. Using ϕ alone as the roll position error has just the opposite effect and increased degradation occurs. Note that using derived rate merely accentuates the degradation since the rate signal is also the wrong sign.

Typical recordings of the pure derived rate cases for γ_{is2} and γ_{is3} are shown in Figures 5.16 and 5.17, respectively.

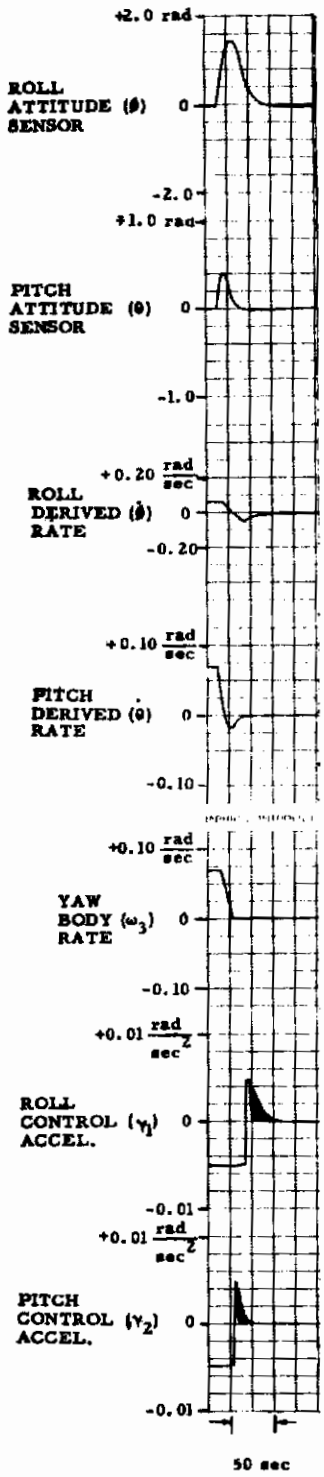

Figure 5.16 Acquisition of Bang-Bang System (PD, γ_{is2}, No Euler Angle Saturation)

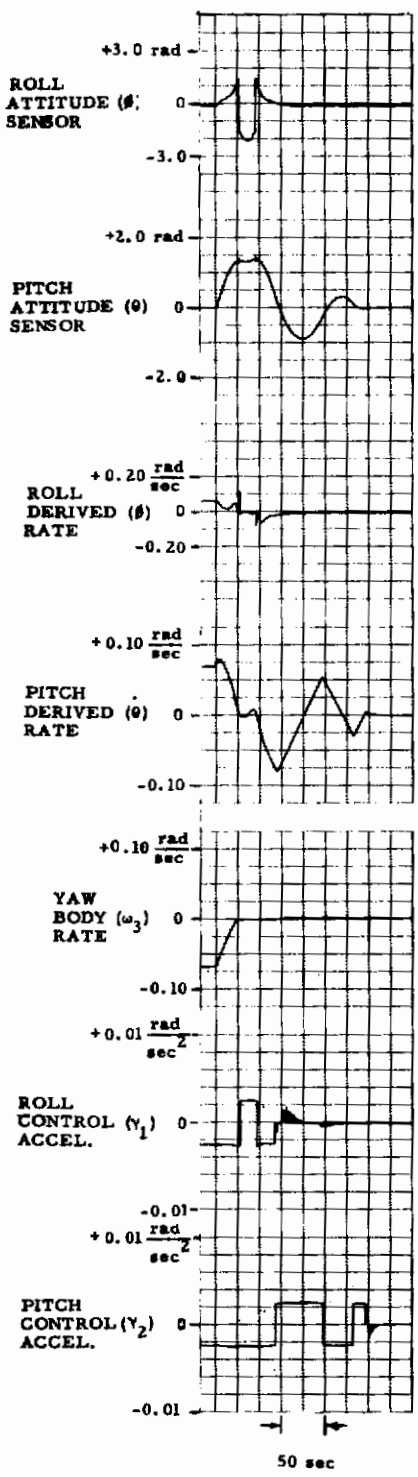

Figure 5.17 Acquisition of Bang-Bang System (PD, γ_{is3}, No Euler Angle Saturation)

TABLE 5.4

RATE SENSING MODES VS. CONTROL ACCELERATION LEVEL RESULTS FOR 4 EULER ANGLE SENSOR CONFIGURATIONS AND SELECTED CASES OF ROLL SENSOR BLANKING (Bang-Bang Control)

Euler Angle Sensor Saturation Level	Roll Sensor Blanked for $a_{33} < 0$	Rate Sensing		γ_{is1}			γ_{is2}			γ_{is3}		
		Roll	Pitch	$\bar{t}_c$	$\bar{I}_n$	#	$\bar{t}_c$	$\bar{I}_n$	#	$\bar{t}_c$	$\bar{I}_n$	#
None		G	G	48	.26	98	58	.30	155	93	.38	315
$-\frac{\pi}{2} \le \theta \le \frac{\pi}{2}$		G	PD	46	.24	99	64	.28	160	111	.49	485
$-\pi \le \phi \le \pi$		PD	PD	29	.30	78	47	.35	147	148	.50	660
0.70		G	G	37	.20	66	48	.38	163	132	.57	670
		G	PD	36	.30	94	48	.34	146	136	.63	765
	X	G	PD			94			146	116	.50	518
		PD	PD	25	.34	76	44	.35	137	117	.53	555
	X	PD	PD			76			137	114	.52	530
0.50		G	G				47	.36	151	138	.57	701
		G	PD				48	.34	146	144	.59	758
	X	G	PD						146	121	.50	540
		PD	PD				46	.35	141	128	.57	650
	X	PD	PD						141	135	.57	687
0.25		G	G	40	.20	72	46	.36	148	99	.39	344
		G	PD	30	.27	72	54	.36	173	200	.66	1180
	X	G	PD			72			173	186	.61	1010
		PD	PD	38	.26	88	64	.43	246	206	.80	1470
	X	PD	PD			88			246	183	.78	1270

Initial rates of 4 deg/sec each control axis (average value of 8 cases)

5.5 Comparison of Rate Sensing Schemes with Saturated Euler Angle Attitude Sensing and Bang-Bang Torque

The remainder of Table 5.4 is devoted to the saturated sensor cases (both blanked and unblanked) as a function of the γ_{is} levels with bang-bang torque and the same sensor saturation levels as in the direction cosine cases. Again, all results are for initial rates of 4 deg/sec, averaged over 8 cases with "optimized" gains selected from the ranges given in Table 5.2.

5.5.1 Gyro Rate Sensing

For the rate gyro control law on each axis, there is little significant difference at the intermediate torque saturation level, γ_{is2}, for any level of sensor saturation. At γ_{is3} the performance is degraded at the higher sensor saturation levels compared to the unsaturated case. However, the performance improves again at the lowest sensor saturation level. This demonstrates the imperfection of the Euler angle control law where grossly nonlinear operation of the acquisition system results. For low control acceleration levels the satellite tumbles and in this case the Euler attitude errors are in significant error. Therefore, low saturation values on the sensor output prevents inefficient control action and improves system performance.

5.5.2 Pure Derived Rate and Gyro Sensing

In this case, the pitch gyro is removed and the pitch rate signal becomes $\dot{\theta}$ which is defined by

$$\dot{\theta} = \begin{cases} \dot{\theta}\ , & |\theta| < \theta_s \\ \\ 0\ , & |\theta| \geq \theta_s \end{cases} \qquad (5.17)$$

where

θ_s = pitch sensor saturation level

Unblanked Roll Sensor: From Table 5.4, it is clear that unblanking the roll sensor degrades performance for γ_{is2} and γ_{is3}, and becomes more marked as γ_{is} and the sensor saturation levels are lowered.

Blanked Roll Sensor for $a_{33} < 0$: By blanking the roll sensor for roll or pitch errors in excess of 90 deg, the performance criteria decreases for every sensor saturation level and the lowest torque saturation level (with one exception).

Recordings of typical blanked and unblanked cases for γ_{is2} and intermediate sensor saturation level are given in Figures 5.18 and 5.19, respectively.

5.5.3 Pure Derived Rate Sensing (PD)

For the final rate sensing control law, the roll gyro is removed and the roll rate signal, $\dot{\phi}$, is given by

$$\dot{\phi} = \begin{cases} \dot{\phi}\ , & |\phi| < \phi_s \\ \\ 0\ , & |\phi| \geq \phi_s \end{cases} \tag{5.18}$$

where

ϕ_s = roll sensor saturation level

Unblanked Roll Sensor: In these cases there is improvement over the previous unblanked cases for the highest sensor saturation level and degradation for the lowest sensor saturation level. Previous results where pure derived rate on the Euler angles was favored over gyro sensoring were also observed. Although these results are not universal it is interesting to note this occurrence since only for large γ_{is} did this occur in the direction cosine derived rate cases, and even then the results were within possible machine errors.

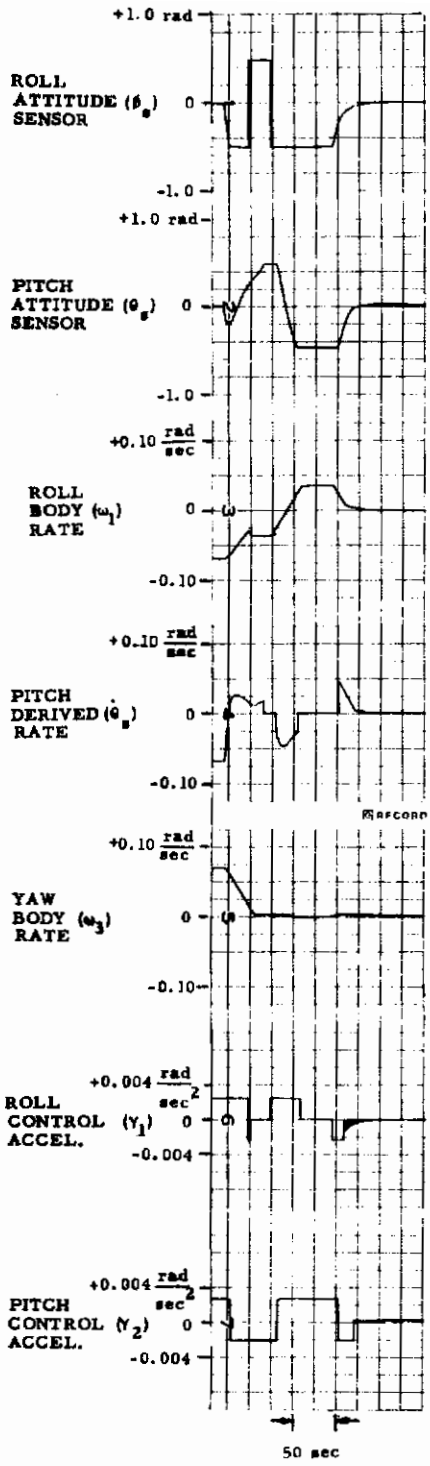

Figure 5.18 Acquisition of Bang-Bang System (PD, Blanking, γ_{is2}, Euler Angle Saturation Level = 0.5)

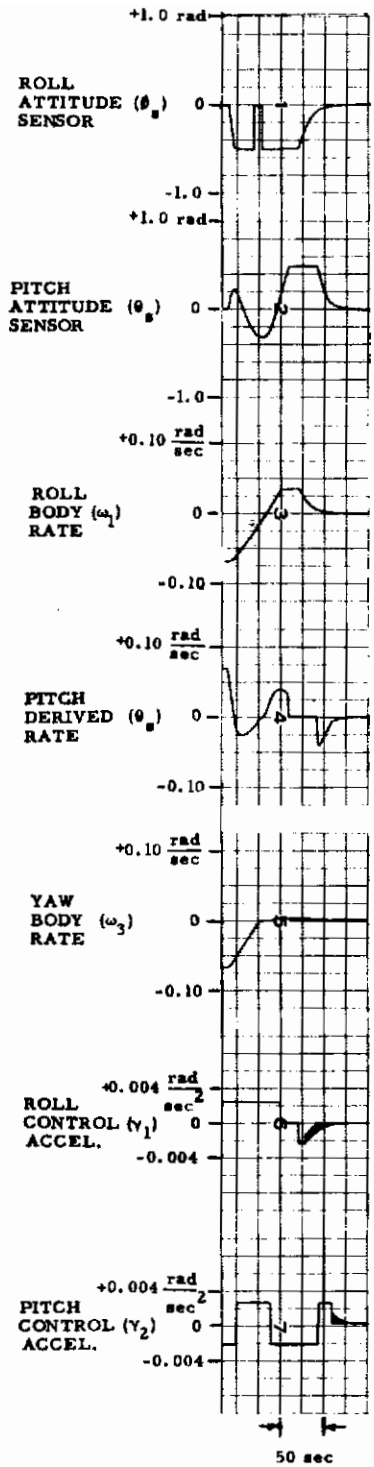

Figure 5.19 Acquisition of Bang-Bang System (PD, No Blanking, γ_{is2}, Euler Angle Saturation Level = 0.5).

Blanked Roll Sensor: The only improvement obtained by blanking the sensor is for the lowest sensor saturation level and γ_{is3}. This suggests that the system performance is dominated more by the sensor saturation level than by the effect of roll sensor blanking for the pure derived rate cases.

5.6 Comparison of Equivalent Direction Cosine and Euler Angle Cases

5.6.1 Gyro Rate Sensing

With rate gyro control laws in both pitch and roll, the direction cosine and Euler angle sensors error criteria Φ are plotted vs. sensor saturation level in Figure 5.20 with γ_{is} as a parameter. The two systems are equivalent for the γ_{is1} and γ_{is2} but show a large divergence for γ_{is3} at the lowest sensor saturation levels. This is partly due to the omission of roll sensor blanking.

5.6.2 Pure Derived Rate Sensing

Equivalent direction cosine and Euler angle sensor cases for the pure derived rate control laws are shown in Figure 5.21. It is noted here that the Euler angle data pertains to a blanked roll sensor and hence the equivalence of the systems is more marked but both show serious degradation of performance at γ_{is3}.

5.6.3 Combination Rate Sensing

In Figure 5.22 the direction cosine sensor cases with (PD) in roll, (SC) in pitch are compared to the Euler angle cases with (PD) in pitch and gyro sensing in roll. Again, the results are consistent for the higher torque levels but show fairly large divergence for γ_{is3}.

5.6.4 Small Initial Momentum Cases

Table 5.5 summarizes the results of system performance for initial rates of 1.5°/sec. For γ_{is3} the position errors always remain very small even for the lowest sensor saturation level of 0.25 radians.

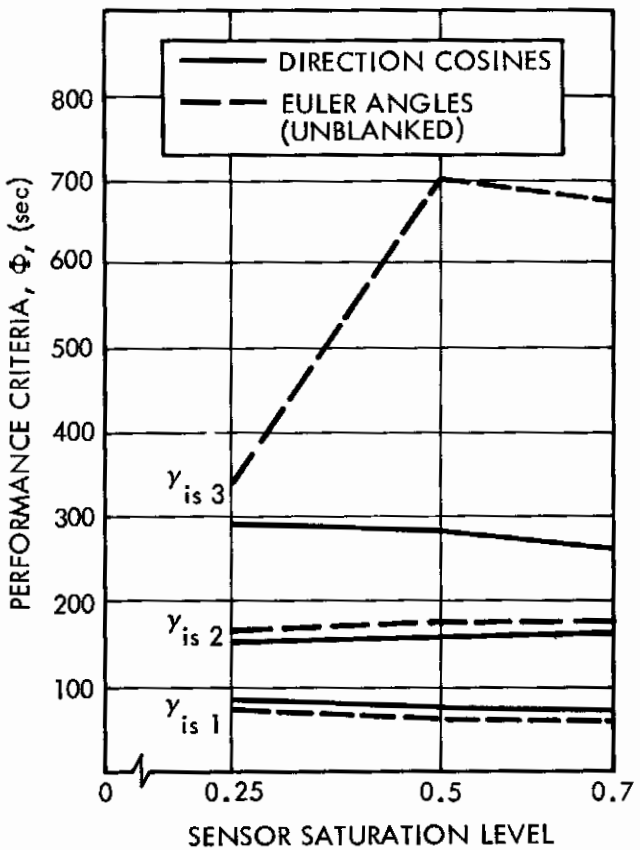

Figure 5.20 Comparison of Attitude Sensing Methods with Three Rate Gyros

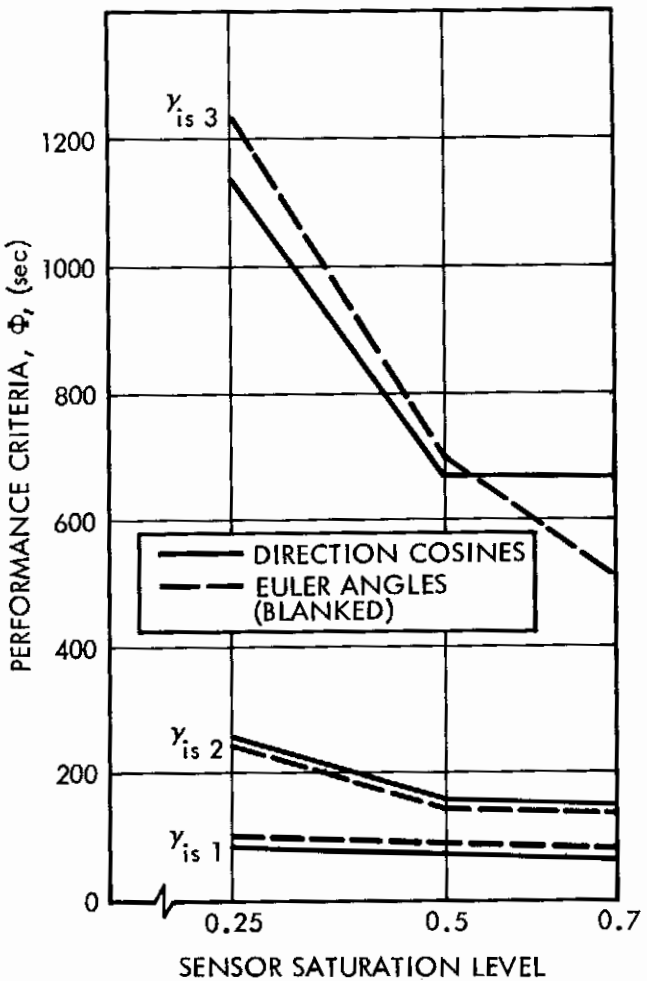

Figure 5.21 Comparison of Attitude Sensing Methods with Derived Rates

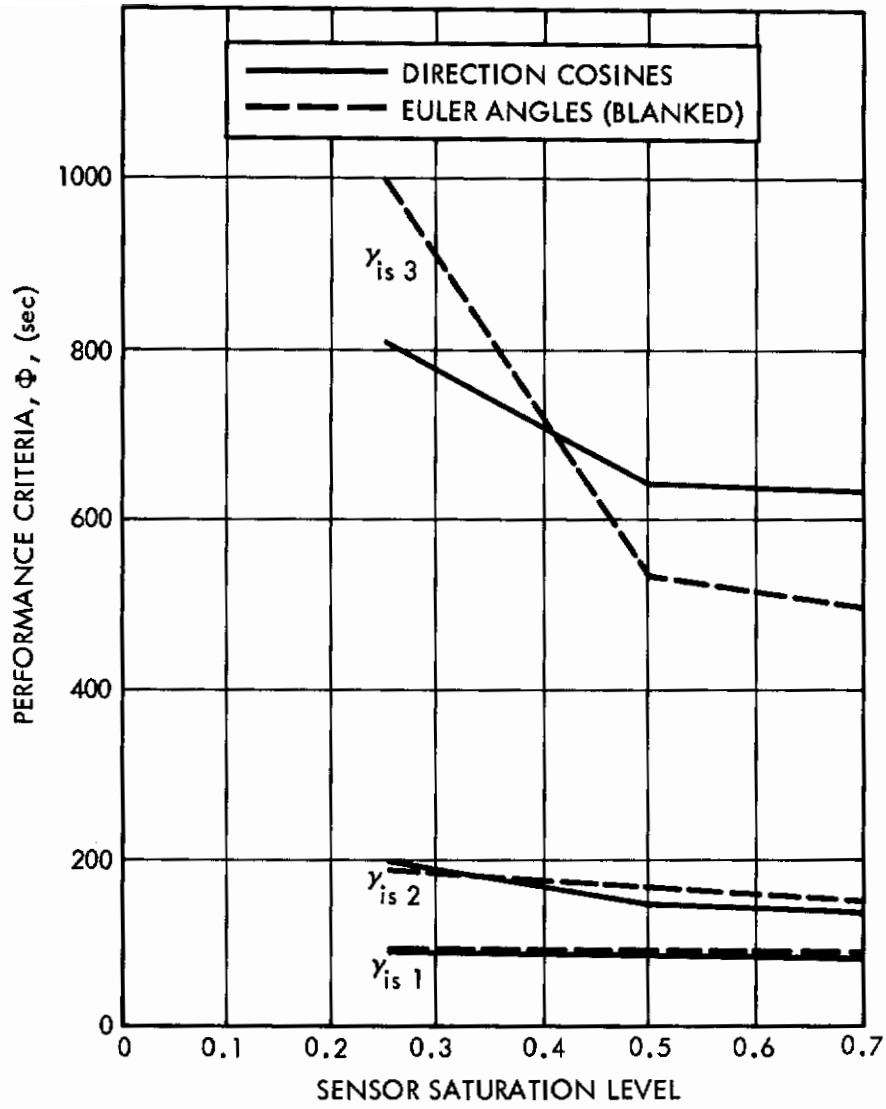

Figure 5.22 Comparison of Attitude Sensing Methods with PD in Roll and SC in Pitch with Direction Cosine Sensing and G in Roll and PD in Pitch with Euler Angle Sensing

Hence, the results are approximately equivalent for all rate sensing modes in both the direction cosine and Euler angle sensing cases. It was noted in the simulation that at γ_{is3} and the lowest sensor saturation level, initial rates of 1.75 deg/sec barely caused the position error to saturate the sensors for both types considered.

TABLE 5.5

RATE SENSING MODES VS. CONTROL ACCELERATION LEVEL RESULTS

(Initial rates of 1.5°/sec each control axis)

Attitude Sensing	Roll and Pitch Rate Sensing		Control Acceleration Level γ_{is1}		γ_{is2}		γ_{is3}		Torque Mode	Idealized Proportional Torque	
			t_c	I_n	t_c	I_n	t_c	I_n		t_c	I_n
Direction Cosine Sensors	G									20	.09
	G		20	.09	20	.09	32	.10	PS		
	G		5	.08	5	.08	5	.08	BB		
	IC		10	.09	.2	.10	32	.11	BB		
	AC						30	.11	BB		
	SC						30	.12	BB		
	PD						30	.12	BB		
	ASC						30	.12	BB		
Euler Angle Sensors	Roll	Pitch									
	PD	PD								24	.09
	PD	PD					45	.16	PS		
	PD	PD	5	.09	15	.10	35	.06	BB		
	G	PD	5	.09	15	.10	25	.14	BB		
	G	G			15	.08	30	.15	BB		

SECTION VI

OPTIMIZATION OF ACQUISITION SYSTEMS

The ultimate goal of every control system synthesis is to optimize its performance within the constraints allowed the design. The study of generalized optimization procedures to achieve this goal has recently received considerable attention. The techniques that have shown the most promise are: 1) classical variational methods (via Euler-Lagrange Equations), 2) Pointryagin's maximum principle, 3) Bellman's dynamic programming, and 4) search techniques. The classical variational methods are most easily adapted to linear, time continuous systems as they make much use of analysis and calculus (both of which have well developed theory only in linear function spaces). Pointryagin's maximum principle gives only necessary conditions for an optimum and relies on the intuition of the user to suggest the optimum controls. Dynamic programming, with its roots from operations analysis and decision theory, has difficulty providing practical solutions for continuous, highly nonlinear, dynamic systems. Search techniques appear the most universally applicable. Much less information is required about the control system before an efficient approach to the solution can be found (although more information could always be used to advantage). Search techniques were chosen as the basic approach for this study because they appeared to offer the highest probability of success.

Search techniques are basically organized trial and error schemes. An initial control design is proposed. The performance criteria of the system is measured for this design. A procedure or algorithm is developed for testing other control designs until an optimum is believed found. An example of a search procedure is the exhaustive procedure where every possible control design is tested. If the allowable space of the control parameters happens to be continuous, this is

obviously an impractical technique, as an infinite number of samples must be tested. Efficient techniques must then be developed that give a reasonable confidence that the optimum design will be found without searching every point. If nothing is known of the relations of changes of the error criterion due to changes in control design, every point not tested will reduce the probability that the best design has been found. Certain general assumptions usually can be made which, if valid, will allow convergence with fewer test points. These assumptions are: sample continuity (for a point tested, it is assumed that a certain minimum distance in the parameter space will be required to produce a significant change), and a general analytical smoothness throughout most of the parameter space (allowing derivative information to predict, with some confidence, likely directions). A desirable technique is one which efficiently uses what information is known about the system and yet remains general so a variety of problems may be solved using the same technique. Since all search techniques assume machine computers, the search techniques must also lie within the computer capabilities of the user. For the present study, the needs of search techniques appear best suited to a hybrid simulation. An analog computer provides the acquisition simulation for which it is so well suited (integration is simple). A digital computer provides the memory and logic required for the search procedure. The present study has developed three general search algorithms (relaxation, random and steep descent) whose memory requirements lie well within the ability of the Raytheon 250 that was used to implement the algorithms. Another scheme (PARTAN [19]) which looks promising would require capabilities in excess of this and was not studied.

In order to utilize any optimization scheme, the following must be given quantitatively: a) a description of the plant to be controlled, b) a description of what is required (what the control should accomplish), c) a description of the class of permissible controls (called parameter space), and d) an optimization criterion.

The plant that is discussed in this report is a satellite performing the acquisition function. As the actual satellite cannot be studied, a simulation is necessary. The equations necessary to adequately describe the satellite have already been developed. Simulation of continuous, dynamic systems are best simulated by analog computers due to its ease of integration with resulting speed of solution. The use of an analog simulation, however, introduces problems related to speed of operation, noise and machine accuracy. The Beckman 2132 computer utilized in this study provides sufficient speed (a typical simulated acquisition took approximately 0.5 second). Techniques to cope with the problems related to machine accuracy must be developed. These techniques involve an intimate knowledge of the causes of computer noise which allow statistical averaging techniques to be used and a knowledge of the sources of computer malfunction so these malfunctions can be discovered and treated so as to not to impede the optimization.

If it is desired for a satellite to acquire an attitude, the state when acquisition is accomplished must be quantitatively defined. It is not sufficient to say that all state variables must go to zero simultaneously. An analog computer will never yield zero outputs for the state variables. Tolerances must then be found which acceptably define the end of run and at the same time is not so demanding of the computer that noise sources will unduly influence the repeatability of the results. These considerations will determine an end-of-run criterion that will end the simulated acquisition.

The sensors and means of providing angular accelerations have been considered previously in this report. The designer is, however, free to suggest modes of operation (for example, bang-bang or proportional), compensation networks and possibly change the sensor and torquer configurations based on his studies. The optimization techniques discussed in this section can merely optimize the parameters for a given configuration. It will not determine how the configuration was arrived at.

The optimization criterion must be well enough defined to permit calculation of a number derived from and associated with acquisition of a system with a particular set of parameters. Examples of suitable criteria which are studied in this report are: acquisition time, fuel consumed during acquisition, maximum thrust level required of the torquers for acquisition within a specified time. The resulting criterion values permit an ordering of the parameter space. An optimization is merely an attempt to find the point in parameter space which has the largest or smallest (depending on what is desired) associated criterion value. In this report, the parameter space ordered with respect to a criterion will be called the criterion space. It should be noted that finding satisfactory quantitative criteria are quite often the most difficult area of an optimization. Usually, what is desired is a "good" response or a "reliable" or "cheap" acquisition system. Minimum fuel, for example, is merely an approximation to a "least weight" system although a more realistic model would also consider weight tradeoffs for size of torquers necessary. There is also a dependence of the values assigned the criterion space on the initial conditions of the variables. A differential equation does not yield a unique solution (and, therefore, a unique optimization criterion if one is determined from these differential equations) unless a complete set of initial conditions is given. The solution (and, therefore, criterion) will vary with the initial conditions. With a nonlinear differential equation, superposition does not hold and, therefore, the relative ordering of a criterion space may vary with the initial conditions.

In order to study a specific acquisition problem optimization techniques must be developed, the acquisition problem must be well defined and techniques to optimize the use of the existing computer hardware must be found. This section then: a) develops the optimization algorithms to be used, b) develops a computer program for properly evaluating the initial condition problem, c) presents an analog computer simulation of the acquisition problem and the necessary

interface with a digital computer, and finally, d) applies these three general areas to optimization of a specific satellite configuration.

6.1 Optimization Algorithms

Search strategies fall into two general classes. One strategy consists of systematically eliminating sections of the parameter space from consideration as a likely location for the criterion optimum [20]. This strategy has shown success only in a smooth parameter space where the criterion is strongly unimodal. The more popular strategy consists of approaching the optimum along a line. Once an initial point has been established, a search is initiated in plausible directions until an improvement is found, in which case the point is updated. In this manner, a monotonically improving path is formed until no further improvement is possible. The last point on this path is assumed the optimum. Clearly this strategy may find a local optimum in any reasonably smooth criterion space, not necessarily the true optimum. If two local optima exist, only one will be found and there is no assurance this is the correct one. Search strategies which locate the local optima will be called local searches. A strategy which attempts to determine a better local optimum once one has already been found will be called a global search.

A great variety of local search algorithms has been developed, each particularly suited to special problems and adaptable to specific computer capabilities. The most challenging problems that arise in developing an algorithm are: a) once an improved point has been found, what direction should be explored to find further improvement, b) at what distance from the present point should the search be made, and c) how to determine when the search is complete. By far the most critical and best studied area is that of direction finding. In fact, the three algorithms studied in this report are named for the manner in which the directions are searched. The global search strategies are less thoroughly studied. The approach that appears most promising

is a random search used in this study. The concepts of these procedures are presented below while Appendix C gives the details of the actual programs used in the study.

6.1.1 Relaxation

This is perhaps the simplest technique. It has produced great successes in linear programming. The strategy consists of inspecting the effect on F (criterion to be optimized) of changes in each parameter while holding all other parameters constant. Assume the parameters available for optimization are denoted by α_i, where i denotes the parameter (1 = first, etc.). Suppose parameter α_i is being searched (relaxed). All $\alpha_j \neq \alpha_i$ are held constant. The parameter α_i is varied until a local optimum is found. When all the parameters have been relaxed in this manner, the process is reiterated until it is concluded that a local optimum has been found. Many variations exist. These variations concern themselves with step sizes and the decision, if an improvement is found, concerning whether to continue along α_i until the best possible criterion is found, or upgrade α_i and immediately search a new parameter.

In the present study, a small initial step size was selected for the search with the provision for expanding the step size based on the number of successive trials before an F is found worse than the preceding trial. At this time, an increment in α_i produces a detriment to F and further search in the same direction is assumed fruitless. Either a local optimum has been found or the optimum is in the opposite direction. Search is then initiated in the opposite direction until a detriment is found. The value for α_i corresponding to the best F found is, at this point, assumed the local optimum. Each time all the parameters have been iterated the step sizes are reduced on the assumption that the optimum is nearer and a finer search may be necessary. Also, each parameter is optimized one at a time rather than immediately upgrading and searching a new parameter. A significance test was also

instituted. In this manner an improvement or detriment in F must be significantly better than the previous F in order to be so classed. The importance of significance tests lies in the use of an analog computer to calculate F. The significance tests should be large enough to screen potential noises and inaccuracies in the analog computation from giving false conclusions as to the change in F. The relaxation search procedure is diagramed in Figure 6.1.

6.1.2 Random Search

This strategy, rather than attempting to guess which direction to search, allows a random noise generator to determine the direction. The search reduces to a random walk, for which several modifications have been successfully used in this study. A pure random walk is accomplished by sampling a random voltage for each parameter direction, scaling the voltages to provide a desirable average step size, and searching in this direction. If a failure occurs, a new direction is found from the noise generator. If a success occurs, the α_i's are updated and a new random direction is searched from this new point. Previous studies [21-22] have differed from the present study in that a predetermined step size for each parameter is given and merely the sign of the direction is found from the noise generator. It is felt the present approach allows a purer random walk as directions other than along parameter axes or midway between these axes (which is all that the previous studies provided) are searched. Several modifications have also been studied. The modifications have been concerned with biasing the search and changing the variance of the noise (changing the expected step sizes). If a reasonably smooth criterion space is assumed, the presence of a success indicates the most likely direction for future success should be in the same direction. Absolute positive biasing (where the incremental step that gave a success is used continuously until it fails to yield a success) has been tried and converged quicker than a strictly random walk for the acquisition

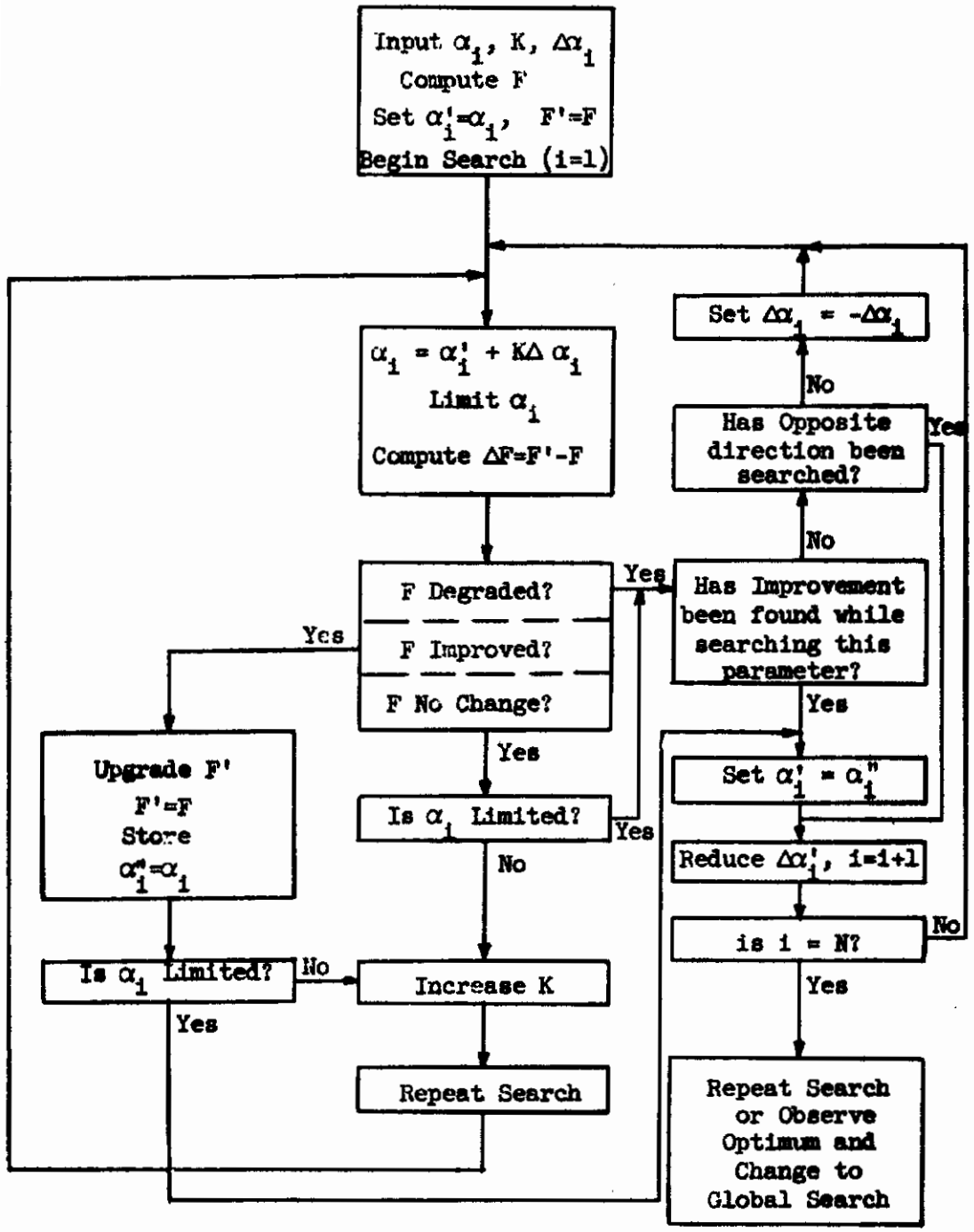

Figure 6.1

Relaxation Local Search Flow Diagram

case studied. Absolute negative biasing (where a step that produced significant detriment causes the computer to search in the opposite direction for the next trial) also aided in convergence. Insufficient time prevented investigating non-absolute biasing. It should be noted that in this case significant detriment does not have the same meaning as in the relaxation case. Significant detriment is a value that is large enough to suggest a slope, but looking approximately opposite to the desired direction. The optimal procedure for the change in variance is to start with a reasonably large variance (so much ground can be covered if need be) and reduce this as the optimum is approached. With little knowledge of the space, it is very difficult to ascertain how close the parameters are to the optimum. No significant improvement was found in convergence by varying the variance. The global technique discussed later does provide for the opportunity to change the variance and appears sufficient. Figure 6.2 is a block diagram of the logic used in the random search algorithm which gave the best results (absolute positive and negative biasing).

6.1.3 Steep Descent

Perhaps the oldest and most intuitively attractive search technique is that of steep descent. In this case, a search direction is selected based on calculation of $\bar{\nabla} F$

$$\bar{\nabla F} = \sum_{\text{all } i} \frac{\partial F}{\partial \alpha_i} \left| \frac{\bar{\alpha}_i}{\alpha_i} \right|$$

If the search direction is directly proportional to $\bar{\nabla F}$, the technique is called the method of steepest descent [23]. A scaling difficulty occurs in attempting to calculate the relative magnitudes of $\frac{\partial F}{\partial \alpha_i}$, as the units of α_i are in general not all the same.

This algorithm consumes the greatest effort of the three in finding the direction to search, as the slope along each α_i must be found

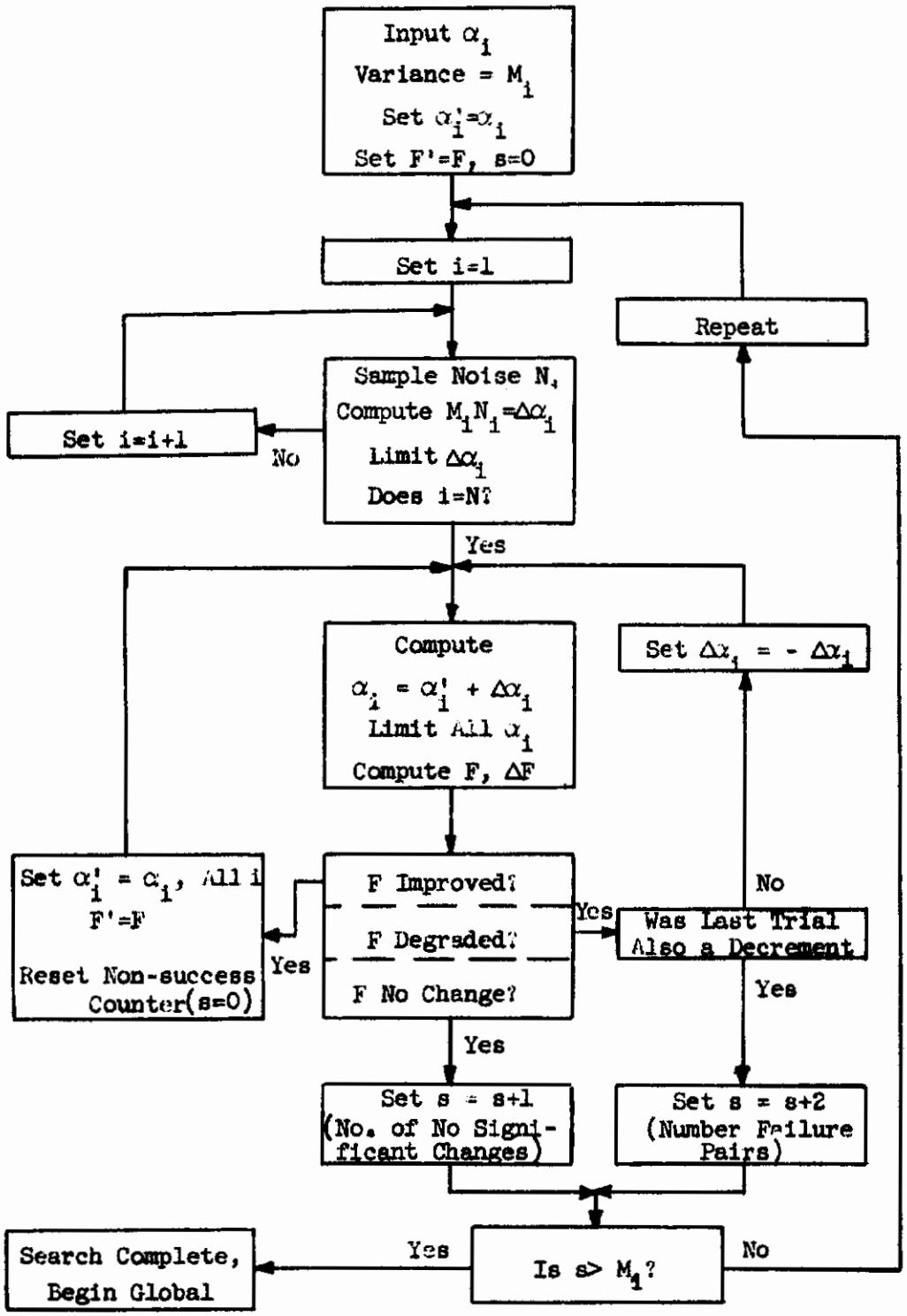

Figure 6.2

Absolutely Biased Local Random Search

Flow Diagram

before an exploration is initiated. For smooth criteria spaces, the added expense is often well rewarded by an attendent reduction in the number of times a direction must be found. Variations in the basic technique occur in: 1) the manner in which $\bar{\nabla}F$ is calculated, 2) the direction of search based on $\bar{\nabla}F$, and 3) the step size strategy once a direction has been found. In this study, these areas were approached as follows and are illustrated in Figure 6.3a. and 6.3b.

(1) A minimum step size is selected for each parameter. The parameters are then individually searched in a fashion similar to Relaxation until a significant change is produced. If no significant change is produced, the step is increased. This is continued until either a limit is reached, detriment or improvement occurs. If a limit is reached or detriment occurs, a search is started in the opposite direction. If no improvement is found along the parameter, the slope is assumed zero. If an improvement does occur, the slope is calculated. If the slope is significant, it becomes a component of $\bar{\nabla}F$, if not, the slope is assumed zero. The reason for searching more than a local region is to insure search along a direction which may be momentarily on a plateau but eventually produces significant change. It is hoped that this technique will reduce the number of times new directions must be found.

(2) Two alternates are available for selecting a search direction. In one case, the steepest descent is implemented (with the tacit assumption that proper scaling has been chosen) so the weighting along each parameter is directly proportional to its slope. Another technique which shows more promise is to weight each direction inversely as a function of its slope (once a significant slope has been found). In this manner, if the function space were linear, a step along the selected direction would produce an improvement to which each parametric direction's contribution is equal.

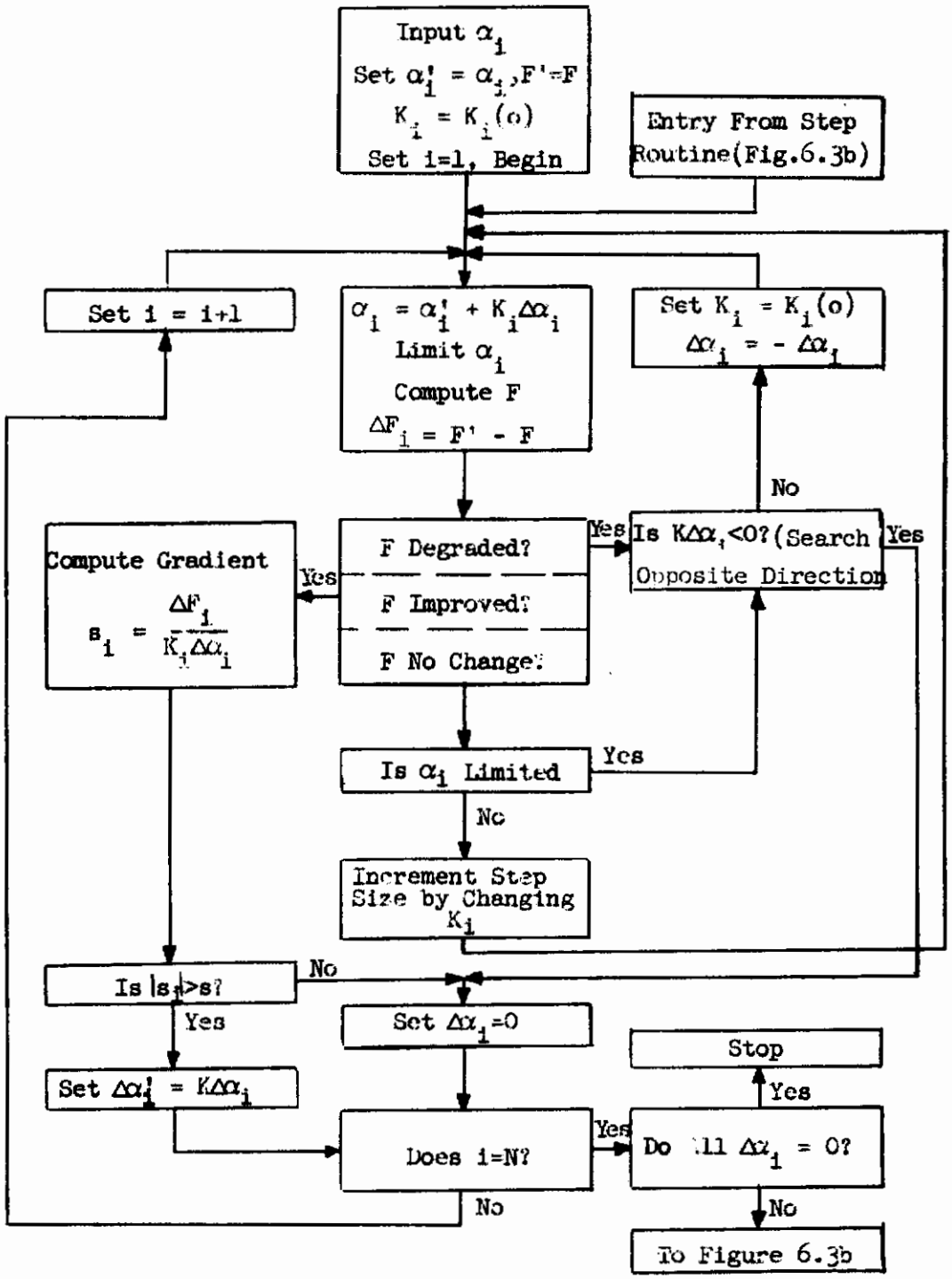

Figure 6.3a

Steep Descent Direction Search

Flow Diagram

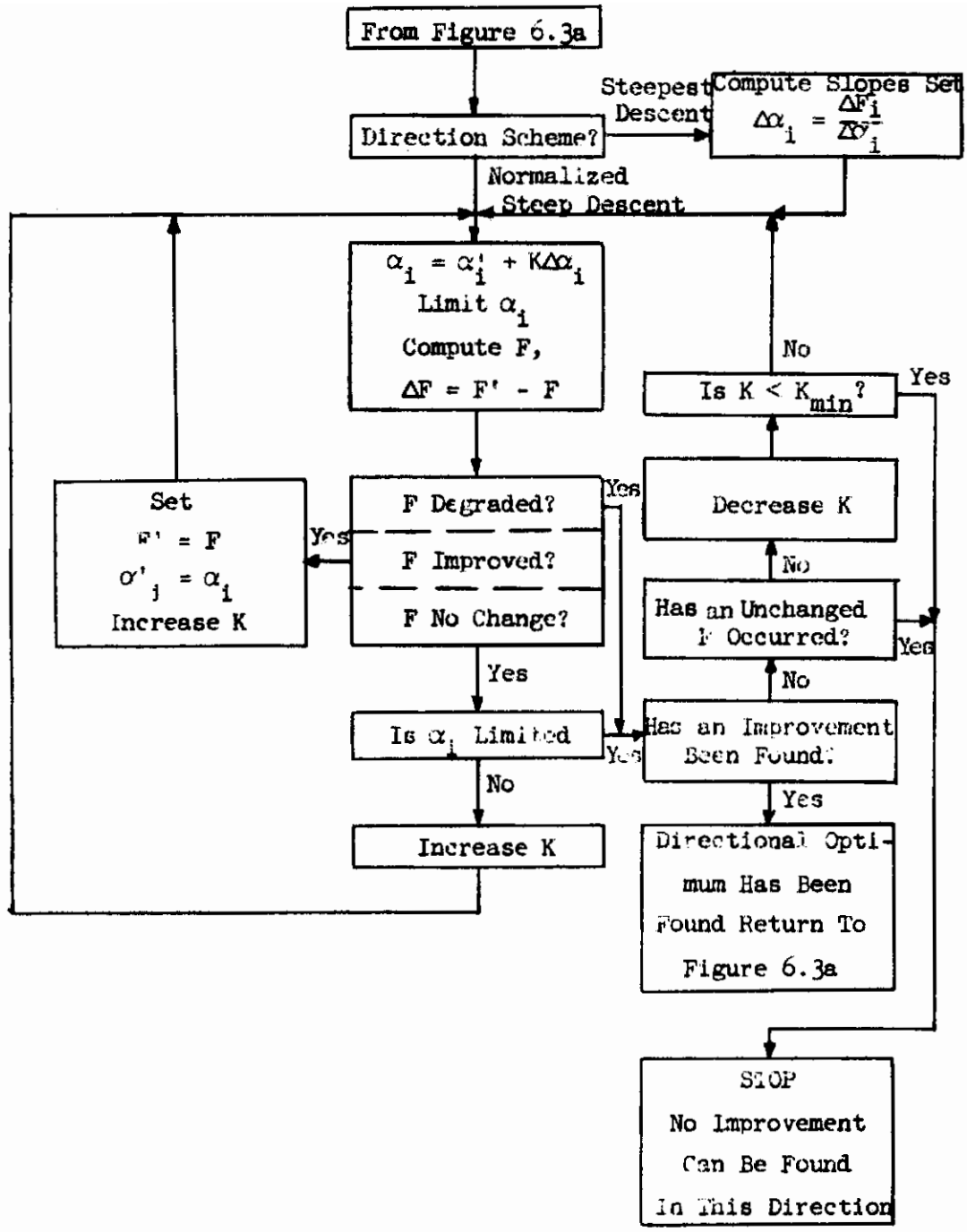

Figure 6.3b

Steep Descent Search Normalization

And Step Flow Diagrams

(3) The facility for accelerating the step size has been implemented similar to the relaxation scheme. The two differences are that the reverse direction is never searched and if a failure occurs before any success is found, the step size is reduced to search closer to the initial point. If no success can be found, the algorithm fails and control is transferred to the operator.

6.1.4 Global Statistical Search

Once a local optimum has been found, the problem remains of substantiating that this is indeed the global optimum. The approach selected in this study is a random search. This allows much flexibility in that the statistics may be adjusted to correspond to educated estimates of other likely optima. For the present case, it was felt the space near the local optimum was the most likely location for an even better optimization criterion. The strategy then consisted of randomly sampling numbers corresponding to the parameter (as in the local random search), starting with a very small variance and expanding this variance slowly if no better points are found. If an improvement is found, a local search strategy is once again initiated. Figure 6.4 gives the flow detail of the global random search algorithm.

6.2 Initial Condition Set Selection

In a nonlinear dynamic control system, the law of superposition does not hold. One of the far reaching consequences of this is: for a given set of parameters, responses of the system to all possible initial conditions cannot be compactly described by a small set of generalized responses which for different initial conditions merely changes the appropriate linear scaling factors. A control system may be designed to give optimal response at a given initial condition, and this may not necessarily be optimal for a small change in the initial condition. An acquisition system must acquire a desired attitude for any possible initial state. If it is to be optimal, it should optimize some criterion function while doing this. It is apparent that in a nonlinear dynamic system, one set of parameters may not optimize the cost

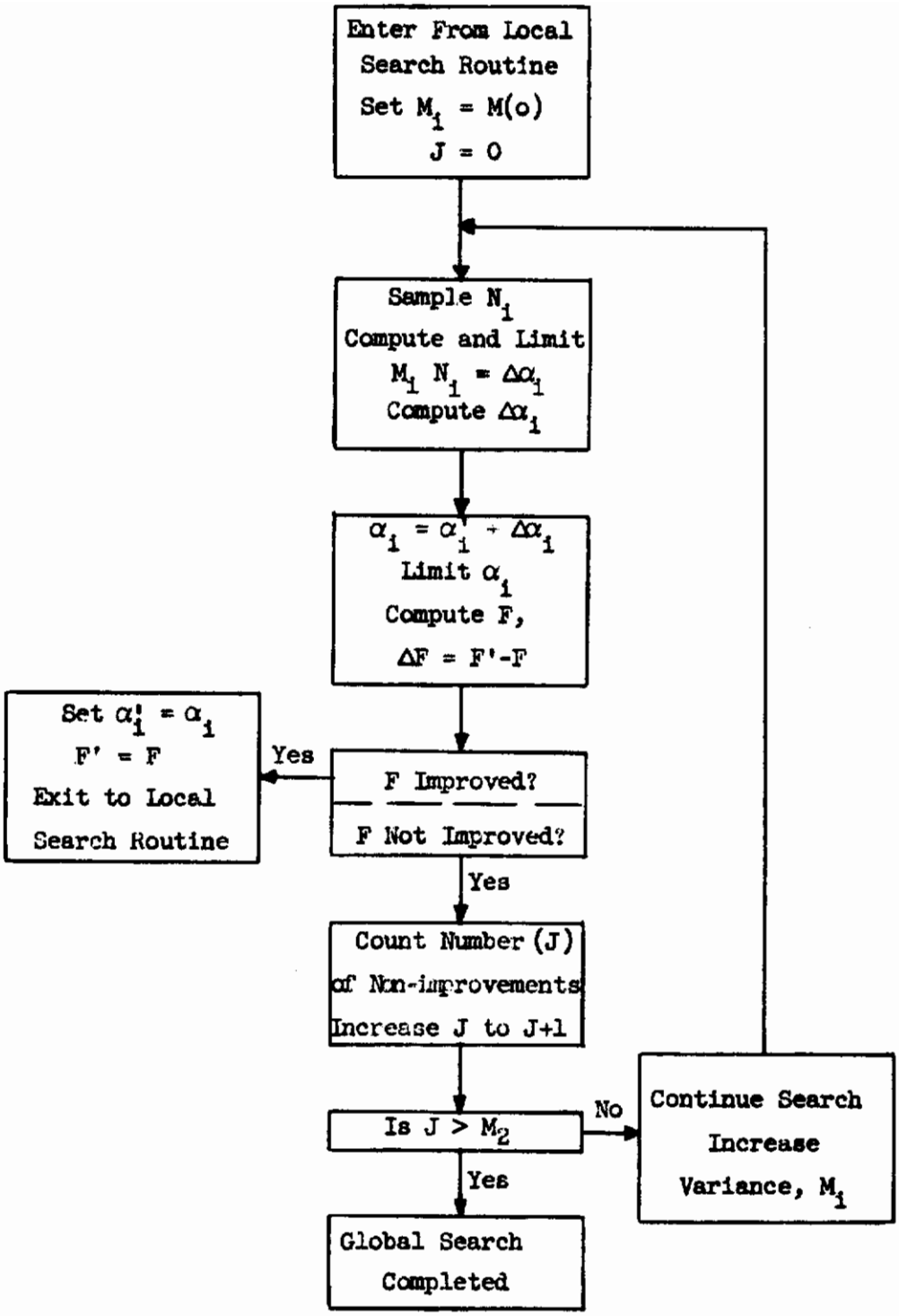

Figure 6.4

Random Global Search Flow Diagram

function (F) for all initial conditions. A different F_{IC} (denoted in this manner to emphasize the F is a function of the IC selected) exists for each initial condition. In order to provide a single F for the optimization algorithm, some synthesis must be made giving F = F (all F_{IC}'s). As an infinite number of IC's exist, apparently not all F_{IC}'s can be considered. The two-fold problem then exists: 1) which initial conditions should be considered, and 2) how should the synthesis be accomplished.

6.2.1 Initial Condition (IC) Selection

If the criterion space is reasonably smooth it can best be described by partitioning the space and inspecting an initial condition from each partition. For the case of six variables (and, therefore, six initial conditions), as may exist for the satellite dynamic and kinematic equations, partitioning each variable into as few as five equal partitions yields 5^6 = 15,625 different initial conditions. This increased cost due to high dimensions has been aptly described by Bellman as the "curse of dimensionality."

In an optimization problem, not all initial conditions are important. It frequently happens that all that is desired is a reasonable set of initial conditions which will describe the worst possible conditions for the optimization criterion. For example, if fuel is being minimized and the initial condition set which maximizes the fuel is given, a design can be found which will minimize the amount of fuel necessary to insure acquisition for any initial condition set. It may not only be desired to minimize the criterion for a maximum IC set, but also good performance may be desired from other more probable IC's. The design for the worst IC set may be found to be too expensive. It may be more desirable to approach the acquisition from a probabilistic approach, where the more probable IC sets will be weighted more heavily than events that have little chance of occurring. Another problem yet remains. The F_{IC}'s are also functions of the parameters. As the

parameters are varied during an optimization study, the original F_{IC}'s may no longer retain their relative ordering and conclusions based on earlier IC sets may no longer be valid. For example, the IC set which yields the worst criterion case for an initial set of conditions may no longer be the worst case after the optimization. It is desirable to initially select not only those IC sets which accomplish the desired effect for the present parameters but also those IC sets which have the same effect on future parameters. In order to do this, certain assumptions must be made about the relations between the parameter space and initial condition space. These will be founded on past experience with acquisition systems. For example, in acquisition systems such as studied in this report, the worst initial conditions may, as a rule, be assumed those with highest initial rate or furthest from the desired attitude. This will probably be the case no matter what the parameter settings. When the parameters change so radically that one set of initial conditions is not satisfactory, a new set must be found. This suggests that the IC space may be searched several times during an optimization.

Alternatively, although not evaluated in this study, the same algorithm employed to minimize F via parameter variation could maximize F via IC variation. In this way the originally worst case IC set could be maintained as worst case throughout the optimization process. For other F synthesis procedures other, perhaps much more complex, applications of this technique may prove feasible.

Initial Condition Space Search: The initial condition space for acquisition problems of the type to be discussed in this report can be assumed fairly smooth. The variables that will be considered are three angular rates and three direction cosines. It is not unreasonable to assume that the criterion performance can be described by partitioning the rates into five areas - $\pm$ maximum expected rates, $\pm$ average expected rates, 0 rate. All possible values for the direction cosines

will be assumed equally probable. Some locations, however may be of particular interest. These locations are: the attitude which is desired - to be called the nominal attitude, satellite pointing directions which lie along one of the coordinates of the direction cosines (this includes the first case as a subcase) - to be called the minimum attitude set, and satellite pointing directions which lie either along one of these coordinates or midway between the three axes - to be called the maximum attitude set. Particular combinations of the above sets may be desired when the expense of searching all combinations is considered too great. A digital program (called the search selection program) has been written which will search the initial condition space at the sets of locations described in Table 6.1. In this manner the initial condition space can be searched in one of seventeen possible ways, depending on the thoroughness of the space inspection desired.

Process Procedure: The results of the search selection provides a reasonable coverage of the initial conditions but yields an unusually large number of cases. In order to further reduce the number of cases and yet retain those which are significant for optimization, a digital program has been written which processes the F_{IC}'s calculated in any of the sets listed in the search selection with the following procedures:

Procedure 1: First, the IC's are sorted in descending order with respect to the F_{IC}. A series of q (arbitrary) initial conditions are selected which list those IC's corresponding to either the q largest or q smallest F_{IC}'s.

Procedure 2: The average F_{IC} is computed and the series of q initial conditions nearest (F_{IC}) average is printed out.

TABLE 6.1

SEARCH SELECTION SUBROUTINES

Initial Condition Set Number	Maximum Rates (a)	Average Rates (b)	Zero Rate (c)	Nominal Attitude (d)	Minimum Attitudes (e)	Maximum Attitudes (f)	Number Elements In Set	Includes Set Numbers
1	X			X			8	
2	X		X	X			27	1
3	X			X	X		48	1
4	X		X	X	X		170	2,3
5	X			X	X	X	112	3
6	X		X	X	X	X	264	4
7		X		X			8	
8		X	X	X			27	7
9		X		X	X		48	7
10		X	X	X	X		170	8
11		X		X	X	X	112	9
12		X	X	X	X	X	264	10
13	X	X		X			64	1,7
14	X	X	X	X			141	2,8,13
15	X	X		X	X		400	3,9,13
16	X	X	X	X	X		775	14,15
17	X	X	X	X	X	X	1750	5,6,11,12,16

(a) Maximum Rates include all sign permutations of $\pm$ maximum angular rates on each axis.
(b) Average Rates include all sign permutations of $\pm$ average angular rates on each axis.
(c) Zero Rate used only with maximum or average rates in all combinations.
(d) Desired acquisition attitude.
(e) Five additional attitudes.
(f) Eight additional attitudes.

Procedure 3: The initial conditions are divided into quadrants and the worst q cases in each quadrant is printed out. A quadrant in this sense is defined as a permutation of a plus or minus or zero value for each initial rate or direction cosine.

6.2.2 F Synthesis

Once a set of F_{IC}'s have been designated, the problem of their synthesis remains. The approach used in this study was the most obvious linear relation - an unweighted average

$$F = \sum_{i}^{q} (F_{IC_i}) \ / \ q$$

However, the flexibility for using other approaches are incorporated in the computer program. Other approaches may be:

$$1) \quad F = \sum_{i}^{q} (F_{IC_i})^{x_i} \ / \ q$$

in order to weight the larger F_{IC}'s more heavily (x_i is a number $\geq$ 1):

$$2) \quad F = \sum_{i}^{q} \left| F_{IC_i} - (F_{acceptable})_i \right| \ / \ q$$

in order to insure that any F_{IC_i} will acquire within an acceptable value for the error criterion;

$$3) \quad F = \text{Max} \ (F_{IC})$$

which gives the classical minimization of the maximum F_{IC}.

6.3 Simulation Discussion

The optimization algorithms and initial condition space search techniques have been developed. Before a specific acquisition can be found, the tasks of implementing an analog simulation of the acquisition problem and tying these three areas together remain. Throughout this study, the digital and analog implementation is kept very general so that a wide class of optimization problems can be optimized. The optimization algorithms will optimize any criterion space provided quantitative criteria can be defined and calculated from a given parameter space. The initial condition space search will search any six dimensional state variable space but are programmed to be meaningful for acquisition problems. An analog simulation must necessarily be somewhat less general, although a very large class of acquisition problems can still be simulated. Many of the techniques related to analog error detection, digital to analog interface and confidence tests are applicable to practically any optimization problem for which the analog computes the optimization criterion.

6.3.1 Simulated Equations

The general acquisition problem to be considered is that of aligning a single axis of a satellite parallel to a desired vector and driving the angular rotation about this axis to zero. This is the previously defined one axis acquisition problem. The reference coordinate frame is a three dimensional, cartesion set ($\bar{i}_1$, $\bar{i}_2$, $\bar{i}_3$) with the 3 axis defining the desired pointing direction. The kinematic representation is the three direction cosines of the satellite axis to be aligned with the reference 3 axis. The control system can consist of any collection of sensors (that can be described by the six variables) whose outputs are processed by a compensation network which can be described by the parameters to be optimized. The outputs of the networks are then used to drive angular acceleration devices (torquers). In order to provide a more concrete control equation, the sensors are assumed three rate sensors and two direction cosine sensors. The

control laws are proportional but saturable control. The equations expressing the acquisition dynamics, kinematics, control law, several potential optimization criteria and the end of run criterion are given in Table 6.2.

6.3.2 Analog Simulation

The above-mentioned equations were simulated on a Beckman 2132 analog computer. A detailed description of the simulation is presented in Appendix C. The end of run criterion is necessary to determine when acquisition is complete. This is especially critical when the time of acquisition is the optimization criterion. The criterion selected is the absolute value of a weighted sum of the variables biased by some fixed voltage (see Table 6.2). The criterion is assumed satisfied when this sum becomes zero. The bias is necessary as noises and drifts by the analog would prevent an unbiased zero from ever occurring. The bias level selected is more a function of actual voltage levels than their equivalent variable units.

6.3.3 Digital-Analog Interface

The digital computer provides those functions it is best suited for. It provides the optimization algorithm, initialization search procedure, controls and analog modes (Initial Condition, Operate), provides voltages for the initial conditions of the variables and parameter settings, and reads the optimization criterion from the analog.

In order to better understand the operations of the various elements of the optimization process a logical flow of the entire computer operations in the optimization phase (rather than the space search phase) are shown in Figure 6.5. Ignoring the minimum thrust criterion for the moment, the procedure is outlined below. An optimization criterion is selected (for example, minimum fuel or time). A set of initial conditions for the variables is selected based on the space search that has already been run. A best initial guess for the parameters is made. The error criterion (F) for this initial setting will

TABLE 6.2

SIMULATED ACQUISITION EQUATIONS

Item Description	Equations	Discussion
Kinematics	$\dot{a}_{13} = \omega_2 a_{33} + \omega_3 a_{23}$ $\dot{a}_{23} = \omega_1 a_{33} - \omega_3 a_{13}$ $\dot{a}_{33} = \omega_2 a_{13} - \omega_1 a_{23}$	a_{i3} - Direction cosine from i body axis to 3 inertial ω_i - Body rate about i body axis
Dynamics	$\dot{\omega}_1 = \left[(I_2-I_3)/I_1\right] \omega_2\omega_3 + \gamma_1$ $\dot{\omega}_2 = \left[(I_3-I_1)/I_2\right] \omega_1\omega_3 + \gamma_2$ $\dot{\omega}_3 = \left[(I_1-I_2)/I_3\right] \omega_1\omega_2 + \gamma_3$	I_i - Inertia about i principal inertia axis γ_i - Control angular acceleration about i axis
Control Laws	$\gamma_1 = -\alpha_1 (a_{23} + \alpha_4 \omega_1)$ $\gamma_2 = -\alpha_2 (-a_{13} + \alpha_5 \omega_2)$ $\gamma_3 = -\alpha_3 \omega_3$	$\alpha_i (i = 1,2,3,4,5)$ - control law gain constants
End-Of-Run Criterion	$\sum_{i=1}^{3} b_i \lvert\omega_i\rvert + \sum_{i=1}^{2} c_i \lvert a_{i3}\rvert - K = 0$	b_i, c_i - Weighting and scaling constants K - a constant
Minimum Fuel Criterion	$F = \int_o^T \sum_1 \lvert\gamma_i\rvert \, dt$	
Minimum Time Criterion	$F = \int_o^T dt$	
Constraints	$\alpha_7, \alpha_9, \alpha_6$ α_8, α_{10} $\alpha_{11}, \alpha_{12}, \alpha_{13}$	Limits on magnitude of γ_1, γ_2, γ_3, respectively Saturation values of a_{13} and a_{23}, respectively Saturation values of ω_1, ω_2, ω_3, respectively

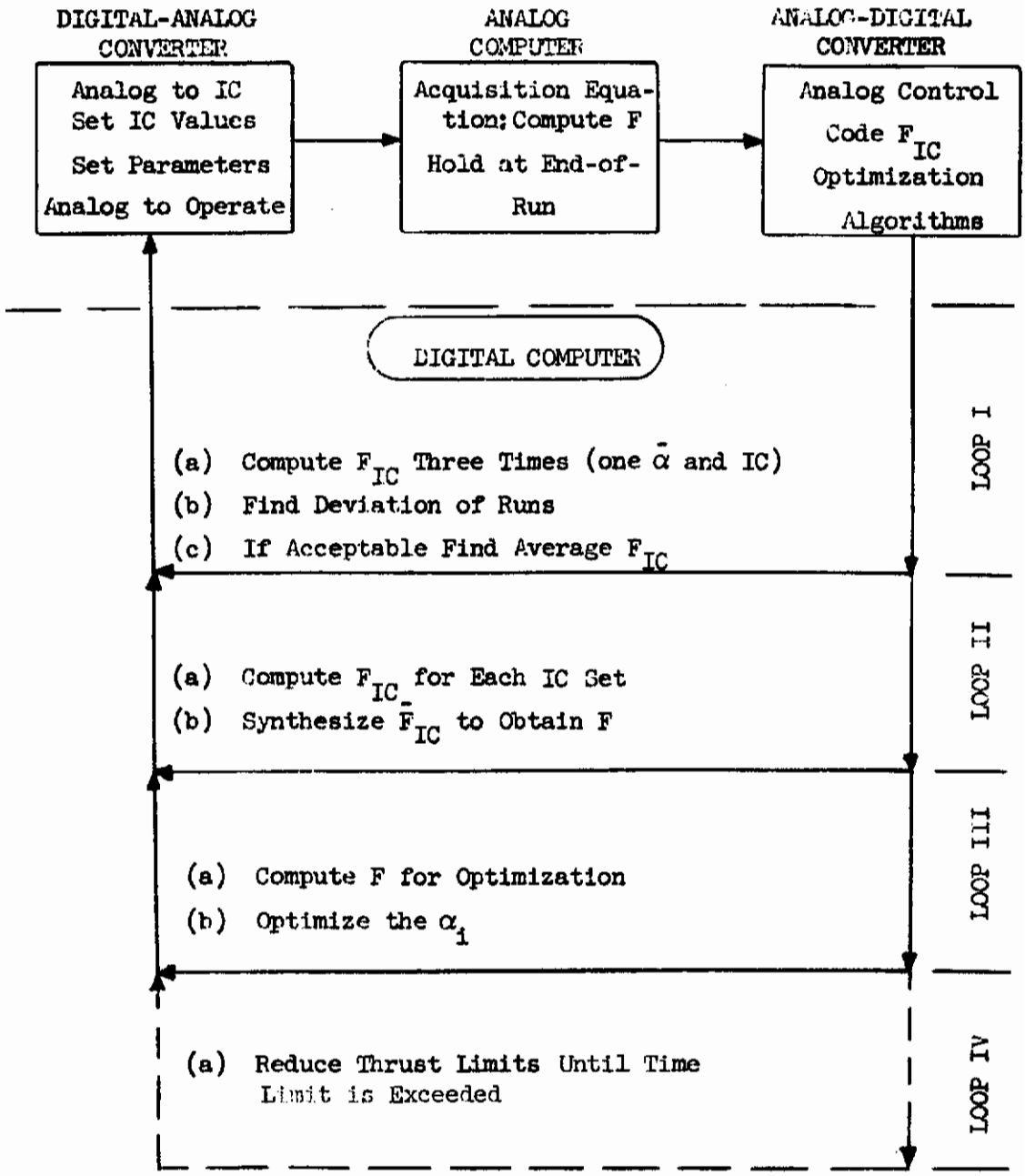

Figure 6.5

Optimization Master Logic Flow Diagram

be assumed already calculated. A new point in parameter space is selected by the optimization algorithm (for example, relaxation). For each set of variable initial conditions, three analog computer runs are made giving a F_{IC} for each run. The three F_{IC}'s are compared to check parity (the reasons are explained later). If their standard deviation is within tolerance, the mean F_{IC} for the three is selected as the criterion for this set of IC's. This is the innermost loop (Loop I). This process is repeated for each set of IC's (Loop II). The F_{IC}'s for each IC set is averaged to give F. This is the F used to determine (Loop III) whether the explored point is better than the present point. If minimum thrust criterion is used, Loop III minimizes time as the error criterion. Once an improvement is found, the time is compared with an acceptable time. If the time is unacceptable, the optimization continues (optimization of all parameters but the thrust saturation levels). If time is made acceptable Loop IV reduces the thrust limits and calculates the time of run criterion for the reduced thrust limits with the other parameters set to the last values found in the time optimization loop (Loop III). The new time will differ from the previous value, as the thrust limits have been reduced. If this time is still acceptable, the thrust limits are further reduced until an unacceptable time is produced. At this point, Loop III optimizes until another thrust limit reduction can be made or no acceptable time can be found. When the thrust limits are so low that the latter situation occurs (no acceptable time can be found), the last set of parameters (including thrust limits) that gave an acceptable time of run is accepted as the optimum set for minimum thrust.

6.3.4 Computer Error Detection

The speed and accuracy of convergence of the optimization procedure is directly related to the accuracy and repeatability of the analog simulation. Extensive testing of the analog computer found that for many runs in succession or even on separate days with identical inputs, the optimization criterion would be repeatable to within

a volt unless an obvious malfunction occurred. The prime source of malfunctions were: a) a bit lost in the analog to digital converter, b) a momentarily defective electronic switch, c) drift in the electronic multipliers. Most malfunctions were of a momentary nature so that for over 99% of the time no more than two successive runs were adversely affected. In light of this knowledge, the computer was programmed in the following manner to prevent computer malfunctions from negating an algorithm or consuming excessive time in trouble shooting.

Overload: An overload in the analog computer indicates one of two possibilities: the parameter settings yield an unstable differential equation, or the analog equipment has malfunctioned. In either case, the computer requires some time to come out of overload. The digital computer is then programmed to stop on overload, allow the operator to diagnose the problem and either re-run the same case or continue to the next case.

Maximum Allowable Time is Exceeded Before the End of Run Criterion is Met: This most frequently occurs intentionally, such as when fuel is minimized and low thrust rates are desired. Naturally, the acquisition time is extended. The lowest possible thrust level is zero in which case acquisition time approaches infinity. Occasionally however, drift in a multiplier will produce the same effect. The computer is programmed to print out when time was exceeded and retry the problem. If time is exceeded again, it is printed out, and a large value is assigned the optimization criterion and the optimization continues. The assumption is made that the parameters violate the acquisition time condition and are, therefore, unacceptable. If the operator suspects computer malfunction, he may stop the computer. If the time is not exceeded on the second trial, the error criterion for the previous trial is erased and optimization continues.

Standard Deviation Test: The computer makes three runs with the same inputs. If the standard deviation is less than a volt, operation is assumed normal and the optimization continues. If the standard deviation is greater than a volt, malfunction is assumed. In this case, the large standard deviation is printed out and another set of three runs attempted. If this set is accepted, the first set is discarded and the optimization is continued. The operator may stop the computation if he desires.

These three checks appeared to eliminate most of the possible error sources, as only twice during the study were poor results obtained that could be attributed to machine error. Additional justification for this test is presented below.

Confidence Test: The use of confidence tests provides a powerful tool for improving the accuracy of analog computer studies as well as detecting deterioration in its performance. Assume the errors in analog results normally distributed with zero mean and a known bias σ. If N samples are tested and a sample mean calculated

$$\bar{M} = \sum_{i=1}^{N} F_i/N$$

where F_i is the result of the computer trial, the probability that this sample mean lies within a valid x of the true mean (the F_i without error) is:

$$p(x) = \frac{1}{2\pi} \int_{-\frac{x\sigma}{\sqrt{N}}}^{+\frac{x\sigma}{\sqrt{N}}} e^{-\frac{t^2}{2}} dt$$

In this manner, if σ is known, it is possible to state that for N trials, the sample mean differs from the true value by no more than x with confidence p(x). Values for p(x) given σ, x and $\sqrt{N}$ are given in any normal distribution table.

σ may be evaluated by making a very large number of identical acquisition trials with the analog computer. The sample variance

$$V = \sum_{i=1}^{N} \frac{(F_i - \bar{M})}{N-1} \sim \sigma^2$$

may be used to approximate the true variance. This sample variance also approaches the true variance as N increases.

Once σ has been estimated, N is determined by the accuracy and confidence desired. Use can also be made of the sample variance (V_s) of the new trial. If the computer is operating as well during the sample as when σ was estimated, the sample variance would be expected to compare closely with σ. The Fisher Z distribution states the explicit relation that with confidence Z ($\sqrt{V_s}$, σ) that $\sqrt{V_s}/\sigma$ is less than a given number. This test can be used to determine, with probability Z whether the computer is operating significantly worse than normal. For example, suppose it is desired to be confident with probability .95 the computer has no more noise than when σ was estimated. For N samples ($2 \leq N \leq 5$), $\sqrt{V_s}$ must be:

N	$\sqrt{V_s}$ requirement
2	$\sqrt{V_s} \leq 3.84\sigma$
3	$\sqrt{V_s} \leq 3.00\sigma$
4	$\sqrt{V_s} \leq 2.60\sigma$
5	$\sqrt{V_s} \leq 2.37\sigma$
∞	$\sqrt{V_s} \leq 1.965$

When the allowable variance is exceeded it is assumed that the computer is not operating properly. The assumption that the analog computer noise has zero mean and has a normal distribution can be justified on the following grounds: 1) an attempt is made to balance the computer continuously, 2) the actual bias is considerably smaller than the noise for normal computer operation (bias can be ignored), 3) the noise comes from many sources (it can be shown that as the number of sources increase the distribution approaches a normal distribution no matter what the individual noise source distributions).

In an earlier section, the decision to select three trials for measuring standard deviation was based on the above (in order to be 95% confident the computer noise level is acceptable provided a standard deviation 3σ is found). By averaging the three samples and using this result, the accuracy of the optimization criterion is increased by a factor $\sqrt{N}$.

6.4 A specific Acquisition Optimization

All the techniques necessary for acquisition optimization have been developed. A specific satellite acquisition will now be studied. The satellite will be assumed to have three rate gyros, two direction cosine sensors and three mass expulsion torquers. The control law is assumed of the form shown in Table 6.2. The torques are assumed in units of angular acceleration, allowing a slightly more general study. In this manner, the inertias need not be given, merely the inertia ratios. This study will apply to any satellite with these given ratios. The error criteria that were studied are acquisition time, fuel consumption for acquisition and maximum thrust level with a time constraint. All three will be minimized. The initial condition set studied will expand from a study of several process procedures for permutations of possible rates about the nominal attitude to a study of average expected rates for all attitudes which the initial condition space search will examine. This procedure allows initial optimization studies in

the linear region of the satellite kinematics (so hand analysis can more easily be used to correlate the data found) and more severe acquisition problems later once some confidence in the optimization procedures has been developed. The parameters in the study will initially be the five gain parameters of the control system and will be expanded to these five plus four limit parameters. Due to the limited number of digital to analog channels, only nine independent parameters can be studied at one time. Two of the limit parameters (the two direction cosine limits) will then be proportional. The values assumed for possible initial conditions on the variables and parameter limits are shown in Table 6.3. These upper bounds on the parameters were selected for the following reasons. The position gains (α_1 and α_2) were limited due to the expected noise level for the sensors. α_3 was limited similarly. The rate to position gains were limited at 10 seconds as it was desired the satellite response be no slower than this. The torque limits were selected as a reasonable upper bound on the mass-expulsion torque of the type that might be used. The direction cosine sensors essentially have no upper limits as unity is the upper bound for the direction cosines. The lower bounds were 1% of the upper bounds which was the effective dynamic range of the analog equipment used. It was planned if any parameters were driven to their lower bounds, the computer would be rescaled.

The following discusses in more detail what was done. A discussion of the significance of these results is presented in the next section.

6.4.1 Initial Condition Space Search

The initial condition space search is used to provide a desirable set of initial conditions for the variables. An initial estimate of the parameters is needed. For the 5 parameter study, the gain parameters were set at 0.5 their upper bound. The limit parameters α_6-α_{10} were set at their upper limits. For the 10 parameter study, all

TABLE 6.3

DEFINITIONS AND NUMERICAL VALUES FOR ACQUISITION OPTIMIZATION STUDY

Parameter	Description	Assumed Value or Range of Values	Units
ω_{im}	Maximum Initial Rate	$\pm$ 70	milliradians / sec
ω_{ia}	Average Initial Rate	$\pm$ 26	milliradians / sec
a_{ijn}	Nominal Direction Cosines	$a_{13}=a_{23}=0 \quad a_{33}=+1$	-
a_{ijmin}	Minimum Initial Attitudes	$0, \pm 1$ *	-
a_{ijmax}	Maximum Initial Attitudes	$0, \pm 1, \pm 1/\sqrt{3}$ *	-
$(I_2-I_3)/I_1$	Inertia Ratios	+ 0.311	-
$(I_3-I_1)/I_2$	Inertia Ratios	- 0.802	-
$(I_1-I_2)/I_3$	Inertia Ratios	+ 0.643	-
α_1	Roll Position Gain	0.001 to 0.100	sec^{-2}
α_2	Pitch Position Gain	0.001 to 0.100	sec^{-2}
α_3	Yaw Rate Gain	0.010 to 1.00	sec^{-1}
α_4	Roll Rate to Position Gain	0.100 to 10.0	sec
α_5	Pitch Rate to Position Gain	0.100 to 10.0	sec
α_6	Yaw Torque Limit	0.001 to 0.100	rad/sec^2
α_7	Roll Torque Limit	0.001 to 0.100	rad/sec^2
α_8	Pitch Direction Cosine Limit	0.01 to 1.00	-
α_9	Pitch Torque Limit	0.001 to 0.100	rad/sec^2
α_{10}	Roll Direction Cosine Limit	0.01 to 1.00	-

* All physically realizable combinations.

parameters were set at 0.5 their upper limit. The first space search series used was series 14 (nominal attitude and all permutations of 0, ± average or ± maximum rates). In order to better compare the importance of which initial condition set is selected, initial condition sets from all three procedures (worst cases, average cases, worst quadrant cases) were studied. It was found (as will be seen later) that optimization appeared most plausible when either an average or worst quadrant set was selected. Based on this knowledge, when the next space search series (series 12 - all possible attitudes for ± average or zero rates) was used, the average procedure was used. A large number of IC's were selected from around the average F and the two initial conditions that appeared in the most diverse quadrants were used as the optimization initial condition set. The initial condition sets selected for optimization studies (following from the above discussion) are listed in Table 6.4.

6.4.2 Optimization Study

The following optimization studies were made:

(1) With the 5 gain parameters variable (the 5 limit parameters fixed at their upper bounds), initial condition sets I, II and III were used for each of the following: a) minimum time criterion, relaxation and pure random walk local search algorithms (no global searches), b) minimum fuel criterion, relaxation and pure random walk local search algorithms (no global searches). These studies established the superiority of the random search over the relaxation and desirability of average or worst quadrant IC sets.

(2) With the 5 gain parameters variable (5 limit parameters fixed at their upper bounds), initial condition set IV, minimum time criterion and the random global search were used for each of the following: a) relaxation local searches,

TABLE 6.4

INITIAL CONDITION SETS FOR ACQUISITION OPTIMIZATION

IC Set Number	Search Set No.	Process Procedure	IC Number	ω_1 (mr/sec)	ω_2 (mr/sec)	ω_3 (mr/sec)	a_{13}	a_{23}	a_{33}
I	14	2-(Average)	1	-70	-26	-26	0	0	+1
			2	+70	-26	+70	0	0	+1
II	14	1-(Worst)	1	+70	+70	+70	0	0	+1
			2	-70	+70	-70	0	0	+1
III	14	3-(Quadrant)	1	+26	+70	+70	0	0	+1
			2	+70	0	+70	0	0	+1
			3	+70	-70	0	0	0	+1
			4	0	+70	-70	0	0	+1
IV	12	2-(Average)	1	-26	-26	-26	+1	0	0
			2	-26	+26	+26	0	+1	0

b) pure random walk local search, and c) absolutely biased random search. These studies established the advantage of a global search and the superiority of the absolutely biased local random search.

(3) With all nine parameters variable, initial condition set IV and random global search were used for each of the following: a) time criterion with absolutely biased random and relaxation local searches, and b) fuel criterion and random local search were studied. These studies provided the final information for the optimal design of the acquisition system for minimum time or fuel.

A summary of the pertinent details of these studies is presented in Tables 6.5, 6.6, and 6.7. Figures 6.6, 6.7, and 6.8 show sample variations of the parameters for relaxation, absolutely biased random local and random global, respectively, during the optimization. These samples were run with nine parameter variation and time as the criterion.

To indicate the improvements in system response during the optimization, Figure 6.9 gives the time response of five independent variables (ω_1, ω_2, ω_3, a_{13}, a_{23}), the end-of-run criterion, time of run and fuel consumption for: 1) the initial parameter settings, 2) the optimized minimum time settings, and 3) the optimized minimum fuel settings. This is for case 1 of IC set number IV. The runs did not terminate at the satisfaction of the end-of-run criterion (as during the search) to ascertain that little motion took place after this point (indication of a satisfactory level for end-of-run criterion). The x's indicate the position of the optimization criterion at the end-of-run.

A maximum thrust level criterion was studied. This thrust level was minimized subject to the additional constraint that acquisition

TABLE 6.5

MINIMUM TIME OPTIMIZATION RESULTS WITH FIVE FREE PARAMETERS

Description	IC Set I		IC Set II		IC Set III				
					Relaxation		Random Walk		
	Relaxation	Random Walk	Relaxation	Random Walk	Case A(a)	Case B(a)	Case A(a)	Case B(a)	Case C(a)
T for Initial Parameter Settings (sec)	31.1	31.1	40.6	39.4	22.9	23.1	23.1	23.3	23.3
T for Optimum Parameter Settings (sec)	10.4	10.0	15.1	14.0	13.8	13.6	11.6	11.3	11.6
Total Runs	139	291	-	275	137	124	146	177	204
Runs to Optimum	91	166	79	146	51	50	25	56	82
Random Walk Runs to Improve Relaxation Results	-	107	-	80	-	-	3	19	35
Optimal α_1 [b] (sec^{-2})	0.099[c]	0.099	0.100	0.096	0.100	0.100	0.089	0.089	0.100
Optimal α_2 (sec^{-2})	0.099	0.099	0.066	0.047	0.060	0.060	0.049	0.052	0.051
Optimal α_3 (sec^{-1})	0.990	0.918	0.500	0.965	0.999	0.999	0.728	0.999	0.621
Optimal α_4 (sec)	8.20	9.90	8.20	9.90	9.90	9.90	8.60	9.90	8.40
Optimal α_5 (sec)	9.90	9.90	9.90	9.90	6.50	6.50	9.90	9.90	9.90

(a) Different cases run on different days to check repeatability.

(b) All initial parameter values were 0.500 upper bound.

(c) All parameters limited between 0.010 and 0.999 as listed in table.

TABLE 6.6

MINIMUM TIME OPTIMIZATION RESULTS WITH FIVE AND NINE FREE PARAMETERS AND IC SET IV

Description	Five Free Parameters				Nine Free Parameters			
	Relaxation to Biased Random Walk[a]	Biased Random Walk With 200 Run Global	Biased Random Walk With 100 Run Global	Random Walk	Relaxation	Biased Random Walk[b]	Biased Random Walk	Biased Random Walk[c]
T for Initial Parameter Settings (sec)	31.1	31.2	31.1	31.1	36.3	36.3	36.3	16.9
T for Optimum	17.5	17.2	17.8	17.6	19.4	17.4	16.9	16.9
Total Runs	370	451	175	244	287	385	453	122
Runs to Optimum	250	124	52	124	183	165	233	-
Optimal α_1 (sec^{-2})	0.078	0.051	0.051	0.055	0.066	0.050	0.047	0.050
Optimal α_2 (sec^{-2})	0.050	0.047	0.051	0.050	0.046	0.052	0.048	0.050
Optimal α_3 (sec^{-1})	0.660	0.511	0.741	0.668	0.500	0.519	0.447	0.999
Optimal α_4 (sec)	4.20	9.90	9.20	9.10	6.00	9.90	9.90	9.90
Optimal α_5 (sec)	9.90	9.90	9.10	9.90	9.90	9.20	9.90	9.90
Optimal α_6 (sec^{-2})	-	-	-	-	0.099	0.098	0.099	0.099
Optimal α_7 (sec^{-2})	-	-	-	-	0.050	0.052	0.064	0.099
Optimal α_8 & α_{10}	-	-	-	-	0.900	0.993	0.999	0.999
Optimal α_9 (sec^{-2})	-	-	-	-	0.050	0.096	0.028	0.099

(a) 143 runs made in relaxation and remainder in random walk.
(b) Threshold to detect significant improvement was lowered by factor of three.
(c) Started at suspected optimum with no further improvement found.

TABLE 6.7

MINIMUM FUEL OPTIMIZATION RESULTS WITH FIVE AND NINE FREE PARAMETERS

Description	Five Free Parameters						9 Parameters	
	IC Set I		IC Set II		IC Set III		IC Set IV	
	Relaxation	Random Walk	Relaxation	Random Walk	Relaxation	Random Walk	Biased Random Walk	
							Case A[a]	Case B
Initial F (mr/sec)	133.4	132.5	162.0	162.4	131.0	130.9	223.2	225.2
Optimal F(mr/sec)	104.9	103.2	132.8	125.5	110.8	105.6	81.3	79.6
Minimum Possible F (mr/sec)	91.5	91.5	121.2	121.2	99.0	99.0	65.0	65.0
Total Runs	--[b]	173	--[b]	315	86	185	413	438
Runs to Optimum	111	51	132	189	73	65	293	314
Optimal α_1(sec^{-2})	0.060	0.059	0.082	0.098	0.050	0.044	0.095	0.089
Optimal α_2(sec^{-2})	0.099	0.100	0.100	0.100	0.090	0.087	0.082	0.088
Optimal α_3(sec^{-1})	0.038	0.032	0.500	0.999	0.050	0.034	0.090	0.089
Optimal α_4(sec)	5.00	4.80	99.90	9.60	5.00	3.60	2.30	2.00
Optimal α_5(sec)	9.00	6.60	99.90	9.90	5.00	9.50	0.90	0.80
Optimal α_6(sec^{-2})	-	-	-	-	-	-	0.091	0.085
Optimal α_7(sec^{-2})	-	-	-	-	-	-	0.034	0.041
Optimal α_8 and α_{10}	-	-	-	-	-	-	0.152	0.152
Optimal α_9(sec^{-2})	-	-	-	-	-	-	0.089	0.080

(a) Different cases run on different days.

(b) Not recorded.

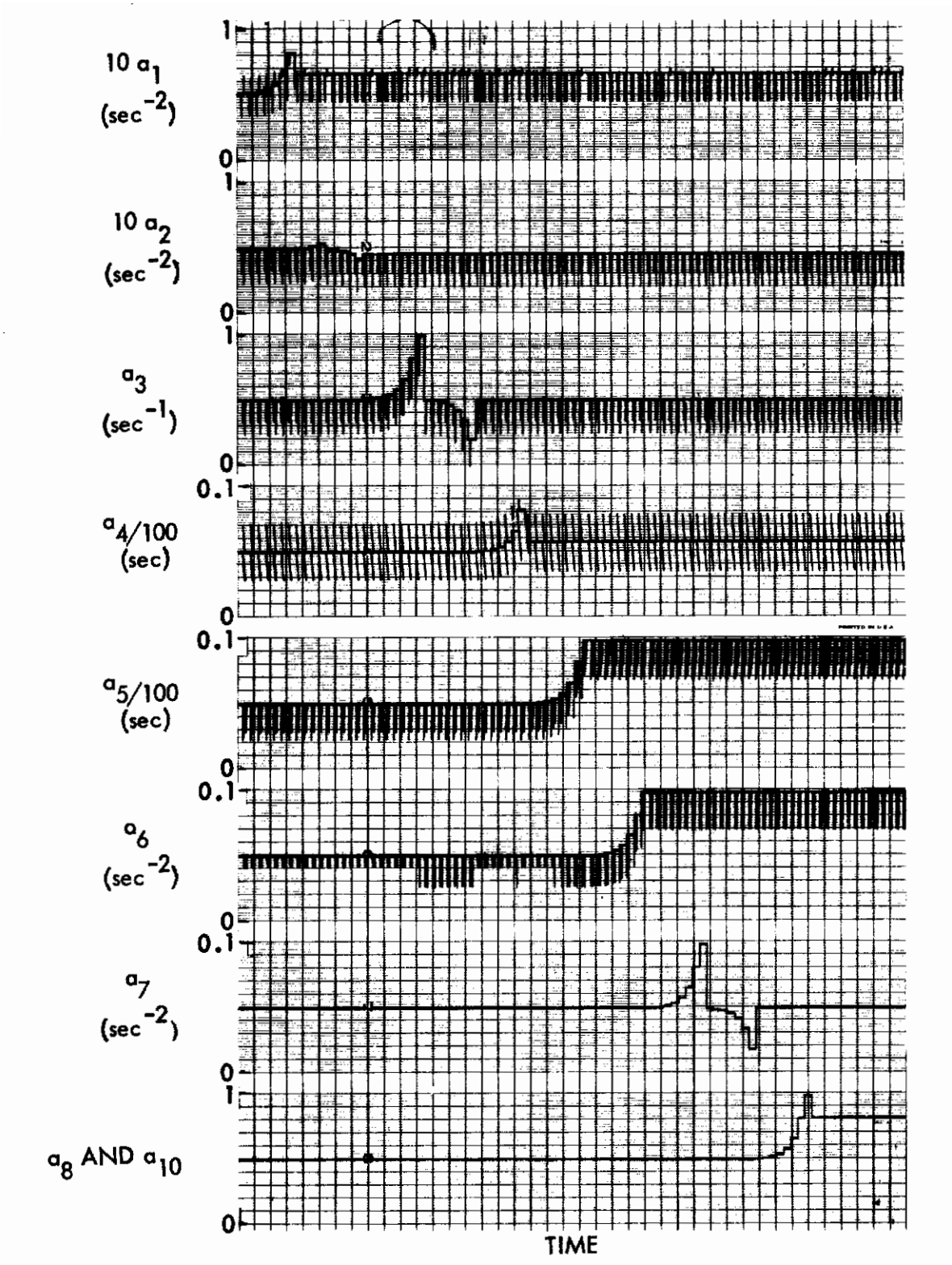

Figure 6.6 Nine Parameter Minimum Time Optimization Using Relaxation Local Search. Vertical lines are resetting of analog computer.

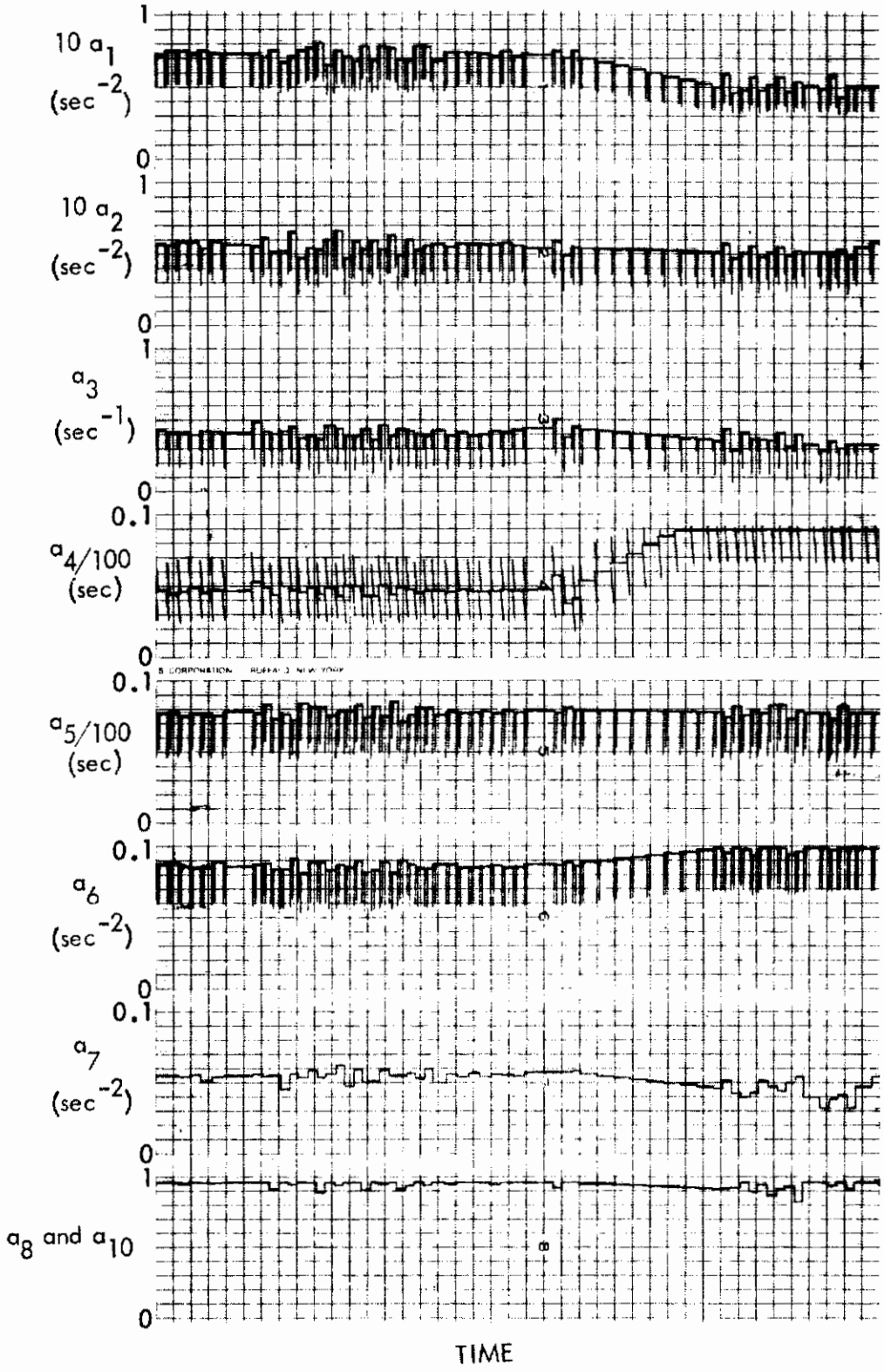

Figure 6.7 Nine Parameter Minimum Time Optimization Using Absolutely Biased Local Random Search

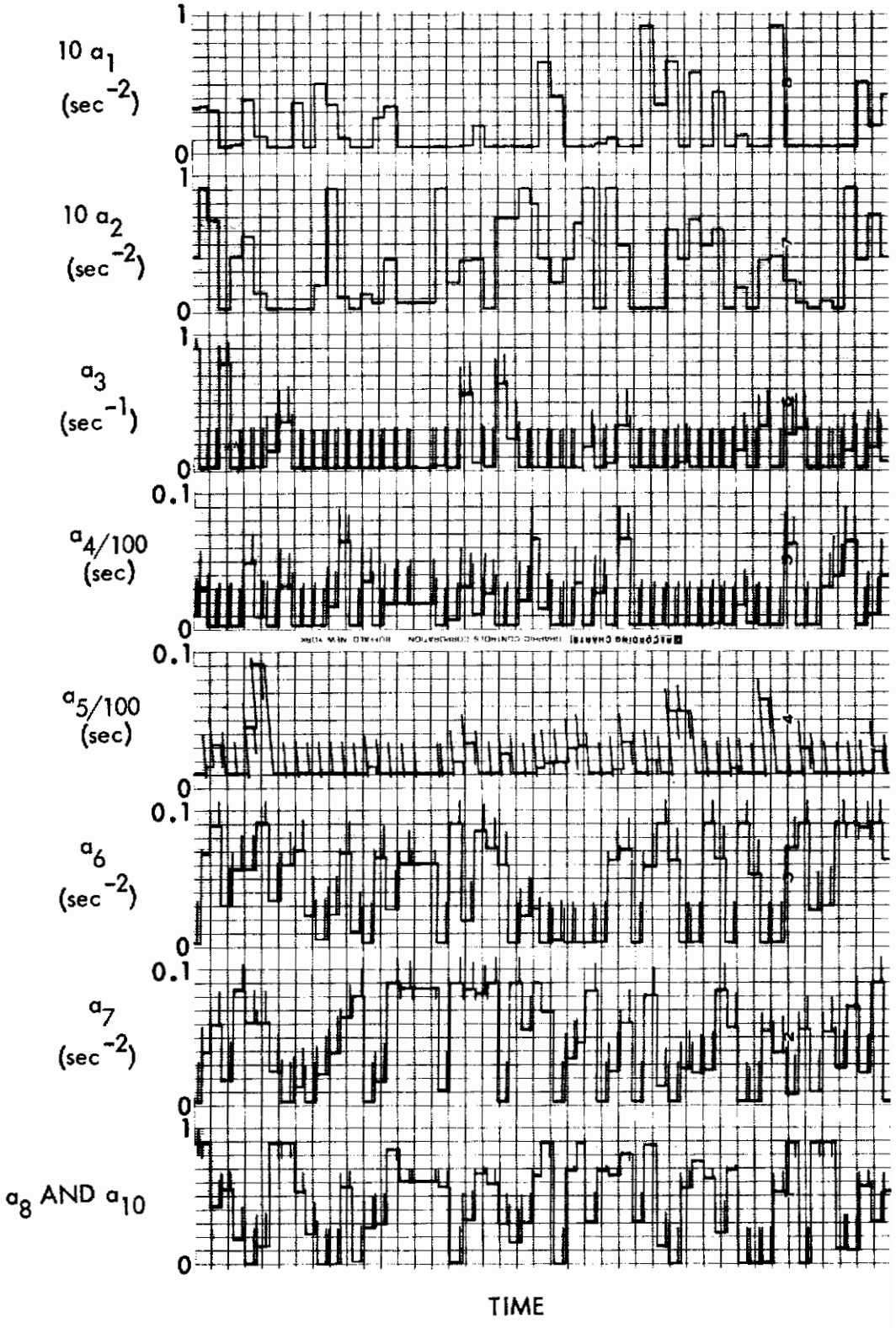

Figure 6.8 Nine Parameter Minimum Time Optimization Using Global Random Search

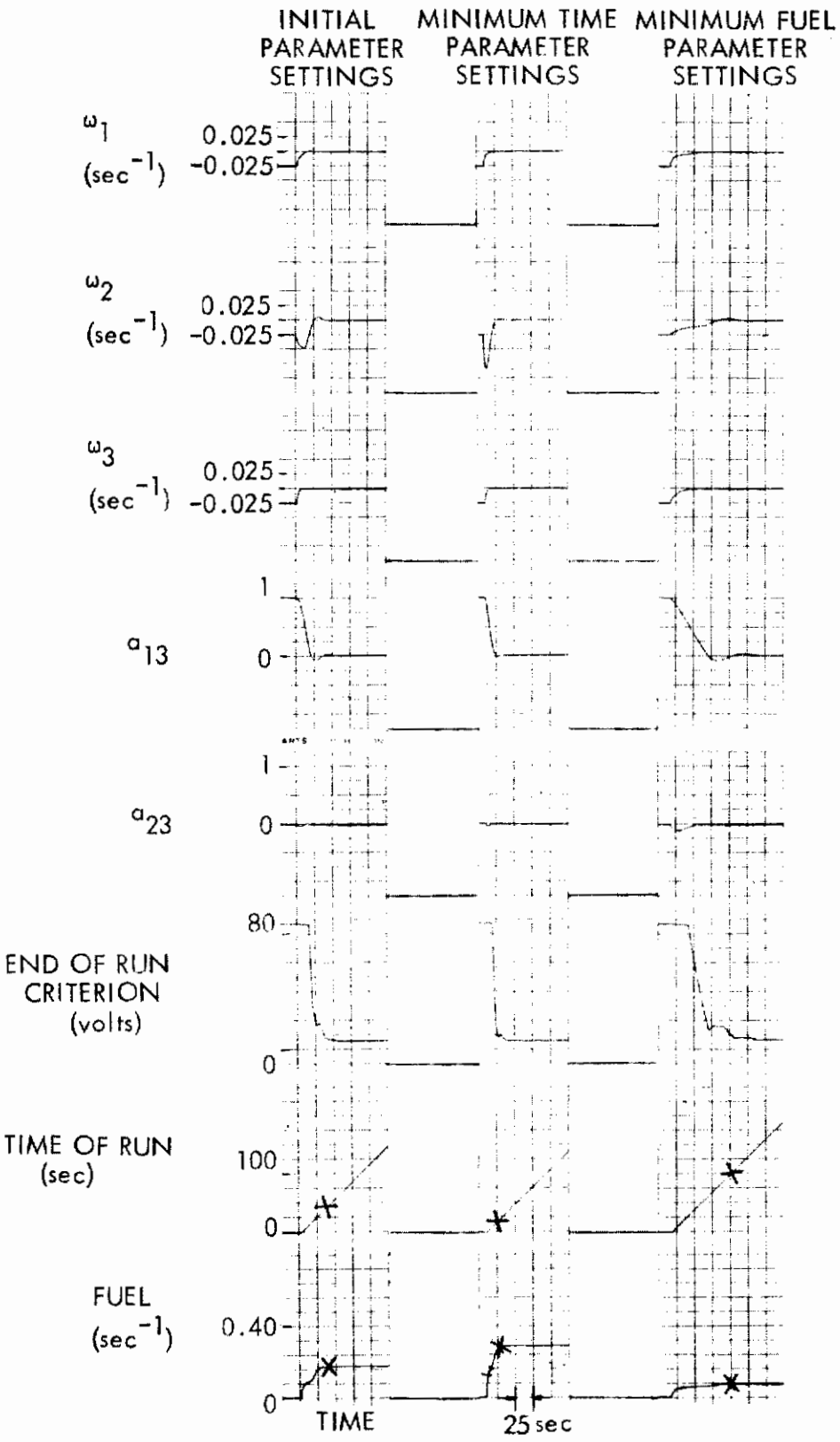

Figure 6.9 Comparison of Minimum Time and Minimum Fuel Optimal Solution with Pre-Optimization Solution

must be accomplished within 30 seconds. The other 7 parameters were adjusted via an absolutely biased random local-random global serach in order to satisfy this time constraint as the thrsut levels were reduced. Initial condition set IV was used. All initial parameter guesses were 0.5 their upper bound with the exception of the torque limits. The limits were found to go so low that the computer was rescaled so that the upper bound (and initial guess) on these limits were .01 rad/sec^2.

The thrust limits were reduced to 5.4 mr/sec^2 before time optimization was required. The final thrust limits of 1.4 mr/sec^2 were achieved after 154 optimization trials (100 additional runs were run to ascertain that this was an optimum).

The final parameter settings were found to be:

$$\alpha_1 = .0957 \text{ sec}^{-2}$$
$$\alpha_2 = .0954 \text{ sec}^{-2}$$
$$\alpha_3 = .0316 \text{ sec}^{-1}$$
$$\alpha_4 = 9.999 \text{ sec}$$
$$\alpha_5 = 9.463 \text{ sec}$$
$$\alpha_6 = \alpha_7 = \alpha_9 = 1.4 \text{ mr/sec}^2$$
$$\alpha_8 = \alpha_{10} = .6175 \text{ unitless}$$

Figure 6.10 shows a typical case of minimum thrust optimization. Notice the alternating reductions of thrust (α_6 and α_7) and the other parameter variations to minimize time.

6.5 Conclusions

The conclusions from studying the acquisition system of Section 6.4 divide into two general classes: those regarding the efficiency of the various techniques developed, and those regarding a desirable design for this system.

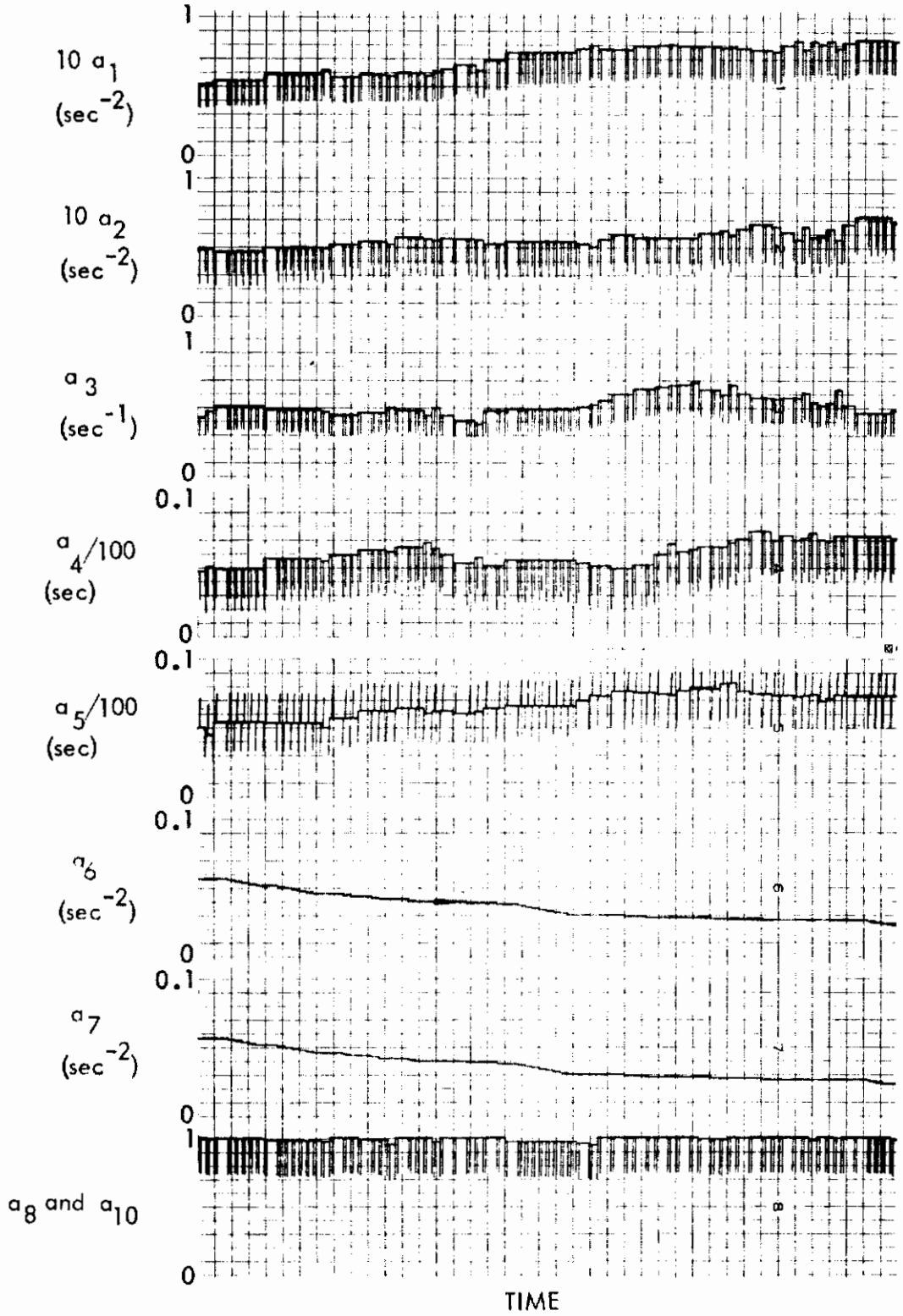

Figure 6.10 Minimizing Required Thrust Level with Acquisition Time Constraint Using Absolutely Biased Local Random Search

6.5.1 Technique Efficiency

The results from this study indicate that search techniques can be used to optimize acquisition control system parameters. However, these techniques cannot indiscriminately be applied. The control system must already be conceptually designed. Only after the basic form of a control design has been formulated can search techniques be of any use. The search technique will designate optimal gains and other parameter settings, but the parameters must already be defined. A satisfactory criterion must be given in sufficient quantitative form that a number can be computed and used as an ordering for the criterion space. A fast and accurate computer is necessary. A hybrid computer used in this study proved satisfactory in both respects as an F for a new point in parameter space was calculated in less than 12 seconds and the optimization criterion converged to within a few percent of the same value each time the case was run (suggesting accuracy to this extent).

Space Search: The variability of the optimization criterion as a function of initial condition sets is well illustrated in the five parameter studies of Tables 6.5 and 6.7 where three different initial sets were used in minimizing time or fuel. It can easily be seen that the "optimal" parameter settings of the three IC sets vary considerably. It, therefore, becomes important to have a tool such as this space search program to assist in evaluating which set of initial conditions will prove satisfactory. In a smooth criterion space as studied in this report, little need was found for using space search more than once--that for the initial set. The lack of need for additional searches is illustrated by the relative value for F before and after the optimization (the worst case remains the worst). Slight variations do however occur as it becomes more difficult to reduce the F for a larger number of IC's (compare IC sets II and III). This indicates that, as expected, the greater the number of conditions the more difficult it is to "tune" the controls for these conditions. As the controls become more nonlinear, it is expected that it will become

necessary to utilize the program during the optimization to update the initial condition set. From experience gained during the study, it was concluded that, in general, an initial condition set which gives large initial conditions to one channel at a time, such as done in IC sets III and IV is desirable. In this manner, if an initial condition in one direction happens to have predominant effect on the criterion, it will not prevent optimization on the other channels. Also, the "tuning to one condition" is most easily removed in this manner without requiring a very large number of initial conditions.

Optimization Algorithms: Time constraints did not allow applications of steep descent algorithm to the simulation, although the algorithm has been programmed. The following briefly discusses the conclusions that can be drawn from the work that was done concerning the relative merits and problems of the relaxation and random search algorithms.

The success of the relaxation scheme is critically dependent upon the appropriate parameter choices. For example, the x control loop could equivalently be written as: $\alpha_1 (a_{23} + \alpha_4 \omega_1)$ or $\alpha_1 a_{23} + \beta \omega_1$ where $\beta = \alpha_1 \alpha_4$. The choice of which parameter set to consider (α_1 and α_4 or β and α_1) should be based on which provides the most efficient convergence. In the case of relaxation, parameters must be selected in order to minimize cross-correlation (as independent of each other as possible). As quite often this is not known before a design, particularly where a large number of nonlinearities exist, this is a basic problem in the use of relaxation techniques. For the choice of parameters chosen in the present study and the equations simulated, relaxation gave very poor results. In fact, for each case that relaxation and random searches were performed on identical problems, the random search found a better set of parameters. For this reason, relaxation was discarded in the latter portion of the studies. The addition of a global search did permit the relaxation to find the optimum, but the local random search always converged faster when used

in conjunction with the global search. Much success has been achieved elsewhere using relaxation and it would probably prove an efficient scheme in a near linear criterion space where the effects of the control design on the criterion is already fairly well understood. But for these acquisition studies, it does not appear promising.

The random search technique shows great promise. One appeal of this technique is the limited demands placed on the criterion space. If pure random walk is assumed, the speed of convergence can be estimated for simple criterion spaces. If more information is available to the designer, this information can efficiently be used by adjusting the bias and variance of the samples. This is demonstrated by the success of the absolutely biased search. The assumptions about the criterion space were: if a success of a certain significance level is found, future successes are most likely to occur along the same direction; and if a failure below a certain significance level is found, future successes are most likely to occur in the opposite direction. These assumptions always hold on very smooth criterion spaces. However, additional work is required in refining the values selected as significance levels and the proper weight to give conclusions about the location of the next sample. For absolute biasing, the above logic determined the direction of the bias. The step length was selected identical to the previous step and the variance was reduced to zero. This technique, as presently implemented, is highly successful as evidenced in Tables 6.6 and 6.7. A successful strategy for changing the variance during the search (if no positive success or failure was found) was never found. The variance finally selected was 4 percent of the span (upper limit to lower limit) of each parameter. One reason for such success with no variance change was the global search strategy selected. This complemented the local search as a change in variance is programmed in the global search.

The random global search technique proved to be very useful. The strategy that appears most useful is that of using the local optimum as the origin and initiating the purely random (no biases) search with a very small variance. After each search, the variance is widened until any point in the parameter space has some chance of being inspected. For the most successful strategy found in the study, the variance was initially set equal to 0.5 percent the span (upper limit to lower limit) of each parameter which was incremented by a factor of 1.02 every trial until the variance reached 50 percent the span. The reasoning being, the probability of a further improvement is most likely near the local optimum and decreases linearly as the distance from the local optimum. The specific strategy must be selected from experience with the acquisition problem and knowledge of the weaknesses of the local search algorithms. For both the local search algorithms studied, the possibility of a nearby improvement was high. The relaxation may get stranded on a saddle point and the fixed variance of the local random search may require a varied variance about the local optimum (either larger or smaller). In nearly every search for which the global random search was used, an improvement was found due to the global search.

Minimum-maximum thrust level optimization provided the greatest exercise for the search procedure, as a time optimization routine became a subsystem for this program. Here, thrust levels were lowered until the acquisition time became unacceptable at which time all other parameters were adjusted in an attempt to give an acceptable acquisition time. The optimization appeared to converge quite efficiently (as indicated in Figure 6.10). This indicates that multi-criterion optimizations or optimizations with constraints which require sub-optimizations for satisfaction are feasible.

6.5.2 Acquisition System Design

Tables 6.5, 6.6, and 6.7 show what control system designs should be used as a function of the optimization criterion, initial condition set and number of parameters available for adjustment. The following observations and conclusions regarding the control design are results of the optimizations performed.

Parameters Available for Adjustment: Table 6.6 shows the results of optimizing identical systems with the exception of the number of parameters available for adjustment. As may be expected, the 10 parameter study allows slightly improved results. The 5 parameter study should never yield a better result than with 10 parameters as the 5 parameter results lies in the 10 parameter criterion - space. A poorer 10 parameter result would indicate a poor optimization algorithm or a poor choice of initial parameter guesses. The significance of the individual parameters will be discussed later.

Acquisition Time Criterion: Tables 6.5 and 6.6 show the desired parameters for minimum acquisition time. Much can be gained by considering the linearized dynamics and kinematics, in which case, acquisition behaves like a second order system with poles described by:

$$s^2 + \alpha_1\alpha_4\, s + \alpha_1 \text{ or } s^2 + \alpha_2\alpha_5 + \alpha_2$$

where s is the Laplacian operator. Consider the generalized form: $s^2 + 2\,\delta\,\omega\, s + \omega^2$ where ω is the natural frequency and δ the damping. The ω_3 channel is described by the first order pole: $s + \alpha_3$; and may be compared to the general form: $s + k$ where k is the time constant of the system. Although the system studied is highly nonlinear, use of the linear terminology defined above does add some insight into the problem.

Consider first the 5 parameter studies with initial conditions at the nominal attitude. In these cases high nonlinearities and saturations are minimized. The results from the relaxation studies will not be considered due to the inferior optimizations. For all IC sets, the rate gains were, in general, raised to their highest values. An apparent insensitivity of the 3 axis control is shown by considerable variation in α_3. This is due to the speed with which the third axis acquires. The x_3 axis rate is reduced so quickly that it has little effect on the total acquisition time. The upper limit for α_3 would suggest a time constant of 1 second as contrasted to the excess of 10 seconds required for acquisition. The position gains (α_1 and α_2) also showed some variability. This can be understood in the linear case, where, if the damping lies in an acceptable range, the time response is primarily determined by the distance of the poles from the imaginary axis (α_4 or α_5). This is especially true where a severe end-of-run criterion (such as was used in this case) is used which does not tolerate overshoots. The greater uniformity of α_2 and α_5 than α_1 and α_4 indicates that the 2 axis (ω_2, a_{13}) is a more critical axis than the 1 axis.

The addition of other initial direction cosine combinations and the 5 limit parameters as permissible variables compounds the nonlinearity. All nonlinearities occur as a form of gain reduction (as with the five limits or reduction in a_{33}) or cross coupling. The effect of the gain reductions can be explained in this manner: gain reductions in the higher order integration paths (such as the $a_{33}\,\omega_1$ or $a_{33}\,\omega_2$ paths) are equivalent to introduction of additional plant lag. In a linear system, this is usually remedied by slowing down the control system sensitivity (reductions in α_1 and α_2). In this manner, the satellite momentum is never allowed to build up for large initial positions to the point that the torquers with their saturation limits cannot drive this to zero as the nominal attitude is approached. In other words--the chance of overshoots is reduced. Inspection of

Table 6.6 indicates this has happened. The natural frequency is driven to around .24 rad/sec. Maximum allowable damping is still desired raising α_4 and α_5 to their upper limits. α_3 has still been found to be rather insensitive. The only limits which appeared desirable to reduce are the T_1 and T_2 torque limits. Reduction in these apparently further prevent this momentum buildup.

Inspection of the time minimum parameter response shown in Figure 6.10 indicates that minimum time is bought at considerable fuel expense.

Fuel Criterion: Table 6.7 shows the desired parameters for minimum fuel consumption. Use of the linearized equations in understanding the minimum fuel optimization is more difficult. In the case of minimum time, the most efficient strategy is to accelerate the satellite toward the desired axis as quickly as possible and, as the nominal axis is approached, the linearized theory becomes a better model of what is happening. When the momentum is quickly decreased (even if not in the best direction) the satellite becomes more responsive and acquisition becomes quick. In the case of minimum fuel, the problem is greatly different. As the units of fuel have been selected as sec^{-1}, there exists a strong correlation between angular velocity change and fuel. In fact, minimum fuel is the sum of the absolute value of all the changes in angular velocity. It is apparent that the limiting fuel condition would be equal to the initial angular velocity of the satellite. This case would indicate that all fuel has been used in reducing angular velocity in the proper vector directions. A simple control law is assumed for the case studied which does not take into consideration cross-coupling. When the satellite attitude greatly differs from the nominal attitude, the sensors are actually providing incorrect signals. In fact, controls may even increase the total satellite angular velocity in an attempt to reduce this same velocity. For example, when $a_{13} = 1$, an ω_1 sensed will produce a torque T_1

which changes the angular velocity about the 3 axis (ω_3). It becomes apparent, then, that low gains are desired, especially at large attitude errors. This decrease in gains causes the acquisition time to grow. It is necessary to add an acquisition - time constraint to the optimization, for, in the limit an infinite acquisition time is required to produce a perfectly efficient acquisition. The control law is only accurate with nominal attitude and $\omega_3 = 0$. The ideal acquisition would allow torques at this condition only (a point at a time). As these are merely points in time, and only a finite torque is allowed, an infinite time is required in order for the integral of these two to reduce the velocity to zero. The time constraint used for the study was 100 seconds.

The results of Table 6.7 can now be understood. The parameter settings for the highest rates, nominal attitude IC set (set II) require very high gains. This is necessary in order to prevent the attitude from changing and further increasing the nonlinearities of the dynamics. In the other nominal attitude IC sets (sets I and III), the angular rates were not so severe and a slower acquisition will keep the controls in the linear region. Note the α_3 is reduced to a very low number. This is to prevent wasting fuel in the T_3 axis when this angular acceleration couples into the other axes. When large attitude conditions are allowed such as shown in IC set IV and limit parameters are allowed as variables, the gains can be seen to be further reduced. This is especially apparent in the rate gains. The optimal time to reduce rates with this control law is once again at the nominal attitude. Low rate gains permit attitude acquisition before rate acquisition.

Note that with an allowable 100 second acquisition time, the acquisition is quite efficient. This is seen by comparing the F final with the F lower limit. The response of the system with the minimum fuel parameters is shown in Figure 6.9. It can be seen that in this case, overshoots are not nearly so critical as in the minimum time case.

SECTION VII

STABILITY OF ACQUISITION SYSTEMS

This section is concerned with investigating the stability of acquisition systems via the Second Method of Lyapunov. Often this approach will provide stability and convergence information associated with the system differential equations even when a closed form solution is not available. In many practical problems these are the only characteristics of importance. In particular, stability is not assured when applying the optimization schemes of Section VI. The confidence in the utility of this approach to optimization is greatly enhanced if quantitative proof of stability can be established for the resulting optimal designs. In fact, true validity of the practical significance of the optimization approach requires that such stability information be available.

In Section IV complete stability of a particular idealized acquisition system was analytically established using the Second Method of Lyapunov. Extension of these results to more practical systems is not trivial. Indeed, the desire to eventually include the effects of control torque source and sensor saturation characteristics etc, greatly complicates the analytic problem. However, several unique aspects of the acquisition problem make it reasonable to explore techniques for determination of stability that may not be applicable in the general nonlinear control system case. First, the initial condition set is bounded, at least with respect to the angular rate variables. Therefore, proof of complete system stability is neither necessary nor desirable. In fact requiring the acquisition system to be stable independent of the initial state may impose implementation constraints which are totally unreasonable or impractical. Secondly, the problem relates to a physical process. Hence a great deal of prior knowledge

and theory are available to improve the understanding of the problem. In addition, valuable intuitive insight can successfully be employed in describing the characteristics of performance. Thirdly, the class of practically implemented acquisition system for various missions is not large. This allows rather specific analytic techniques to be developed for this problem which may not be of general validity or importance. Also, successful analysis of a particular acquisition system provides a significantly broad base for approaching a new system with slightly increased complexities. In this way a learning process can be employed to eventually cover all significant acquisition systems.

7.1 A Lyapunov Approach for Acquisition

In Section III significant effort was devoted to establish a satisfactory set of state variables for the acquisition problem. Independent of the choice of the kinematic representation the acquisition problem can be expressed in the usual vector differential equation form

$$\dot{\bar{y}} = \bar{g}(\bar{y}) \tag{7.1}$$

where $\bar{y}$ is the state vector.

A first step in the stability investigation of any nonlinear system is to establish all the singular points. The singular points are defined by the states $\bar{y} = \bar{y}_k$ such that

$$\bar{g}(\bar{y}_k) \equiv 0 \tag{7.2}$$

By introducing the transformation of coordinates,

$$x_i = y_i - y_{ik} \tag{7.3}$$

Equation (7.1) is transformed to

$$\dot{\bar{x}} = \bar{f}(\bar{x}) \qquad \bar{x}(0) = \bar{0} \tag{7.4}$$

where the singular point under investigation is now the origin of x-space. In this way all investigations can be described in terms of stability to the origin.

For the acquisition problem it is only necessary to establish the stability over some bounded region R in x-space. If in terms of the original y-space this region is R', and if more than one $\bar{y}_k \in R'$ exists then either: 1) the acquisition system should be discarded or 2) each of the singular points must be analyzed for stability and the implications on system performance evaluated. The limitation of interest to the bounded region R is of fundamental importance for the development of the potentially practical approach to quantitative stability analysis given in this section.

The fundamental theorem upon which is based the present approach is given by LaSalle and Lefschetz [24] and represents an extension of the original Lyapunov work.

Theorem 7.1

Let $V(\bar{x})$ be a scalar function with continuous first partial derivatives. Let Ω_ℓ designate the region of the state space where $V(\bar{x}) < \ell$ ($\ell > 0$). Assume that Ω_ℓ is bounded and that for every $\bar{x} \in \Omega_\ell$

$$V(\bar{x}) > 0 \qquad \bar{x} \neq 0 \tag{a}$$

$$\dot{V}(\bar{x}) \leq -\epsilon < 0 \qquad \bar{x} \neq 0 \tag{b}$$

then the origin is asymptotically stable and every solution of Equation (7.4) initiating in Ω_ℓ tends to the origin as $t \rightarrow +\infty$.

For some practical acquisition systems condition (b) of Theorem 7.1 may not be satisfied. For example, systems which tend to a limit cycle about the origin as their ultimate state solution will not be acceptable. These systems can readily be handled by the present approach by introducing the concepts of Lagrange Stability (Practical Stability) and ultimate boundedness. In this case the following theorem is useful.

Theorem 7.2

Let $V(\bar{x})$ be a scalar function with continuous first partial derivatives. Let Ω_ℓ and Ω_r designate regions where $V(\bar{x}) < \ell$ and $V(\bar{x}) < r$, $(\ell, r > 0)$ respectively, and $r < \ell$. Further, let U_o define a region within Ω_r, i.e., $U_o \subset \Omega_r$. If

$$V(\bar{x}) > 0 \text{ for } \quad \bar{x} \in \Omega_\ell \text{ and } \bar{x} \neq 0 \qquad \text{(a)}$$

$$\dot{V}(\bar{x}) \leq -\epsilon < 0 \text{ for } \quad \bar{x} \in U_o{}^c \cap \Omega_\ell \qquad \text{(b)}$$

$$\dot{V}(x) \lesseqgtr 0 \text{ for } \quad \bar{x} \in U_o \qquad \text{(c)}$$

then every solution to Equation (7.4) initiating in $U_o{}^c \cap \Omega_\ell$ will eventually enter U_o and never thereafter leave Ω_r.

The acquisition stability problem now can be formulated as establishing a function $V(\bar{x})$ such that conditions (a) and (b) of Theorems 7.1 or 7.2, as applicable, are satisfied and that $R \subset \Omega_\ell$.

Although numerous methods have been proposed for establishing suitable candidates for $V(\bar{x})$ no generally applicable approach exists. Nonetheless, for particular system classes the stability problem has been solved completely. For example, the Lure' transform reduces the problem of stability to satisfying certain simple algebraic constraints for a class of systems incorporating a nonlinear gain element. In general this, and other techniques, are not applicable to the

---

* $\cap$, $\cup$, and a superscript c denote set intersection, union and complement respectively.

acquisition problem. Instead other, more fruitful, approaches exist and for the most part these have been left relatively unexplored.

Recently R. Pringle [25] has suggested that for mechanical systems a very useful "testing function" (candidate) for a Lyapunov function, $V(\bar{x})$, is the Hamiltonian. As this work points out, a fundamental distinction between the total system energy and the Hamiltonian exists for problems involving rotating coordinates or cyclic variables. Since in acquisition system formulation the kinematic variables fall into this category the importance of the observation is apparent. Whereas it is frequently convenient to choose the total system energy as a candidate for $V(\bar{x})$, usually this does not suffice. In Section IV an intuitive approach was successfully employed to establish a suitable $V(\bar{x})$.

A suitable Lyapunov function to establish a regional lower bound on the extent of stability can be obtained for any continuous nonlinear system not possessing an ultimate state limit cycle. The nonlinear system is linearized about the desired equilibrium point and the stability of the linear approximation is established. Since a Lyapunov function for the linear system is always available, this function can be used as a candidate for the nonlinear system. Linearizing Equation (7.4) gives

$$\dot{\bar{x}} = [A]\,\bar{x} \tag{7.5}$$

where [A] is a constant matrix. The linear system is stable if the real parts of the eigenvalues of the matrix [A] are all negative. If some of the eigenvalues are identically zero or pure imaginary pairs no information on stability can be obtained by investigation of the linear system. These cases are the so-called Lyapunov Critical Cases

and the stability is ascertained only by consideration of the nonlinear terms [26]. Even in the critical cases a Lyapunov function can be found to establish the stability of the equilibrium point.

For the case where the linear approximation is stable, a Lyapunov function can be found to be

$$V_L(\bar{x}) = \bar{x}^T \left[P\right] \bar{x} \tag{7.6}$$

where $\bar{x}^T$ is the transpose of $\bar{x}$ and $\left[P\right]$ is a symmetric positive definite matrix satisfying the equation

$$\left[A\right]^T \left[P\right] + \left[P\right] \left[A\right] = - \left[I\right] \tag{7.7}$$

where $\left[I\right]$ is the unit matrix.

Equation (7.7) can always be solved and the resulting $V(\bar{x})$ is both <u>necessary</u> and <u>sufficient</u> for the linearized system of Equation (7.5).

Since the linear approximation must be valid for $\bar{x}$ sufficiently near the equilibrium condition, the function $V_L(\bar{x})$ must be capable of establishing a region of stability for the nonlinear system as well. All that must be accomplished is to take the total differential of Equation (7.6) with respect to time and utilize Equation (7.4). This gives

$$\dot{V}_{NL}(\bar{x}) = \bar{x}^T \left[A\right] \bar{f}(\bar{x}) + \left[\bar{f}(\bar{x})\right]^T \left[A\right] \bar{x} \tag{7.8}$$

For application of Theorem 7.1 it is required to establish the largest ℓ, $V_L(\bar{x}) = \ell$, such that for $\bar{x} \in \Omega_\ell$ then $\dot{V}_{NL}(\bar{x}) \leq - \epsilon < 0$. This is most easily accomplished by finding a suitable region S in x-space, wherein $\dot{V}_{NL}(\bar{x}) \leq - \epsilon < 0$ and then establishing the largest ℓ such that $\Omega_\ell \subset S$.

This proves stability of the nonlinear system within Ω_ℓ. The fundamental study of this section is concerned with establishing a practical means for establishing S and Ω_ℓ.

Combining the approaches of linearization, intuition and application of the Hamiltonian provides a powerful starting point for establishing potentially useful candidates for $V(\bar{x})$.

7.2 Stability Study Approach and Scope

The present study has been devoted to investigating the utility of digital computation for establishing the regions S and Ω_ℓ. This represents a considerable task since the basic evaluations required are analytic in nature rather than purely computational. The desired result is to establish a computational algorithm which can prove the sign definiteness of an analytic function over a finite region in x-space and establish the bound of this region.

The development of such an algorithm, based upon a Taylor Series expansion, is the subject of the remainder of this section. The algorithm developed was limited to the case in which both $V(\bar{x})$ and $\dot{V}(\bar{x})$ are polynomial functions. Although the nature of the acquisition problem makes this choice a particularly useful one, it will become evident that the class of allowable functions can be extended by employing techniques similar to those given.

The desire to utilize digital computation to accomplish the stated task is evident if the complexities of the acquisition problem are considered. Even though the candidate function $V(\bar{x})$ may be of relatively simple form, the resulting $\dot{V}(\bar{x})$ is much more complex. Therefore, for higher order systems it is a nontrivial task, except in limiting cases, to analytically evaluate the character of the latter. It would be highly desirable to be able to use the digital computer for this tedious task. Not only would this allow evaluation of more

candidate $V(\bar{x})$ functions in a reasonable time, but greater insight into the problem characteristics would be obtained by observing the nature of past results (or failures).

7.3 Description of the Algorithm

7.3.1 General Development

To demonstrate the method employed in developing the algorithm, $\bar{x}$ is assumed to be of dimension two, namely $\bar{x} = (x,y)$. Then $V(\bar{x}) = V(x,y)$ and using Equation (7.4) define

$$F(x,y) = -\dot{V}(x,y) = -\nabla V(x,y) \cdot \bar{f}(x,y) \tag{7.9}$$

The object is to determine whether $F(x,y)$ is positive in the region

$$R_o = \left\{ (x,y) : |x| \leq x_f, \ |y| \leq y_f \right\} \tag{7.10}$$

for given bounded values of x_f and y_f. Only the first quadrant of R_o need be considered if a function $F_k(x,y)$ is defined which behaves in the first quadrant identically to the way that $F(x,y)$ behaves in the k-th quadrant. The relationship of $F(x,y)$ and $F_k(x,y)$ are given by Table 7.1, with the result that when interest in $F(x,y)$ is focussed on the k-th quadrant, $F_k(x,y)$ be utilized instead over the region

$$R_1 = \left\{ (x,y) : 0 \leq x \leq x_f , \ 0 \leq y \leq y_f \right\} \tag{7.11}$$

TABLE 7.1

DETERMINATION OF $F_k(x,y)$

k	$F_k(x,y)$
1	$F(x,y)$
2	$F(-x,y)$
3	$F(-x,-y)$
4	$F(x,-y)$

With this identification, it is sufficient merely to consider the characteristics of $F(x,y)$ for $(x,y) \in R_1$. The $F_k(x,y)$ $(k = 2,3,4)$ can then be handled in a similar fashion.

The method adopted for determining the merits of a Lyapunov candidate in R_1 consists of two parts. The first part is a qualitative test of the function $F(x,y)$ designed to screen most of the unacceptable Lyapunov candidates without undue use of computer time. This method is inexact in that there is no guarantee that it will reject all improper candidates. However, no promising candidates will be rejected. Only if a function passes this test will it be subjected to the quantitative evaluation which, although mathematically precise, is significantly more expensive.

The qualitative test can assume several forms all of which are simple in concept. One approach would be to select sequences of distinct values of the variables, viz,

$$\begin{aligned} 0 = x_1 < x_2 < x_3 < \ldots < x_n = x_f \\ 0 = y_1 < y_2 < y_3 < \ldots < y_m = y_f \end{aligned} \tag{7.12}$$

with a mesh finiteness, Δ, given by

$$\Delta = \max \left[(x_{i+1} - x_i) , (y_{i+1} - y_i) \right] \tag{7.13}$$

For every i and j, $F(x_i, y_j)$ is computed and F is rejected in any region in which it takes on negative values. If no negative values of F appear, Δ can be reduced by interposing additional points in the sequences of Equation (7.12) and the procedure repeated. However, no matter how small Δ becomes, the positiveness of $F(x_i, y_j)$ for every i and j never absolutely assures the positive definiteness of $F(x,y)$. It can, at best, be a strong indicator as to whether $F(x,y)$ is a Lyapunov

function or not. When, for reasonable mesh size, the function $F(x,y)$ is positive at all (x_i, y_i) over the desired region D it becomes a more likely candidate for a Lyapunov function and the qualitative test is terminated and the quantitative evaluation initiated. Only the quantitative evaluation will be considered here because of the simplicity in mechanizing the former. Alternate implementations of the qualitative test are possible such as random sampling. Study of this area would be fruitful in that confidence levels could be established regarding the sign nature of the function $F(x,y)$ over D.

The quantitative evaluation uses as its basic philosophy the expansion of the given function $F(x,y)$ in a Taylor Series with a remainder R. The procedure employed is illustrated in Figure 7.1. Assuming that $F(x_o, y_o) > 0$, values of x_μ and y_μ are to be determined such that it is known with certainty that $F(x,y) > 0$ whenever

$$(x,y) \in \left\{ (x_\lambda, y_\lambda) : x_o \le x_\lambda \le x_\mu,\ y_o \le y_\lambda \le y_\mu \right\} \equiv D \qquad (7.14)$$

A new operating point $(x_1,y_1) \in D$ is now selected and the process repeated to establish an addition region, E, wherein $F(x,y) > 0$. Figure 7.1 illustrates the case for which $(x_1,y_1) = (x_\mu, y_o)$. Continual repetition of this process results in operating point sequences $\left\{x_k\right\}$, $\left\{y_k\right\}$, which if properly chosen, causes the overlap of incremental regions to eventually exhaust R_1 provided $F(x,y) > 0$ in this region. Note that the operating point sequences necessarily contain subsequences $\left\{x_{k_i}\right\}$, $\left\{y_{k_i}\right\}$ satisfying

$$x_{k_{i+1}} - x_{k_i} \ge 0$$

$$y_{k_{i+1}} - y_{k_i} \ge 0$$

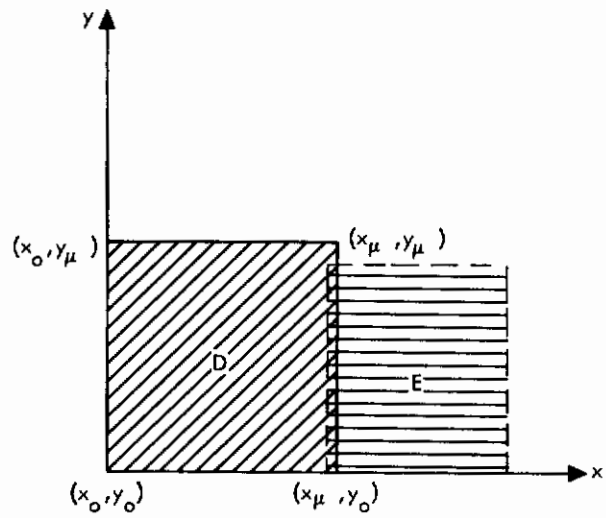

Figure 7.1 Domain of F(x,y)

The computer cannot, by this process, include any points where $F(x,y) \leq 0$. Should the computer approach a zero of F, it will begin to accept smaller and smaller rectangles in its attempt to surpass the zero. This is an indication that the function F is approaching zero and a simple decision process will halt the machine for operator observation.

Now sufficient conditions for accepting incremental regions, such as illustrated in Figure 7.1, will be considered. The main results are presented in the following two theorems.

Theorem 7.3

Given the function of two variables F(x,y) defined on

$$D = \left\{(x_\lambda, y_\lambda) : x_o \leq x_\lambda \leq x_1,\ y_o \leq y_\lambda \leq y_1\right\}$$

Suppose that $\frac{\partial F}{\partial x}$ and $\frac{\partial F}{\partial y}$ exist for all $(x,y) \in D$, and that P_x and P_y are lower bound for $\frac{\partial F}{\partial x}$ and $\frac{\partial F}{\partial y}$ respectively when $(x,y) \in D$. Defining

$$P_x^* = \begin{cases} P_x \text{ if } P_x < 0 \\ 0 \text{ if } P_x \geq 0 \end{cases} \tag{7.15}$$

$$P_y^* = \begin{cases} P_y \text{ if } P_y < 0 \\ 0 \text{ if } P_y \geq 0 \end{cases} \tag{7.16}$$

and

$$R_m = P_x^*(x_1 - x_o) + P_y^*(y_1 - y_o) \tag{7.17}$$

Then

$$F(x_o,y_o) + R_m > 0$$

implies

$$F(x,y) > 0 \text{ for } (x,y) \in D$$

Proof:

Under the hypothesis of the theorem, F(x,y) can be expanded in a Taylor Series with remainder about (x_o,y_o), namely

$$F(x,y) = F(x_o,y_o) + R(x,y) \qquad (x,y) \in D \tag{7.18}$$

where

$$R(x,y) = \left.\frac{\partial F}{\partial x}\right|_{\substack{x_o+\theta(x-x_o) \\ y_o+\theta(y-y_o)}} (x-x_o) + \left.\frac{\partial F}{\partial y}\right|_{\substack{x_o+\theta(x-x_o) \\ y_o+\theta(y-y_o)}} (y-y_o) \qquad 0 \leq \theta \leq 1 \tag{7.19}$$

It is to be noted that the partial derivatives are evaluated at some point in D. Utilizing Equation (7.17), where the partials are evaluated as in Equation (7.19), gives

$$\left.\begin{aligned} R(x,y) - R_m &= \frac{\partial F}{\partial x}(x-x_o) + \frac{\partial F}{\partial y}(y-y_o) - P_x^*(x_1-x_o) - P_y^*(y_1-y_o) \\ &= \left(\frac{\partial F}{\partial x} - P_x^*\right)(x-x_o) + \left(\frac{\partial F}{\partial y} - P_y^*\right)(y-y_o) \\ &\quad - P_x^*(x_1-x) - P_y^*(y_1-y) \end{aligned}\right\} \quad (7.20)$$

Now by definition P_x^* and P_y^* are non-positive lower bounds to $\frac{\partial F}{\partial x}$ and $\frac{\partial F}{\partial y}$, respectively. Thus since $x_o \le x \le x_1$ and $y_o \le y \le y_1$, each term on the right hand side of Equation (7.20) is non-negative. Thus

$$R(x,y) \ge R_m \qquad (x,y) \in D \quad (7.21)$$

By Equation (7.18)

$$F(x,y) = F(x_o,y_o) + R(x,y) \ge F(x_o,y_o) + R_m \quad (7.22)$$

and

$$F(x_o,y_o) + R_m > 0 \quad (7.23)$$

necessarily implies $F(x,y) > 0$ for any $(x,y) \in D$.

Note that it is not sufficient merely to define $P_x^* = P_x$ and $P_y^* = P_y$. In this case, the third and fourth terms on the right hand side of Equation (7.20) could be negative. It is an easy matter to construct an example for which $R(x,y) < R_m$ under these circumstances.

Corollary: Under the hypothesis of Theorem 7.3, and assuming $F(x_o,y_o)>0$, there exists an $\epsilon > 0$ such that $x_1 - x_o < \epsilon$ and $y_1 - y_o < \epsilon$ implies $F(x,y) > 0$ for $(x,y) \in D$.

Proof:

Since $F(x,y)$ is continuous in the neighborhood of (x_o,y_o), its partial derivatives are bounded there. Thus P_x^* and P_y^* are also bounded. Let

$$Q = \min (P_x^*, P_y^*)$$

and let $\beta > 0$ be such that $F(x_o,y_o) > \beta$. Now select $\epsilon > 0$

$$\epsilon = \frac{\beta}{4|Q|} \tag{7.24}$$

Then by Equation (7.22), noting that $Q \leq 0$

$$F(x,y) \geq F(x_o,y_o) + R_m > \beta + Q \left[(x_1-x_o) + (y_1-y_o)\right]$$

$$> \beta + Q \left[\frac{\beta}{4|Q|} + \frac{\beta}{4|Q|}\right] = \beta - \frac{\beta}{2} > 0$$

Thus the ϵ given by Equation (7.24) satisfies the assertion made in the Corollary.

This Corollary implies that the expansion process cannot terminate at (x_o,y_o) if $F(x_o,y_o) > 0$. However, there is no guarantee that the expansion process will accept values of (x,y) arbitrarily close to (x_o,y_o) in the case where $F(x,y) > 0$ but $F(x_o,y_o) = 0$. The following theorem considers this problem.

Theorem 7.4

Suppose that the expansion process is taking place in the domain

$$D_1 = \{ (x,y) : 0 \leq x;\ 0 \leq y \}$$

Let (x_n,y_n) $n = 0, 1, 2, \ldots$ represent the sequence of operating points in the expansion process and assume the expansion process is such that $x_n - x_m > 0$ and $y_n - y_m \geq 0$ if $n > m$. Now suppose that $F(x_\lambda,y_\lambda) = 0$, but that there exists a rectifiable arc*, $\gamma(t) : (x(t), y(t))$, (for which x and y are parameterized in terms of t) joining some point $A \in D$ to (x_λ,y_λ); and that $F(x,y) > 0$ for $(x,y) \in \gamma$. Finally assume that x(t) and y(t) are monotone increasing with t. Then, under the hypothesis of Theorem 7.3, an expansion process for which the dimensions of each incremental neighborhood are of the same order can extend along γ to an arbitrarily small neighborhood of (x_λ, y_λ).

Proof:

The situation is illustrated by Figure 7.2. Assume the contrary, namely that there exists a neighborhood of (x_λ,y_λ) for which expansion along γ cannot enter. Then there exists points on γ other than (x_λ,y_λ) which cannot be covered by the expansion process. Let

$$P_\mu = (x_\mu,y_\mu) = \inf_t \{ (x(t), y(t)) : (x(t), y(t)) \text{ cannot be covered} \}^{**} \quad (7.25)$$

---

* Rectifiable is defined as: Let the curve $\gamma(t) = [x(t),y(t)]$ be described by a parameter t for $a \leq t \leq b$. Let $|\gamma(t)| \equiv [x^2(t)+y^2(t)]^{1/2}$ and let π be a partition of t, $a = t_1 < t_2 < t_3 < \ldots < t_n = b$. Let $S(\pi) = \sum_{i=1}^{n} |\gamma(t_{i+1}) - \gamma(t_i)|$ and let $S = \sup_\pi S(\pi)$, i.e., the supremum of $S(\pi)$ over all possible partitions. Then γ is rectifiable if S is finite.

** $\inf_t (f(t))$ means the greatest lower bound with respect to values of t in the domain of the function f.

This point is well defined since γ is rectifiable. The definition of P_μ, the rectifiability of γ, and the continuity of $F(x,y)$ implies that for any given $\epsilon > 0$, there exists an M such that

$$x_\mu - x_M < \epsilon$$

$$y_\mu - y_M < \epsilon \qquad (7.26)$$

$$|F(x_M,y_M) - F(x_\mu,y_\mu)| < \epsilon$$

(x_M, y_M) will now be utilized as an operating point to determine (x_{M+1}, y_{M+1}). This results in

$$R_m = P_x^*(x_1-x_M) + P_y^*(y_1-y_M) \geq -K[(x_1-x_M) + (y_1-y_M)]$$

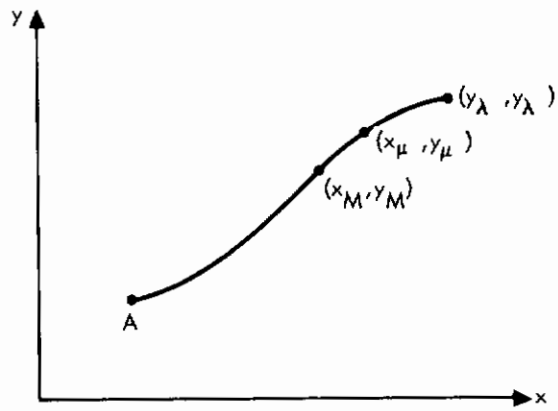

Figure 7.2 Expansion Along γ

where K is a finite constant $(0 \leq K < \infty)$ such that

$$-K < \min(P_x^*, P_y^*)$$

Then

$$F(x_M,y_M) + R_m > F(x_M,y_M) - K[(x_1-x_M) + (y_1-y_M)]$$

Thus if

$$(x_1 - x_M) + (y_1 - y_M) \leq \frac{F(x_M, y_M)}{K}$$

it necessarily follows that

$$F(x_M, y_M) + R_m > 0 \tag{7.27}$$

Thus the expansion process can take place along γ at least to the point (x_{M+1}, y_{M+1}) where

$$\left.\begin{aligned} x_{M+1} &= x_M + \frac{F(x_M, y_M)}{K}\alpha_1 \\ y_{M+1} &= y_M + \frac{F(x_M, y_M)}{K}\alpha_2 \end{aligned}\right\} \tag{7.28}$$

where $0 < \alpha_i \leq \frac{1}{2}$ $(i = 1,2)$ and the α_i are chosen in such a way that $(x_{M+1}, y_{M+1}) \in \gamma$. Therefore,

$$x_{M+1} - x_\mu = (x_M - x_\mu) + \frac{F(x_M, y_M)}{K}\alpha_1 \tag{7.29}$$

But since $F(x,y) > 0$ on γ except at (x_λ, y_λ), it follows that there exists a $\beta > 0$ such that $F(x_M, y_M) > \beta$. Then in view of Equation (7.26)

$$x_{M+1} - x_\mu > \alpha_1 \frac{\beta}{K} - \epsilon \tag{7.30}$$

or

$$x_{M+1} > x_\mu \tag{7.31}$$

since ϵ can be selected arbitrarily small. Similarly

$$y_{M+1} > y_\mu \tag{7.32}$$

But this is impossible by the definition of (x_μ, y_μ) and so this contradiction implies that the expansion process along γ exists to an arbitrary neighborhood of (x_λ, y_λ).

In particular, if the point A is the origin of D, an expansion process beginning at the origin eventually reaches an aribitrarily small neighborhood of (x_λ, y_λ).

Utilizing the methods described in the previous theorems for establishing neighborhoods, along with a suitable neighborhood expansion or overlapping method, a region including (0,0) can eventually be established in which $F(x,y) = \frac{-dV}{dt}$ is greater than zero. In the limiting case, the boundary of this region satisfies $F(x,y) = 0$. This region, R_2, is shown in Figure 7.3 which also plots the loci of constant V functions $V(x,y) = V_i$ $(i = 0,1,2,3,4,5)$. Unfortunately, it is not in general possible to deduce system stability to (0,0) for any $(x,y) \in R_2$. For assume the system is at point A at time t_o. Since $A \in R_2$, the function must decrease, but there is no assurance that the system trajectory will not pass through point B for some time greater than t_o,

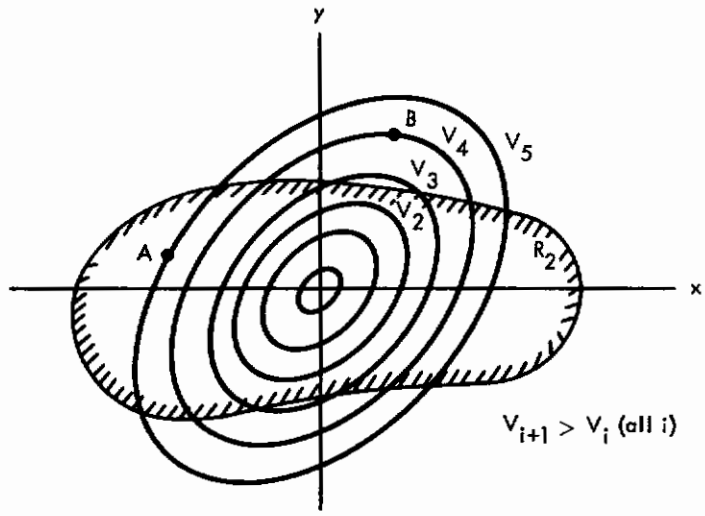

Figure 7.3 R_2 and Loci of Constant (x,y) Functions in x, y plane

since $V_4 < V_5$. But at point B, $\frac{dV}{dt}$ can be positive and so the system trajectory may possibly never again enter R_2.

The acceptable region to illustrate asymptotic stability is thus the interior of the boundary determined by the largest V_i function which lies solely within R_2. In Figure 7.3 this is given by the V_i function whose value is V_3. In general, if D_i corresponds to the domain whose boundary has the V functional value V_i then asymptotic stability to (0,0) is assured for $(x,y) \in D_K$ where D_K is the maximal subset of R_2 for which $(x,y) \in D_K$ implies $V(x,y) \leq V(x_\mu, y_\mu)$ for every (x_μ, y_μ) in the complement of R_2. This results in Theorem 7.1, given previously.

To find V_K and D_K once R_2 has been established is nontrivial. A sequence of points $p_n = (x_n, y_n)$ arbitrarily close to the boundary of R_2 can be established, and $V(x_n, y_n)$ computed for all n. If the points lie sufficiently close to each other, a good approximation to the maximum acceptable value of V_i, say V_K, will be established by this method. It remains to show rigorously that the corresponding domain $D_K \subset R_2$. Then finally $(x,y) \in D_K$ implies asymptotic stability to (0,0).

Thus, for some analyst chosen $\epsilon > 0$, consider the function

$$G(x,y) = V(x,y) - V_K + \epsilon \tag{7.33}$$

By the previous paragraph, it has been established that $G(x_n, y_n) > 0$ for all of the boundary points (x_n, y_n). Consider two adjacent points p_n and p_{n+1}. It is sufficient to show that $G(x, y) > 0$ on this line segment and to do this for all n.

On the line segment, y can be simply related to x provided $\frac{dy}{dx} < \infty$, a case which can always be avoided by proper selection of the p_n. Thus, writing $y = f(x)$, it is required that

$$G(x,y) = G(x,f(x)) = H(x) > 0 \tag{7.34}$$

Instead of dealing directly with H(x), consider instead H(z) where z = x on the condition that $x_{n+1} > x_n$ and z = -x if $x_{n+1} < x_n$. It is desired to prove that

$$H(z) > 0 \tag{7.35}$$

on the line segment. But this is the one dimensional analog of the problem considered in Theorem 7.3, and specifically, all the previous theorems apply. Thus letting z_o correspond to the point p_n gives

$$H(z) \geq H(z_o) + R_m \tag{7.36}$$

and it is required to select, if possible, a distance along the line segment sufficiently small so that

$$H(z_o) + R_m > 0 \tag{7.37}$$

In this case, R_m is given by

$$R_m = P_z(z_1 - z_o) \tag{7.38}$$

where P_z need merely be a lower bound on $\frac{dH}{dz}$. If a finite number of expansions eventually include p_{n+1}, then clearly V_K is less than V(x,y) for (x,y) on the line segment. If this holds true for all line segments, then D_K is truly a domain of asymptotic stability. If this procedure fails for some segment, a lower value of V_K must be assumed and the entire process repeated. Eventually this method will generate an acceptable domain.

7.3.2 F(x,y) A Polynomial

Consider the previous discussion limited to the case in which F(x,y) is a polynomial

$$F(x,y) = \sum_{i+j\le m} a_{ij} x^i y^j \tag{7.39}$$

To apply the methods previously described, it is only necessary to determine suitable lower bounds, P_x and P_y for $\frac{\partial F}{\partial x}$ and $\frac{\partial F}{\partial y}$, respectively.

Theorem 7.5

Supose that in D

$$\frac{\partial F}{\partial x} = \sum_{i+j\le m} b_{ij} x^i y^j = \Sigma b^+_{ij} x^i y^j + \Sigma b^-_{ij} x^i y^j \tag{7.40}$$

where $b^+_{ij} \ge 0$ and $b^-_{ij} < 0$. Then a suitable value of P_x is given by

$$P_x = \Sigma b^+_{ij} x_o^i y_o^j + \Sigma b^-_{ij} x_1^i y_1^j \tag{7.41}$$

Proof: For any $(x, y) \in D$, $x_o \le x \le x_1$ and $y_o \le y \le y_1$, therefore,

$$\begin{aligned} \Sigma b^+_{ij} x^i y^j &\ge \Sigma b_{ij} x_o^i y_o^i \\ \Sigma b^-_{ij} x^i y^j &\ge \Sigma b^-_{ij} x_1^i y_1^j \end{aligned} \tag{7.42}$$

Thus in view of Equations (7.40) and (7.42)

$$P_x \le \frac{\partial F}{\partial x} \qquad (x, y) \in D \tag{7.43}$$

which proves the theorem.

Similarly, if

$$\frac{\partial F}{\partial y} = \Sigma\, c_{ij}\, x^i\, y^j = \Sigma\, c^+_{ij}\, x^i\, y^j + \Sigma\, c^-_{ij}\, x^i\, y^j \qquad (7.44)$$

where $c^+_{ij} \geq 0$, $c^-_{ij} < 0$. Then a suitable lower bound to $\frac{\partial F}{\partial y}$ if given by

$$P_y = \Sigma\, c^+_{ij}\, x_o{}^i\, y_o{}^j + \Sigma\, c^-_{ij}\, x_1{}^i\, y_1{}^j \qquad (7.45)$$

7.3.3 Overlapping the Neighborhoods

To complete the algorithm description, it remains to describe a method for overlapping acceptable neighborhoods in some orderly fashion in order to establish the domain within which the given function is sign definite. Many possible approaches exist, but the reduction to a computer algorithm of even the simpliest approach is not generally an easy task. Consider a function of two variables. Suppose, as in Figure 7.4, a number of rectangular neighborhoods are overlapped, where the origin of each neighborhood lies on the boundary of some previously accepted neighborhood. It is evident from this figure that the irregularity of the shaded portion of Figure 7.4 results in a difficult analytic description of the area yet to be covered, in that the computer is required to store a great many coordinate values, (x,y), in order to adequately define the boundary between the two areas. Using the point A as an operating point for a new rectangle D, the computer program would have to possess the capability to establish and store the points B and C which must be used for future operating points. Geometrically, the situation is quite clear, but the reduction of this type of expansion process to a set of formal computer programming statements, while presenting no essential difficulties, is nevertheless quite complex.

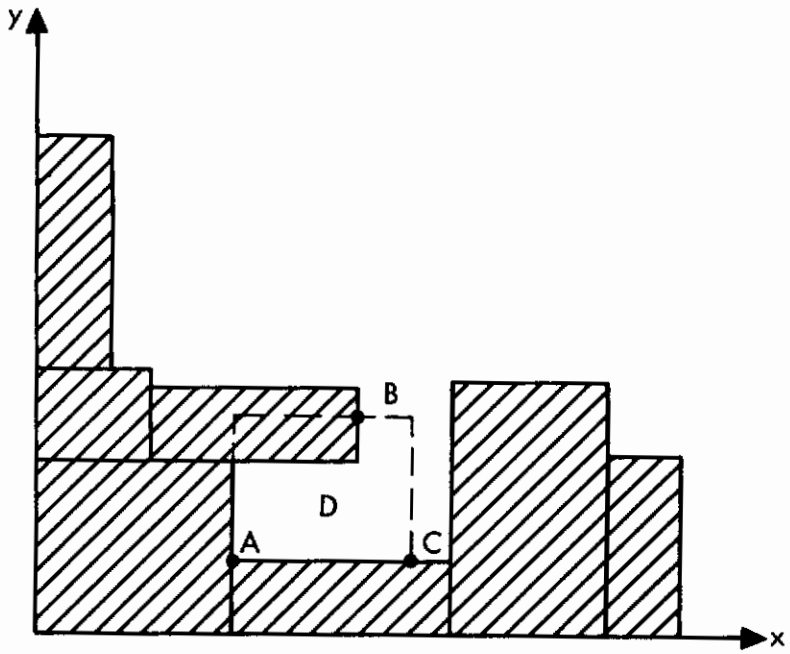

Figure 7.4 Overlapping Neighborhoods

Contrast this expansion process to the simpler one illustrated in Figure 7.5. Here assume that, by some auxiliary means (linearization, etc.), all points in the very small rectangle denoted by the number 1 yield positive functional values. A line a - a' parallel to the y axis is then established using the methods of Theorem 7.3 such that positive functional values are assured in rectangle 2. Such a line exists by the corollary to this theorem. Next a line b - b', parallel to the x axis is similarly established such that rectangles 3 and 4 can be accepted. Then c - c' is established to accept 5 and 6, d - d' is selected to accept rectangles No. 7, 8, and 9, etc. In general, the expansion program iterates between the two axes, exhausting area in an orderly fashion that requires relatively little computer memory. Only the incremental values along the coordinate axes must be stored, namely the points f, b, d..., e', a', c'..., etc.

Unfortunately, the method described in the preceding paragraph and illustrated by Figure 7.5 possesses a limitation in that it does not meet the requirements of Theorem 7.4. This is because the acceptance of each new rectangle keeps one dimension fixed, reducing the second dimension until Equation (7.23) is satisfied. Since both dimensions cannot be reduced to arbitrarily small values this expansion process can limit at points where $F(x,y) > 0$. Thus from a single origin, 0, the entire domain for which $F(x,y) > 0$ cannot be obtained in general. This difficulty can be overcome by resetting the computer origin to limit points with non-zero functional values, and beginning a new expansion process. In this way the entire acceptable domain can be obtained.

In order to keep these stability studies within reasonable bound, it was important from the start to avoid non-essential programming complexities at the sacrifice of some program flexibility. Thus despite the inefficiency of the latter overlapping approach, this method was the one selected for digital programming. The program was written to handle three state variables, so the three-dimensional

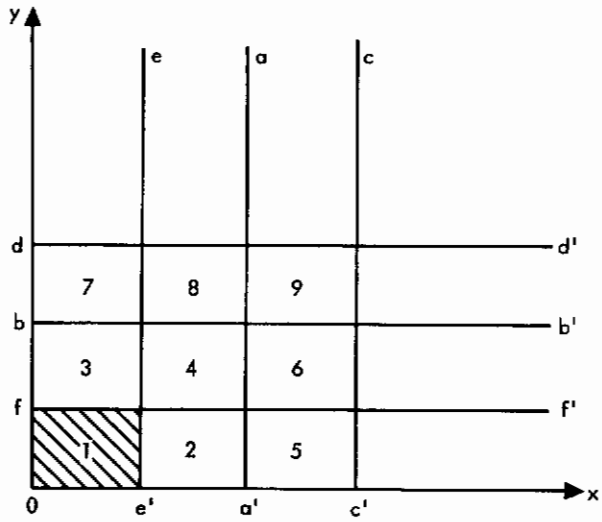

Figure 7.5 Simplified Overlapping Method

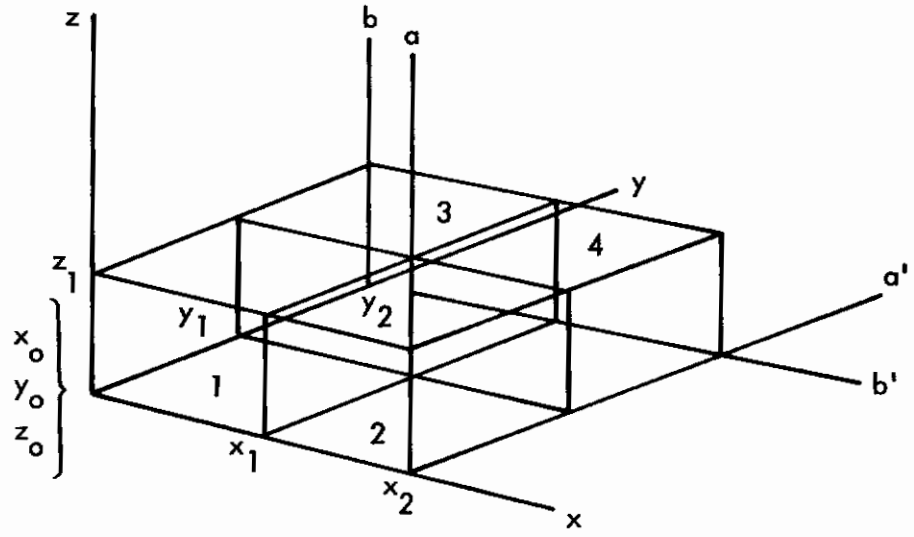

Figure 7.6 Start of the Cube Growing Process

analog of this method, illustrated by Figure 7.6, was employed. Starting with "cube" No. 1 and then selecting a plane a - x_2 - a' parallel to the z - y plane in such a way that cube No. 2 can be accepted demonstrates the analogy. Then a plane b - y_2 - b', parallel to x - z is picked such that cubes No. 3 and 4 meet the requirements; and finally a plane parallel to x - y is selected to fit in the four "cubes" above those in Figure 7.6. Then attention is focussed on a new plane normal to the x axis and the whole procedure repeated. Again this programming method iterates among the coordinate axes in such a way as to enlarge, in an orderly fashion, the region within which $F(x, y, z) > 0$.

It is evident that this overlapping method could easily be extended to spaces of any finite dimension. Fundamentally, the algorithm does not change. To fit in a new n dimensional cube, n-1 dimensions are held fixed while an n-1 dimensional plane is added in such a way that the required inequalities are met. There are merely more cubes to consider and more coordinate axes over which to iterate.

A simplified version of the computer flow diagram appears in Figure 7.7. The three coordinate axes are labeled z_o, z_1, z_2, and the computer is presently attempting to fit in a new plane on the z_s axis (s = 0, 1, 2). The basic computations involving the original function, its partials, R_m, etc. are performed in the Polynomial Computer. The result is tested to see whether $F_o + R_m > 0$. If not, the increment is reduced. If the test is passed, the computer indexes to a new cube by iterating in the $z_{(x+1) \bmod 3}$* direction. This procedure is continued until the "end" of the cube is reached at which point iteration occurs in the $z_{(x+2) \bmod 3}$ direction. Once this

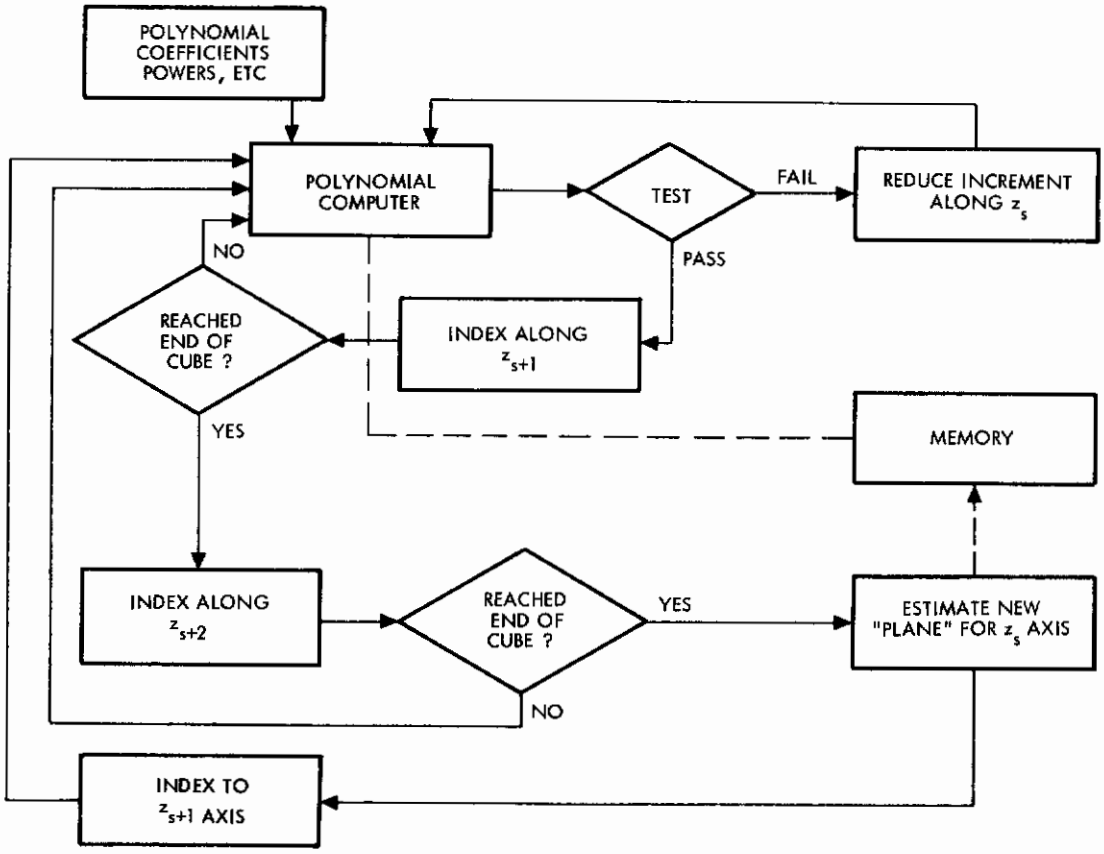

Figure 7.7 Simplified Computer Flow Diagram

* $z = x \bmod y = \inf_{z'} \left\{ \left[z' : z' = x \pm ky \right] \left[k = 0, \pm 1, \pm 2 \ldots \right] \cap \left[z' : z' \geq 0 \right] \right\}$

iteration ceases, the computer "estimates" a new plane for the z_s axis (which it will utilize upon its return to this axis) and then indexes to the $z_{(s+1) \bmod 3}$ axis. The entire procedure is now repeated on this new axis, etc. A very detailed description of the program with a complete flow diagram appears in Appendix D.

7.4 Computer Solutions of Well-Behaved Polynomials

The computer program was first considered for polynomials which contained no negative terms and were thus obviously positive definite in the first quadrant of the space pertinent to its independent variables. The purpose of this exercise was to establish some measure of how much time the program requires to exhaust a given space, and how this time varies with the dimensionality and degree of the polynomial in question. Because of the positiveness of each term, the polynomials considered result in computer operating times that are somewhat lower than would be expected in most cases. This is due to the fact that R_m equals zero in all the computations, and therefore, there can be no failures resulting from poor incremental guesses. Thus while the computer employs the same computations for these simple cases as for the more complex problems, it is essentially unrestricted in its neighborhood expansion process. However, it should be noted that if a candidate is truly a Lyapunov Function in some region, it too will exhibit well behaved characteristics resulting, perhaps, in R_m values which are zero or only slightly negative over much of the domain of function definition. Thus it may well be that many practical cases of this sort involve computer operating times which tend to approach those to be specified.

In any event, effects of polynomial dimension and degree for the general case can probably be derived from these examples. In all of the following examples the expansion process in each variable extended

from 0.2 to 4.88 x 10^5, or better than a six order magnitude change. This change in every case was obtained by eleven increments in each variable, the computer printing out the run time required to the nearest second. The results are summarized in Table 7.2.

TABLE 7.2

COMPUTER RUN TIMES VS. POLYNOMIAL CONSIDERED

Number	Polynomial	Time Req'd To Expand All Variables from 0.2 to 4.88 x 10^5 (sec)
1	$x^2y^2z^2 + y^2z^2 + x^2z^2 + x^2y^2 + x^2 + y^2 + z^2$	39
2	$x^2x^2y^2 + \frac{1}{2}x^2y^2 + \frac{1}{2}x^2y^2 + x^2x^2 + x^2 + \frac{1}{2}y^2 + \frac{1}{2}y^2$	5
3	$x^2x^2x^2 + \frac{1}{3}x^2x^2 + \frac{1}{3}x^2x^2 + \frac{1}{3}x^2x^2 + \frac{1}{3}x^2 + \frac{1}{3}x^2$	2
4	$x^2y^2 + x^2 + y^2$	3
5	x^2	1

Table 7.2 clearly illustrates the detrimental effect of system dimension. The first three entries possess terms of comparable complexity, yet there exists a very significant difference in the computing time required. This, of course, is to be expected since many more neighborhoods must be evaluated as the dimension increases. The polynomial complexity does not appear to be as significant a factor. For example, comparison of numbers 3 and 5 shows a time ratio of only a factor of two despite the fact that there is a vast difference in the complexity of the functions.

In the next section, an example will be considered for which the polynomial does not possess the ideal characteristic here.

7.5 An Example

7.5.1 Problem Description

Consider a satellite in an earth orbit tumbling solely about its pitch axis under the influence of the Earth's gravitional field. Figure 7.8 illustrates this situation and defines principle body axes (x_1, x_2, x_3) and corresponding geocentric reference axes (x_1^R, x_2^R, x_3^R). Since the satellite is assumed to possess no roll or yaw attitude error or error rates, $x_2 = x_2^R$ and (x_1, x_2, x_3) is related to (x_1^R, x_2^R, x_3^R) by the direction cosine matrix

$$\begin{bmatrix} x_1 \\ x_2 \\ x_3 \end{bmatrix} = \begin{bmatrix} a_{33} & 0 & a_{13} \\ 0 & 1 & 0 \\ -a_{13} & 0 & a_{33} \end{bmatrix} \begin{bmatrix} x_1^R \\ x_2^R \\ x_3^R \end{bmatrix} \tag{7.46}$$

Euler's dynamical equation for the pitch axis is

$$I_2 \dot{\omega}_2 + 3\omega_o^2 (I_1 - I_3) a_{13} a_{33} + T_c = 0 \tag{7.47}$$

where ω_2 is the pitch body rate, I_1, I_2, and I_3 are the roll, pitch, and yaw moments of inertia, respectively, ω_o is the orbital rate, and T_c, the control torque on the pitch axis. The kinematic equations relating direction cosines to the body rates are

$$\left.\begin{aligned} \dot{a}_{13} &= -(\omega_2 + \omega_o) a_{33} \\ \dot{a}_{33} &= (\omega_2 + \omega_o) a_{13} \end{aligned}\right\} \tag{7.48}$$

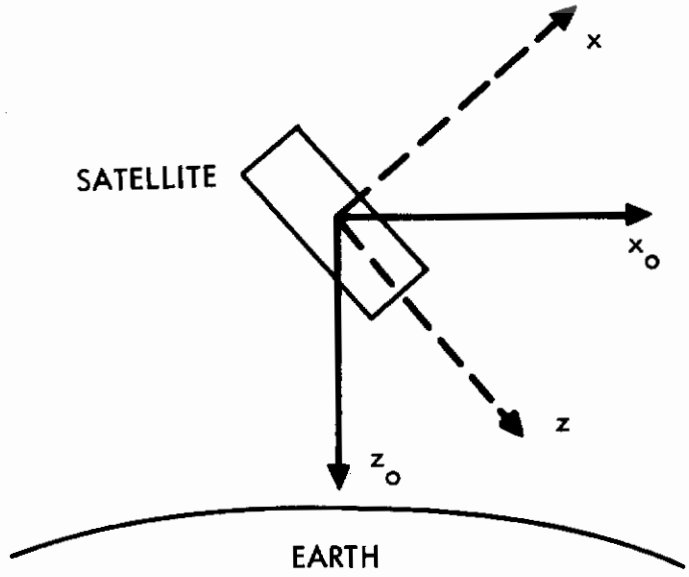

Figure 7.8 Satellite Tumbling in Pitch

Writing Equations (7.47) and (7.48) as a set of three first order equations, the result is

$$\left.\begin{aligned} \dot{\alpha} &= \beta\omega - \omega \\ \dot{\beta} &= -\alpha\omega \\ \dot{\omega} &= A\alpha - A\,\alpha\beta + \gamma \end{aligned}\right\} \qquad (7.49)$$

where

$$\left.\begin{aligned} \alpha &= a_{13} \\ \beta &= 1 - a_{33} \\ \omega &= \omega_2 + \omega_o \\ \gamma &= T_c/I_y \\ A &= 3\omega_o^2 \left(\frac{I_1 - I_3}{I_2}\right) \end{aligned}\right\} \qquad (7.50)$$

It remains to select a control law. A rather simple control system is one employing a reaction wheel. The control law chosen is

$$H_w = -k_o\, a_{13}\, a_{33} \qquad (7.51)$$

where H_w is the reaction wheel momentum and k is a gain constant. If $k = k_o/I_2$, then by Equations (7.49) it follows that

$$\begin{aligned} \gamma &= k\,\dot{\alpha} - k\,(\alpha\dot{\beta} + \beta\dot{\alpha}) \\ &= k\,(1-\beta)\,(\beta\omega - \omega) + k\alpha^2\,\omega \end{aligned} \tag{7.52}$$

Substituting Equation (7.52) into Equation (7.49) the state equations become

$$\left.\begin{aligned} \dot{\alpha} &= \beta\omega - \omega \\ \dot{\beta} &= -\alpha\omega \\ \dot{\omega} &= A\,\alpha - A\alpha\beta + 2k\beta\omega - k\beta^2\omega - k\omega + k\alpha^2\,\omega \end{aligned}\right\} \tag{7.53}$$

In order to investigate the stability of the system given by Equations (7.53), it is desirable to determine a Lyapunov function for the system, namely a positive definite scalar function, V, of the state variables whose time derivative is negative definite except, perhaps, at certain locally unstable points where $\frac{dV}{dt}$ is permitted to take on zero values. The determination of a suitable V function is no simple task. A start can be made by finding a Lyapunov function for the linearized system corresponding to Equations (7.53). In this way, at least a small portion, D, of the three dimensional state space can be found such that $(\alpha, \beta, \omega) \in D$ implies asymptotic convergence to (0, 0, 0). With good fortune, the function obtained may turn out to be a Lyapunov function for the nonlinear system as well or provide an indication of what modifications can be made in the function such that it is suitable for this system.

The first step in this investigation is to determine over what state space region the linear system Lyapunov function is a Lyapunov function for the nonlinear system as well. For this determination, the polynomial computer will be utilized. Since the purpose of this example is to demonstrate the utility of the computer program, this is the only part of the problem that will be considered. Once this region has been determined, human judgments and subsequently another routine can be emplo

Linearizing Equation (7.53), the result is

$$\left.\begin{aligned} \dot{\alpha} &= -\omega \\ \dot{\beta} &= 0 \\ \dot{\omega} &= A\alpha - k\omega \end{aligned}\right\} \tag{7.54}$$

Provided that the system possesses complex roots and that A and k are both greater than zero, a Lyapunov function and asymptotic stability for the linear system can be implied from the function

$$V = \alpha^2 - \frac{k}{A}\,\alpha\omega + \frac{1}{A}\,\omega^2 \tag{7.55}$$

since

$$\dot{V}_L = -kV \tag{7.56}$$

and V is positive definite since complex characteristic roots imply

$$k^2 - 4A < 0 \tag{7.57}$$

Considering the V function of Equation (7.55) for the nonlinear system, it follows that

$$\begin{aligned} \dot{V}_{NL} = &-\left[\frac{k}{A}\,\omega^2 - \frac{k^2}{A}\,\alpha\omega + k\alpha^2\right] + \frac{k}{A}\,(3\beta\omega^2 - 2\beta^2\omega^2) \\ &+ \left(2\frac{k}{A}\,\alpha^2\omega^2 - \frac{k^2}{A}\,\alpha^3\omega\right) + \frac{k^2}{A}\,(-2\alpha\beta\omega + \alpha\beta^2\omega) + k\alpha^2\beta \end{aligned} \tag{7.58}$$

where

$$0 \le \beta \le 2, \quad -1 \le \alpha \le 1 \text{ and } \omega \text{ is unrestricted.}$$

The negative of Equation (7.58) was utilized by the digital routine to establish the state space region within which $\dot{V}_{NL} \leq 0$. By employing symmetry considerations, all quadrants are covered if $\omega \geq 0$ but α assumes both plus and minus values.

The parameter k is chosen such that the linear system has a damping ratio of 0.5 and the moments of inertia are taken to satisfy

$$3\left(\frac{I_1 - I_3}{I_2}\right) = 2.25 \tag{7.59}$$

Taking

$$\eta = \frac{\omega}{\omega_o} \tag{7.60}$$

Equation (7.58) becomes

$$\begin{aligned}\frac{\dot{V}_{NL}}{\omega_o} = &- \left[0.66\,\eta^2 - \alpha\eta + 1.50\,\alpha^2\right] + \left[2.00\,\beta\eta^2 - 200\,\alpha\beta\eta\right. \\ &\left. + 1.50\,\alpha^2\beta\right] + \left[-1.33\,\beta^2\eta^2 + 1.33\,\alpha^2\eta^2\right. \\ &\left. - \alpha^3\eta + \alpha\beta^2\eta\right]\end{aligned} \tag{7.61}$$

Determination of part of the region for which this equation is negative will now serve as an example for the digital computer routine previously described.

7.5.2 Computer Results

The negative of Equation (7.61), namely

$$F(\eta, \alpha, \beta) = -\frac{\dot{V}_{NL}}{\omega_o} \tag{7.62}$$

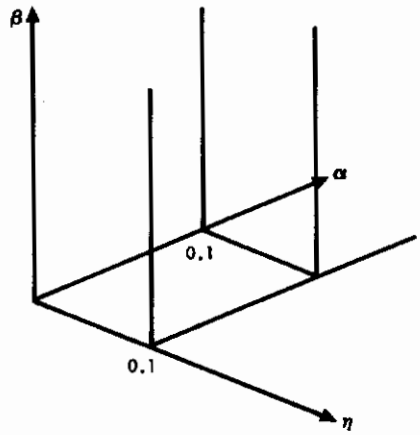

Figure 7.9 Space Associated with Example Problem

was specified to the polynomial computer using the initial operating point $(\eta_o, \alpha_o, \beta_o) = (0.1, 0, 0)$ as illustrated in Figure 7.9. It was not possible to begin the expansion at (0, 0, 0) since F(0, 0, 0) = 0. The computer was instructed to expand, if possible, to final values $(\eta_f, \alpha_f, \beta_f) = (10, 1, 2)$ within the constraint of a 5 minute time limit. Since this approach leaves the region $0 < \eta < 0.1$, $0 < \alpha$, $0 < \beta$ unaccounted for, a second computer application, under the same time constraint, was initiated at (0, 0.1, 0) with expansion, if possible, to (0.1, 1, 2). No attempt was made to exhaust any additional volume lying close to the β axis since $F(0, 0, \beta) = 0$ for all β. Physically, a system trajectory can cross the β axis only at $\beta = 0$ or 2 so this is no real limitation. This will be discussed more fully later.

For the first run described above, the computer, within the five minute time limit reached the point $(\eta, \alpha, \beta) = (10, 0.35, 0.13)$. Thus it expanded to its final desired value in only one of the three variables. From the nature of the print out data, it is evident that 0.35 and 0.13 represent limit values of α and β of the expansion in that the computer reached these values in a relatively short time, devoting most of the five minute running time to iteration in very small neighborhoods of these values. Since $F(\eta, \alpha, \beta)$ is not close to zero in this neighborhood, the program has obviously approached a limit point of the type described in Section 7.3.3. This is a charac-

teristic only of the expansion method rather than the basic algorithm, and this problem can be surmounted as described previously. No attempt to reset the computer to this limit point was made here since the primary purpose of this example is demonstration of the program rather than solution of the problem.

The second run described above achieved somewhat better results in that the final values of (η, α, β) were (.1, 1, 0.41). Here only the third coordinate, β, failed to reach its desired limit, limiting instead in a similar manner described above.

As described at the end of Section 7.5.1, the polynomial $F(\eta, -\alpha, \beta)$ also required consideration. The same two types of runs illustrated by Figure 7.9 were considered here also. The first of these expanded from (.1, 0, 0) to (7.5, .54, .18) (instead of (10, 1, 2)) and the second expanded from (0, .1, 0) to (.1, 1, .53) (instead of (.1, 1, 2)). Again the limit points were of the nature described above. A typical illustration of one of these runs is given in Figure 7.10. z_1, z_2, and z_3 represent the variables (η, α, β), P_1 is the value of F, NFT records the number of computer estimation failures, and U(s) represent values utilized by the computer to form its expansion estimations.

These results will now be applied to the physical problem at hand. First of all, it is clear that for analytical convenience the three dimensional problem was constructed from one that is essentially two dimensional. This is because α and β have been unconstrained relative to each other whereas in reality

$$a_{13}^2 + a_{33}^2 = \alpha^2 + (1-\beta)^2 = 1 \qquad (7.63)$$

	η	α	β	$F(\eta,\alpha,\beta)$		
S	Z1	Z2	Z3	P1	NFT	U(S)
1	1.50000E-01	0	0	1.48500E-02	0	3.03484E-01
2	1.50000E-01	3.00000E-02	0	1.16771E-02	0	1.00157E-01
3	1.50000E-01	3.00000E-02	5.00000E-02	9.87318E-03	1	1.63272E-03
1	2.00000E-01	3.00000E-02	5.00000E-02	1.83580E-02	1	2.27150E-01
2	2.00000E-01	6.00000E-02	5.00000E-02	1.66847E-02	1	1.56832E-01
3	2.00000E-01	6.00000E-02	7.50000E-02	1.52784E-02	2	4.48294E-02
1	3.10697E-01	6.00000E-02	7.50000E-02	3.86033E-02	2	1.12103E-01
2	3.10697E-01	1.02019E-01	7.50000E-02	3.62676E-02	3	2.06537E-01
3	3.10697E-01	1.02019E-01	8.75816E-02	3.46375E-02	4	5.89796E-02
1	5.21973E-01	1.02019E-01	8.75816E-02	1.01571E-01	4	3.30987E-01
2	5.21973E-01	1.36208E-01	8.75816E-02	9.56751E-02	4	8.83066E-02
3	5.21973E-01	1.36208E-01	9.50005E-02	9.28755E-02	4	1.98460E-02
1	8.27987E-01	1.36208E-01	9.50005E-02	2.48436E-01	5	3.57227E-01
2	8.27987E-01	1.98643E-01	9.50005E-02	2.19812E-01	6	2.73468E-01
3	8.27987E-01	1.98643E-01	1.04170E-01	2.11078E-01	7	3.50514E-02
1	1.18357E 00	1.98643E-01	1.04170E-01	4.53025E-01	7	1.48713E-01
2	1.18357E 00	2.40887E-01	1.04170E-01	4.10524E-01	8	6.79240E-02
3	1.18357E 00	2.40887E-01	1.89118E-01	4.00716E-01	8	1.24020E-02
1	2.04724E 00	2.40887E-01	1.09118E-01	1.30919E 00	8	2.08854E-01
2	2.04724E 00	2.85114E-01	1.09118E-01	1.15757E 00	9	1.09405E-01
3	2.04724E 00	2.85114E-01	1.14760E-01	1.12248E 00	10	2.30121E-02
1	3.42467E 00	2.85114E-01	1.14760E-01	3.40838E 00	10	2.07263E-01
2	3.42467E 00	3.13235E-01	1.14760E-01	3.11866E 00	11	1.24710E-01
3	3.42467E 00	3.13235E-01	1.17722E-01	3.06512E 00	11	1.05330E-02
1	5.95283E 00	3.13235E-01	1.17722E-01	9.93493E 00	11	2.15528E-01
2	5.95283E 00	3.33449E-01	1.17722E-01	9.28023E 00	13	1.20969E-01
3	5.95283E 00	3.33449E-01	1.20955E-01	9.09819E 00	14	1.69114E-02
2	5.95283E 00	3.41023E-01	1.20955E-01	8.84470E 00	15	5.63008E-02
3	5.95283E 00	3.41023E-01	1.22640E-01	8.75034E 00	15	4.91596E-03
2	5.95283E 00	3.46643E-01	1.22640E-01	8.55941E 00	17	3.34894E-02
3	5.95283E 00	3.46643E-01	1.24439E-01	8.45904E 00	18	1.64055E-03
2	5.95283E 00	3.48365E-01	1.24439E-01	8.40009E 00	19	2.55350E-02
3	5.95283E 00	3.48365E-01	1.25356E-01	8.34905E 00	20	2.82195E-04
2	5.95283E 00	3.49340E-01	1.25356E-01	8.31552E 00	20	4.93976E-03
3	5.95283E 00	3.49340E-01	1.25818E-01	8.28987E 00	22	5.78858E-03
2	5.95283E 00	3.50416E-01	1.25818E-01	8.25284E 00	23	3.65845E-03
3	5.95283E 00	3.50416E-01	1.25933E-01	8.24642E 00	23	2.43608E-03

Figure 7.10 Typical Digital Output for Algorithm

Thus the computer obtained results can actually be plotted in two dimensions where the acceptable limit on α, α_1, is given by

$$\alpha_1 = \min \left[\alpha_1, \sqrt{1 - (1-\beta_1)^2} \right] \tag{7.64}$$

where α_1 and β_1 are the final computer values. The previous computer results then reduce to the illustration in Figure 7.11, where the shaded region represents the domain the computer has accepted. It is assumed that the small rectangle near the origin can be shown to possess positive functional values by some other means, for example, from a consideration of the dominating terms of $F(\eta, \alpha, \beta)$.

The Lyapunov candidate can be written as

$$V(\alpha, \eta) = (\alpha - .330\,\eta)^2 + .115\,\eta^2 \tag{7.65}$$

As described in Section 7.1, it is necessary to find the minimum value of Equation (7.4-20) on the outer boundary of Figure 7.11. A simple computation demonstrates that the minimum value of the V function on this boundary is V = .0642. Thus, stability to (0, 0) is assured as long as (η, α) are such that $V(\eta, \alpha) < .0642$. This curve is illustrated in Figure 7.11.

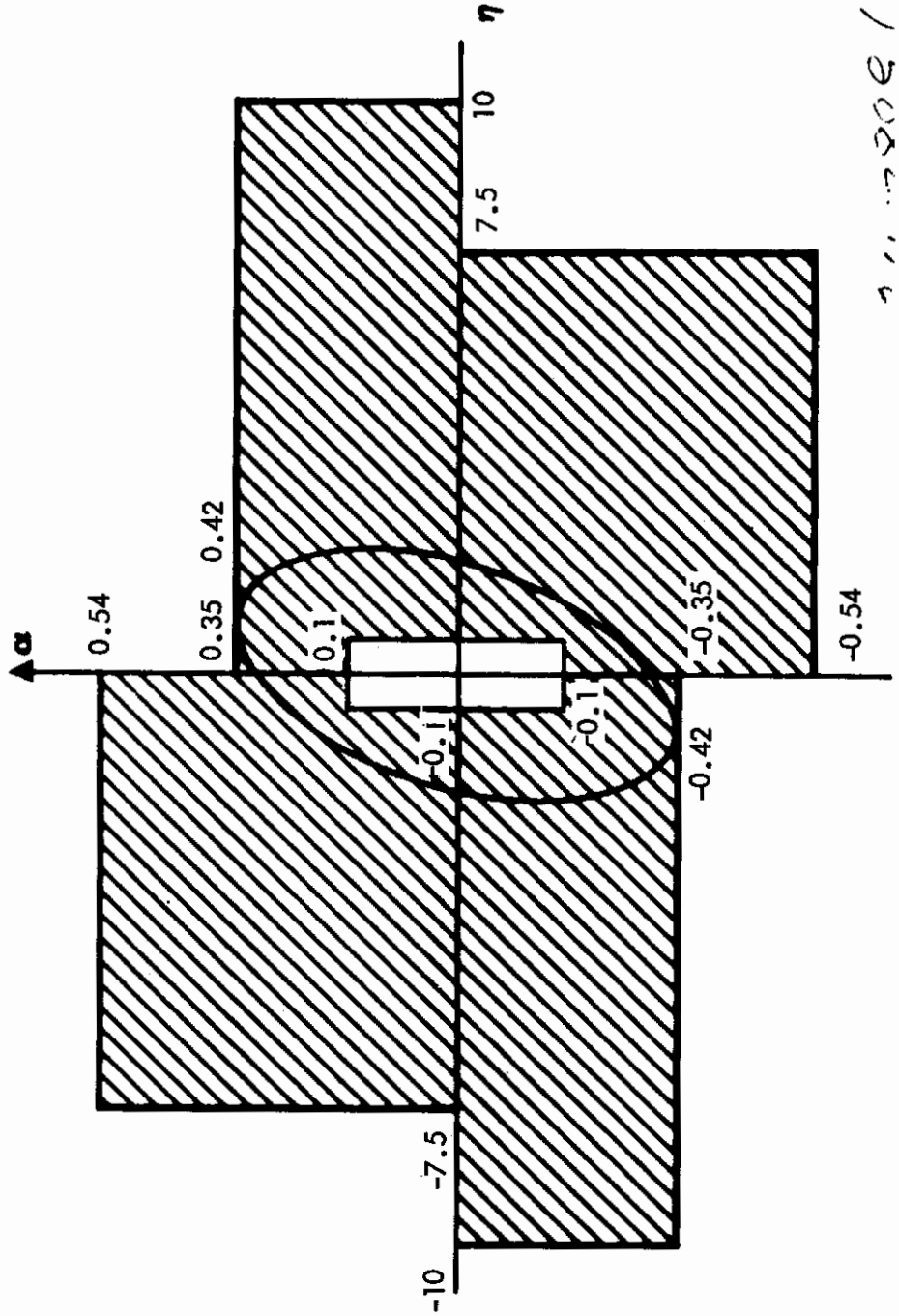

Figure 7.11 Computer Accepted Area (for $a_{33} > 0$)

SECTION VIII

CONCLUSIONS

The basic analytic sections of the report from which general conclusions can be drawn concern the kinematic representations (Section III), the comparison of possible acquisition schemes (Section V), the optimization study (Section VI), and the stability study (Section VII).

8.1 Kinematic Representations

There still does not exist a universally acceptable and readily applicable kinematic representation for rigid body motion. For complete three axis acquisition simulation studies the Euler symmetrical parameters appear most suitable. For the one axis acquisition problem three appropriate direction cosines provide simple analytic and simulation capabilities. The utility of the latter approach was demonstrated in Sections IV, V, and VI where significant use of this representation appears. For analytic studies of the complete three axis acquisition problem the appropriate choice of representation is not clear. In Appendix A the Gibbs vector is successfully utilized for a solution to this problem. In this application the control law was admittedly artificially chosen to "match" the kinematic representation. For simplicity of representation it was demonstrated in Section III that the kinematic representation employed should be closely related to the acquisition system sensor characteristics. Since available sensing techniques give outputs nearly proportional to the cosine of the angle between sensing axis and sensed object, the advantage of direction cosines in this respect is clear. Thus it seems that the only worthy conclusion is that the analyst should possess a familiarity with each of the available representations so that all can be considered for each application.

8.2 Acquisition Systems Comparisons

In comparing the various acquisition systems of Section V several interesting conclusions were established. Perhaps of major significance, and also the major limiting factor in the general application of these particular results, is the advantage obtained by initiating the acquisition maneuver near the desired final equilibrium point and having available sufficient control acceleration to prevent significant divergence from this point. This is not a revelation but rather a confirmation of hypothesis. It does establish the advantage available from an attitude stabilized launch vehicle in that the design based on this initial attitude apparently approaches the theoretically optimal performance for various constraints on control law implementation. For the lowest control acceleration level tested the tradeoffs in other system parameters - rather than just control acceleration level - were more apparent. The increase in convergence time and decrease in fuel with decreases in the direction cosine sensor saturation level were most readily observed for the low torque case with gyro rate sensing. Again, for the low torque case the direction cosine sensors, a major decrement in performance occurred in changing from AC to SC rate sensing modes. The lower the sensor saturation level the less pronounced this effect, being approximately a 65% decrement with saturation at 0.7 and about 40% at 0.25. A second major decrement in performance occurred in changing from ASCBR to PDR rate sensing modes. In this case the effect was most pronounced for the lowest sensor saturation level, being over 100% in this case and only about 20% for the higher sensor saturation levels. If, for a particular application, the sensor saturation level is unavoidably low it appears desirable to incorporate improved body rate information over that available by passive means.

For Euler angle sensing the results presented in Table 5.4 demonstrate an advantage in blanking the roll signal. In this case a general decrement in performance is noted as the sensor saturation level is decreased. On the other hand the use of PD control provides improved

performance over that available with G control for intermediate sensor saturation levels and low control acceleration levels. The reason for such improvement has not yet been firmly established. Comparison of Euler angle and direction cosine sensing shows no essential difference for large control acceleration levels. This is expected for this nearly linear operation mode since the two sensing approaches are nearly equivalent. However, even with low control acceleration levels no clear distinction exists, except perhaps with high sensor saturation levels and gyro rate sensing in which case direction cosines are favored (see Figure 5.20).

8.3 Acquisition System Optimization

The optimization approach of Section VI provides a practically implemented technique for pseudo-optimal design of acquisition systems. The technique is efficient in that even for many free parameters (say nine) and several initial conditions (say four) an optimal parameter set can be found in about one hour at a total machine cost expenditure of less than a hundred dollars. Even for more complete optimizations involving more parameters and more initial conditions the time and cost are small.

The utility of the optimization approach for providing practically useful results has been demonstrated. The capability of working with combined optimization criteria was demonstrated by the minimum thrust-minimum time optimization results. Other results have demonstrated the capability for these optimization algorithms to establish parameter saturation values for optimal control which could not have been obtained in a quantitative manner by any other method. For example, the requirements to have no direction cosine sensor saturation for minimum time optimal control, very low sensor saturation for minimum fuel optimal control and intermediate sensor saturation for minimum thrust optimal control are not readily predicted in a quantitative manner by other means. The capability for investigating a set of initial conditions simultaneously provides a key advantage to this scheme over other less

quantitative techniques. Future improvements potentially can provide even greater capabilities and understanding for complex nonlinear systems.

8.4 Acquisition System Stability

The approach to stability investigations of nonlinear control systems described in Section VII may have considerable practical value. The studies performed, although limited in scope, have demonstrated the potential utility of employing digital computers as analytic aids in these stability analyses. Even for the relatively crude first steps taken here, the computational requirements do not appear to be excessive for systems of reasonable order. A great deal of work remains to be done to definitely establish the practical significance of the approach and the classes of problems which can be expected to fit into the allowable category.

SECTION IX

NEW TECHNOLOGY

The ideas presented in Section VII are considered new concepts, and the hybrid optimization of Section VI represents, to our knowledge, the most successful undertaking of this sort thus far attempted.

SECTION X

REFERENCES

1. Ergin, E., Norum, V., Windeknecht, T., Techniques for Analysis of Nonlinear Attitude Control Systems for Space Vehicles, ASD-TDR-62-208, June 1962.

2. Flugge-Lotz, I., Marbach, H., "The Optimal Control of Some Attitude Control Systems for Different Performance Criteria," Journal of Basic Engineering, June 1963.

3. Wheeler, P. C., "Magnetic Attitude Control of Rigid Axially Symmetric Spinning Satellites in Circular Earth Orbits," SUDAER No. 224, Stanford University, April 1965.

4. Farrenkopf, R., Sabroff, A., Wheeler, P., "Integral Pulse Frequency On-Off Control," AIAA Guidance and Control Conference Paper 63-328, MIT, August 1963.

5. Scott, E. D., "Control Moment Gyro Gravity Stabilization," AIAA Guidance and Control Conference Paper 63-324, MIT, August 1963.

6. Sabroff, A. E., "A Summary of Gravity Gradient Stabilization of Earth Satellites," TRW/STL Report 9990-6715-RU001, 27 July 1964.

7. Fletcher, H. J., Rongved, L., and Yu, E. Y., "Dynamics Analysis of a Two-Body Gravitationally Oriented Satellite," Bell System Technical Journal, September 1963, pp 2239-2266.

8. Fishell, R. E. and Mobley, F. M., "A System for Passive Gravity Gradient Stabilization of Earth Satellites," AIAA Guidance and Control Conference paper 63-326, MIT, August 1963.

9. Pringle, R., "On the Captive, Stability, and Passive Damping of Artificial Satellites," Stanford University, April 1964.

REFERENCES

10. Roberson, R. E., "Attitude Control of Satellite Vehicles -- An Outline of the Problem," Proc. of VIII International Astro. Fed. Congress, Barcelona, 1957, Springer-Verlag, Wien, 1958.

11. Goldstein, H., Classical Mechanics, Addison-Wesley, Cambridge, Massachusetts, 1953.

12. Smirnov, Academician V. I., Linear Algebra and Group Theory, trans. and ed. by R. A. Silverman, McGraw-Hill Book Co., New York, 1961.

13. Whittaker, E. T., A Treatise on the Analytical Dynamics of Particles and Rigid Bodies, Cambridge University Press, Cambridge, England, 1960.

14. Gibbs, J. W., The Scientific Papers of J. Willard Gibbs, Edited by H. A. Bumstead and R. G. Van Name, Dover, 1961.

15. Hamilton, Sir W. R., Elements of Quaternions, Longmans, Green and Co., London, England, 1866.

16. Robinson, A. C., On the Use of Quaternions in Simulation of Rigid Body Motion, WADC Technical Report 58-17, December 1958.

17. De Bra, D. B., "The Large Attitude Motions and Stability, Due to Gravity, of a Satellite with Passive Damping in an Orbit of Arbitrary Eccentricity About an Oblate Body," Stanford University, May 1962.

18. Windeknecht, T. G., "On Design of In-The-Large Stability in Spacecraft Attitude Control," TRW/STL Report 9344-6001-KU000, 24 July 1962.

19. Shah, B. V., Buehler, R. J., Kempthorne, O., "The Method of Parallel Tangents (PARTAN) for Finding an Optimum" Technical Report No. 2, Office of Naval Research, Contract No. 530(05), Iowa State Statistical Doc.

REFERENCES

20. Wilde, D. J., "Optimization by the Method of Contour Tangents," American Institute of Chemical Engineers Journal, Vol. 9 (March 1963) pp 186-190.

21. Mitchell, B., "A Hybrid Analog-Digital Parameter Optimizer for Astroc II," Proc. AFIPS Spring Joint Computer Conference, V. 25, pp 271-285, 1964.

22. Rostrigin, L. A., "The Convergence of the Random Search Method in the External Control of a Many-Parameter System," Academy of Science, U.S.S.R., Automation and Remote Control, Vol. 24, No. 11, November 1963.

23. Buehler, R. J., Shah, B. V., and Kempthorne, O., "Some Properties of Steepest Ascent and Related Procedures for Finding Optimum Conditions," Iowa State Statistical Laboratory (April 1961) pp 8-18.

24. LaSalle, J., Lefschetz, S., Stability by Lyapunov's Direct Method With Applications, Academic Press, New York, 1961.

25. Pringle, R., "Stability of Mechanical Systems," AIAA Journal, Vol. 3, No. 2, February 1965.

26. Malkin, I. G., "Theory of Stability of Motion", AEC-tr-3352, Physics and Mathematics.

27. Mortensen, R. E., "On Systems for Automatic Control of the Rotation of a Rigid Body", unpublished

APPENDIX A

MORTENSEN'S ACQUISITION EXAMPLE

In Reference [27], Mortensen uses the Second Method of Lyapunov in describing an acquisition system that is asymptotically stable in the large. Since it is felt that this particular example has some merit, it is presented in this Appendix.

It proves advantageous to make a slight reformulation of the dynamical principles given in Section III in order to investigate the application of various control techniques for attitude control. Define the angular momentum vector, $\bar{L}$, which is related to the angular velocity vector $\bar{\omega}$ by

$$I = \begin{bmatrix} L_x \\ L_y \\ L_z \end{bmatrix} = \begin{bmatrix} I_x & 0 & 0 \\ 0 & I_y & 0 \\ 0 & 0 & I_z \end{bmatrix} \begin{bmatrix} \omega_x \\ \omega_y \\ \omega_z \end{bmatrix} = \bar{\bar{I}}\,\bar{\omega} \qquad (A.1)^*$$

where I_x, I_y, I_z are the principal moments of inertia of the body inertia matrix $\bar{\bar{I}}$. In terms of the angular momentum components L_x, L_y, L_z, Euler's equations may be rewritten in matrix form

$$\begin{bmatrix} \dot{L}_x \\ \dot{L}_y \\ \dot{L}_z \end{bmatrix} = \begin{bmatrix} 0 & \frac{L_z}{I_z} & -\frac{L_y}{I_y} \\ -\frac{L_z}{I_z} & 0 & \frac{L_x}{I_x} \\ \frac{L_y}{I_y} & -\frac{L_x}{I_x} & 0 \end{bmatrix} \begin{bmatrix} L_x \\ L_y \\ L_z \end{bmatrix} + \begin{bmatrix} M_x \\ M_y \\ M_z \end{bmatrix} \qquad (A.2)$$

* Note that Mortenson's notation replaces the subscripts 1, 2, 3 used earlier by x, y, and z respectively.

From Section III, the components of the Gibbs vector α, β, γ and their derivatives are related by

$$2\begin{bmatrix}\dot{\alpha}\\ \dot{\beta}\\ \dot{\gamma}\end{bmatrix} = \begin{bmatrix}\omega_x\\ \omega_y\\ \omega_z\end{bmatrix} + \begin{bmatrix}\alpha^2 & \alpha\beta & \alpha\gamma\\ \beta\alpha & \beta^2 & \beta\gamma\\ \gamma\alpha & \gamma\beta & \gamma^2\end{bmatrix}\begin{bmatrix}\omega_x\\ \omega_y\\ \omega_z\end{bmatrix} + \begin{bmatrix}0 & -\gamma & \beta\\ \gamma & 0 & -\alpha\\ -\beta & \alpha & 0\end{bmatrix}\begin{bmatrix}\omega_x\\ \omega_y\\ \omega_z\end{bmatrix} \qquad (A.3)$$

Define the scalar S by the bilinear form

$$S = \begin{bmatrix}\alpha & \beta & \gamma\end{bmatrix}\begin{bmatrix}\frac{1}{I_x} & 0 & 0\\ 0 & \frac{1}{I_y} & 0\\ 0 & 0 & \frac{1}{I_z}\end{bmatrix}\begin{bmatrix}L_x\\ L_y\\ L_z\end{bmatrix} \qquad (A.4)$$

Then, Equation (A.3) may be rewritten in the equivalent form

$$\begin{bmatrix}\dot{\alpha}\\ \dot{\beta}\\ \dot{\gamma}\end{bmatrix} = \frac{1}{2}\begin{bmatrix}S & \frac{L_z}{I_z} & -\frac{L_y}{I_y}\\ -\frac{L_z}{I_z} & S & \frac{L_x}{I_x}\\ \frac{L_y}{I_y} & -\frac{L_x}{I_x} & S\end{bmatrix}\begin{bmatrix}\alpha\\ \beta\\ \gamma\end{bmatrix} + \frac{1}{2}\begin{bmatrix}\frac{1}{I_x} & 0 & 0\\ 0 & \frac{1}{I_y} & 0\\ 0 & 0 & \frac{1}{I_z}\end{bmatrix}\begin{bmatrix}L_x\\ L_y\\ L_z\end{bmatrix} \qquad (A.5)$$

Combining Equations (A.2) and (A.5) into a six-dimensional vector-matrix differential equation gives a complete dynamical description of the motion of a rigid body subject to any external moments:

$$\begin{bmatrix} \dot{L}_x \\ \dot{L}_y \\ \dot{L}_z \\ \dot{\alpha} \\ \dot{\beta} \\ \dot{\gamma} \end{bmatrix} = \begin{bmatrix} 0 & \frac{L_z}{I_z} & -\frac{L_y}{I_y} & 0 & 0 & 0 \\ -\frac{L_z}{I_z} & 0 & \frac{L_x}{I_x} & 0 & 0 & 0 \\ \frac{L_y}{I_y} & -\frac{L_x}{I_x} & 0 & 0 & 0 & 0 \\ \frac{1}{2I_x} & 0 & 0 & \frac{S}{2} & \frac{L_z}{2I_z} & -\frac{L_y}{2I_y} \\ 0 & \frac{1}{2I_y} & 0 & -\frac{L_z}{2I_z} & \frac{S}{2} & \frac{L_x}{2I_x} \\ 0 & 0 & \frac{1}{2I_z} & \frac{L_y}{2I_y} & -\frac{L_x}{2I_x} & \frac{S}{2} \end{bmatrix} \begin{bmatrix} L_x \\ L_y \\ L_z \\ \alpha \\ \beta \\ \gamma \end{bmatrix} + \begin{bmatrix} M_x \\ M_y \\ M_z \\ 0 \\ 0 \\ 0 \end{bmatrix} \quad \text{(A.6)}$$

Consider (A.6) as the fundamental dynamic description of a rigid body for the acquisition control problem.

For attitude control problems, the moment vector acting on the rigid body is the sum of the control torques u_x, u_y, u_z applied by the control system and disturbance torques d_x, d_y, d_z resulting from external causes. For acquisition the disturbances can usually be neglected. Therefore,

$$\begin{bmatrix} M_x \\ M_y \\ M_z \\ 0 \\ 0 \\ 0 \end{bmatrix} = \begin{bmatrix} u_x \\ u_y \\ u_z \\ 0 \\ 0 \\ 0 \end{bmatrix} \quad \text{(A.7)}$$

Using the definition (A.4) of the quantity S appearing in the matrix in (A.6), it is possible to rewrite this matrix so that the dependence on L_x, L_y, L_z, α, β, γ appears explicitly. Making this revision and incorporating (A.7), the fundamental dynamic equation becomes

$$\begin{bmatrix} \dot{L}_x \\ \dot{L}_y \\ \dot{L}_z \\ \dot{\alpha} \\ \dot{\beta} \\ \dot{\gamma} \end{bmatrix} = \begin{bmatrix} 0 & \frac{L_z}{I_z} & -\frac{L_y}{I_y} & 0 & 0 & 0 \\ -\frac{L_z}{I_z} & 0 & \frac{L_x}{I_x} & 0 & 0 & 0 \\ \frac{L_y}{I_y} & -\frac{L_x}{I_x} & 0 & 0 & 0 & 0 \\ \frac{1+\alpha^2}{2I_x} & \frac{\alpha\beta}{2I_y} & \frac{\alpha\gamma}{2I_z} & 0 & \frac{L_z}{2I_z} & -\frac{L_y}{2I_y} \\ \frac{\beta\alpha}{2I_x} & \frac{1+\beta^2}{2I_y} & \frac{\beta\gamma}{2I_z} & -\frac{L_z}{2I_z} & 0 & \frac{L_x}{2I_x} \\ \frac{\gamma\alpha}{2I_x} & \frac{\gamma\beta}{2I_y} & \frac{1+\gamma^2}{2I_z} & \frac{L_y}{2I_y} & -\frac{L_x}{2I_x} & 0 \end{bmatrix} \begin{bmatrix} L_x \\ L_y \\ L_z \\ \alpha \\ \beta \\ \gamma \end{bmatrix} + \begin{bmatrix} u_x \\ u_y \\ u_z \\ 0 \\ 0 \\ 0 \end{bmatrix} \qquad \text{(A.8)}$$

As an application of the formulation just developed, consider the acquisition control stability problem. Let the components of the state vector have any initial values L_{xo}, L_{yo}, L_{zo}, α_o, β_o, γ_o whatsoever at time $t = 0$. The desired orientation of the body is defined as $\alpha = \beta = \gamma = 0$ with zero rate (i.e., maintain the state vector at zero).

The problem is to find a suitable control law which makes the control moment vector (u_x, u_y, u_z) a function of the state vector

$(L_x, L_y, L_z, \alpha, \beta, \gamma)$ such that the resulting acquisition system may be proven asymptotically stable in the large by means of the Second Method of Lyapunov.

Mortensen proposed the following, admittedly artificial, control law.

$$\begin{bmatrix} u_x \\ u_y \\ u_z \\ 0 \\ 0 \\ 0 \end{bmatrix} = \begin{bmatrix} -k_x & 0 & 0 & -k_p\left(\frac{1+\alpha^2}{2I_x}\right) & -k_p\left(\frac{\beta\alpha}{2I_x}\right) & -k_p\left(\frac{\gamma\alpha}{2I_x}\right) \\ 0 & -k_y & 0 & -k_p\left(\frac{\alpha\beta}{2I_y}\right) & -k_p\left(\frac{1+\beta^2}{2I_y}\right) & -k_p\left(\frac{\gamma\beta}{2I_y}\right) \\ 0 & 0 & -k_z & -k_p\left(\frac{\alpha\gamma}{2I_z}\right) & -k_p\left(\frac{\beta\gamma}{2I_z}\right) & -k_p\left(\frac{1+\gamma^2}{2I_z}\right) \\ 0 & 0 & 0 & 0 & 0 & 0 \\ 0 & 0 & 0 & 0 & 0 & 0 \\ 0 & 0 & 0 & 0 & 0 & 0 \end{bmatrix} \begin{bmatrix} L_x \\ L_y \\ L_z \\ \alpha \\ \beta \\ \gamma \end{bmatrix} \qquad (A.9)$$

where k_x, k_y, k_z, and k_p are all constants (i.e., "control gains"). Substitution of (A.9) into (A.8) yields:

$$\begin{bmatrix} \dot{L}_x \\ \dot{L}_y \\ \dot{L}_z \\ \dot{\alpha} \\ \dot{\beta} \\ \dot{\gamma} \end{bmatrix} = \begin{bmatrix} -k_x & \frac{L_z}{I_z} & -\frac{L_y}{I_y} & -k_p\left(\frac{1+\alpha^2}{2I_x}\right) & -k_p\left(\frac{\beta\alpha}{2I_x}\right) & -k_p\left(\frac{\gamma\alpha}{2I_x}\right) \\ -\frac{L_z}{I_z} & -k_y & \frac{L_x}{I_x} & -k_p\left(\frac{\alpha\beta}{2I_y}\right) & -k_p\left(\frac{1+\beta^2}{2I_y}\right) & -k_p\left(\frac{\gamma\beta}{2I_y}\right) \\ \frac{L_y}{I_y} & -\frac{L_x}{I_x} & -k_z & -k_p\left(\frac{\alpha\gamma}{2I_z}\right) & -k_p\left(\frac{\beta\gamma}{2I_z}\right) & -k_p\left(\frac{1+\gamma^2}{2I_z}\right) \\ \frac{1+\alpha^2}{2I_x} & \frac{\alpha\beta}{2I_y} & \frac{\alpha\gamma}{2I_z} & 0 & \frac{L_z}{2I_z} & -\frac{L_y}{2I_y} \\ \frac{\beta\alpha}{2I_x} & \frac{1+\beta^2}{2I_y} & \frac{\beta\gamma}{2I_z} & -\frac{L_z}{2I_z} & 0 & \frac{L_x}{2I_x} \\ \frac{\gamma\alpha}{2I_x} & \frac{\gamma\beta}{2I_y} & \frac{1+\gamma^2}{2I_z} & \frac{L_y}{2I_y} & -\frac{L_x}{2I_x} & 0 \end{bmatrix} \begin{bmatrix} L_x \\ L_y \\ L_z \\ \alpha \\ \beta \\ \gamma \end{bmatrix} \qquad \text{(A.10)}$$

Equations (A.10) are the dynamical equations for the closed-loop behavior of an acquisition system employing a set of control laws which apply restoring moments according to (A.9). For brevity, make the following definitions. The state vector is denoted by $\bar{w}$

$$\bar{w} = \begin{bmatrix} L_x \\ L_y \\ L_z \\ \alpha \\ \beta \\ \gamma \end{bmatrix} \qquad \text{(A.11)}$$

The matrices $\bar{\bar{K}}$ and $\bar{\bar{R}}$ are defined as follows:

$$\bar{\bar{K}} = \begin{bmatrix} -k_x & 0 & 0 & 0 & 0 & 0 \\ 0 & -k_y & 0 & 0 & 0 & 0 \\ 0 & 0 & -k_z & 0 & 0 & 0 \\ 0 & 0 & 0 & 0 & 0 & 0 \\ 0 & 0 & 0 & 0 & 0 & 0 \\ 0 & 0 & 0 & 0 & 0 & 0 \end{bmatrix} \tag{A.12}$$

$$\bar{\bar{R}} = \begin{bmatrix} 0 & \frac{L_z}{I_z} & -\frac{L_y}{I_y} & -k_p\left(\frac{1+\alpha^2}{2I_x}\right) & -k_p\left(\frac{\beta\alpha}{2I_x}\right) & -k_p\left(\frac{\gamma\alpha}{2I_x}\right) \\ -\frac{L_z}{I_z} & 0 & \frac{L_x}{I_x} & -k_p\left(\frac{\alpha\beta}{2I_y}\right) & -k_p\left(\frac{1+\beta^2}{2I_y}\right) & -k_p\left(\frac{\gamma\beta}{2I_y}\right) \\ \frac{L_y}{I_y} & -\frac{L_x}{I_x} & 0 & -k_p\left(\frac{\alpha\gamma}{2I_z}\right) & -k_p\left(\frac{\beta\gamma}{2I_z}\right) & -k_p\left(\frac{1+\gamma^2}{2I_z}\right) \\ \frac{1+\alpha^2}{2I_x} & \frac{\alpha\beta}{2I_y} & \frac{\alpha\gamma}{2I_z} & 0 & \frac{L_z}{2I_z} & -\frac{L_y}{2I_y} \\ \frac{\beta\alpha}{2I_x} & \frac{1+\beta^2}{2I_y} & \frac{\beta\gamma}{2I_z} & -\frac{L_z}{2I_z} & 0 & \frac{L_x}{2I_x} \\ \frac{\gamma\alpha}{2I_x} & \frac{\gamma\beta}{2I_y} & \frac{1+\gamma^2}{2I_z} & \frac{L_y}{2I_y} & -\frac{L_x}{2I_x} & 0 \end{bmatrix} \tag{A.13}$$

In order to investigate the stability of the differential equations (A.10), choose as a candidate for a Lyapunov function, V, the following quadratic form:

$$V = \begin{bmatrix} L_x & L_y & L_z & \alpha & \beta & \gamma \end{bmatrix} \begin{bmatrix} 1 & 0 & 0 & 0 & 0 & 0 \\ 0 & 1 & 0 & 0 & 0 & 0 \\ 0 & 0 & 1 & 0 & 0 & 0 \\ 0 & 0 & 0 & k_p & 0 & 0 \\ 0 & 0 & 0 & 0 & k_p & 0 \\ 0 & 0 & 0 & 0 & 0 & k_p \end{bmatrix} \begin{bmatrix} L_x \\ L_y \\ L_z \\ \alpha \\ \beta \\ \gamma \end{bmatrix} \qquad (A.14)$$

Denoting the matrix in (A.14) by G, the equation may be written in symbolic form as

$$V = \bar{w}^T \, \bar{\bar{G}} \, \bar{w} \qquad (A.15)$$

The system of differential equations (A.10) may be written using the definitions (A.12) and (A.13) as

$$\dot{\bar{w}} = \bar{\bar{K}} \, \bar{w} + \bar{\bar{R}} \, \bar{w} \qquad (A.16)$$

The transposed equations may be written as

$$\dot{\bar{w}}^T = \bar{w}^T \, \bar{\bar{K}}^T + \bar{w}^T \, \bar{\bar{R}}^T \qquad (A.17)$$

Since $\bar{\bar{G}}$ is a constant matrix, the time derivative of V is:

$$\dot{V} = \dot{\bar{w}}^T \, \bar{\bar{G}} \, \bar{w} + \bar{w}^T \, \bar{\bar{G}} \, \dot{\bar{w}} \qquad (A.18)$$

Substituting the Equations (A.16) and (A.17) for $\dot{\bar{w}}$ and $\dot{\bar{w}}^T$ into (A.18), the time derivative of V is found as

$$\dot{V} = \bar{w}^T \, \bar{\bar{K}}^T \bar{\bar{G}} \, \bar{w} + \bar{w}^T \bar{\bar{R}}^T \, \bar{\bar{G}} \, \bar{w} + \bar{w}^T \, \bar{\bar{G}} \, \bar{\bar{R}} \, \bar{w} + \bar{w}^T \, \bar{\bar{G}} \, \bar{\bar{R}} \, \bar{w} \qquad (A.19)$$

Using the definitions (A.13) and (A.14), one may readily verify the following identities:

$$\bar{\bar{K}}^T \bar{\bar{G}} = \bar{\bar{G}} \bar{\bar{K}} = \bar{\bar{K}} \; ; \; \bar{\bar{R}}^T \bar{\bar{G}} = -\bar{\bar{G}} \bar{\bar{R}} \tag{A.20}$$

Therefore, Equation (A.19) reduces simply to

$$\dot{V} = 2 \bar{w}^T \bar{\bar{K}} \bar{w} \tag{A.21}$$

which may be written explicitly as

$$\dot{V} = -2 (k_x L_x^2 + k_y L_y^2 + k_z L_z^2) \tag{A.22}$$

The quadratic form V, Equation (A.14), will be positive definite provided

$$k_p > 0 \tag{A.23}$$

Furthermore, although $\dot{V}$ as given by (A.22) is not negative definite, it is constrained to be non-positive definite by the additional requirements

$$k_x > 0 \; ; \; k_y > 0 \; ; \; k_z > 0 \tag{A.24}$$

Under conditions (A.24), the only instants of time at which $\dot{V}$ can be zero are when L_x, L_y, L_z are <u>all</u> zero, i.e., when the body is at rest. It is then necessary to eliminate the possibility that the body, governed by the dynamical equations (A.10), remains at rest given that L_x, L_y, and L_z are all zero but that at least one of α, β, or γ, is not zero (i.e., although the body is at rest an attitude displacement error exists). This is equivalent to inquiring whether it is possible for $\dot{L}_x$, $\dot{L}_y$, and $\dot{L}_z$ all simultaneously to be zero given that L_x, L_y, L_z

are all zero, but that at least one of the components α, β, γ is <u>not</u> zero. From examination of the dynamic equations (A.10), this is equivalent to determining whether any non-trivial solutions exist of the equation

$$-\frac{k_p}{2}\begin{bmatrix} \frac{1+\alpha^2}{I_x} & \frac{\beta\alpha}{I_x} & \frac{\gamma\alpha}{I_x} \\ \frac{\alpha\beta}{I_y} & \frac{1+\beta^2}{I_y} & \frac{\gamma\beta}{I_y} \\ \frac{\alpha\gamma}{I_z} & \frac{\beta\gamma}{I_z} & \frac{1+\gamma^2}{I_z} \end{bmatrix}\begin{bmatrix} \alpha \\ \beta \\ \gamma \end{bmatrix} = \begin{bmatrix} 0 \\ 0 \\ 0 \end{bmatrix} \qquad \text{(A.25)}$$

The constants I_x, I_y, I_z are the principal moments of inertia of the rigid body, and in any physical situation must be positive. Expanding (A.25) and using the condition (A.23), it may be shown that (A.25) will have a non-trivial solution if and only if the following set of equations has a non-trivial solution,

$$\begin{aligned} \alpha\,(1+\alpha^2+\beta^2+\gamma^2) &= 0 \\ \beta\,(1+\alpha^2+\beta^2+\gamma^2) &= 0 \qquad \text{(A.26)} \\ \gamma\,(1+\alpha^2+\beta^2+\gamma^2) &= 0 \end{aligned}$$

It is clear that the Equations (A.26) do not have a non-trivial solution since α, β, and γ are all real. Therefore, if $\dot{V}$ given by (A.22) vanishes instantaneously, $\dot{L}_x$, $\dot{L}_y$, and $\dot{L}_z$ cannot simultaneously also vanish unless α, β, γ are all zero, i.e., if the state vector $\bar{w}$ is zero. But if at least one of $\dot{L}_x$, $\dot{L}_y$, or $\dot{L}_z$ is non-zero, then the function $\dot{V}$ given by (A.22) cannot remain zero, and by conditions (A.24), if $\dot{V}$ is not zero it can only be negative. Therefore, the positive-definite function V

defined by (A.14) must be monotonically decreasing with time, i.e., V necessarily approaches zero from above as $t \rightarrow \infty$. The only question remaining is whether V possesses suitable boundedness properties for all possible states of the system.

From the definition (A.14), the function V may be written as

$$V = (L_x^2 + L_y^2 + L_z^2) + k_p (\alpha^2 + \beta^2 + \gamma^2) \qquad (A.27)$$

The quantity $(L_x^2 + L_y^2 + L_z^2)$ is by definition the squared magnitude of the total angular momentum vector of the rigid body, which cannot be infinite unless the angular momentum of the body is infinite and cannot be zero unless the angular momentum is zero (i.e., the body is at rest). Recall the following definition involving α, β, and γ given in Section III:

$$\alpha^2 + \beta^2 + \gamma^2 = \tan^2 \frac{\Phi}{2} \qquad (A.28)$$

where Φ is the total angle of equivalent rotation. Therefore, in order to keep the function V bounded, Φ must be restricted to the open interval

$$-\pi < \Phi < +\pi \qquad (A.29)$$

For any possible initial conditions α_o, β_o, γ_o on the displacement of the body from the desired orientation, it must be possible to find some (direction cosine) matrix $\bar{\bar{A}}$ as defined in Section III which generates this rotational displacement. This matrix $\bar{\bar{A}}$ must be an orthogonal transformation belonging to the rotation group defined by Smirnov [12] as discussed earlier. Recalling Smirnov's remark about the rotation group being isomorphic to the points of a sphere of radius π, it is seen that the only initial conditions α_o, β_o, γ_o

which do not meet the restriction (A.29) correspond to points lying on the very outer surface of this sphere. As a matter of fact, as was pointed out earlier, because the components of the eigenvector $\hat{e}$ may take on any values between +1 and -1 consistent with $e_1^2 + e_2^2 + e_3^2 = 1$, the angle Φ may actually be restricted to the closed interval $0 \leq \Phi \leq \pi$ and any possible distinguishable member of the rotation group may still be generated. Excluding infinite angular momentum, the state vector $\bar{w}$, whose displacement components are α, β, γ, therefore, becomes infinite only for rotational displacements corresponding to points on the boundary of the set of all points (Smirnov's sphere) representing all possible displacements of the body from its desired orientation. In addition, the state vector $\bar{w}$ vanishes when and only when the body is at rest in the desired orientation. The vector $\bar{w}$ which has been chosen as the state vector therefore provides an adequate description of all possible states of motion of the rigid body. Furthermore, the function V defined by the equivalent equations (A.14), (A.15), and (A.27) is a continuous (scalar) function of $\bar{w}$ which becomes infinite when and only when $\bar{w}$ is infinite and vanishes when and only when $\bar{w}$ vanishes. The restriction (A.29) is therefore actually unnecessary.

Since it has been shown that the function $V(\bar{w})$ enjoys all of the required properites[24], it is concluded that $V(\bar{w})$ is a Lyapunov function for the system of differential equations (A.10). Therefore, the acquisition control system incorporating the plant described by (A.6) and employing the control law (A.9) is completely stable for all $k_x > 0$, $k_y > 0$, $k_z >$, $k_p > 0$.

APPENDIX B

ACQUISITION SYSTEMS COMPARISON DIAGRAMS

B.1 Block Diagrams

The block diagram for the direction cosine attitude sensors simulation is presented in Figure B.1. Various combinations of measured body rate, computed body rate, or pure derived rate are indicated as inputs to the rate sensor block.

Figure B.2 presents the block diagram for the Euler angle sensors simulation and indicates the method of obtaining Euler angles from explicit solutions in terms of direction cosines. Combinations of measured body rate and derived Euler rates are indicated as inputs to the rate sensor block.

B.2 Analog Computer Diagrams

The dynamics and kinematics integration indicated in Figures B.1 and B.2 for both types of attitude sensing is shown in the analog diagram of Figure B.3. This diagram corresponds to the simulation of Equations (5.1) and (5.3).

Simulation of the "controller" block is presented in Figure B.4 and again refers to both types of attitude sensing. Formation of the error criteria is also shown. Figure B.4 represents the simulation of Equations (5.2) and (5.4).

The simulation methods of obtaining the various direction cosine control laws is shown in Figure B.5. This diagram covers Equations (5.5) through (5.8) and (5.10) through (5.14).

In Figure B.6, the Euler angle attitude sensing control laws are presented. This diagram corresponds to the simulation of Equations (5.15) through (5.18).

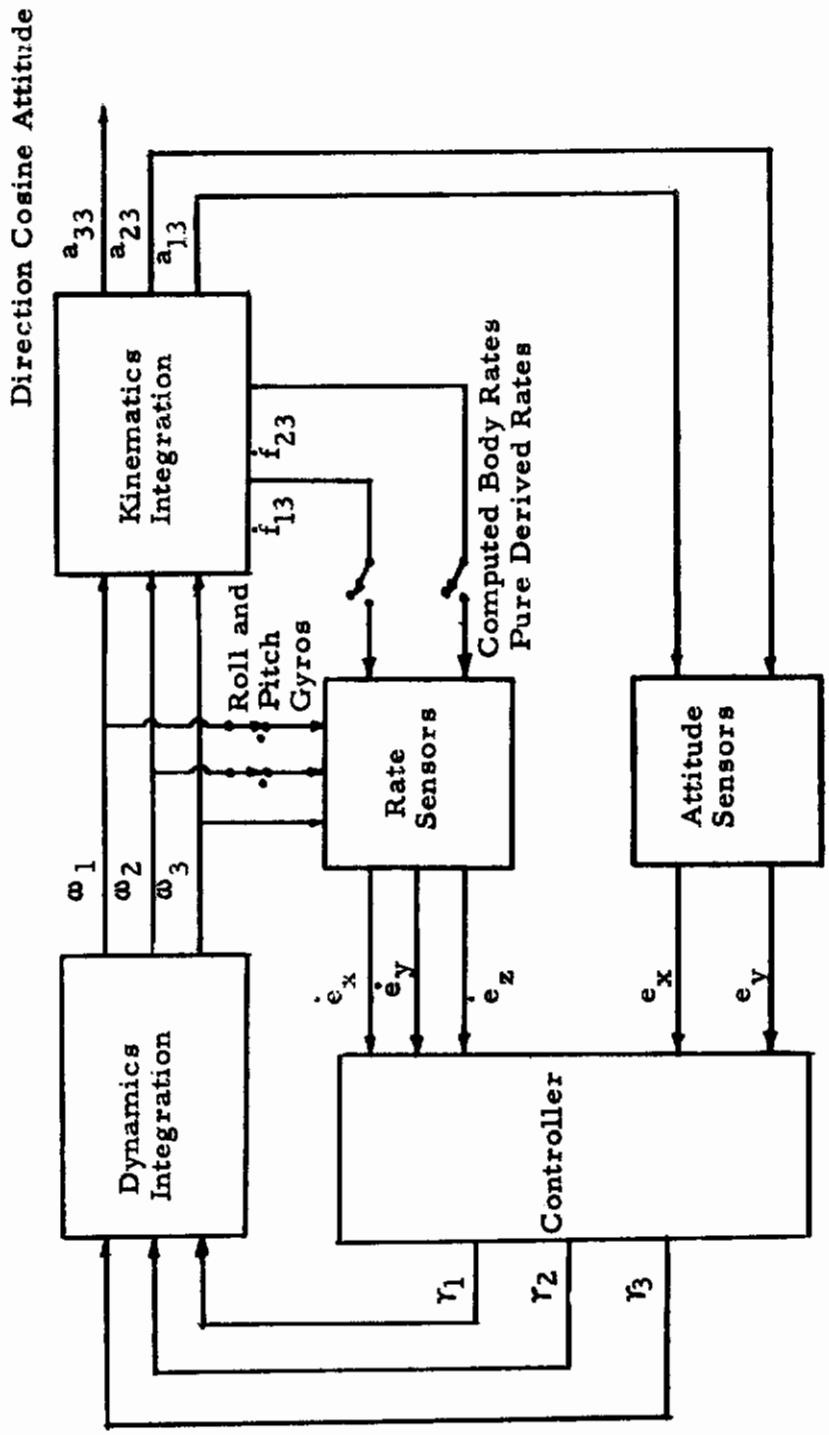

Figure B.1 Direction Cosine Sensors Simulation Block Diagram

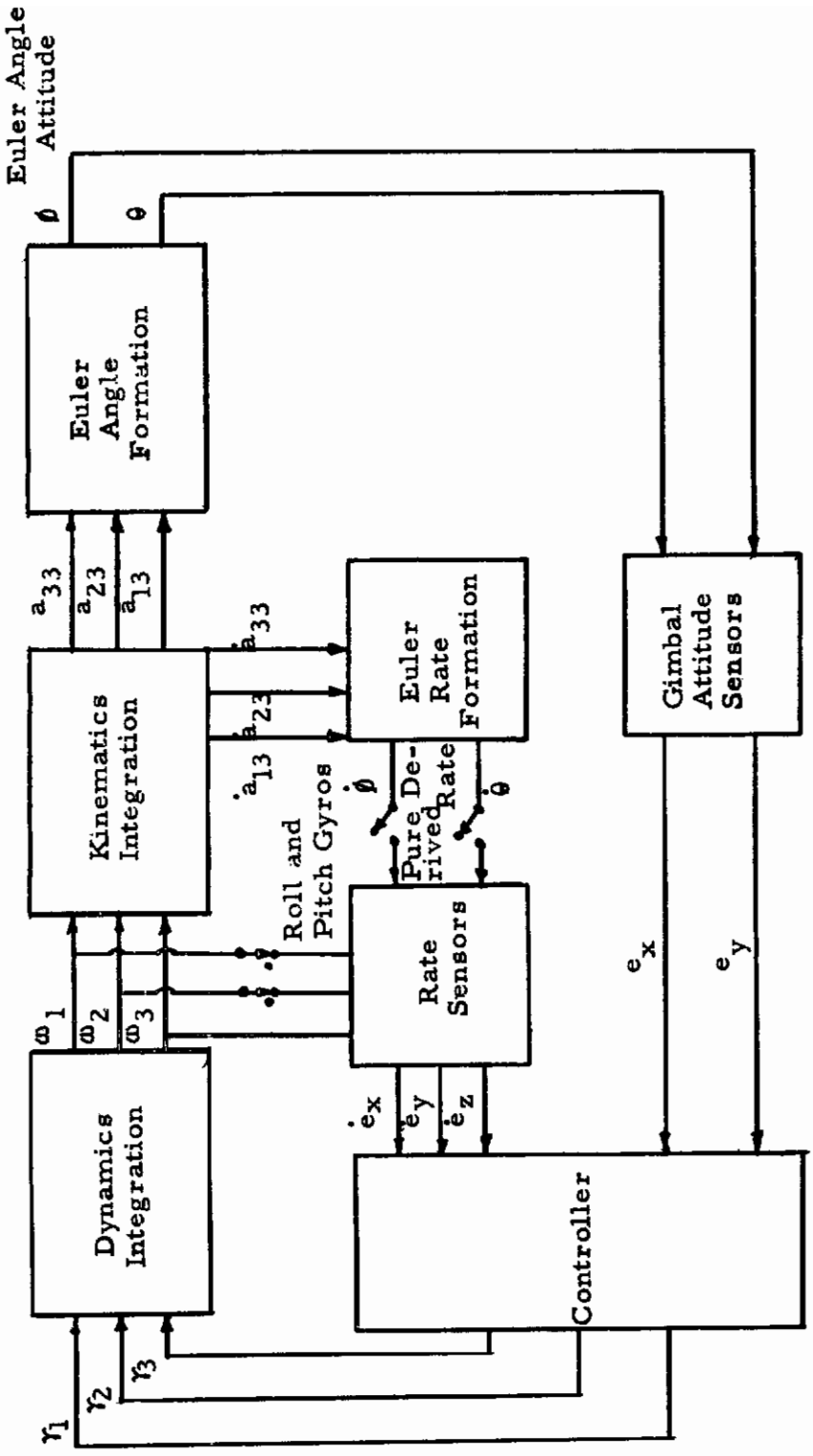

Figure B.2 Euler Angle Sensors Simulation Block Diagram

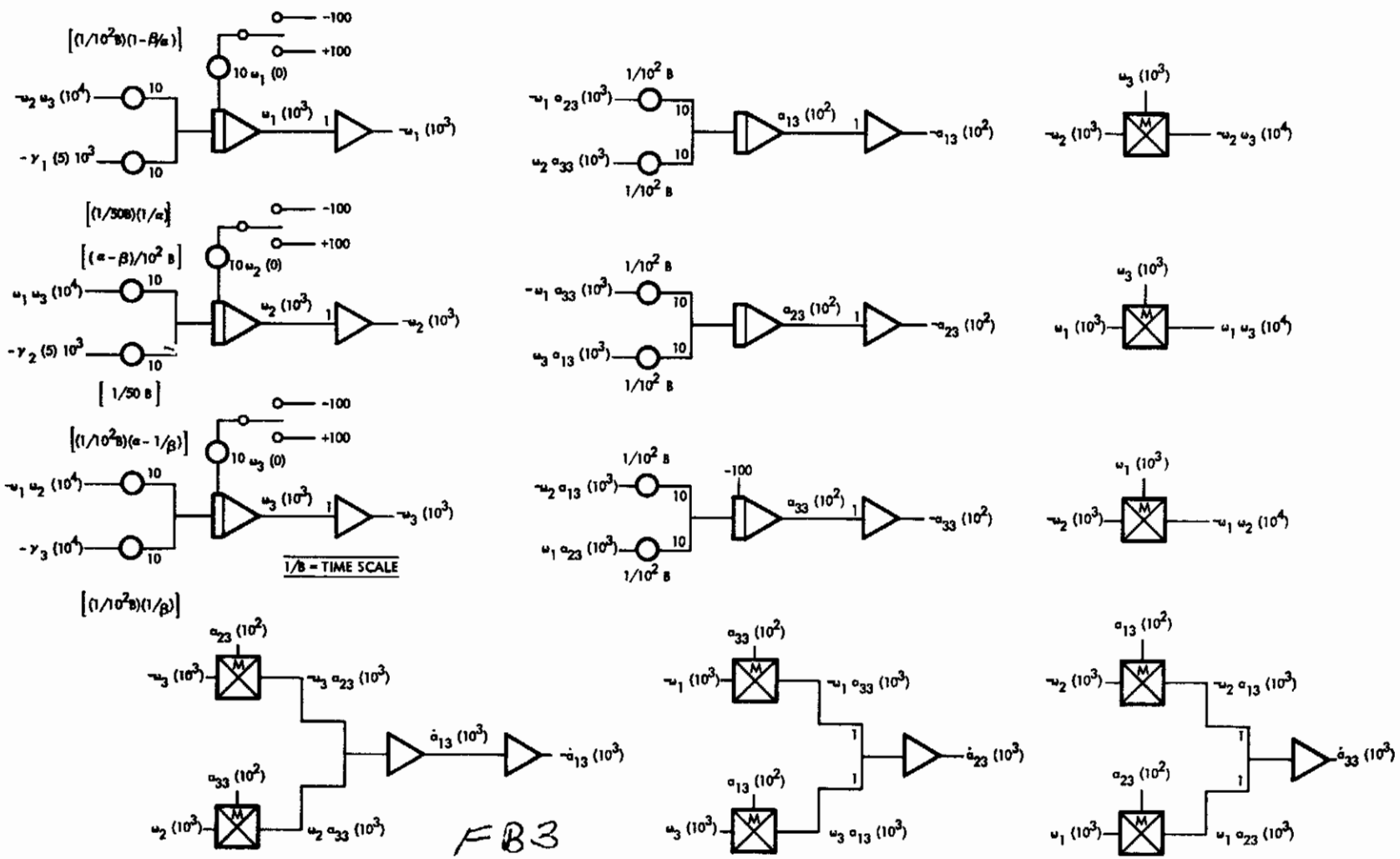

Figure B-3 Simulation Diagram Dynamics and Kinematics

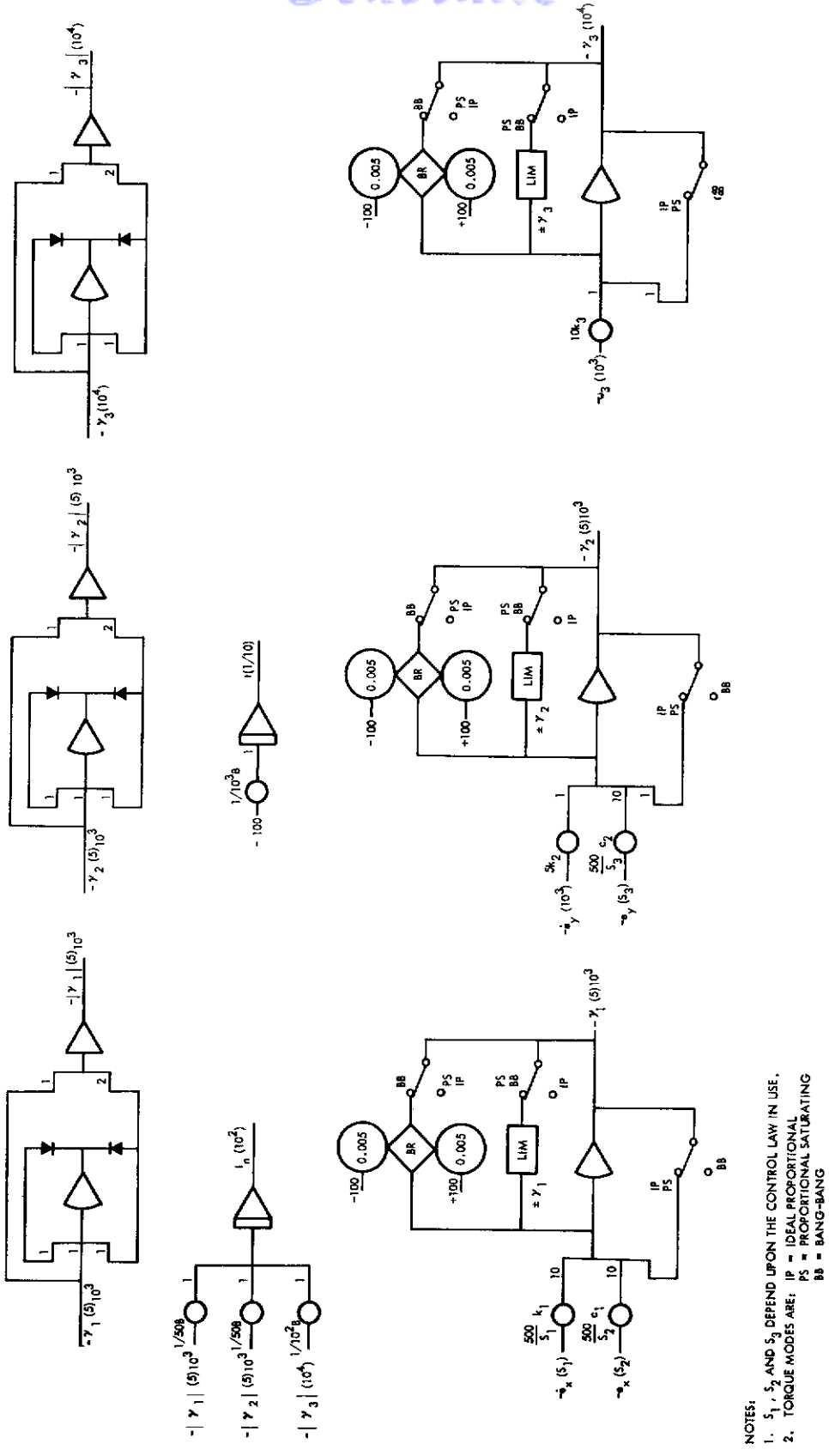

Figure B-4 Simulation Diagram Control Accelerations and Error Criteria

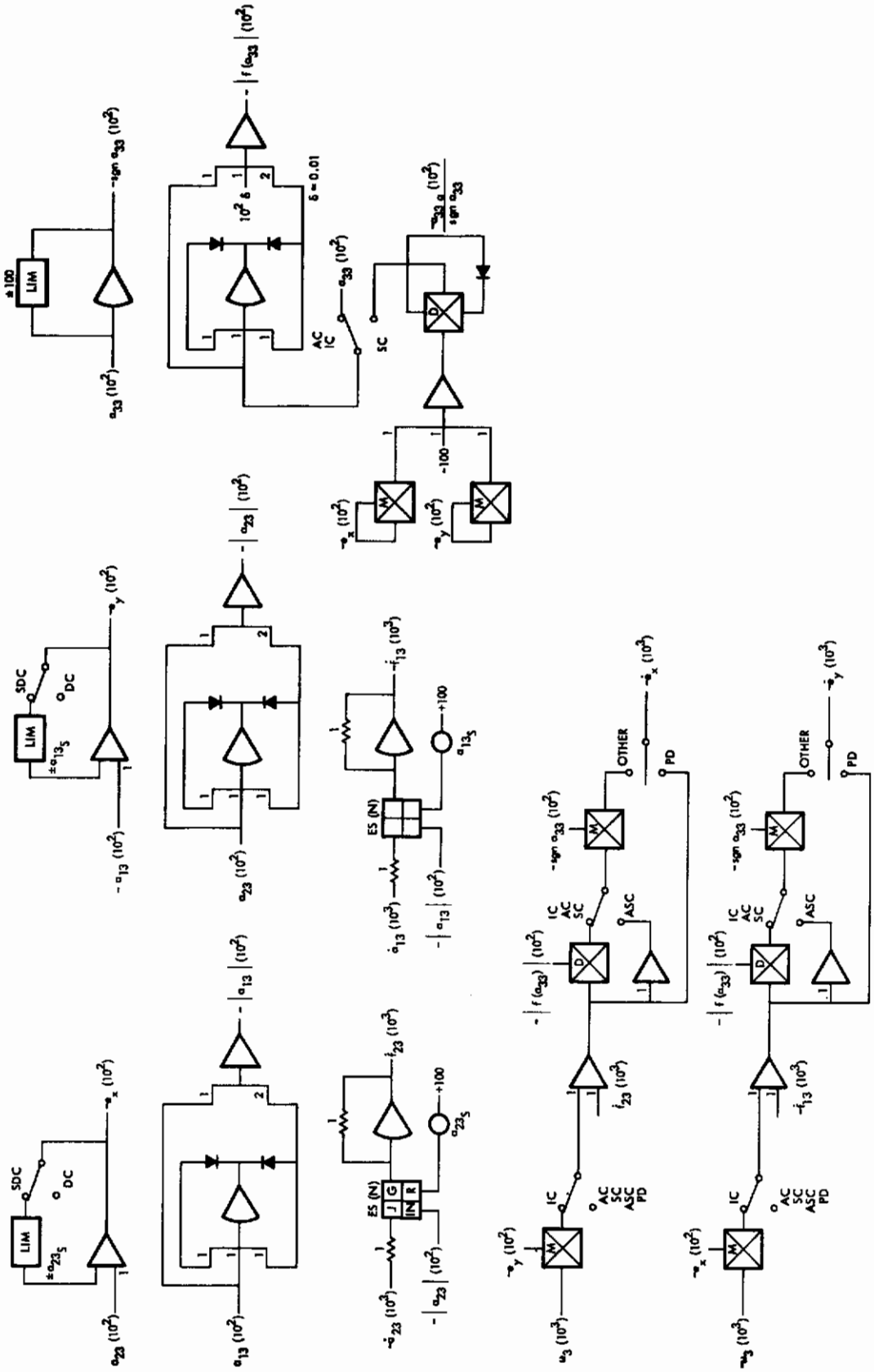

Figure B-5 Simulation Diagram Direction Cosine Attitude Sensing Control Laws

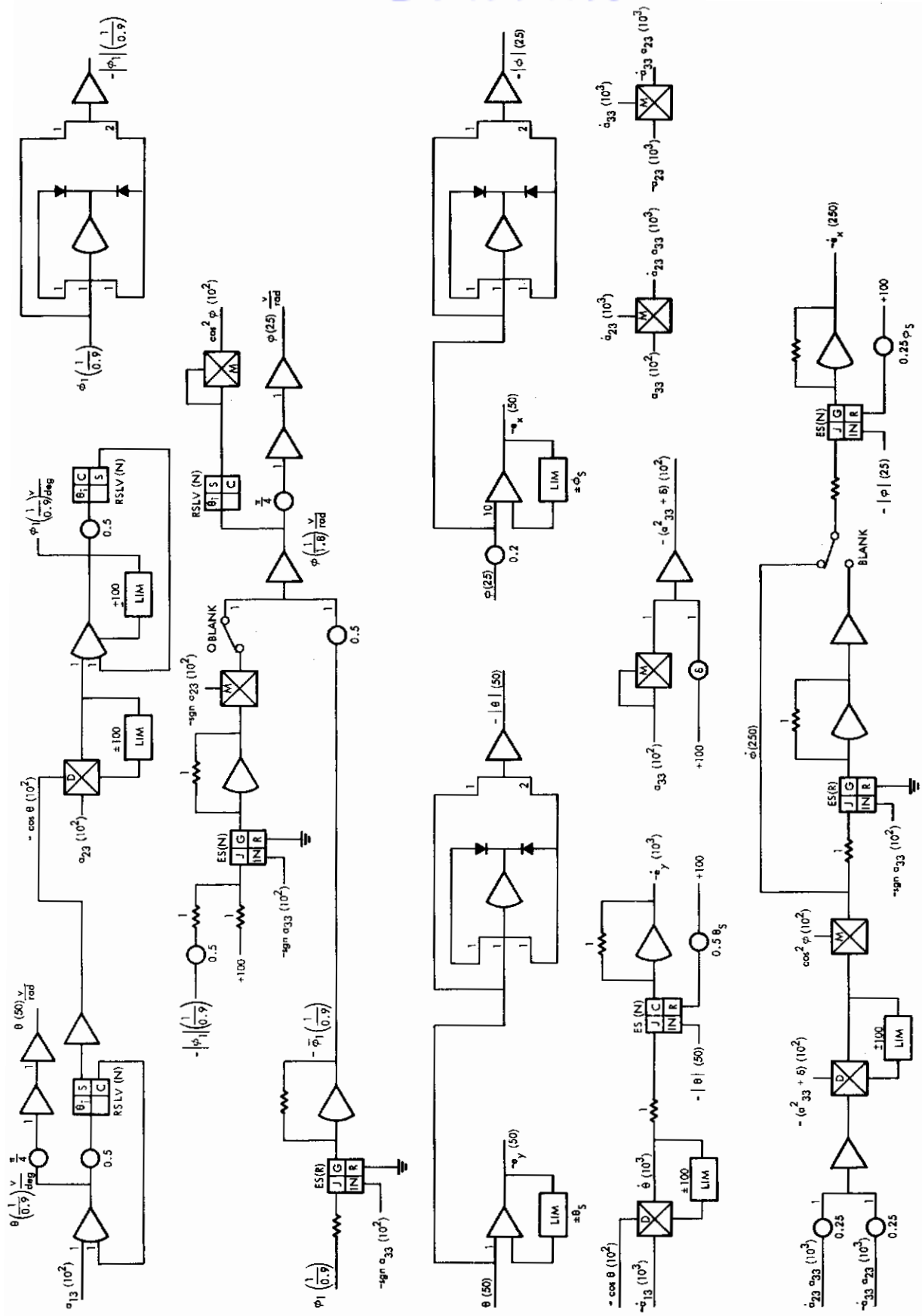

Figure B-6 Simulation Diagram Euler Angle Attitude Sensing Control Laws

APPENDIX C

COMPUTER MECHANIZATION OF OPTIMIZATION STUDY

C.1 Introduction

This appendix describes the programming details of the parameter optimization study using a hybrid computer. The hybrid programming can be divided into the following major subgroups:

a) Initial condition space search.

b) Optimization algorithms.

   1) Relaxation local search.
   2) Random local and global searches.
   3) Steep descent.
   4) Minimum-maximum thrust level criterion.

c) Analog simulation.

Each of the subprograms is self-contained with supplementary initialization and input/output routines. In this manner, they can function independently, although normal operation links these subgroups in order to provide a smooth operation. The following presents flow charts of the subprograms and brief explanatory remarks where needed.

C.2 Initial Condition Space Search

This program provides a means of selecting initial conditions for the analog computer. In order to provide sufficient memory for the larger initial condition sets (the largest consists of 1750 initial condition sets) in a computer with only 4,000 memory cells, a certain amount of storage location coding is required. A given set of initial conditions

will be used in the analog simulation to compute an $F_{I.C.}$ (optimization criterion) to be associated with this I.C. set. As many as 1750 $F_{I.C.}$'s are required to be stored. The storage location of the $F_{I.C.}$ is used to describe its associated initial condition set. Each storage location is described by 6 digits. The digits correspond to the following initial conditions: 1st digit = ω_1(I.C.), 2nd digit = ω_2, 3rd digit = ω_3, 4th digit = a_{13}, 5th digit = a_{23}, 6th digit = a_{33}.

One of five different integers can be assigned each digit. This correspondence is:

1) For first 3 digits; integer "1" = + maximum rate
integer "2" = - maximum rate
integer "3" = zero
integer "4" = + average rate
integer "5" = - average rate

2) For last 3 digits: integer "1" = + 1
integer "2" = - 1
integer "3" = 0
integer "4" = $+\frac{1}{\sqrt{3}}$
integer "5" = $-\frac{1}{\sqrt{3}}$

In this manner, the initial condition set associated with a particular $F_{I.C.}$ is given by its location in the computer memory. The first three digits will be denoted by C_ω and the last by C_a.

C.2.1 Initial Condition Search Selection

The assignment of the initial conditions is governed by the keywords C_{ω} and Ca, which are processed in accordance with the "Search Selection Logic" to provide a series of sets of initial conditions.

The search Selection Logic consists of 17 series as follows:

Series		No. of I.C. Sets
1	Case 1 with nominal attitude	8
2	Case 2 with nominal attitude	27
3	Case 1 with minimum attitude	48
4	Case 2 with minimum attitude	162
5	Case 1 with maximum attitude	112
6	Case 2 with maximum attitude	378
7	Case 3 with nominal attitude	8
8	Case 4 with nominal attitude	27
9	Case 3 with minimum attitude	48
10	Case 4 with minimum attitude	162
11	Case 3 with maximum attitude	112
12	Case 4 with maximum attitude	378
13	Case 5 with nominal attitude	64
14	Case 6 with nominal attitude	125
15	Case 5 with minimum attitude	384
16	Case 6 with minimum attitude	750
17	Case 6 with maximum attitude	1750

where

Case 1: all combinations of $\pm$ maximum value on each of the rates

Case 2: all combinations of $\pm$ maximum and zero values

Case 3: all combinations of $\pm$ minimum value only

Case 4: all combinations of $\pm$ minimum and zero value

Case 5: all combinations $\pm$ maximum and $\pm$ minimum values

Case 6: all combinations of $\pm$ maximum, zero and $\pm$ minimum values

Nominal attitude: $a_{13} = 0 \quad a_{23} = 0 \quad a_{33} = 1$

Minimum attitude: all possible combinations of $\pm$ 1 and 0 on each element in group 2

Maximum attitude: all possible combinations of $\pm$ 1, 0 $\pm 1/\sqrt{3}$

For example:

If series 2 is chosen, the following keywords are evident:

Cω ranging from 111 through 333

Ca = 331

C.2.2 Process Procedure

For each set of initial conditions, there is a corresponding criterion function "$F_{I.C.}$". The criterion functions for the entire series are stored in the memory which can then be processed in one of the following procedures:

Procedure 1

Sort the F's in descending order and select the first q sets of initial conditions corresponding to the F's.

Procedure 2

Compute an average value $\bar{F}$ of the entire series and select q cases closest to $\bar{F}$.

Procedure 3

Subdivide the F's into quadrants corresponding to the initial conditions and select q worst cases in each quadrant where q is an arbitrary number of cases.

C.2.3 Summary

The initial condition space search subprogram logic flow is shown in Figures C.1 to C.5. The logic for all these figures have been described in the above sections. Figure C.5 gives the detailed interface between the digital search and analog simulation. This shows the error detection logic discussed in Section 6.3 of the report.

C.3 Parameter Optimization

The various optimization techniques employed by this study are listed as subprograms (1), (2), (3) and (4) where (1) relaxation, (2) random, (3) steep descent and (4) thrust level criterion. Detailed flow charts are shown in Figures C.6 to C.11. For clarification, the following general points are observed:

(1) Computation of Fi

For simplicity the detail of this subroutine is not shown. Except for the handling and initial condition and trial parameter, the analog mode control and status replies are identical to Figure C.4 and is discussed in Section 6.3 of the report.

For each set of trial parameters there are n sets of initial conditions. The criterion function (F_i) for the trial set (i) of parameters is:

$$F_i = \frac{\sum_{j=1}^{n} F_{ij}}{n}$$

where $n = 1, 2 \ldots 8$

j = jth set of initial conditions

(2) Linkage (Not shown in flow chart)

Linkages are provided between subprograms as mentioned before. They merelytransfer the results of one subprogram into the next or vice versa. This allows use of various combinations of local and global search.

(3) Criterion Function

Subprograms (1), (2), and (3), are designed for optimization of the following functions:

1 - minimum time

2 - minimum fuel

3 - minimum thrust

Item 3 required the additional programming of subprogram (4) which is shown in Figure C.11.

An additional, specific discussion of the optimization algorithms is presented below.

C.3.1 Relaxation Notes (See Figure C.6)

The basic logical flow is as follows:

(1) An initial parameter set is selected, all α_i' (i = 1, i max) are set equal to the initial parameter settings; F' is set equal to the criterion calculated; all relaxation counters (i and H) are initialized and the first parameter is ready to be relaxed. δ is set = - 1 if a function is minimized (+1 for maximization).

(2) $\alpha_i = \alpha_i' + K\, a^n \Delta\alpha_i$ (K = + 1, n = 0) is calculated, it is limited so the parameter bounds are not exceeded, a new F is calculated and $\Delta F = F' - F$ is calculated.

(3) If $\delta\Delta F - \Delta F_j$ min is positive, F is concluded significantly worse than F' and search in this direction is curtailed.

(4) If I is positive, no previous successes have been found and the program goes to (5) or (6).

(5) If K = +1, search has not been made in the opposite direction; search will then be made in opposite direction by setting K = -1 and returning to (2).

(6) If K = -1, search has been unsuccessful in both directions along α_i, a local optimum is assumed, the initial step size $\Delta\alpha_i$ is reduced for the next search and a new parameter is tried.

(7) If I is negative, a previous success has been found. The last success is assumed the local optimum, the sign of $\Delta\alpha_i$ is set so the next search begins in what is most likely the correct direction $\Delta\alpha_i$ is reduced, and the next parameter is searched.

(8) If $\delta\Delta F - \Delta F_1$ min is negative and $\delta\Delta F + \Delta F_2$ min is positive, no significant change in F is assumed. If α_i is limited, control is transferred to (4) or (7)(depending on I). If α_i is not limited, the step size is increased by incrementing n and control is returned to step (2).

(9) If $\delta\Delta F - \Delta F_1$ min is negative and $\delta\Delta F + \Delta F_2$ min is negative, a significant improvement is assumed. If α_i is limited, note of this is printed out, the new α_i is assumed a local optimum and the next parameter is searched. If α_i is not limited, the estimated local optimum point (α_i'') is upgraded, the step size increased (n = n + 1) and control is returned to step (2).

(10) After all parameters have been relaxed, the H counter is tested to see if any successes have been found. If $H \neq 0$, at least one success has been found and control returns to step (1). If H = 0, no successes have been found and the optimum is assumed found.

C.3.2 Absolutely Biased Random Local Search Notes (See Figure C.7)

(1) As portions of this algorithm will be used in global search, the appropriate flags and exits are set.

(2) The initial guess parameter set is chosen, α_i' ($i = 1, i_{max}$) set equal to these parameters, an F is computed and F' is set = F.

(3) The noise generator is sampled i_{max} times and a trial step $\Delta\alpha_i$ is applied to each parameter direction (modified by preset variances M_i). These $\Delta\alpha_i$ are limited between upper and lower bounds.

(4) $\alpha_i = \alpha_i' + K\Delta\alpha_i$ ($K = +1$) is computed and bounded for each i.

(5) F and $\Delta F = F' - F$ are computed.

(6) If $\delta\Delta F - \Delta F_1$ min is positive, a significant failure is assumed and control goes to (7) or (8).

(7) If $K = +1$, the opposite direction has not been searched and will be by returning to step (4) with K set = -1 (a new noise sample is not made).

(8) If $K = -1$, the number of paired failures is counted ($S = S + 2$).

(9) If $S > M$, a local optimum is assumed found and the program exits to the global routine.

(10) If $S \leq M_1$, a new trial is attempted by going to step (3).

(11) If $\delta\Delta F - \Delta F_1$ min is negative and $\delta\Delta F + \Delta F_2$ min is positive, no significant change is assumed and the fact that a non-success has occurred is recorded by incrementing $S = S + 1$ and going to step (9) or (10) as a function of what S is.

(12) If $\delta\Delta F - \Delta F_1$ min and $\delta\Delta F + \Delta F_2$ min are negative, a success is assumed. All α_i" are updated ($\alpha_i' = \alpha_i$) and $F' = F$. Another step in the same direction is attempted by returning to step (3).

C.3.3 Global Random Search Notes (See Figures C.7 and C.8)

The global search uses the identical noise sampling as the local random. The primary differences are: (1) There is no biasing. This

implies that only a significant improvement test is required (in any other case, the variance is changed, a counter is incremented and another sample is made). (2) If an improvement is found, the global exits to a local search.

C.3.4 Steep Descent Local Search Notes (See Figures C.9 and C.10)

The basic logic flow is as follows.

Direction Search and Normalization (Figure C.9)

(1) The initial parameters are given, α_i' and F' are computed and the various counters and flags (such as Z_1 and Z_2) are initialized. Search begins with the first parameter ($i = 1$).

(2) $\alpha_i = \alpha_i' + ab\Delta\alpha_i$ is computed ($a = b = +1$) and bounded. F and $\Delta F = F' - F$ are computed.

(3) If $\delta\Delta F - \Delta F_1$ min is negative, a significant improvement has been found and a slope S_i is computed. If S_i is significant, set $\Delta\alpha_i = ab\Delta\alpha_i$; if not, set $\Delta\alpha_i = 0$. Control is transferred to step (7).

(4) If $\delta\Delta F - F_i$ min is positive, the limit is tested. If α_i has been limited, go to step (6); if not go to step (5).

(5) $\delta\Delta F + F_1$ min is tested. If negative, no significant change has been found, the step size is increased ($b = 2b$) and go back to (2). If positive, go to step (6).

(6) A is tested to see if the opposite direction has been searched. If A = + 1, it has not; A is set to = -1 and the opposite direction is searched by going to step (2). If A = -1, the opposite direction has been searched, concluding that the steep descent search should not go along α_i and therefore set $\Delta\alpha_i = 0$ and go to step (7).

(7) Repeat step (2) for $\omega_i = 1, i_{max}$ then proceed to step (8) or (9). If all $\Delta\alpha_i = 0$ ($C = i_{max}$), a local optimum has been found and stop.

(8) If normalization is used go directly to step search.

(9) If normalization is not used, $\Delta\alpha_i$ are set equal to the gradient of F in the parameter space (steepest descent) and go to step search.

Step Search (Figure C.10)

(1) A new $\bar{\alpha} = \sum_{i=1}^{i_{max}} (\alpha_i' + b\Delta\alpha_i)$ is computed and limited. F and ΔF are calculated (all done by logic of Figure C.9).

(2) If $\delta\Delta F - \Delta F_1$ min is negative, an improvement has been found. $\bar{\alpha}'$ and F' are updated, noting that an improvement has been made, enlarge the step (b = 2b), and return to (1).

(3) If $\delta\Delta F - \Delta F_1$ min is positive and $\delta\Delta F + \Delta F_2$ min is positive, a definite failure has been found; go to (4) or (5).

(4) If a success has been found along this direction (Z = -1), return to direction search looking for a new direction.

(5) If no success had been found ($Z_1 = 0$), check to see if a step giving no significant change in F had been found (check Z_2). If $Z_2 = -1$, stop, as previously, since b had increased and the next instruction is to decrease b. The operator must decide what to do. If $Z_2 = -1$, decrease the step size ($b = \frac{b}{2}$) and search again (return to step (1)).

(6) If $\delta\Delta F - \Delta F_1$ min is positive and $\delta\Delta F + \Delta F_2$ min is negative, no significant change is concluded, the step size is increased ($b = 2b$) and return to (1). If, however, $\bar{\alpha}$ has a limited parameter, chances are that this strategy will do no good and control transfers to step (4) or (5).

C.4 Analog Simulation

A discussion of the equations simulated is presented in Section 6.3 of the report. These equations are simulated on a Beckman analog computer. The patch diagrams are shown in Figures C.12, C.13 and C.14. Figure C.12 gives the dynamics and kinematics. Figure C.13 gives the control laws. Figure C.14 gives the optimization and end-of-run criterion.

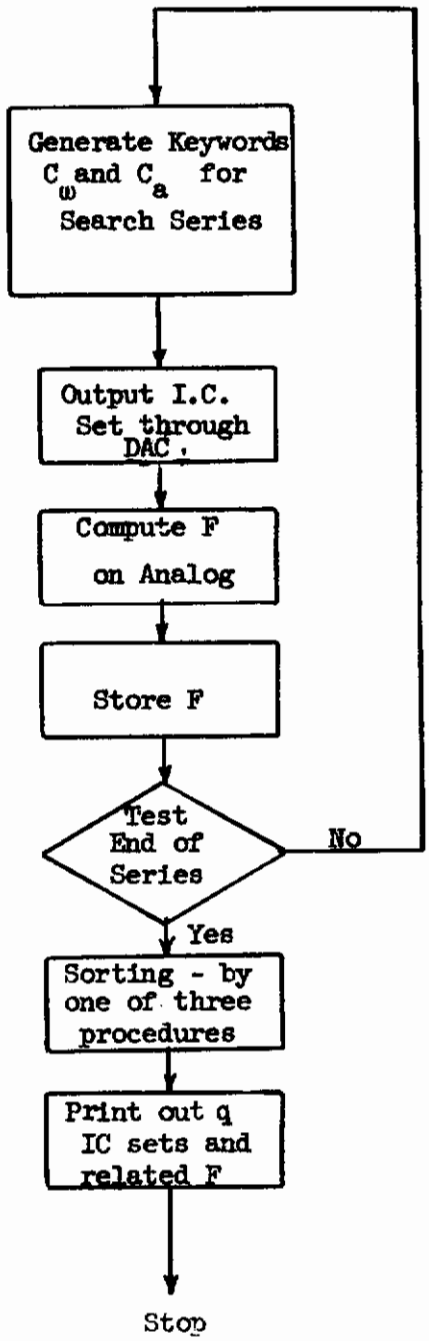

Figure C.1 Master Logic For Space Search

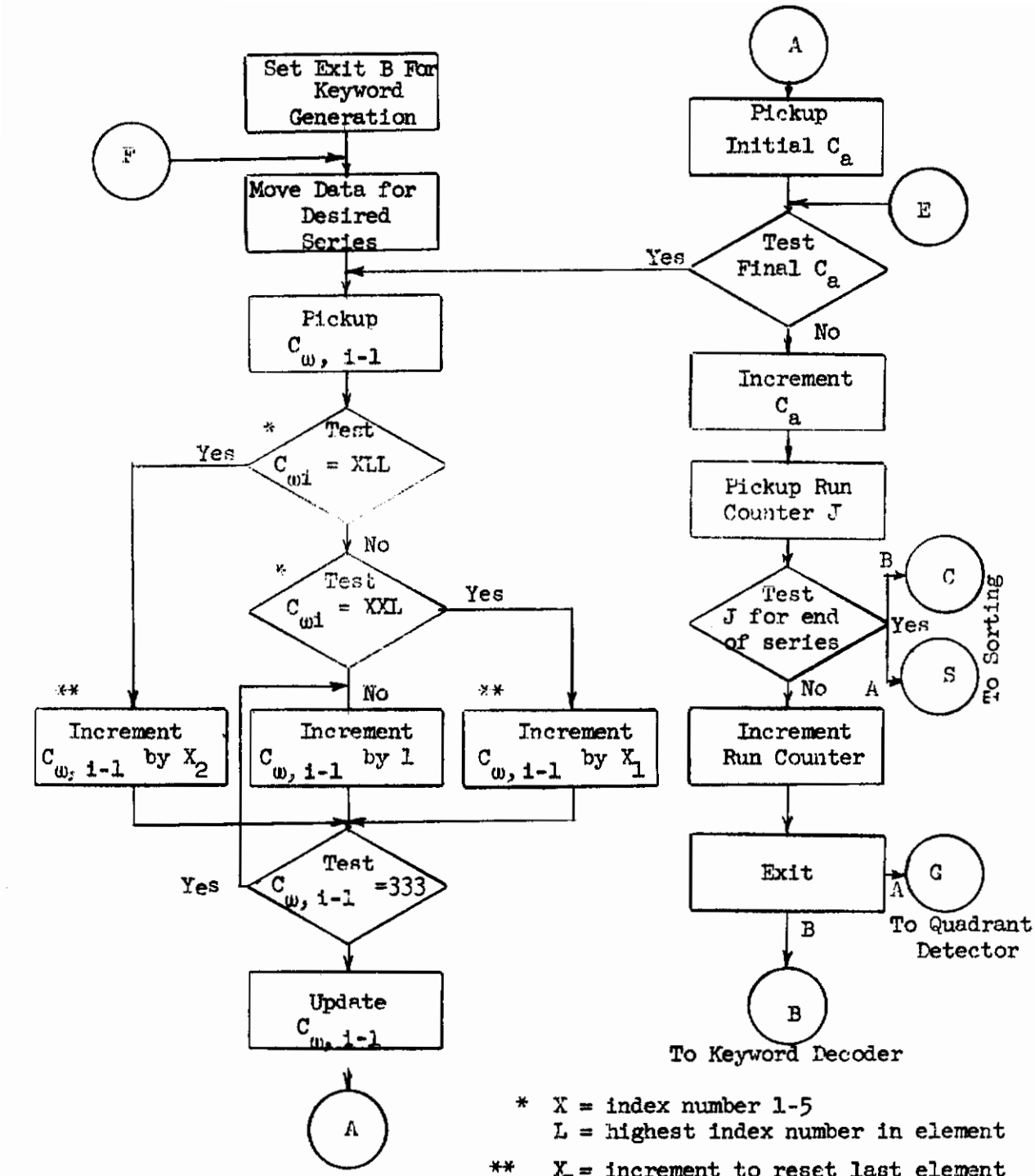

Figure C.2 Space Search Keyword Generation Subroutine

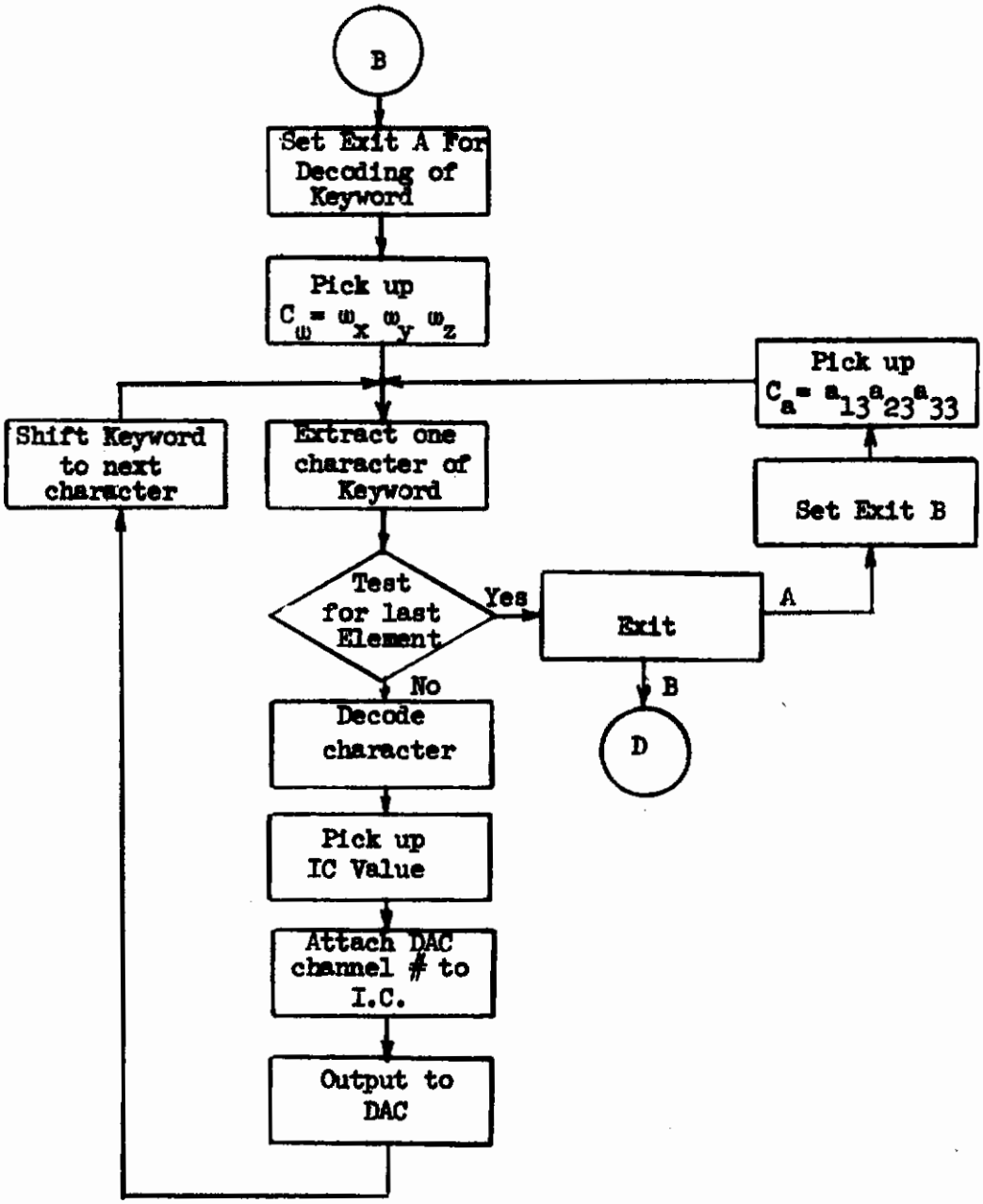

Figure C.3 Keyword Decoding Subroutine

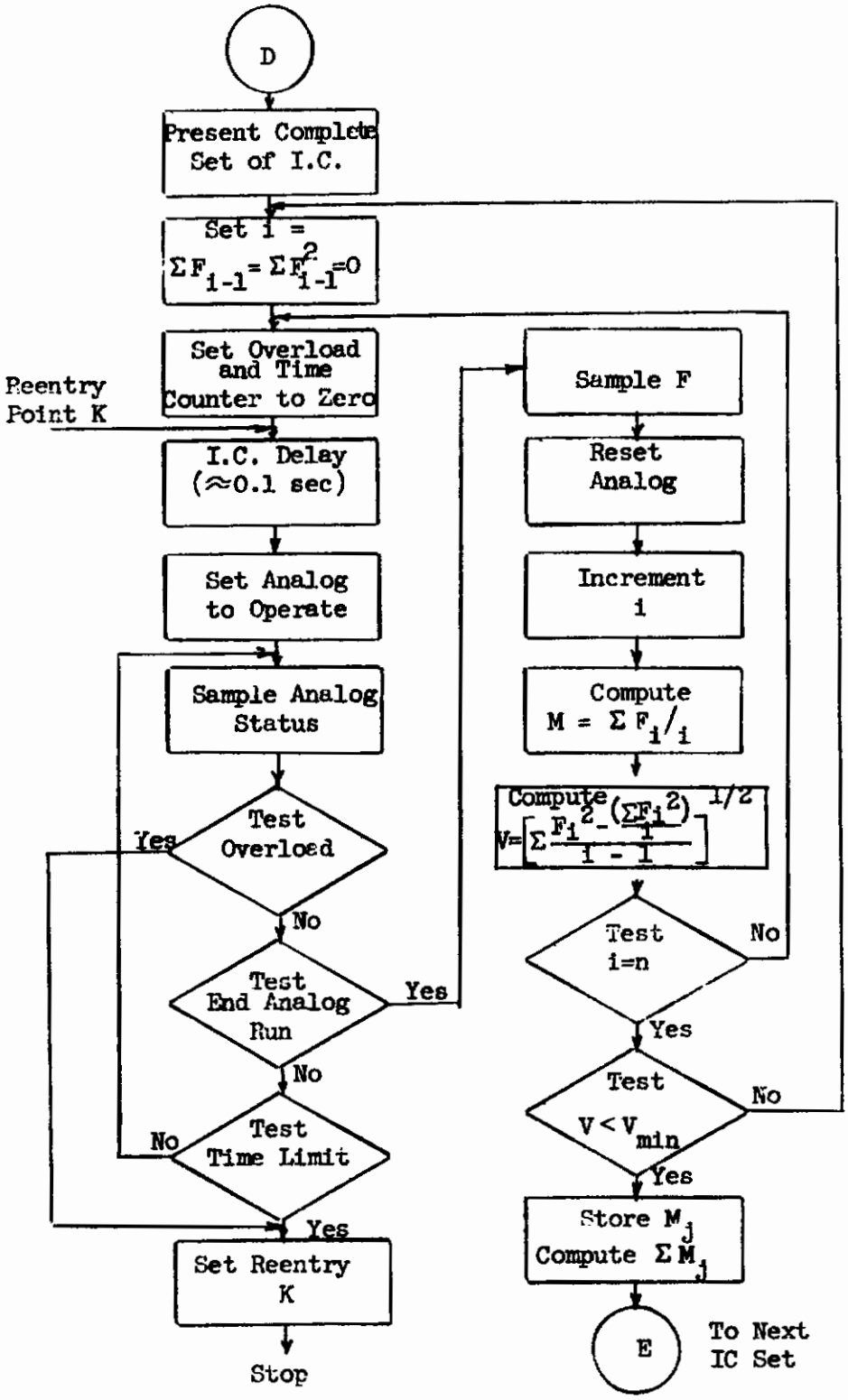

Figure C.4 Space Search Analog Control and Status

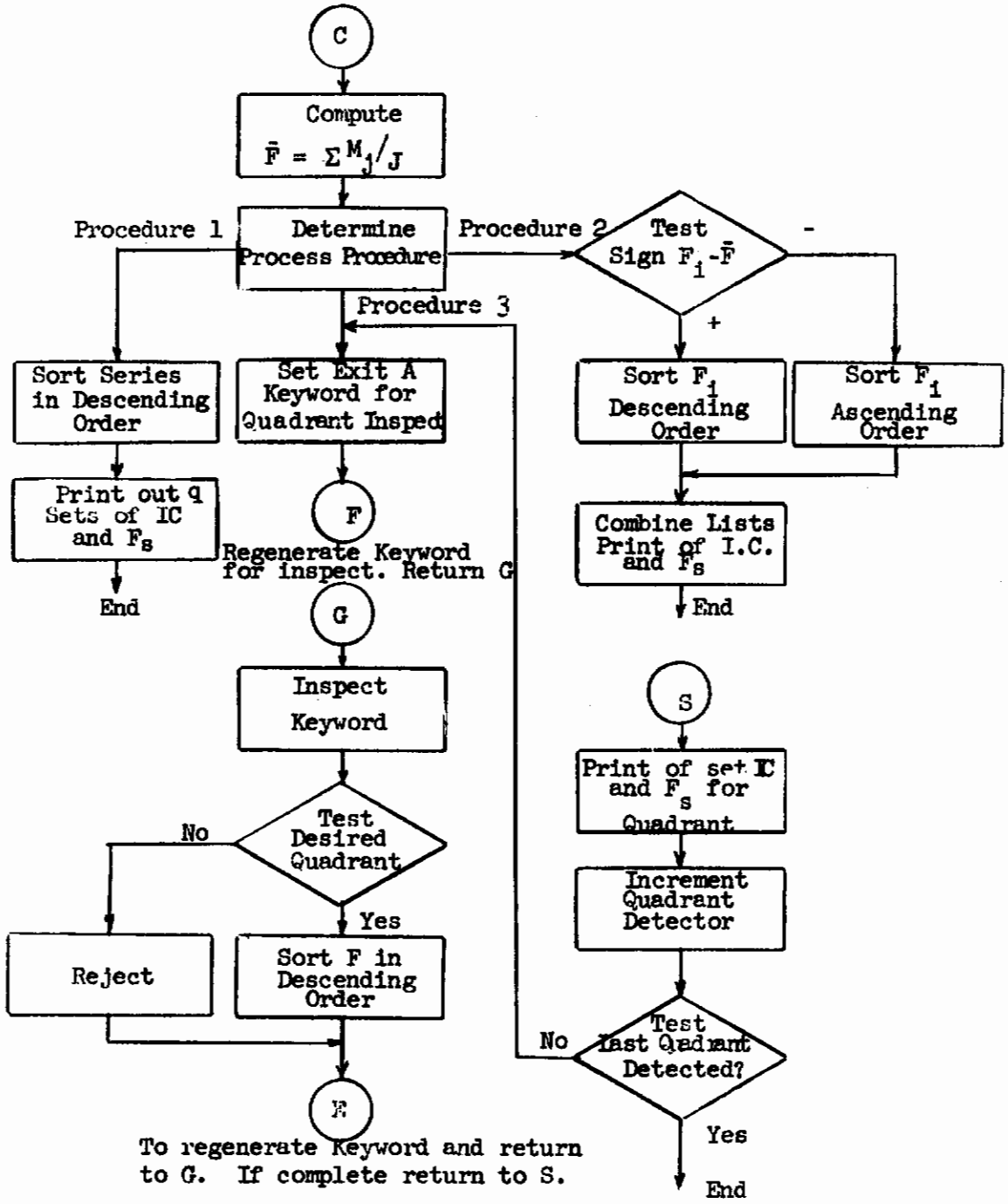

Figure C.5 Space Search - Sorting Subroutine

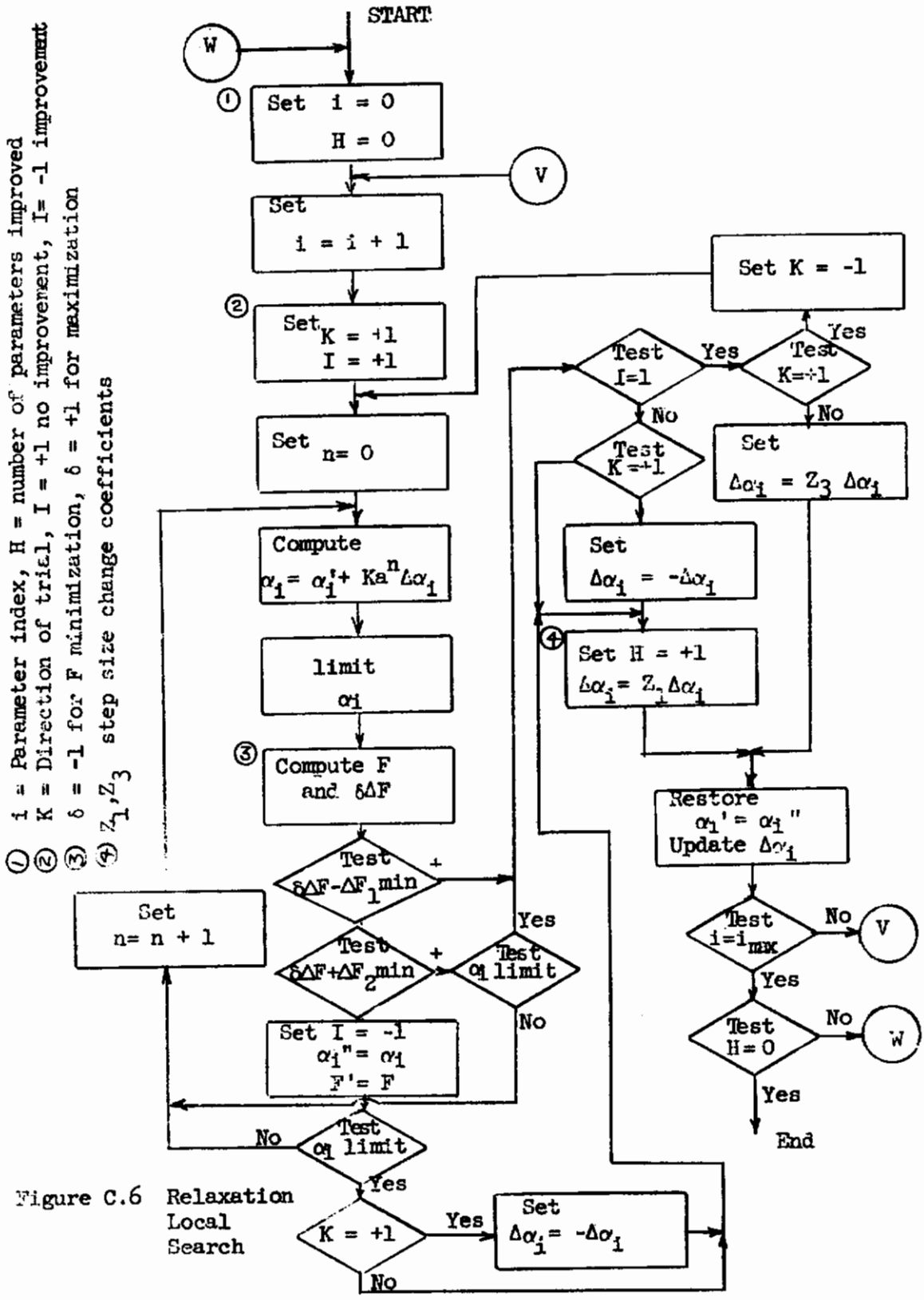

Figure C.6 Relaxation Local Search

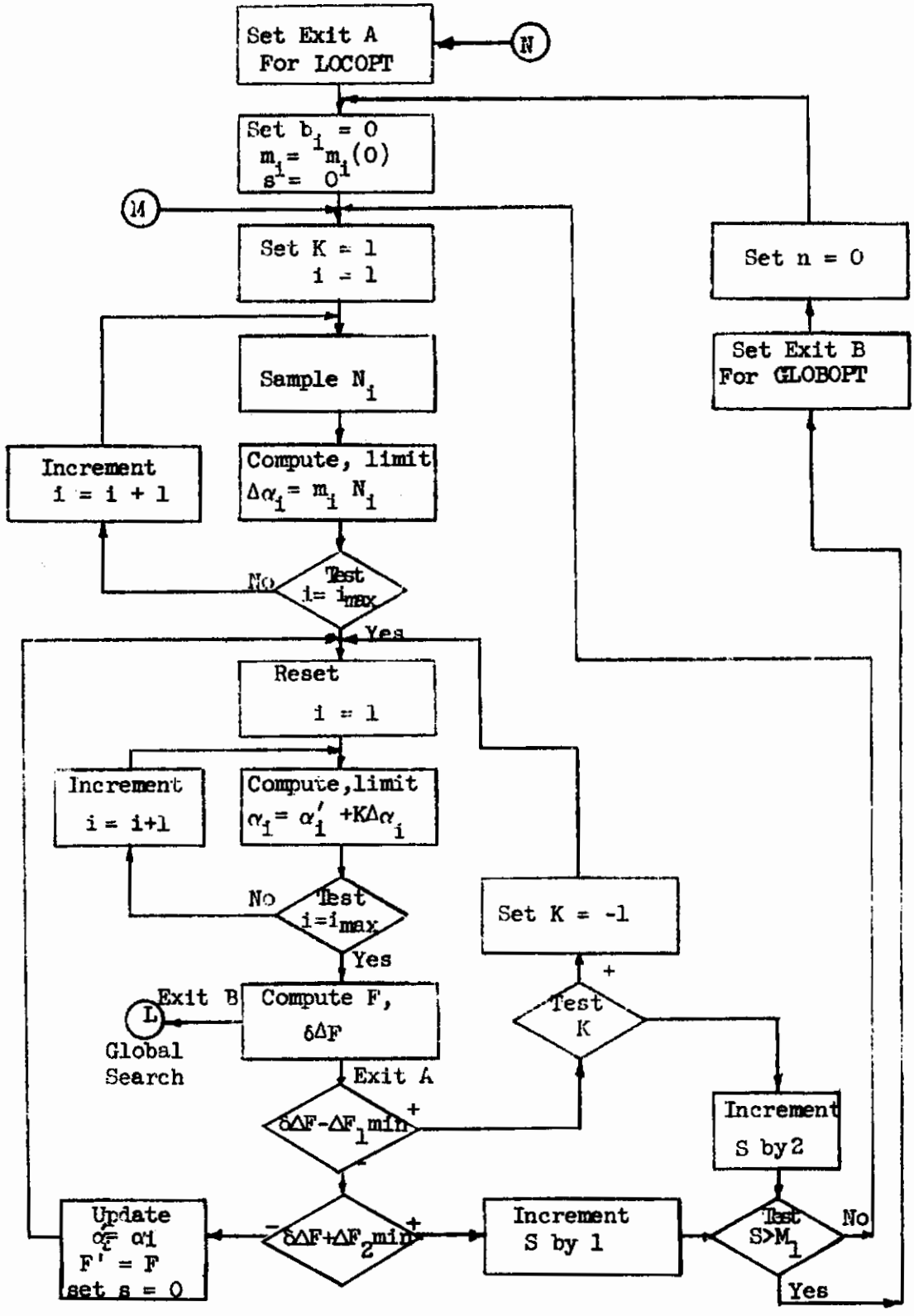

Figure C.7 Absolutely Biased Local Random Search

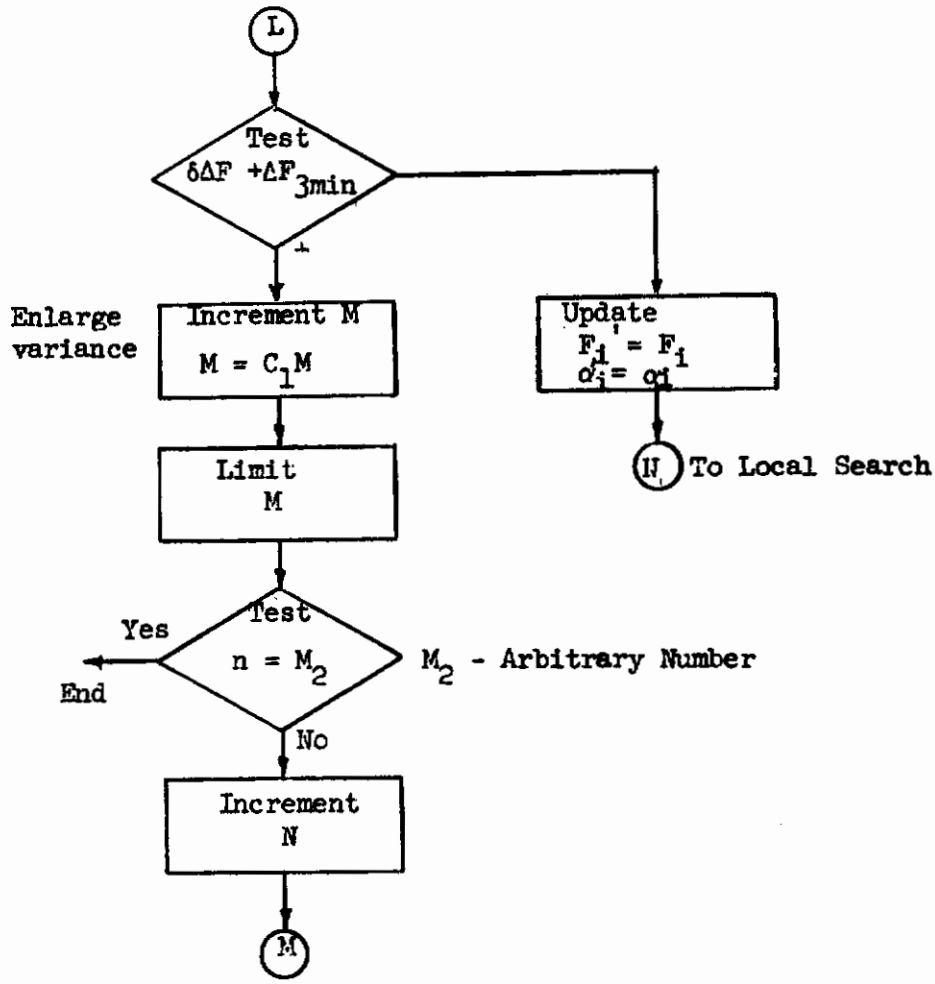

Figure C.8 Random Global Search

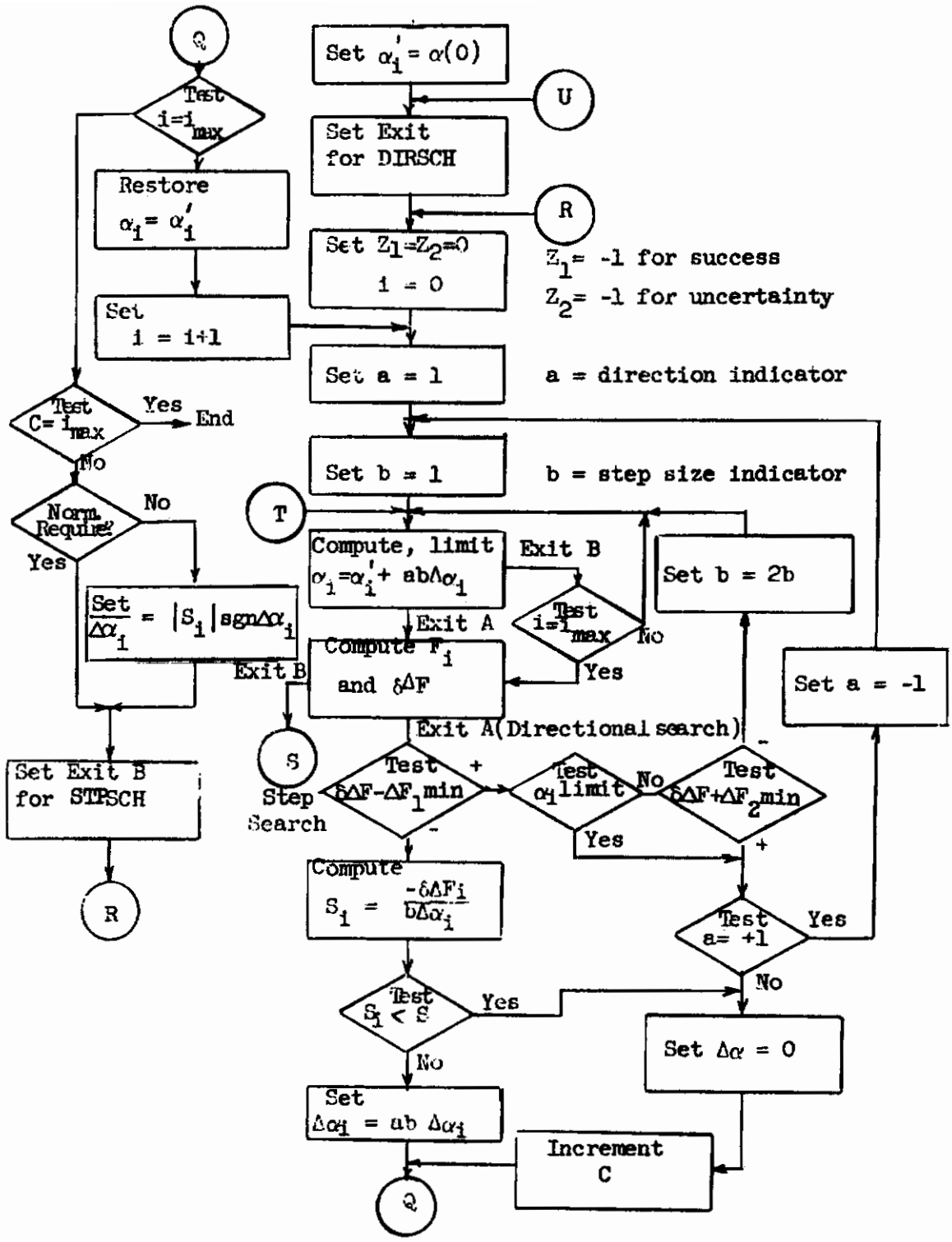

Figure C.9 Steep Descent Directional Local Search

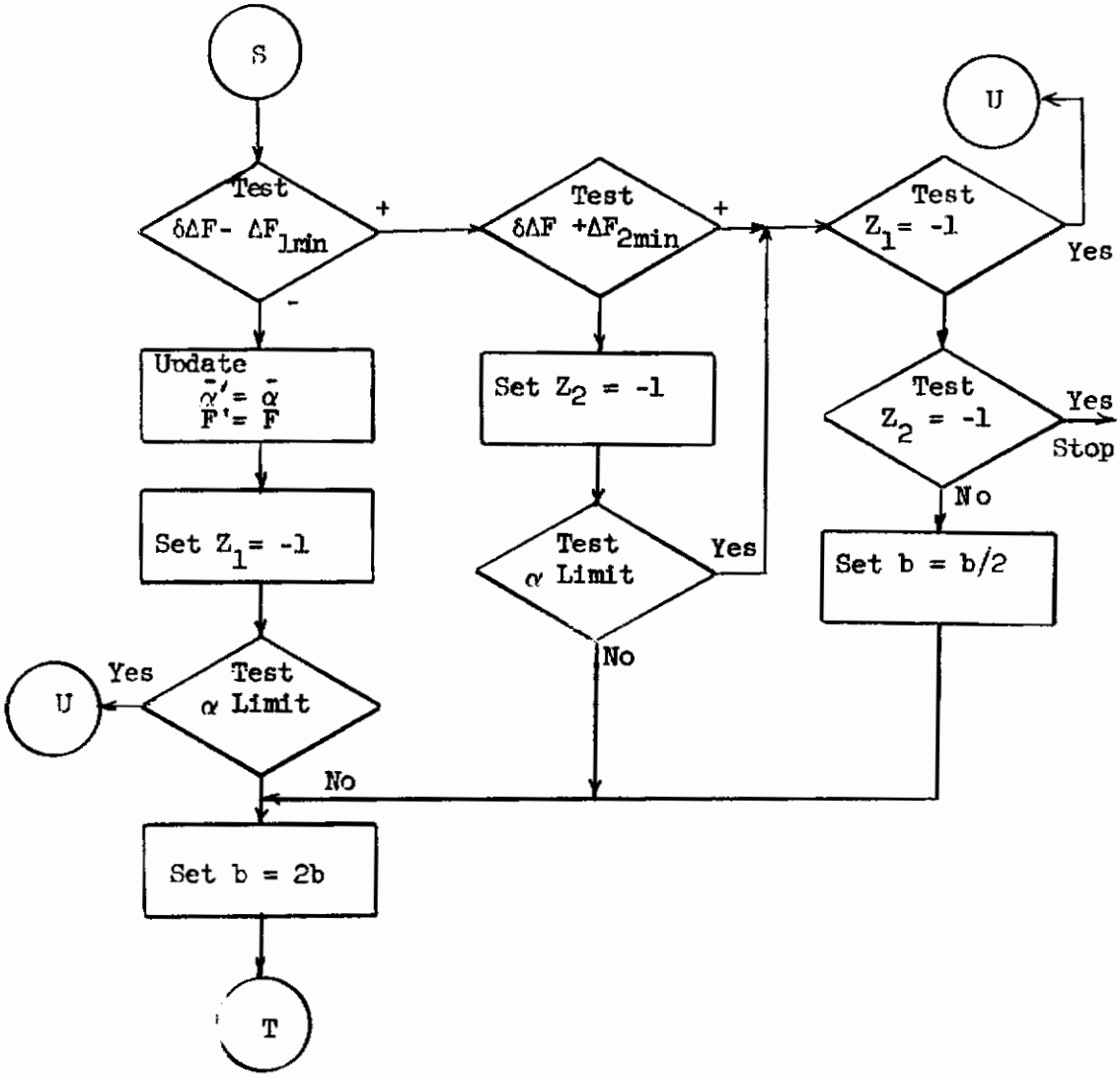

Figure C.10 Steep Descent Step Search
Portion of Local Search

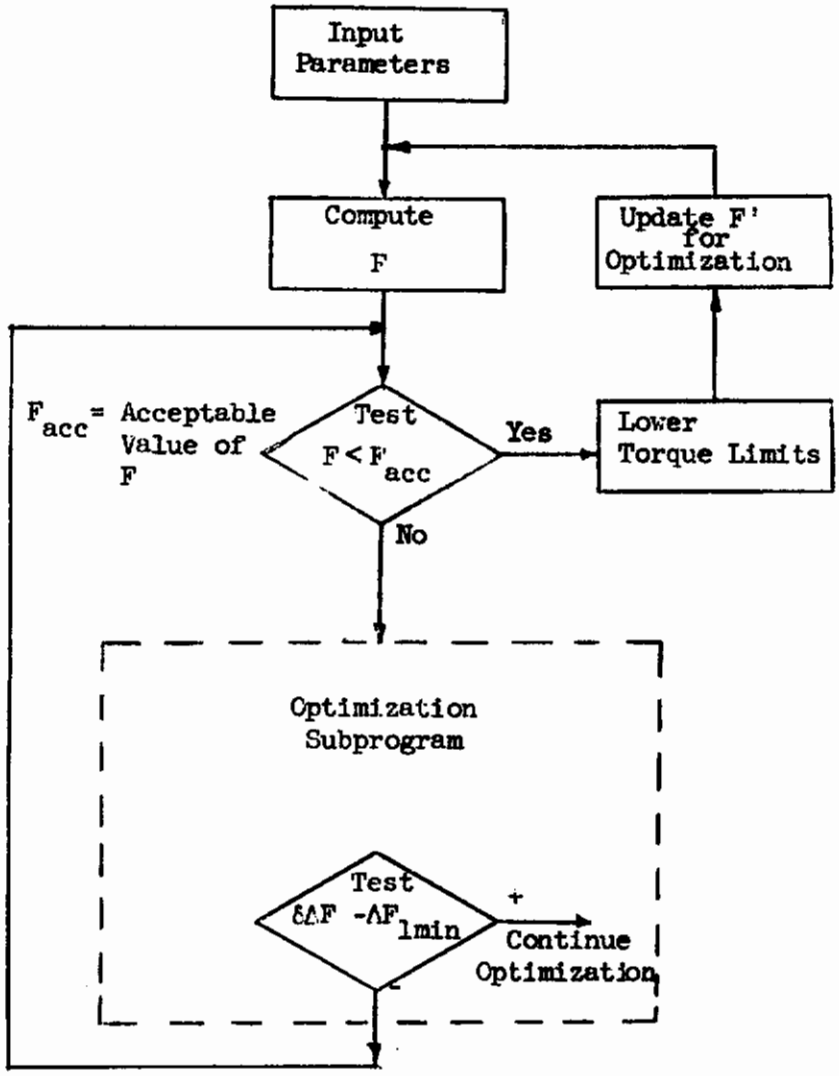

Figure C.11 Minimum Torque Modifications

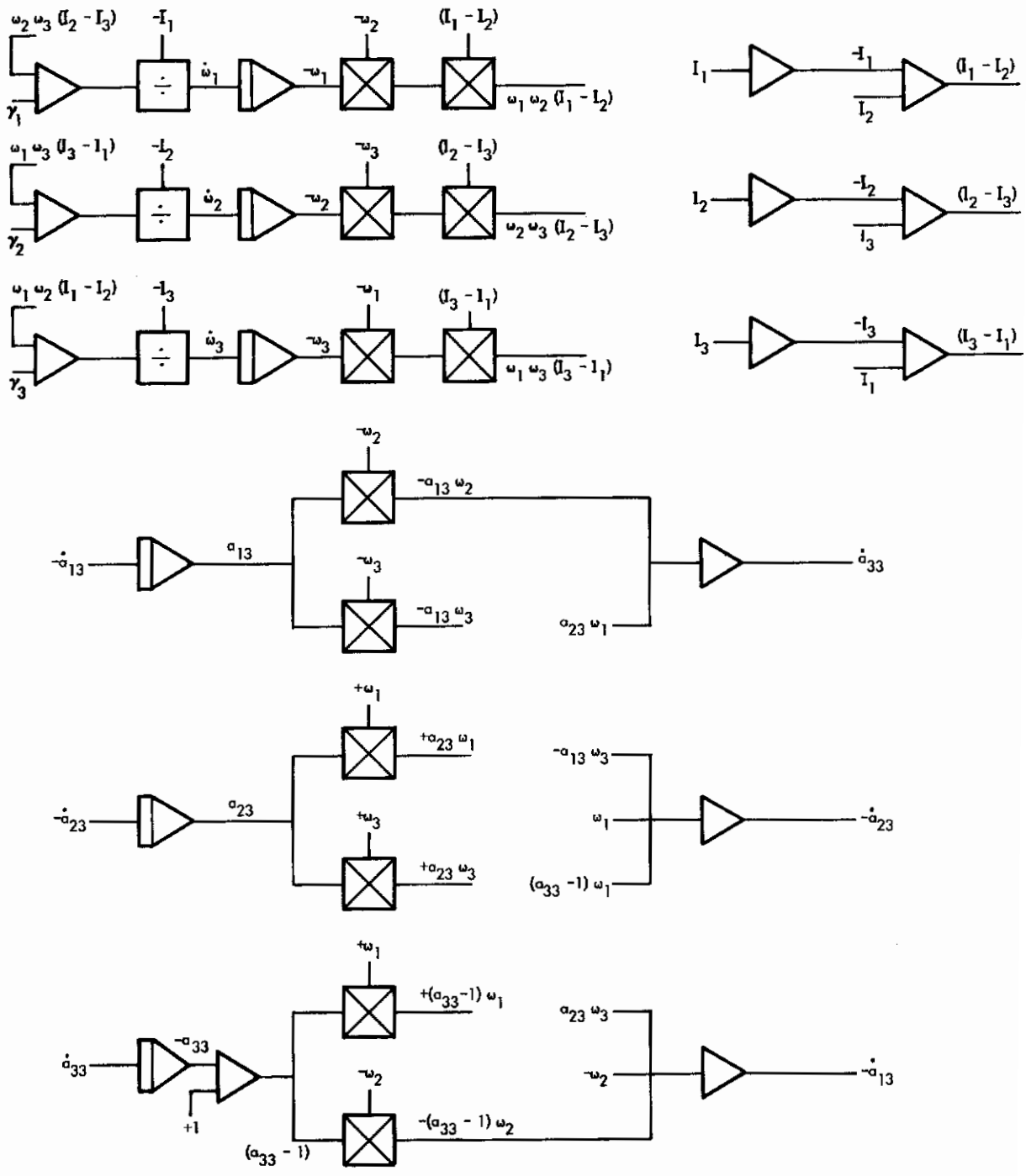

Figure C.12 Dynamics and Kinematics Simulation

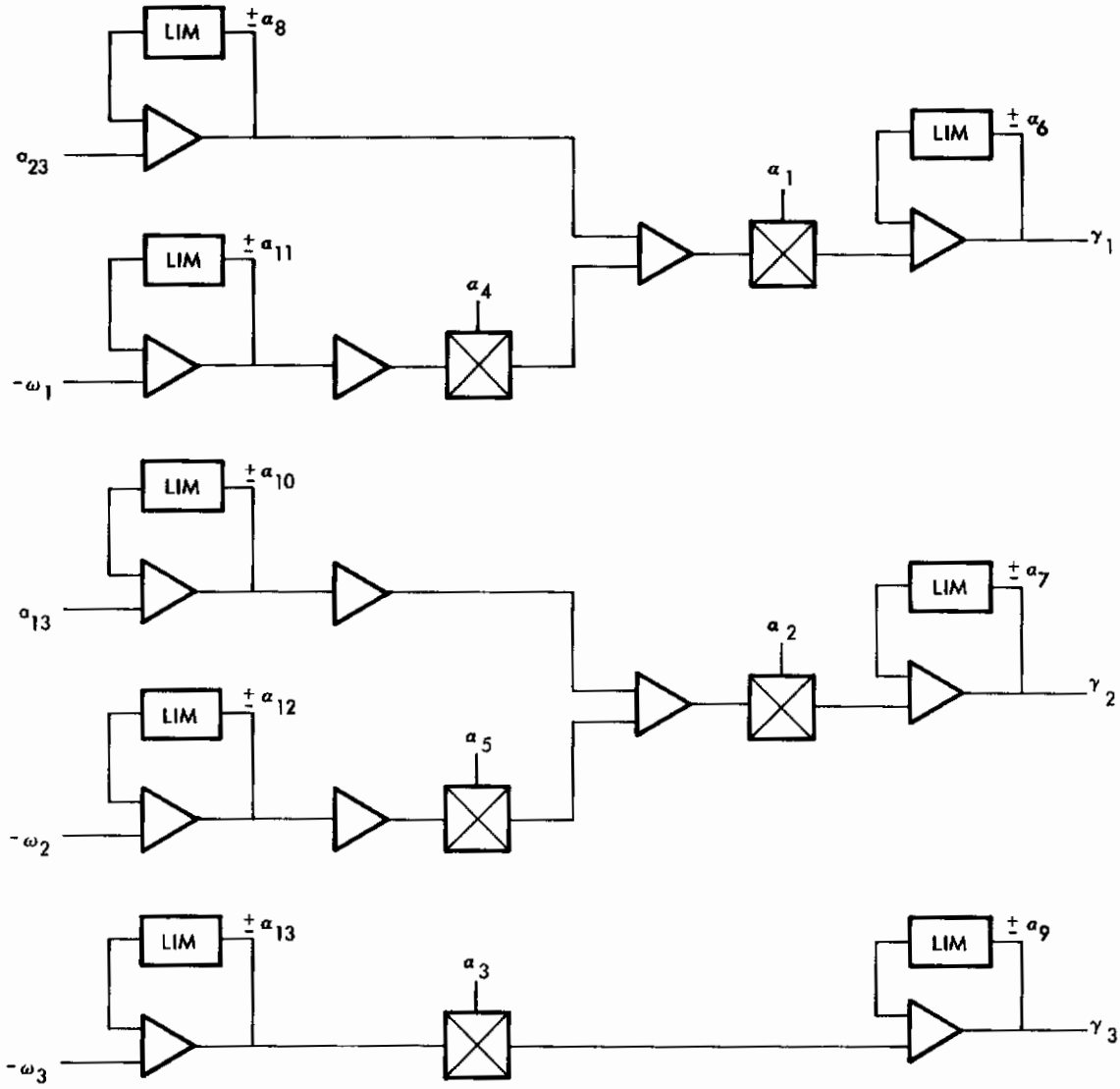

Figure C.13 Control Law Simulation

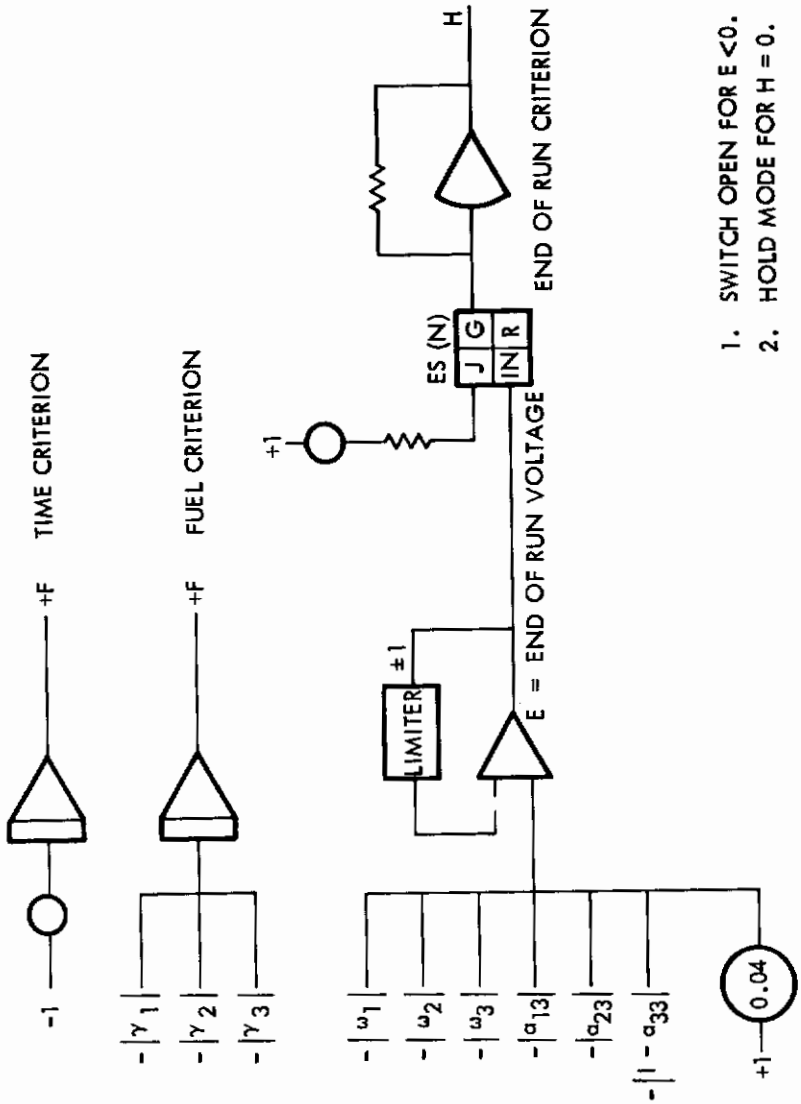

Figure C.14 Criteria Simulation

APPENDIX D

DESCRIPTION OF DIGITAL PROGRAM FOR STABILITY STUDIES

The computer programming philosophy has been briefly outlined in Section VII. This appendix presents the detailed flow diagrams along with a short description of the program itself.

The computer flow diagrams, Figures D.1 and D.2 will be explained making use of Figure D.3, an illustration of the "cube" at some intermediate point. Assume the computer is operating on the Z_1 axis (state S = 1), attempting to insert cube #1 based upon its estimate of $Z_{1,5}$, namely ZT_1.* In this case $I_1 = 4$, $I_2 = 1$, and $I_3 = 1$. This new cycle begins at point 100 in Figure D.1. One is put into $U_S = U_1$ (to be explained later), $Z_{S,I_S} = Z_{1,I_1} = Z_{1,4}$ is put into $Z_S = Z_1$, the Z_1 input of the polynomial evaluation portion of the program. One is also put into J, K, L and M. Here J and K are floating indices which identify which of the 9 possible cubes along the surface $Z_1 = Z_{1,4}$ is being considered. J in this case represents the index along the Z_2 axis and K along the Z_3 axis. In general, J is the index along the $Z_{\overline{S+1}}$ axis and K that along the $Z_{\overline{S+2}}$ axis where,

$$\overline{S} = \begin{cases} S \text{ if } S-3 \leq 0 \\ S-3 \text{ if } S-3 > 0 \end{cases}$$

M represents a polynomial index that identifies which of seven polynomials is being evaluated in order to form R; the polynomials

* ZT_1 differs from $Z_{1,5}$ in that ZT_1 is a trial value for $Z_{1,5}$ that must be evaluated over the entire Z_1 face of the cube. $Z_{1,5}$ becomes equal to the minimum value of ZT_1 after the entire Z_1 face of the cube has been tested.

corresponding to $P(Z_1, Z_2, Z_3)$ and the positive and negative portions for each of the three polynomials $\partial P/\partial Z_S$ (S = 1, 2, 3). The coding is as follows:

M	Polynomial
1	$P(Z_1, Z_2, Z_3)$
2	$\partial P/\partial Z_1^+$
3	$\partial P/\partial Z_2^+$
4	$\partial P/\partial Z_3^+$
5	$\partial P/\partial Z_1^-$
6	$\partial P/\partial Z_2^-$
7	$\partial P/\partial Z_3^-$

Next in the diagram (Point 101) $Z_{\overline{S+2}} = Z_{3,1}$ is put into the Z_3 polynomial register. NF is set to zero (to be explained) and $Z_{2,1}$ goes into the Z_2 polynomial register. This completely identifies cube #1 of Figure D.3 and the polynomial computer evaluates and stores $P(Z_1, Z_2, Z_3)$. M is then indexed, and the computer repetitively cycled back to point 103 to compute and store $\partial P/\partial Z_1^+$, $\partial P/\partial Z_2^+$, and $\partial P/\partial Z_3^+$. At this point M = 5 and the inputs to Z_1, Z_2, and Z_3 are changed to their maximum values in cube #1 as required by the discussion centering around Equation (7.41). With these inputs, the remaining three polynomials are evaluated until M > 7 at which time the computation passes to the Evaluation Routine (Point 200). This routine computes R. At point 230 the routine checks to see if the analog of Equation (7.23) is satisfied. If not, ZT_1 is re-estimated and the polynomials 5-7 recomputed (polynomials 1-4 are not affected by the re-estimation). When an acceptable ZT_1 is found, the initial values are reinserted into the polynomial

registers and J indexed by one. This corresponds to the investigation of cube No. 2 of Figure A-3, since now $Z_{\overline{S+1},J} = Z_{2,2}$ is to be put into the Z_2 register. This entire procedure is then repeated for cube No. 2. If cube No. 2 should fail for the ZT_1 estimate, re-estimation takes place until an acceptable value is found. To simplify the overall figure, all previous cubes bordering on $Z_{1,4}$ (in this case only cube No. 1) are cut back to the same value by setting $Z_{S,I_S+1} = Z_{1,5}$ equal to ZT_1 whenever ZT_1 is reduced. Clearly, the previous cubes need not be re-checked since this is a conservative move.

The indexing along J continues until $J = I_{\overline{S+1}} = 3$, in which case J is reset to one and an increment taken along K, in this case the Z_3 axis. The same process is repeated until all 9 cubes have been fitted along the Z_1 face of the total cube. When this has been accomplished, I_1 is indexed by one (so that $I_1 = 5$). If I_1 has not exceeded IM* and $Z_{1,5}$ has not exceeded $Z_{1,f}$, the computer then estimates a value of ZT_1 to be used the next time indexing is to occur along the Z_1 axis (Point 300-302). In the event that $I_1 > IM$ or $Z_{1,5} > Z_{1,f}$, L_1 is changed from zero to one and estimation is ignored. At this point the computer tests whether or not Z_1, Z_2, and Z_3 have all exceeded their limits. If $\sum_{S=1}^{3} L_S < 3$, then clearly at least one axis still remains to be extended and S is indexed by 1 to $\overline{S+1}$. If the new value of L_S is still zero, Z_S still requires extension, and the computer cycles back to Point 100 in the flow diagram. Assuming all L_S are still zero, in our case the computer now indexes along the Z_2 axis, with the J index occurring along Z_3 and K along Z_1.

The above process is repeated until either the computer halts due to an apparent critical point in the polynomial's domain, as implied

---

*IM is the maximum number of increments to be taken along each axis, and $Z_{S,f}$ is the final value of interest in the S direction (S = 1, 2, 3). Each is specified as part of the input data to the routine.

by NF > NT in the re-estimator loop, or $\Sigma L_S = 3$ indicating that the axes need no longer be extended. The Evaluation Routine and the Estimation Routine (starting at Points 200 and 300 respectively) will now be explained in greater detail.

In the Evaluator (Figure D.2), the computer first forms $\frac{\partial F^+}{\partial Z_1} + \frac{\partial F^-}{\partial Z_1}$. If this result is positive, then according to the philosophy of Equation (7.17) it must be multiplied by either $(Z_{1,I_{S+1}} - Z_{1,I_S})$, $(Z_{1,J+1} - Z_{1,J})$, or $(Z_{1,K+1} - Z_{1,K})$, depending upon the system state, S, in order to form one of the terms in R. Lower bounds on the other two partials are formed in a similar way, and R is evaluated. R is then added to $P(Z_1, Z_2, Z_3)$ and the result stored for subsequent testing.

In the Evaluation Routine, $R + P(Z_1, Z_2, Z_3)$ is ratioed to $P(Z_1, Z_2, Z_3)$. A positive result indicates a successful test. In this event the ratio is compared to the value in U_S (S = 1, 2, 3), and replaces the latter if it is smaller. U_S represents a measure of how close the test has come to failing as J and K index over all their values, and will always be in the range $0 \leq U_S \leq 1$. The final value of U_S after the indexing (in J and K) is finished is then utilized by the Estimator in predicting the next incremental value along Z_S. If the test is successful, the computer is ready to index in J.

If the test fails, U_S is first reset to one, since the value in U_S is based upon an increment in Z_S which will now be reduced. A failure counter, NF, is indexed by one and compared to the maximum allowable number of failures, NT. If NT is not exceeded, re-estimation takes place. The re-estimation is based upon cutting the ΔZ_S increment in half whenever a test failure occurs. The number of re-estimations to be made (NT) is specified in the input data.

Finally, the Estimator element, starting at Point 300 in the flow diagram, will be described. As mentioned before, the estimation for a new Z_S increment is based upon U_S. Basically speaking, the new incremental estimation is taken to be some variable times the last previous estimation. Thus,

$$ZT_S - Z_{S,I_S} = A \left[Z_{S,I_S} - Z_{S,I_S-1} \right]$$

A U_S value near zero indicates a good guess was employed in using $Z_{S,I_S} - Z_{S,I_S-1}$ and retains approximately the same increment for the next expansion in the Z_S direction. If U_S is near one, A is increased, the increase depending upon the operator controlled sensitivity parameter k.

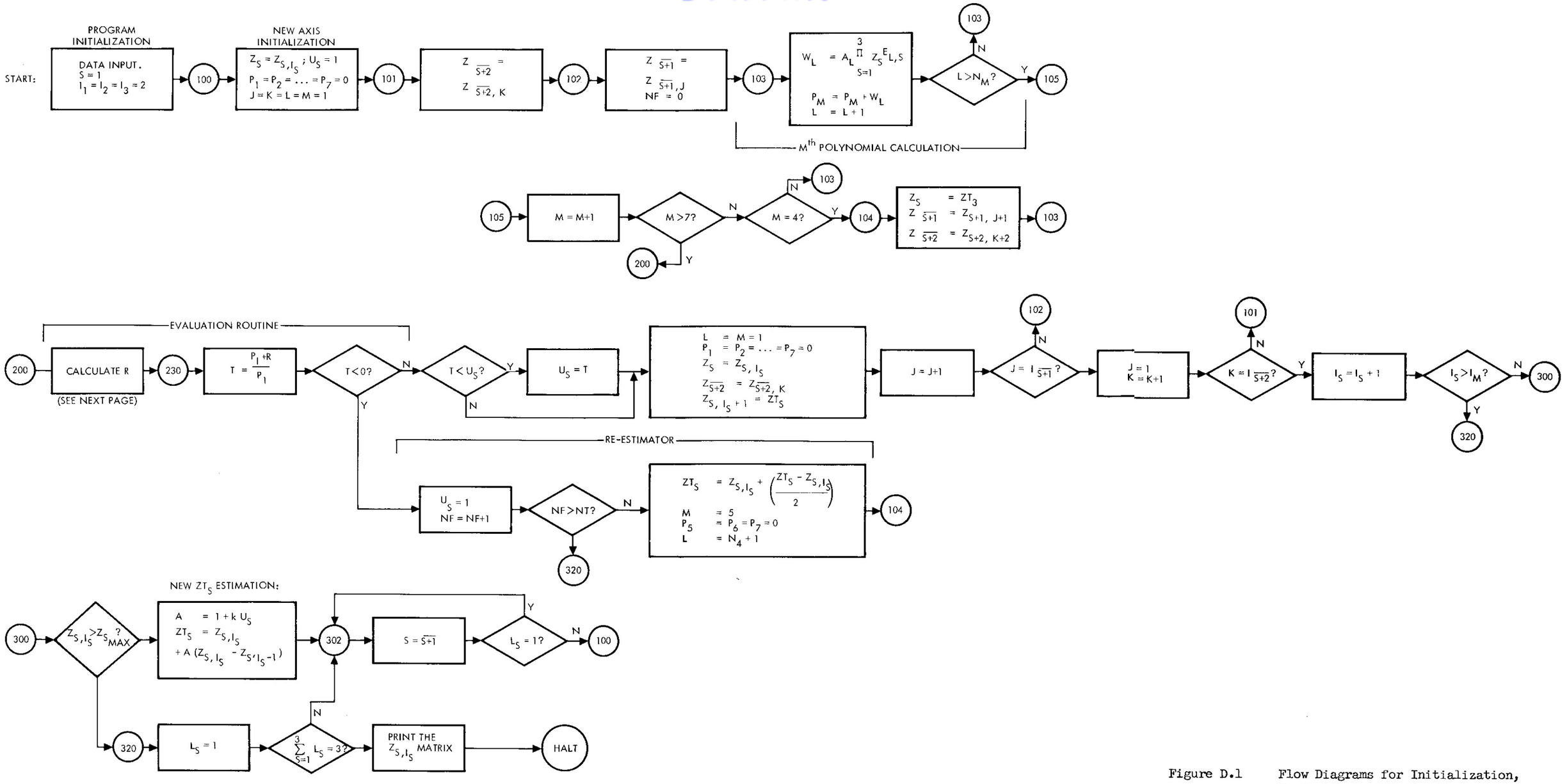

Figure D.1 Flow Diagrams for Initialization, Evaluation and Estimation

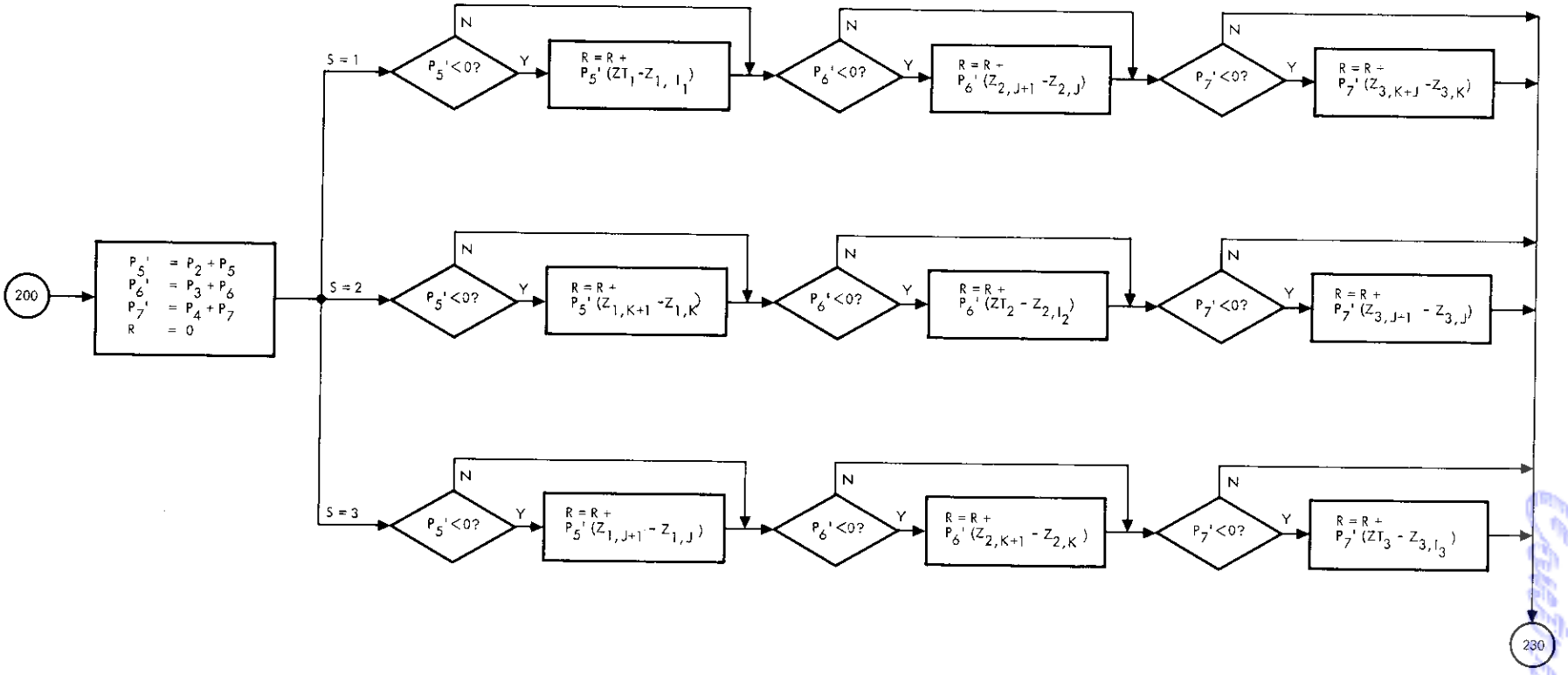

Figure D.2 Computer Flow Diagram

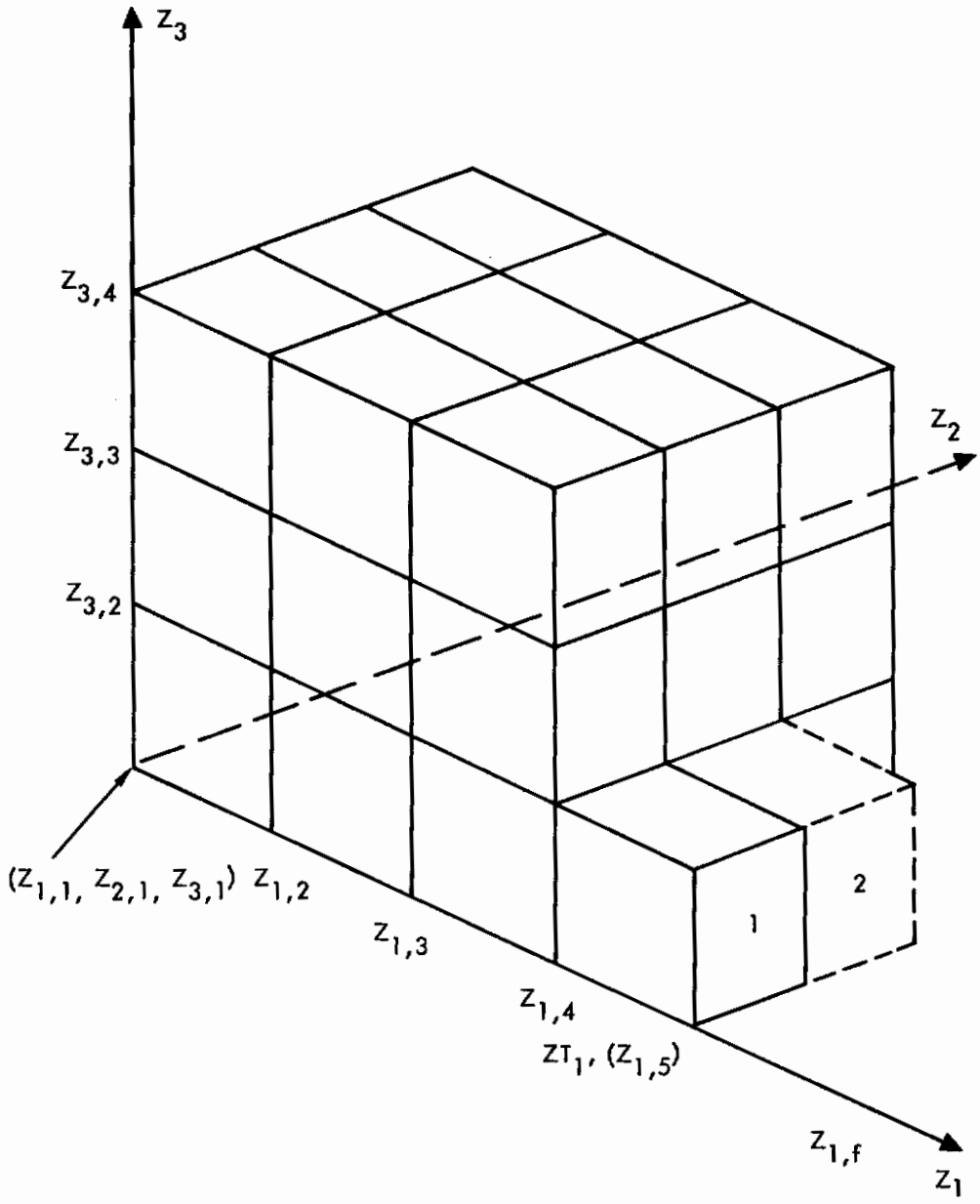

Figure D.3 Intermediate Point in Cube Growing Process

Unclassified
Security Classification

DOCUMENT CONTROL DATA - R&D

(Security classification of title, body of abstract and indexing annotation must be entered when the overall report is classified)

1. ORIGINATING ACTIVITY *(Corporate author)*
TRW Space Technology Laboratories
Redondo Beach, California

2a. REPORT SECURITY CLASSIFICATION
Unclassified

2b. GROUP

3. REPORT TITLE
INVESTIGATION OF THE ACQUISITION PROBLEM IN SATELLITE ATTITUDE CONTROL

4. DESCRIPTIVE NOTES *(Type of report and inclusive dates)*
Final Report 1 April 64 to 31 March 65

5. AUTHOR(S) *(Last name, first name, initial)*
Sabroff, A. E. Frew, A. M.
Farrenkopf, R. L. Gran, M. H.

6. REPORT DATE	7a. TOTAL NO. OF PAGES	7b. NO. OF REFS
December 1965	299	27

8a. CONTRACT OR GRANT NO.	9a. ORIGINATOR'S REPORT NUMBER(S)
AF33(615)1535	AFFDL TR 65-115
b. PROJECT NO. 8219	
c. Task - 821904	9b. OTHER REPORT NO(S) *(Any other numbers that may be assigned this report)*
d.	4154-6008-RU 000 (Originator's number)

10. AVAILABILITY/LIMITATION NOTICES
This report will be available to the Clearing-house for Federal Scientific and Technical Information.

11. SUPPLEMENTARY NOTES	12. SPONSORING MILITARY ACTIVITY
	AFFDL (FDCC) Wright-Patterson AFB, Ohio

13. ABSTRACT

The acquisition function of a spacecraft attitude control system consists of properly orienting the vehicle with respect to specified reference directions starting from large initial attitude and rate errors. The resulting control system design problem was examined by establishing suitable mathematical representations, comparing competing control concepts, developing a practical optimization approach, and evaluating a new technique for applying Lyapunov stability theory to the acquisition problem.

DD FORM 1 JAN 64 1473

Unclassified
Security Classification

Unclassified
Security Classification

14. KEY WORDS	LINK A		LINK B		LINK C	
	ROLE	WT	ROLE	WT	ROLE	WT
Acquisition						
Satellite						
Attitude						
Control						

INSTRUCTIONS

1. ORIGINATING ACTIVITY: Enter the name and address of the contractor, subcontractor, grantee, Department of Defense activity or other organization *(corporate author)* issuing the report.

2*a*. REPORT SECURITY CLASSIFICATION: Enter the overall security classification of the report. Indicate whether "Restricted Data" is included. Marking is to be in accordance with appropriate security regulations.

2*b*. GROUP: Automatic downgrading is specified in DoD Directive 5200.10 and Armed Forces Industrial Manual. Enter the group number. Also, when applicable, show that optional markings have been used for Group 3 and Group 4 as authorized.

3. REPORT TITLE: Enter the complete report title in all capital letters. Titles in all cases should be unclassified. If a meaningful title cannot be selected without classification, show title classification in all capitals in parenthesis immediately following the title.

4. DESCRIPTIVE NOTES: If appropriate, enter the type of report, e.g., interim, progress, summary, annual, or final. Give the inclusive dates when a specific reporting period is covered.

5. AUTHOR(S): Enter the name(s) of author(s) as shown on or in the report. Enter last name, first name, middle initial. If military, show rank and branch of service. The name of the principal author is an absolute minimum requirement.

6. REPORT DATE: Enter the date of the report as day, month, year; or month, year. If more than one date appears on the report, use date of publication.

7*a*. TOTAL NUMBER OF PAGES: The total page count should follow normal pagination procedures, i.e., enter the number of pages containing information.

7*b*. NUMBER OF REFERENCES: Enter the total number of references cited in the report.

8*a*. CONTRACT OR GRANT NUMBER: If appropriate, enter the applicable number of the contract or grant under which the report was written.

8*b*, &c, & 8*d*. PROJECT NUMBER: Enter the appropriate military department identification, such as project number, subproject number, system numbers, task number, etc.

9*a*. ORIGINATOR'S REPORT NUMBER(S): Enter the official report number by which the document will be identified and controlled by the originating activity. This number must be unique to this report.

9*b*. OTHER REPORT NUMBER(S): If the report has been assigned any other report numbers *(either by the originator or by the sponsor)*, also enter this number(s).

10. AVAILABILITY/LIMITATION NOTICES: Enter any limitations on further dissemination of the report, other than those imposed by security classification, using standard statements such as:

(1) "Qualified requesters may obtain copies of this report from DDC."

(2) "Foreign announcement and dissemination of this report by DDC is not authorized."

(3) "U. S. Government agencies may obtain copies of this report directly from DDC. Other qualified DDC users shall request through _____."

(4) "U. S. military agencies may obtain copies of this report directly from DDC. Other qualified users shall request through _____."

(5) "All distribution of this report is controlled. Qualified DDC users shall request through _____."

If the report has been furnished to the Office of Technical Services, Department of Commerce, for sale to the public, indicate this fact and enter the price, if known.

11. SUPPLEMENTARY NOTES: Use for additional explanatory notes.

12. SPONSORING MILITARY ACTIVITY: Enter the name of the departmental project office or laboratory sponsoring *(paying for)* the research and development. Include address.

13. ABSTRACT: Enter an abstract giving a brief and factual summary of the document indicative of the report, even though it may also appear elsewhere in the body of the technical report. If additional space is required, a continuation sheet shall be attached.

It is highly desirable that the abstract of classified reports be unclassified. Each paragraph of the abstract shall end with an indication of the military security classification of the information in the paragraph, represented as *(TS), (S), (C), or (U)*.

There is no limitation on the length of the abstract. However, the suggested length is from 150 to 225 words.

14. KEY WORDS: Key words are technically meaningful terms or short phrases that characterize a report and may be used as index entries for cataloging the report. Key words must be selected so that no security classification is required. Identifiers, such as equipment model designation, trade name, military project code name, geographic location, may be used as key words but will be followed by an indication of technical context. The assignment of links, rules, and weights is optional.

Unclassified
Security Classification